Synthesis of Policy Relevant Findings from the CalNex 2010 Field Study

(California Research at the Nexus of Air Quality and Climate Change)

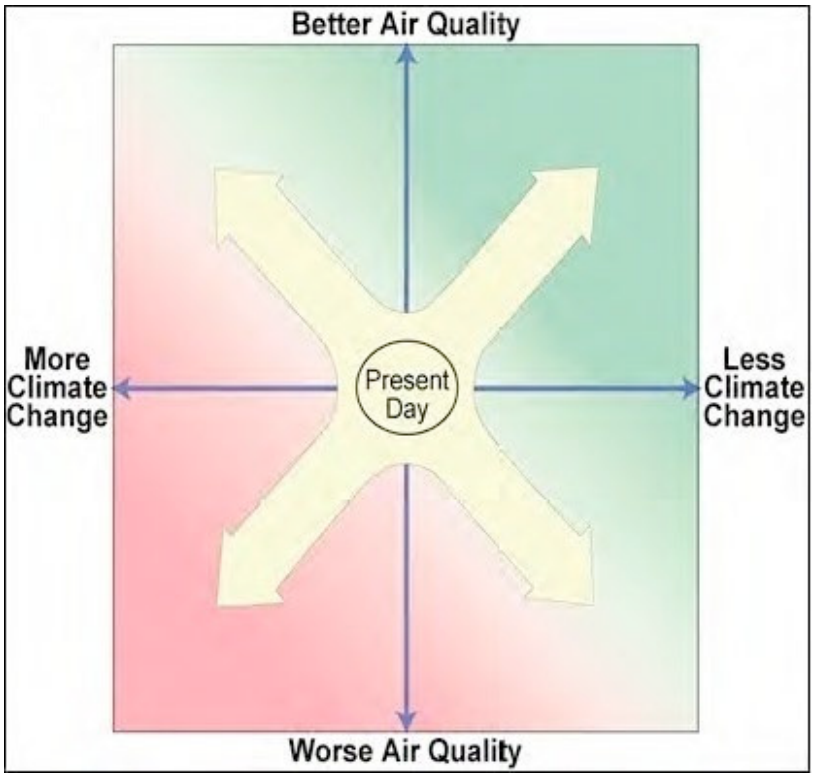

Final Report to the Research Division of the California Air Resources Board

Prepared by **David D. Parrish**
Tropospheric Chemistry Group
NOAA/ESRL/Chemical Sciences Division
325 Broadway R/CSD7
Boulder, CO 80305-3337

ARB Agreement No. 10-326

27 March 2014

Disclaimer

The statements and conclusions in this Report are those of the author from the National Oceanic and Atmospheric Administration, and not necessarily those of the California Air Resources Board. The mention of commercial products, their source, or their use in connection with material reported herein is not to be construed as actual or implied endorsement of such products.

Acknowledgements

A great many people and organizations contributed to the CalNex 2010 research. They are listed in the "Contributors" section near the end of this report. Many of these people also contributed to writing and reviewing this report. ARB staff, most notably Eileen McCauley and Leon Dolislager, provided great help in guiding the writing and in reviewing the report's content and format.

This Report was submitted in fulfillment of ARB contract number 10-326, titled “Synthesis of Policy Relevant Findings from the CalNex 2010 Field Study” by the National Oceanic and Atmospheric Administration under the sponsorship of the California Air Resources Board. Work was completed as of February 20, 2014.

Table of Contents

Abstract 1
Executive Summary 2
Introduction 12
CalNex 2010 Science Questions 15
Glossary of Symbols and Acronyms 19
Summary of Platforms and Sites deployed for CalNex 23
Synthesis of Results - Meteorology and Atmospheric Climatology 24
Question A (Meteorology during CalNex) 24
Question B (Historical context of CalNex) 28
Question C (Seasonal context of CalNex) 31
Question D (Pollutant background concentrations) 34
Synthesis of Results - Emissions 41
Question E (Effectiveness of historical air pollution control efforts) 41
Question F (Accuracy of emission inventories) 45
Question G (Emission insights from VOC measurements) 55
Question H (Improvement of emission estimates) 60
Question I (Impacts of ammonia emissions) 62
Question J (Emission differences between the SJVAB and the SoCAB) 67
Question K (Sulfur sources in the SoCAB) 71
Question L (Impact of biogenic emissions) 73
Synthesis of Results - Climate Processes/Transformations 78
Question M (Spatial and temporal variations of atmospheric chemistry) 78
Question N (Contributors to secondary organic aerosol) 83
Question O (Layers of enhanced ozone aloft) 91
Question P (Ozone weekend effect) 95
Question Q (Aerosol radiative balance) 100
Synthesis of Results - Atmospheric Transport 104
Question R (Pollutant transport between air basins or states) 104
Question S (Pollutant recirculation) 110
Question T (Long-range pollutant transport into California) 115
Synthesis of Results - Modeling 120
Question U (Performance of air quality forecast models) 120
Synthesis of Results - Climate and Air Quality Nexus 124
Question V (Response to pollutant control efforts) 124
Question W (Spatial variability of response to pollutant control efforts) 127
Recommendations for Further Analysis 130
Contributors 132
Appendix A - Sites, Platforms and Instruments deployed during the CalNex 2010 Field Study 136

List of Figures

page

Figure 1	Surface O_3 data, and number of days in exceedance of the state O_3 standards, for selected air basins in California.	13
Figure 2	Operations schedule of CalNex 2010 mobile platforms, ground sites and instrument networks.	23
Figure A1	Meteorological data from selected California sites during the CalNex 2010 field study period.	26
Figure B1	Photograph of the Los Angeles Civic Center area during a severe pollution episode in 1948.	28
Figure C1	Daily maximum 8-hr O_3 concentrations at sites in the SoCAB and the SJV.	31
Figure C2	Comparison of monthly mean fine aerosol composition in California urban areas.	32
Figure D1	Ozone distributions above Trinidad Head, California.	36
Figure D2	Summertime probability distribution functions of CO and O_3 between 2 and 10 km altitude at Portland, Oregon and Los Angeles, California.	36
Figure D3	Vertical profiles for CO, O_3 and PAN boundary conditions for California.	37
Figure D4	Median O_3 profiles above the IONS-2010 ozonesonde sites.	38
Figure E1	Long-term trends of ambient concentrations of primary and secondary pollutants in the SoCAB.	42
Figure E2	Comparison of the temporal evolution of O_3 in the SoCAB and the SJV.	43
Figure E3	Emissions reductions from a marine vessel as a result of the State of California fuel sulfur regulation and vessel speed reduction program.	44
Figure F1	Radiative forcing estimated from the 2009 California greenhouse gas emissions inventory.	46
Figure F2	Estimate of hydrocarbon emissions from six sources in the SoCAB.	48
Figure F3	Trends in NO_X emitted from on-road vehicles in the SoCAB and the SJV	50
Figure F4	Spatial distribution of methane emissions in the SJV	52
Figure G1	Trends in CO and hydrocarbon mixing ratios in Los Angeles during the last 50 years.	56
Figure G2	Comparison of measured emission ratios of VOCs versus the same ratios in two VOC emission inventories.	57
Figure G3	Sum of VOC reactivity with OH and secondary organic aerosol formation potential.	58
Figure I1	NH_3 and HNO_3 partial pressure product in the SoCAB.	63
Figure I2	Airborne measurements of ammonia and nitric acid mixing ratios in the Central Valley.	64
Figure I3	Airborne NH_3 flux measurements in the SJV.	65
Figure J1	Trends in NO_X emitted from on-road vehicles in the SoCAB and the SJV	67

Figure J2	Temperature dependence of formic acid concentrations and reactivity of organic compounds with OH radicals at the Bakersfield site.	68
Figure K1	Dependence of SO_2 on CO_2 in the Long Beach area and in offshore ship plumes.	72
Figure L1	OH reactivity for atmospheric species at the Pasadena and Bakersfield sites.	74
Figure M1	Comparison of radical production mechanisms at the Pasadena site.	81
Figure N1	Average composition of PM measured at the Bakersfield site.	83
Figure N2	Time series for organic aerosol components and O_X at the Pasadena site.	84
Figure N3	Evolution of organic aerosol to CO ratio versus photochemical age at the Pasadena site.	85
Figure N4	Diurnal profiles of the SOA components at the Pasadena site.	86
Figure N5	Diurnal trends in pΣAN, OA, pΣAN/OA, and NO_3 production rate at the Bakersfield site.	87
Figure O1	Latitude-height curtain plot of ozone measured near Joshua Tree National Park.	92
Figure P1	Weekday-to-weekend-day ratios of NO_X emissions in the LA basin.	96
Figure P2	Correlation of benzene and toluene with CO measured on a weekday and a weekend day.	97
Figure P3	NO_X/NO_Y ratio versus NO_Y on weekdays and weekends.	97
Figure P4	Observations of O_X versus NO_Y-NO_X on weekdays and weekends.	98
Figure R1	Average near-surface mixing ratios of each on-road vehicle emission tracer from four source regions.	108
Figure R2	Average of near-surface mixing ratios of each agricultural emission tracer from four source regions.	109
Figure S1	Near-surface mixing ratios of the four CO regional tracers.	111
Figure S2	Base of imaginary cylinder placed over Los Angeles for calculating fluxes of pollutant emissions.	113
Figure S3	Average NO_Y fluxes normal to the cylinder walls defined in Figure S2.	114
Figure T1	Time series of the contribution of stratospheric O_3 to surface concentrations in the greater Los Angeles area	116
Figure T2	Model versus observed MDA8 surface O_3 in the Central Valley, Southern California, and Las Vegas, Nevada.	117
Figure T3	Time series of the contribution of stratospheric O_3 to MDA8 surface O_3 concentrations over the Mojave Desert.	118
Figure U1	Number of days observed and modeled with maximum 8-hr average O_3 concentration $\geq$ 75 ppbv from 19 May to 15 July 2010.	122

Abstract

The CalNex 2010 field study was jointly organized and conducted by the California Air Resources Board (CARB) and the National Oceanic and Atmospheric Administration (NOAA) in the late spring and early summer of 2010, with the goal of investigating scientific issues at the nexus between air quality and climate change. This report is intended to ensure that the results of the analysis of the field observations are made available to California policy makers in a timely fashion. The findings from the CalNex research are here synthesized in a form most useful for those who must deal with air quality and climate change issues. The goal is to provide a comprehensive and integrated presentation of our current understanding of these interrelated issues in California. This Synthesis is organized around 23 policy-relevant Science Questions formulated by CARB in consultation with NOAA. Findings in response to each of these questions address six general areas:

1) Meteorology during the CalNex field study period and atmospheric climatology,
2) An assessment of emission inventories of air pollutants and climate forcing agents, including greenhouse gases,
3) An assessment of climate processes and atmospheric transformations,
4) An overview of important atmospheric transport processes,
5) An assessment of the skill of current air quality modeling and forecasting systems, and
6) A discussion of the areas where it is particularly important to simultaneously consider the air quality and climate impacts of policy decisions.

Executive Summary

This Synthesis is intended to address 23 policy-relevant Science Questions formulated by the California Air Resources Board (CARB) in consultation with the National Oceanic and Atmospheric Administration (NOAA). Answers to these questions are needed by CARB and other stakeholders in California to help fulfill the Board's responsibility to formulate scientifically sound policies to simultaneously address concerns regarding air quality degradation and increasing climate change.

This Report provides statements of Findings in response to each of CARB's policy-relevant Science Questions. These Questions and Findings address six general areas:

1) Meteorology during the CalNex field study period and atmospheric climatology,
2) An assessment of emission inventories of air pollutants and climate forcing agents, including greenhouse gases,
3) An assessment of climate processes and atmospheric transformations,
4) An overview of important atmospheric transport processes,
5) An assessment of the skill of current air quality modeling and forecasting systems and recommendations for improvement of these systems, and
6) A discussion of the areas where it is particularly important to simultaneously consider the air quality and climate impacts of policy decisions.

The Executive Summary organizes the main scientific Findings from the CalNex research for use by CARB managers and other air-quality decision makers and stakeholders in California. It comprises a list of the 23 policy-relevant Science Questions and a series of Findings that have been developed in response to each of these questions. We emphasize that these Findings are based on analysis and interpretation of results that have so far emerged; additional analyses are continuing, and will yield additional important information in the future.

Each section of this report is structured as a Response to address one of the Science Questions, including a numbered sequence of succinctly stated Findings in response to that question. Where useful, the policy relevance of the Science Question is briefly summarized in a text box. Important references are given for publications upon which the Finding is based, and following some Findings is an acknowledgment of the individual(s) whose analyses and data contributed to that Finding, particularly if the analysis has not yet been published. A brief discussion of background and the evidence that supports each Finding is given.

As is common in scientific research, progress in addressing a given set of questions raises new questions suggesting additional analysis. Specific examples of additional analysis suggested by the CalNex results are collected in a concluding section.

The CalNex fieldwork comprised an intensive, relatively short late spring-early summer period. Hence, the results cannot address all aspects of atmospheric issues affecting California's air quality and climate change concerns. Specifically, no data were collected in the cooler winter season when maximum particulate matter (PM) concentrations are usually observed.

A brief summary of platforms and sites deployed for CalNex is included in the body of the report, and Appendix A provides extensive details.

The institutional affiliations of the scientists responsible for the field measurements and the analyses leading to these Findings are given in the Contributors section, which follows the discussion of the Science Questions and Findings.

Findings Related to Study Questions

Meteorology and Atmospheric Climatology

QUESTION A

How did the meteorology during CalNex compare to historical norms?

***Finding A1*:** May 2010 was cooler and wetter than normal, followed by more seasonal warm temperatures in June. In May deep upper level troughs moved into California bringing stratospheric intrusions that affected ozone concentrations in the State.

QUESTION B

How did the CalNex air quality measurements fit in the context of historical measurements?

***Finding B1*:** While nearly all atmospheric pollutants have decreased in California, ethanol is an exception because its use in gasoline has recently increased markedly. During CalNex ethanol was the VOC with the highest ambient concentrations in SoCAB. Acetaldehyde (an air toxic) is a secondary product of the atmospheric oxidation of ethanol, but its concentration has continued to decrease.

QUESTION C

How do the CalNex air quality measurements in late spring and early summer relate to the peak ozone concentrations in summer and the peak PM2.5 concentrations in winter?

***Finding C1*:** The CalNex fieldwork was conducted primarily in May and June, 2010, but included some aircraft flights through mid-July. The measurements provide characterization of the photochemical environment in southern California, particularly in the SoCAB, during its most active period.

***Finding C2*:** The CalNex measurements cannot be used to characterize the peak PM2.5 concentrations observed in the Central Valley in winter. However, they do provide a guide for further studies of this important phenomenon.

QUESTION D

What were the global "background" concentrations observed during CalNex and how did they vary spatially and temporally?

Finding D1: Baseline concentrations of pertinent air quality species have such large variability on time scales of days that average vertical profiles of baseline concentrations provide only poor quantification of boundary conditions for regional air quality modeling.

Finding D2: Along the California coast there is little indication of significant latitudinal gradient in average baseline concentrations of gas phase species important for air quality.

Finding D3: Global chemical transport models (GTMs) capture a significant fraction of the temporal and spatial variability of the baseline concentrations, and hence can provide improved boundary conditions for regional air quality modeling.

Emissions

QUESTION E

How effective have historical air pollution control efforts been? How effective have specific emission control measures been?

***Finding E1*:** The five decades of air pollution controls implemented in the SoCAB have produced remarkable improvement in air quality, with substantial reductions in both primary and secondary air pollutants.

***Finding E2*:** By some measures, O_3 concentrations have decreased more slowly in the SJV than in the SoCAB. Although several factors likely contribute, the cause(s) and significance of this difference is ambiguous at this time.

***Finding E3*:** Compliance of marine vessels with the California fuel quality regulation and participation in the vessel speed reduction program yield the expected reduction in emissions of SO_2, and also provide substantial reductions in emissions of carbon dioxide and primary PM.

QUESTION F

Are emission inventory estimates for air pollutants and climate-forcing agents accurate? Are there under- or over-estimated emissions or even missing emission sources in the emission inventories?

***Finding F1*:** CO_2 emissions for the SoCAB estimated by an observation-based mesoscale inverse modeling technique agree with emission estimates by CARB. Both of these estimates are higher by 15 to 38% than that in the Vulcan inventory of North American CO_2 emissions.

***Finding F2a*:** Total methane emissions for the SoCAB have been consistently underestimated by inventories. CalNex analyses implicate larger-than-expected CH_4 emissions from the oil and gas sector in Los Angeles as the emissions missing from current inventories.

***Finding F2b*:** Methane emissions from landfills and dairies in the SoCAB are accurately estimated in the inventories developed by CARB.

***Finding F2c*:** Annual average methane emissions from rice agriculture are factors of 2 to 3 greater than in the CARB inventory.

***Finding F3*:** Analyses of CalNex nitrous oxide measurements suggest that inventory improvements are needed to correct a potential low bias and improve the spatial and seasonal patterns of emissions.

***Finding F4*:** Top-down assessments of anthropogenic halocarbon emissions are generally consistent with the CARB emission inventory.

***Finding F5*:** Top-down assessments of the CO emissions in 2010 are within 15% of the CARB 2008 emission inventory.

***Finding F6*:** Top-down assessments of NO_X emissions are in general agreement with the CARB emission inventory.

***Finding F7*:** Top-down assessments of VOC emissions of measured species indicate some discrepancies with inventories, but they are not sufficiently large to appreciably affect results of air quality modeling. However, an important, temperature-dependent source of unidentified VOC species is missing from inventories in the SJV.

***Finding F8*:** Measurements at the Bakersfield site have been used to assess the magnitude, composition and spatial distribution of emissions from petroleum and dairy operations and other agricultural activities in the SJV.

QUESTION G

Do the VOC measurements provide any new insights into emission sources?

***Finding G1*:** Ambient VOC concentrations in the SoCAB have decreased by a factor of approximately 50 in the past five decades, but the ambient relative concentrations have remained remarkably constant, indicating that mobile emissions have remained the predominant source over this entire period.

***Finding G2*:** The individual VOC to CO emission ratios observed in the SoCAB can disagree by a factor of four or more with the ratios derived from NEI 2005 and CARB 2008 emission inventories. The agreement is particularly poor for oxygenated VOCs. Nevertheless, the difference between measurements and inventory in terms of the overall OH reactivity is within 15% of that from the CARB inventory, and the potential to form secondary organic aerosols (SOA) agrees within 35%.

***Finding G3*:** Ambient benzene concentrations in the SoCAB have decreased more rapidly than concentrations of other VOCs, which is primarily attributed to efforts to remove benzene from gasoline due to its recognized toxicity.

QUESTION H

Can emission estimates from area sources be improved with the CalNex measurements?

***Finding H1*:** Gaseous elemental mercury emissions from a variety of California sources were estimated, and these estimates generally agreed with inventoried emissions. An exception is that emissions from the Los Angeles urban area were much larger than those in the inventory; reemission of mercury accumulated over the industrialized history of Los Angeles could account for this discrepancy.

QUESTION I

What are the relative roles and impacts of NH_3 emissions from motor vehicles and dairy farms?

***Finding I1*:** Within the SoCAB, conditions observed downwind of the dairy facilities were always thermodynamically favorable for NH_4NO_3 formation due to high NH_3 mixing ratios from those concentrated sources. Although automobile emissions of NH_3 within the basin were of approximately the same magnitude as the dairies, they were more dispersed and thus generated lower NH_3 mixing ratios. However, they are sufficiently high that they can thermodynamically favor NH_4NO_3 formation. Reducing the dairy NH_3 emissions would have a larger impact on reducing SoCAB NH_4NO_3 formation than would reducing automobile NH_3 emissions.

***Finding I2a*:** Within the San Joaquin Valley, despite large concentrations of NH_3 (often many 100's of ppbv) associated with dairies, measured NH_4NO_3 concentrations were relatively low ($\leq 4\ \mu g/m^3$) due to low HNO_3 concentrations resulting from low NO_X emissions.

***Finding I2b*:** Preliminary results indicate that within the San Joaquin Valley, NH_3 emissions could be underestimated in inventories by about a factor of three.

***Finding I3*:** Within the San Joaquin Valley, the large concentrations of NH_3 enhance SOA formation in the atmosphere, likely due to reactions between NH_3 and carboxylic acids.

QUESTION J

Are there significant differences between emissions in the San Joaquin Valley Air Basin (SJVAB) and the South Coast Air Basin (SoCAB)?

***Finding J1*:** NO_X emissions from the on-road vehicle fleet have decreased more rapidly in the SoCAB than in the SJVAB.

***Finding J2*:** There is evidence that temperature dependent VOC emissions from an unidentified source, perhaps associated with agricultural activities and petroleum operations, are important in the SJVAB but absent in the SoCAB.

***Finding J3*:** The relative amounts of ammonia and NO_X emissions are such that formation of ammonium nitrate aerosol (the major component of PM2.5 during many exceedance episodes) is ammonia-limited in the SoCAB and NO_X-limited in the SJVAB.

QUESTION K

What are the significant sources of sulfur in southern California that contribute to enhanced sulfate ($SO_4^=$) concentrations in the SoCAB?

***Finding K1*:** No significant sources of sulfur beyond those included in the CARB inventory could be identified from the CalNex 2010 data.

QUESTION L

What is the impact of biogenic emissions, especially in foothills of the Sierra Nevada?

***Finding L1a*:** Photochemical O_3 formation in the SoCAB is dominated by anthropogenic VOCs rather than biogenic VOCs; this was true in 2010 despite very substantial reductions in anthropogenic VOC emissions over past decades.

***Finding L1b*:** Considering only the individually measured VOCs, photochemical O_3 formation in the SJVAB is also dominated by anthropogenic VOCs. However, on the hotter days in the SJVAB there is evidence that additional VOCs make an important contribution to O_3 formation, and this contribution well may be of biogenic origin.

***Finding L2*:** Biogenic VOCs play significant roles in SOA formation in the SJVAB during both daytime and nighttime; the different processes important during light and dark periods both involve interactions between biogenic VOCs and anthropogenic emissions.

***Finding L3*:** Biogenic VOCs play a significant, but minor role in SOA formation in the SoCAB.

Climate Processes/Transformations

QUESTION M

How does the atmospheric chemistry vary spatially and temporally?

***Finding M1*:** Nighttime atmospheric chemistry plays multiple important air quality roles including interconversion of reactive oxidized nitrogen species, formation of gas phase chlorine species, and formation of aerosol nitrate. It is important that these processes are accurately included in the air quality models from which air quality policy and regulations are generally developed.

***Finding M2*:** $ClNO_2$ and HONO are significant primary radical sources in SoCAB, particularly in early morning when they were the dominant radical source near the surface between sunrise and 09:00 PDT. However, it is important that vertical gradients of radical precursors be taken into account in radical budgets, particularly with respect to HONO.

***Finding M3*:** The propensity of Cl for radical propagation yielding second-generation OH radicals indicates that the relative contributions of Cl and OH to tropospheric oxidation are not accurately captured through simple radical budgets.

QUESTION N

What are the major contributors to secondary organic aerosol (SOA)? What are the relative magnitudes of SOA compared with primary organic aerosols in different areas?

***Finding N1*:** SOA contributions to OA at Pasadena could be identified from 1) their diurnal cycles and their correlations with photochemical ozone production, and 2) an increase in SOA concentration with increasing photochemical processing of urban air.

***Finding N2*:** Averaged over the entire CalNex study, the 24-hour average SOA contributions to total OA in PM1 at the Pasadena (≈ 66%) and Bakersfield (≈ 72%) sites were about two to three times that of primary organic aerosols.

***Finding N3*:** At the Bakersfield site, most nighttime SOA formation is due to the reaction of the NO_3 radical (a product of anthropogenic NO_X emissions) with unsaturated, primarily biogenic VOCs.

***Finding N4*:** Analysis of ambient OA measurements in SoCAB indicate that gasoline emissions dominate over diesel in formation of secondary organic aerosol mass; however, an analysis (based on liquid fuel composition) indicated that diesel dominates over gasoline for the formation of SOA in the southern SJV.

QUESTION O

How do layers of enhanced ozone concentrations form aloft, and how do they impact ground-level ozone concentrations?

***Finding O1*:** Layers of enhanced O_3 concentrations aloft over California reflect the interleaving of layers of air affected by differing O_3 sources. Enhanced O_3 concentrations arise from decent of upper tropospheric air with O_3 of stratospheric origin, long-range transport of anthropogenic emissions (e.g., from Asia), and lofted aged regional pollution (e.g., from California urban areas).

***Finding O2*:** Layers of enhanced ozone concentrations aloft are entrained into the convective boundary layer throughout California, thereby enhancing surface level ozone concentrations.

QUESTION P

What is the prevalence and spatial extent of the ozone weekend effect? What are the contributing factors?

***Finding P1*:** In the SoCAB, NO_X emissions are reduced by nearly half on weekends, while VOC emissions remain approximately constant. As a result, weekend hydroxyl radical concentrations are greater, giving 65%–75% faster photochemical processing. In addition, ozone production efficiency is 20%–50% higher. These effects yield 8-16 ppbv higher average midday ozone concentrations on weekends than on weekdays.

***Finding P2*:** The weekend reduction of NO_X emissions, and the concomitant changes in the photochemical environment in the SoCAB, provides an opportunity to investigate certain aspects of urban photochemistry such as secondary aerosol formation.

***Finding P3*:** Investigation of the history of the weekend O_3 effect in the San Joaquin Valley suggests that NO_X emissions reductions are now effective for reducing maximum O_3 concentrations in the southern and central SJV, or are poised to soon become so.

QUESTION Q

How do the different aerosol compositions in different areas influence radiative balances?

***Finding Q1*:** Climate models need more detailed treatment of direct radiative effects related to black carbon absorption enhancements and also of ammonium nitrate partitioning between aerosol and gas phases.

***Finding Q2*:** The hygroscopicity of particles in the Central Valley is consistent with the emerging global picture of a limited range of hygroscopicities, which may simplify the treatment of indirect aerosol effects in global climate models. However, considerable variability was found in aerosol hygroscopicity in the Los Angeles basin, which may complicate the treatment of this issue in regional climate models.

Atmospheric Transport

QUESTION R

Is there evidence of pollutant transport between air basins or states?

***Finding R1a*:** San Francisco Bay Area anthropogenic emissions are transported efficiently to the Central Valley. Automotive CO emitted in the Bay Area is a significant fraction of total CO found in the San Joaquin Valley.

***Finding R1b*:** Agricultural emissions (as well as emissions from other sources) in the Central Valley can be transported aloft to the Southern California Bight.

***Finding R1c*:** Southern California emissions are typically transported to less-populated areas to the east.

***Finding R2*:** The primary direction of transport of Mexican emissions in the border area (as exemplified by daytime Tijuana emissions) was to the east or southeast. At least during May and June of 2010, the transport of emissions from the Mexican border regions into the San Diego area was not an important influence. However, nighttime Tijuana emissions, which were particularly rich in black carbon, were commonly transported into the US in a northeasterly direction.

QUESTION S

Is there evidence of pollutant recirculation, particularly in the South Coast Air Basin (SoCAB)?

***Finding S1*:** Pollutants from the SoCAB can be recirculated within the Catalina Eddy in the boundary layer over the Southern California Bight. In the process, they can mix with pollutants from the San Francisco Bay Area, which can be transported down the coast. Although pollutant concentrations associated with San Francisco Bay Area emission sources that are offshore of southern California are generally small, they represent the bulk of the pollution in that area during the June 1-15 period of CalNex.

***Finding S2*:** The direction that emissions originating from Los Angeles exit from the basin varies with time of day. From late morning to early evening, most emissions exit toward the east, while during the rest of the day, significant emissions exit to the west and south in shallow layers over the ocean. Both the sea-land breeze circulation and the Catalina Eddy flow over the Southern California Bight bring emissions that had exited the LA basin to the west and south back into the source region. For NO_Y, total inflow from upwind sources and this return flux equals about 40% of that emitted within the basin when averaged over May of 2010.

QUESTION T

Is there evidence of long-range transport during CalNex? What were the relative contributions of the various sources outside the control of emissions within California (i.e., policy-relevant background ozone)?

***Finding T1*:** Transport of baseline O_3 can enhance surface O_3 concentrations to such an extent that the margin for local and regional O_3 production before exceeding the NAAQS is greatly reduced or potentially eliminated, particularly if the NAAQS is revised downward to 60 ppbv.

***Finding T2*:** Transport of baseline ozone accounts for a majority of surface ozone concentrations in California at urban as well as rural locations, both on average and during many exceedance events.

***Finding T3*:** In addition to being a receptor of long-range pollutant transport, California is also a source of transport to downwind areas.

Modeling

QUESTION U

How well did the meteorological and air quality forecast models perform during CalNex? What weaknesses need attention?

***Finding U1*:** Evaluation of different meteorological models against CalNex measurements shows that details of model configuration (physics, initialization, resolution) can impact performance for specific processes and regions. Particular attention needs to be paid to land surface and soil parameters and to clouds offshore. Significant but poorly characterized biases (for example, high wind speeds and weak land breeze) remain in the best available simulations.

***Finding U2a*:** Evaluation of several different real-time air quality forecasts against O_3 and PM2.5 observations show that none of the models perform statistically better than the persistence forecast (i.e., predicting that tomorrow's air quality will be exactly the same as today's air quality). All models show temporal correlations for maximum 8-hr O_3 that beat persistence, but model biases and poor spatial correlations limit overall forecast skill.

***Finding U2b*:** Incorporation of the RAQMS global forecast [*Pierce et al.*, 2003] to modify lateral boundary conditions improved temporal skill for O_3 forecasts but increased model bias.

Climate and Air Quality Nexus

QUESTION V

What pollution control efforts are likely to result in "win-win" or "win-lose" situations?

***Finding V1*:** The approximately 75% reduction of burning crop residue from rice agriculture (a "win" for air quality) increased methane emissions (a "lose" for climate).

***Finding V2*:** Marine vessel emissions changes due to fuel sulfur reductions and speed controls result in a net warming effect (a "lose" for climate), but have substantial positive impacts on local sulfur and primary PM emissions (a "win" for air quality).

QUESTION W

Could the same pollutant control efforts in different air basins (i.e., SJVAB and SoCAB) have different results with respect to changes in air quality and climate (i.e., move toward different nexus quadrants in the figure on the front page of this report)?

***Finding W1*:** The southern SJVAB has an unidentified, temperature-dependent VOC emission source that dominates O_3 production on the hottest days when the highest O_3 concentrations occur. As a consequence, NO_X emission controls are expected to be more effective for reducing maximum O_3 concentrations in the southern SJVAB than in the SoCAB.

***Finding W2a*:** In the SJVAB ammonia is in large excess compared to nitric acid; consequently NH_4NO_3 PM concentrations in the SJVAB will be more responsive to NO_X emissions reductions compared to ammonia emissions reductions.

***Finding W2b*:** In the SoCAB the response of NH_4NO_3 PM concentrations to emission reductions will depend upon meteorological conditions, other aerosol components, and the regional distribution of NH_3 and NO_X emissions.

***Finding W3a*:** In both the SoCAB and the SJVAB, anthropogenic VOCs are believed to be the primary precursors of secondary organic aerosol; thus in both basins organic aerosol concentrations will be sensitive to VOC emissions control.

Finding W3b: Biogenic VOCs oxidized in the presence of NO_X provides additional sources of secondary organic aerosol that are important for the SJVAB, but less so in the SoCAB. Thus, NO_X emissions reductions will be effective for controlling this source of organic aerosol in the SJVAB, but will have less impact in the SoCAB.

Introduction

The California Air Resources Board (CARB) and the National Oceanic and Atmospheric Administration (NOAA) jointly organized an atmospheric field study in the spring and early summer of 2010 (CalNex) that collected atmospheric composition and meteorological data pertinent to addressing issues at the nexus between air quality and climate change (see http://www.arb.ca.gov/research/calnex2010/calnex2010.htm and http://esrl.noaa.gov/csd/calnex/). This report is intended to ensure that the results of the analysis of the field observations are made fully available to California policy makers who must deal with air quality and climate change issues. Much of the material in this report has been presented in *Ryerson et al.* [2013] in a different format with a different emphasis.

As fully as possible, the findings from the CalNex publications and from additional integrated analysis of the diverse data sets from the CalNex researchers, as well as other historical air quality studies in California, are here synthesized in a timely fashion and in a form useful to policy makers. The goal is to provide a comprehensive and integrated presentation of our current understanding of the interrelated air quality and climate issues in California.

The California Research at the Nexus of Air Quality and Climate Change (CalNex) 2010 field project was undertaken to provide improved scientific knowledge for emissions control strategies to simultaneously address the two interrelated issues of air quality and climate change. Air quality and climate change issues are linked because in many cases the atmospheric agents of concern are the same, and the sources of the agents are the same or intimately connected. Examples include tropospheric ozone (O_3), which is both an air pollutant and a greenhouse gas (GHG), and atmospheric particulate matter (PM), which affects the radiative budget of the atmosphere, as well as human and ecosystem health, visibility degradation, and acidic deposition. Efforts to address one of these issues can be beneficial to the other, but in some cases policies addressing one issue without additional consideration can have unintended detrimental impacts on the other. The goal of CalNex 2010 is to improve and advance the science needed to support continued and effective air quality and climate management policy for the State of California.

Over the past several decades in the U.S., emissions reductions implemented for vehicles and point sources have significantly improved air quality in most metropolitan areas. In recent years the rate of improvement in air quality in most regions of the U.S. has slowed, both in terms of regional ozone concentrations and ozone exceedance days (*e.g.*, Figure 1 for California). At the same time, accelerating emissions of greenhouse gases have increased the net radiative forcing of the climate system. Overall, from 1990 to 2005, total emissions of carbon dioxide (CO_2) in the US were estimated to have increased by 20% (from 5062 to 6090 Tg per year) [*EPA*, 2007].

California was chosen as the region for this study because it has well-documented air quality problems and faces the difficult task of managing them with an increasing population and demand for goods and services. The CalNex study was designed to build upon the knowledge developed through decades of previous atmospheric research field projects in California. Consistent themes across the many studies include quantifying anthropogenic emissions and their changes over time, notably in tunnel studies (e.g., [*Harley et al.*, 2005]) and by roadside monitoring (e.g., [*Bishop and Stedman*, 2008]); the role that regional transport plays in shaping pollutant concentrations, forced either by the sea breeze (e.g., [*Boucouvala and Bornstein*, 2003; *Cass and Shair*, 1984; *Shair et al.*, 1982]), by complex terrain (e.g., [*Langford et al.*, 2010; *Skamarock et al.*, 2002; *Wakimoto and McElroy*, 1986]) or both [*Lu and Turco*, 1996; *Rosenthal*

et al., 2003]; the roles of chlorine chemistry (e.g., [*Finlayson-Pitts*, 2003; *Knipping and Dabdub*, 2003]) and the weekend effect (e.g., [*Blanchard and Tanenbaum*, 2003; *Marr and Harley*, 2002]) in ozone formation; and studies of the sources and chemistry leading to atmospheric haze formation (e.g., [*Hersey et al.*, 2011; *Schauer et al.*, 1996; *Turpin and Huntzicker*, 1995]).

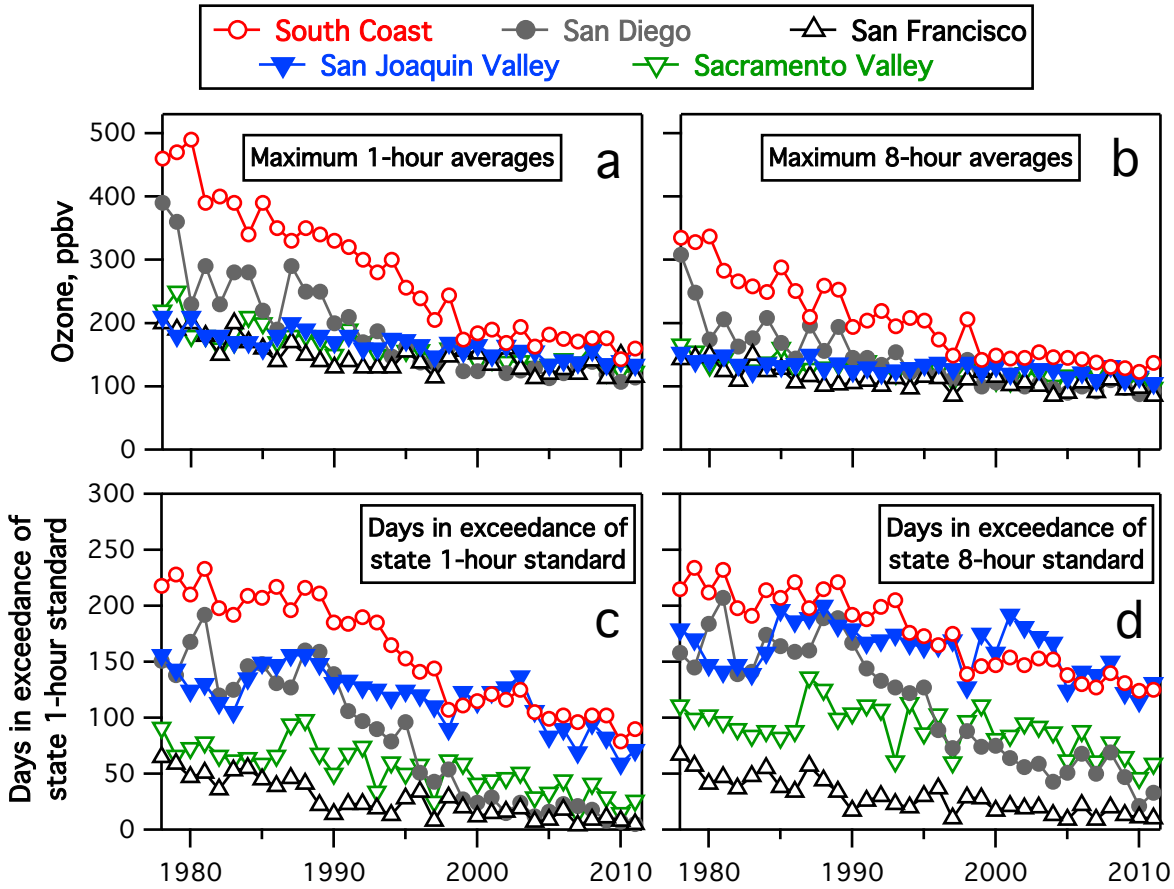

Figure 1. Maximum 1-hour (a) and 8-hour (b) averaged surface O_3 data, and number of days in exceedance of the state 1-hour (c) and 8-hour (d) O_3 standards, for selected air basins in California (www.arb.ca.gov/adam/trends/trends1.php).

The literature from previous field studies in California is extensive; initial descriptions can be found in the project overview papers for the Southern California Air Quality Study (SCAQS; which took place in 1987) [*Hering and Blumenthal*, 1989], the Southern California Ozone Study (SCOS, 1997) (www.arb.ca.gov/research/scos/scos.htm), the California Regional Particulate AirQuality Study (CRPAQS, 1999-2001) [*Chow et al.*, 2006; *Qin and Prather*, 2006; *Rinehart et al.*, 2006], the Central California Ozone Study (CCOS, summer 2000) [*Bao et al.*, 2008a; *Liang et al.*, 2006; *Tonse et al.*, 2008], the Intercontinental Transport and Chemical Transformation (ITCT, spring 2002) study [*Parrish et al.*, 2004], the Intercontinental Chemical Transport Experiment - North America (INTEX-NA, summer 2004) study, the Study of Organic Aerosols at Riverside (SOAR; 2005) [*Docherty et al.*, 2011], the Arctic Research of the Composition of the Troposphere from Aircraft and Satellites-California Air Resources Board (ARCTAS-CARB, summer 2008) study [*Jacob et al.*, 2010], the Pre-CalNex (summer 2009) study [*Langford et al.*, 2010], and the Pasadena Aerosol Characterization Observatory study (PACO, 2009-2010) study [*Hersey et al.*, 2011].

In addition to its long-standing focus on air quality issues, California led the nation's effort to address global climate change by implementing Assembly Bill 32 (AB32; arb.ca.gov/cc/ab32/ab32.htm) as the Global Warming Solutions Act of 2006, mandating controls on the emissions of greenhouse gases within, or attributable to, the State. Thus, California is particularly interested in finding the most effective way to simultaneously manage the two challenges of air quality and climate change. The CalNex study was organized to address issues simultaneously relevant to both, including (1) emission inventory assessment, (2) atmospheric transport and dispersion, (3) atmospheric chemical processing, and (4) cloud-aerosol interactions and aerosol radiative effects.

The CalNex project was loosely coordinated with the Carbonaceous Aerosol and Radiative Effects Study (CARES; http://campaign.arm.gov/cares) sponsored by the U.S. Department of Energy (DOE)in the Central Valley (primarily the Sacramento area), and with the multi-institutional Cal-Mex study (http://mce2.org/en/activities/cal-mex-2010) based in Tijuana, Mexico. CARES took place in June of 2010 with a focus on the evolution of secondary and black carbon aerosols and their climate-relevant properties in the Sacramento urban plume. The scientific objectives, deployment approach, and a summary of initial findings from this project are described in *Zaveri et al.* [2012]. Cal-Mex took place in May and June of 2010 with a focus on characterizing the sources and processing of emissions in the California-Mexico border regions to better understand their transport [*Bei et al.*, 2012], transformation, impacts on regional air quality and climate (*e.g.,* [*Takahama et al.*, 2012]), and to support the design and implementation of emission control strategies at local, regional and trans-boundary scales.

The CalNex fieldwork was planned initially to address twelve general Science Questions (see the CalNex White Paper at http://esrl.noaa.gov/csd/calnex/whitepaper.pdf for a listing) that were formulated to guide the study planning. Those questions address many specific and general science needs required to guide policy approaches to effectively address air quality and climate change issues. The questions addressed pollutant emissions (of greenhouse gases and ozone and aerosol precursors), important atmospheric transformation and climate processes, and pollutant transport and meteorology. Instrumentation and platforms (airborne, ship- and ground-based) were deployed to collect the data sets necessary to address those questions. Analyses of the resulting data sets have been reported in many science publications (96 published or submitted to date), with more expected during coming years. However, most of these publications are intended to further our understanding of the scientific issues at hand, and not necessarily at directly addressing the most policy-relevant issues.

The general Science Questions that were formulated to guide the CalNex field study are here revised into twenty-three specific policy-relevant Science Questions (see text box on next pages) that can be addressed, and ideally fully answered, by CalNex analyses. They provide the organizational framework of this synthesis for presentation of the scientific results of this ongoing analysis in a format that is maximally useful to California policy makers responsible for formulating the State's response to air quality and climate change issues, both at the state and more regional levels. This report brings together in an organized fashion the most important policy-relevant findings to date, and is intended to present them as concise but comprehensive findings. The goals are that: 1) each question/issue be succinctly stated, 2) the policy-relevance is discussed if appropriate, 3) the historical context is given, 4) the analytical approach (along with caveats and uncertainties) is summarized, and 4) the findings and recommendations, if any, are presented succinctly and clearly. Of course, an approximately 6-week sampling program cannot definitively answer all the questions and issues, but it does effectively address and advance our understanding of all twenty-three policy-relevant Science Questions.

CalNex 2010 Science Questions

Meteorology and Atmospheric Climatology

A. How did the meteorology during CalNex compare to historical norms?
B. How did the CalNex air quality measurements fit in the context of historical measurements?
C. How do the CalNex air quality measurements in late spring and early summer relate to the peak ozone concentrations in summer and the peak PM2.5 concentrations in winter?
D. What were the global "background" concentrations observed during CalNex and how did they vary spatially and temporally?

Emissions

E. How effective have historical air pollution control efforts been? How effective have specific emission control measures been?
F. Are emission inventory estimates for air pollutants and climate-forcing agents accurate? Are there under- or over-estimated emissions or even missing emission sources in the emission inventories?
G. Do the VOC measurements provide any new insights into emission sources?
H. Can emission estimates from area sources be improved with the CalNex measurements?
I. What are the relative roles and impacts of NH_3 emissions from motor vehicles and dairy farms?
J. Are there significant differences between emissions in the San Joaquin Valley Air Basin (SJVAB) and the South Coast Air Basin (SoCAB)?
K. What are the significant sources of sulfur in southern California that contribute to enhanced sulfate ($SO_4^{=}$) concentrations in the SoCAB?
L. What is the impact of biogenic emissions, especially in foothills of the Sierra Nevada?

Climate Processes/Transformations

M. How does the atmospheric chemistry vary with time of day?
N. What are the major contributors to secondary organic aerosol (SOA)? What are the relative magnitudes of SOA compared with primary organic aerosols in different areas?
O. How do layers of enhanced ozone concentrations form aloft, and how do they impact ground-level ozone concentrations?
P. What is the prevalence and spatial extent of the ozone weekend effect? What are the contributing factors?
Q. How do the different aerosol compositions in different areas influence radiative balances?

Atmospheric Transport

R. Is there evidence of pollutant transport between air basins or states?
S. Is there evidence of pollutant recirculation, particularly in the South Coast Air Basin (SoCAB)?
T. Is there evidence of long-range transport during CalNex? What were the relative contributions of the various sources outside the control of emissions within California (i.e., policy-relevant background ozone)?

CalNex 2010 Science Questions (cont.)

Modeling

U. How well did the meteorological and air quality forecast models perform during CalNex? What weaknesses need attention?

Climate and Air Quality Nexus

V. What pollution control efforts are likely to result in "win-win" or "win-lose" situations?

W. Could the same pollutant control efforts in different air basins (i.e., SJVAB and SoCAB) have different results with respect to changes in air quality and climate (i.e., move toward different nexus quadrants in the figure on the front page of this report)?

The CalNex fieldwork was conducted during May through July of 2010; hence, the results can only address aspects of atmospheric issues affecting California's air quality and climate change concerns that are relevant to that season, and cannot address some others. Specifically, no data were collected in the cooler winter season when maximum particulate matter (PM) concentrations are usually observed.

CalNex 2010 represents a collaborative, multiagency, intensive effort. Partners in the study included the local air quality districts, universities (both in California and other states), Department of Energy, National Aeronautics and Space Administration (NASA), National Science Foundation, U.S. Environmental Protection Agency, and the Mexican air quality community. The field measurements were executed by a large number of scientists from the study partners. Individual scientists from these institutions have formulated and conducted the analyses that they excitedly believe will reinforce foundational air quality and climate change principles and definitively address outstanding issues and uncertainties. For the most part, these research scientists have and will continue to present their analyses and findings in scientific presentations and publications, and generally all will submit final reports to their respective funding agencies. The Contributors Section contains a more complete listing of the institutions that participated in CalNex.

References

Bao, J. W., S. A. Michelson, P. O. G. Persson, I. V. Djalalova, and J. M. Wilczak (2008), Observed and WRF-simulated low-level winds in a high-ozone episode during the Central California Ozone Study, *Journal of Applied Meteorology and Climatology*, *47*(9), 2372-2394.

Bei, N., et al. (2012), Meteorological overview and plume transport patterns during Cal-Mex 2010, Atmospheric Environment, doi:10.1016/j.atmosenv.2012.01.065.

Bishop, G. A., and D. H. Stedman (2008), A decade of on-road emissions measurements, *Environmental Science & Technology*, *42*(5), 1651-1656, doi:10.1021/es702413b.

Blanchard, C. L., and S. J. Tanenbaum (2003), Differences between weekday and weekend air pollutant levels in southern California, *Journal of the Air and Waste Management Association*, *53*(7), 816-828.

Boucouvala, D., and R. Bornstein (2003), Analysis of transport patterns during an SCOS97-NARSTO episode, *Atmospheric Environment*, *37*(Supplement no. 2), S73-S94, doi:10.1016/S1352-2310(03)00383-2.

Cass, G. R., and F. H. Shair (1984), Sulfate accumulation in a sea breeze/land breeze circulation system, *Journal of Geophysical Research*, *89*, 1429-1438.

Chow, J. C., L. W. A. Chen, J. G. Watson, D. H. Lowenthal, K. A. Magliano, K. Turkiewicz, and D. E. Lehrman (2006), $PM_{2.5}$ chemical composition and spatiotemporal variability during the California Regional PM_{10}/$PM_{2.5}$ Air Quality Study (CRPAQS), *Journal of Geophysical Research*, *111*(D10S04), doi:10.1029/2005JD006457.

Docherty, K. S., et al. (2011), The 2005 Study of Organic Aerosols at Riverside (SOAR-1): instrumental intercomparisons and fine particle composition, *Atmospheric Chemistry and Physics*, *11*, 12387-12420, doi:10.5194/acp-11-12387-2011.

EPA, U.S. (2007), Inventory of U.S. greenhouse gas emissions and sinks: 1900–2005, *Rep. EPA-430-R-07-002*, Washington, D.C.

Finlayson-Pitts, B. J. (2003), The tropospheric chemistry of sea salt: a molecular-level view of the chemistry of NaCl and NaBr, *Chemical Reviews*, *103*, 4801-4822.

Harley, R. A., L. C. Marr, J. K. Lehner, and S. N. Giddings (2005), Changes in motor vehicle emissions on diurnal to decadal time scales and effects on atmospheric composition, *Environmental Science & Technology*, *39*(14), 5356-5362, doi:10.1021/es048172+.

Hering, S. V., and D. L. Blumenthal (1989), Southern California Air Quality Study (SCAQS) description of measurement activities, final report to California Air Resources Board, contract no. A5-157-32.

Hersey, S. P., J. S. Craven, K. A. Schilling, A. R. Metcalf, A. Sorooshian, M. N. Chan, R. C. Flagan, and J. H. Seinfeld (2011), The Pasadena Aerosol Characterization Observatory (PACO): chemical and physical analysis of the Western Los Angeles Basin aerosol, *Atmospheric Chemistry and Physics*, *11*, 7417-7443, doi:10.5194/acp-11-7417-2011.

Jacob, D. J., et al. (2010), The Arctic Research of the Composition of the Troposphere from Aircraft and Satellites (ARCTAS) mission: design, execution, and first results, *Atmospheric Chemistry and Physics*, *10*, 5191–5212, doi:10.5194/acp-10-5191-2010.

Knipping, E., and D. Dabdub (2003), Impact of chlorine emissions from sea-salt aerosol on coastal urban ozone, *Environmental Sciene & Technology*, *37*(2), 275-284, doi:10.1021/es025793z.

Langford, A. O., C. J. Senff, R. J. I. Alvarez, R. M. Banta, and R. M. Hardesty (2010), Long-range transport of ozone from the Los Angeles Basin: a case study, *Geophysical Research Letters*, *37*(L06807), doi:10.1029/2010GL042507.

Liang, J., B. Jackson, and A. Kaduwela (2006), Evaluation of the ability of indicator species ratios to determine the sensitivity of ozone to reductions in emissions of volatile organic compounds and oxides of nitrogen in northern California, *Atmospheric Environment*, *40*, 5156–5166, doi:10.1016/j.atmosenv.2006.03.060.

Lu, R., and R. P. Turco (1996), Ozone distributions over the Los Angeles Basin: Three-dimensional simulations with the SMOG model, *Atmospheric Environment*, *30*, 4155-4176.

Marr, L. C., and R. A. Harley (2002), Modeling the effect of weekday-weekend differences in motor vehicle emissions on photochemical air pollution in central California, *Environmental Science & Technology*, *36*(19), 4099-4106, doi:10.1021/es020629x.

Parrish, D. D., Y. Kondo, O. R. Cooper, C. A. Brock, D. A. Jaffe, M. Trainer, T. Ogawa, G. Hübler, and F. C. Fehsenfeld (2004), Intercontinental Transport and Chemical Transformation 2002 (ITCT 2K2) and Pacific Exploration of Asian Continental Emission (PEACE) experiments: An overview of the 2002 winter and spring intensives, *Journal of Geophysical Research*, 109,D23S01,doi:10.1029/2004JD004980

Qin, X., and K. A. Prather (2006), Impact of biomass emissions on particle chemistry during the California Regional Particulate Air Quality Study, *International Journal of Mass Spectrometry*, *258*, 142–150, doi:10.1016/j.ijms.2006.09.004.

Rinehart, L. R., E. M. Fujita, J. C. Chow, K. Magliano, and B. Zeilinska (2006), Spatial distribution of $PM_{2.5}$ associated organic compounds in central California, *Atmospheric Environment*, *40*, 290–303, doi:10.1016/j.atmosenv.2005.09.035.

Rosenthal, J. S., R. A. Helvey, T. E. Battalino, C. Fisk, and P. W. Greiman (2003), Ozone transport by mesoscale and diurnal wind circulations across southern California, *Atmospheric Environment*, *37*(Supplement no. 2), S51-S71.

Ryerson, T.B., et al. (2013), The 2010 California Research at the Nexus of Air Quality and Climate Change (CalNex) field study. *J. Geophys. Res.-Atmos., 118*, 5830-5866, doi:10.1002/jgrd.50331.

Schauer, J. J., W. G. Rogge, L. M. Hildemann, M. A. Mazurek, and G. R. Cass (1996), Source apportionment of airborne particulate matter using organic compounds as tracers, *Atmospheric Environment*, *30*, 3837-3855.

Shair, F. H., et al. (1982), Transport and dispersion of airborne pollutants associated with the land breeze-sea breeze system, *Atmospheric Environment*, *16*, 2043-2053.

Skamarock, W. C., R. Rotunno, and J. B. Klemp (2002), Catalina eddies and coastally trapped disturbances, *Journal of Atmospheric Sciences*, *59*, 2270-2278.

Takahama, S., S. Liu, and L. M. Russell (2010), Coatings and clusters of carboxylic acids in carbon-containing atmospheric particles from spectromicroscopy and their implications for cloud-nucleating and optical properties, *Journal of Geophysical Research*, *115*(D01202), doi:10.1029/2009JD012622.

Tonse, S. R., N. J. Brown, R. A. Harley, and L. Jin (2008), A process–analysis based study of the ozone weekend effect, *Atmospheric Environment*, *42*, 7728–7736, doi:10.1016/j.atmosenv.2008.05.061.

Turpin, B. J., and J. J. Huntzicker (1995), Identification of secondary organic aerosol episodes and quantitation of primary and secondary organic aerosol concentrations during SCAQS, *Atmospheric Environment*, *29*(23), 3527-3544.

Wakimoto, R. M., and J. L. McElroy (1986), Lidar observation of elevated pollution layers in Los Angeles, *Journal of Climate and Applied Meteorology*, *25*, 1583–1599.

Zaveri, R. A., et al. (2012), Overview of the 2010 Carbonaceous Aerosols and Radiative Effects Study (CARES), *Atmospheric Chemistry and Physics*, *12*, 7647-7687, doi:10.5194/acp-12-7647-2012.

Glossary of Terms, Symbols and Acronyms

^{14}C	carbon 14 isotope
8-h	8-hour
AB32	Assembly Bill 32: Global Warming Solutions Act
AGL	above ground level
AIM/IC	ambient ion monitor/ion chromatograph
AIRNow	web site providing public access to national air quality information
AGU	American Geophysical Union
AM3	Atmospheric model developed by NOAA GFDL
AMS	aerosol mass spectrometer
amu	atomic mass unit
APN	acyl peroxy nitrates
ARB	Air Resources Board
ARCTAS	Arctic Research of the Composition of the Troposphere from Aircraft and Satellites
ASL	above sea level
BAMS	Baron Advanced Meteorological Services
BC	black carbon
BEARPEX	Biosphere Effects on AeRosols and Photochemistry EXperiment
Bight	The Southern California Bight includes the Channel Islands and that part of the Pacific Ocean bounded by the curved coastline of Southern California from Point Conception to San Diego.
BVOC	biogenic volatile organic compound
Cal-Mex	2010 US-Mexico collaborative field study of air quality and climate change in the California-Mexico border that was loosely coordinated with CalNex
CalNex	California Research at the Nexus of Air Quality and Climate Change
CalNex-LA	CalNex super monitoring site in the Los Angeles basin (Pasadena)
CalNex-SJV	CalNex super monitoring site in the San Joaquin Valley (Bakersfield)
CARB	California Air Resources Board
carbonyl	a functional group composed of a carbon atom double-bonded to an oxygen
CARES	Carbonaceous Aerosol and Radiative Effects Study
CBL	convective boundary layer
CCN	cloud condensation nuclei
CFC(s)	chlorofluorocarbon(s)
Cl^-	chloride ion
Cl_2	molecular chlorine
$ClNO_2$	nitryl chloride
CIOA	cooking-influenced organic aerosol
CIMS	chemical ionization mass spectrometer
CIRPAS	the Center for Interdisciplinary Remotely-Piloted Aircraft Studies
CMAQ	Community Multi-scale Air Quality model
CMB	chemical mass balance
CO	carbon monoxide
CO_2	carbon dioxide
COAMPS	Coupled Ocean–Atmosphere Mesoscale Prediction System
DMS	dimethyl sulfide, a reduced sulfur species released by natural sources
DOAS	differential optical absorption spectroscopy

EC	elemental carbon
ECMWF	European Centre for Medium-Range Weather Forecasts
EDGAR	Emission Database for Global Atmospheric Research
EMFAC	Emission model used in California to estimate vehicle emissions
EPA	U.S. Environmental Protection Agency
ER	enhancement ratio or emission ratio
FLEXPART	Lagrangian particle dispersion model for describing atmospheric transport
FTS	Fourier transform spectrometer
GC/MS-FID	Gas Chromatography/Mass Spectrometry-Flame Ionization Detector
GEM	gaseous elemental mercury
GEOS-Chem	a global 3-D model of atmospheric composition
GFDL	NOAA's Geophysical Fluid Dynamics Laboratory
GHG	greenhouse gas
GOCART	the Goddard Chemistry Aerosol Radiation and Transport model
GOME	Global Ozone Monitoring Experiment - a satellite borne instrument
GWP	global warming potential (usually based on 100 year period)
H_2O	water vapor
H_2O_2	hydrogen peroxide
HCFC(s)	hydrochlorofluorocarbon(s)
HCN	hydrogen cyanide
HFCs	hydrofluorocarbon(s)
HNO_3	nitric acid
HO_2	hydroperoxy radical
HOA	hydrogen-like organic aerosol
HONO	nitrous acid
HO_X	$OH + HO_2$
hPa	atmospheric pressure unit - one standard atmosphere equals 1013.25 hPa
IC	ion chromatography
IMPROVE	Interagency Monitoring of Protected Visual Environments
IONS-2010	Intercontinental Chemical Transport Experiment Ozonesonde Network Study - 2010
IPCC	Inter-governmental Panel on Climate Change
km	kilometer
LAT	latitude
LAX	Los Angeles International Airport
LOA	local organic aerosol
LV-OOA	low-volatility OOA
MDA8	daily maximum 8-hour average
MODIS	Moderate Resolution Imaging Spectroradiometer
molec. cm^{-3}	molecules per cubic centimeter
MOZAIC	Measurements of OZone, water vapor, carbon monoxide and nitrogen oxides by in-service AIrbus airCraft)
MOZART-4	global Model for Ozone and Related Chemical Tracers-4
MPAN	methyl peroxy acetyl nitrate
MSD	mass selective detector
N_2O	nitrous oxide
N_2O_5	dinitrogen pentoxide
NAAQS	national ambient air quality standard

NEI	National Emission Inventory
NH_3	ammonia gas
NH_4^+	ammonium ion (also NH_4)
NH_4NO_3	particulate ammonium nitrate
nm	nanometer
NO	nitric oxide
NO_2	nitrogen dioxide
NO_3	nitrate radical
NO_3^-	nitrate ion (also NO_3, depending on context to differentiate from radical)
NOAA	National Oceanic and Atmospheric Administration
NOAA/ESRL	NOAA/Earth System Research Laboratory
NOAA/ESRL/CSD	NOAA/ESRL/Chemical Sciences Division
NOAA/ESRL/GSD	NOAA/ESRL/Global Systems Division
NOAA/NCEP	NOAA/National Centers for Environmental Prediction
NO_X	oxides of nitrogen, NO + NO_2
NO_Y	total reactive oxidized nitrogen, i.e., NO + NO_2 + HONO + HNO_3 + N_2O_5 + …
NR-PM1	non-refractive particulate matter smaller than 1 micron in aerodynamic diameter
N_{TOT}	total particle density (units generally part. cm^{-3})
$O(^1D)$	an excited state of atomic oxygen (free radical)
O_3	ozone
O_X	total oxidant (often estimated as O_3 + NO_2)
OA	organic aerosol
OH	hydroxyl radical
OMI	Ozone Monitoring Instrument - a satellite borne instrument
OOA	oxygenated organic aerosol
P-3	(aka WP-3, or WP-3D) – Lockheed WP-3D Orion Aircraft operated by NOAA
PACO	Pasadena Aerosol Characterization Observatory
PAN	peroxy acetylnitrate
PBL	planetary boundary layer
PDT	Pacific Daylight Time
PFA	Perfluoroalkoxy
PHO_X	HOx Production Rate
PM	particulate matter
PM1	particulate matter smaller than 1 micron in aerodynamic diameter
PM2.5	particulate matter less than 2.5 microns aerodynamic diameter
PO_3	Ozone Production Rate
POA	primary (directly emitted) organic aerosol
POM	particulate organic matter
ppbv	parts-per-billion by volume - mixing ratio unit based on mole ratio
ppmv	parts-per-million by volume - mixing ratio unit based on mole ratio
PPN	peroxy propionyl nitrate
PRB	policy-relevant background
PST	Pacific Standard Time
RACM	Regional Atmospheric Chemistry Mechanism Version 2
RAQMS	Regional Air Quality Modeling System
$RONO_2$	alkyl nitrate
R/V	research vessel

s	second
SCAQS	Southern California Air Quality Study
SCIAMACHY	Scanning Imaging Absorption Spectrometer for Atmospheric Cartography- a satellite borne instrument
SFBA	San Francisco Bay Area
SIP	State Implementation Plan
SJV(AB)	San Joaquin Valley (Air Basin)
SO_2	sulfur dioxide
$SO_4^=$	sulfate ion (also, SO_4)
SO_X	total oxidized sulfur, $SO_2 + SO_4^=$
SOA	secondary (formed in the atmosphere, not directly emitted) organic aerosol
SoCAB	South Coast Air Basin
SST	sea surface temperature
STP	standard temperature and pressure
STT	stratosphere to troposphere
SULEV	super ultra-low emitting vehicle
SV-OOA	semi-volatile OOA
TD-CIMS	Thermal Dissociation Chemical Ionization Mass Spectrometer
TD-LIF	Thermal Dissociation Laser Induced Fluorescence
TES	EOS Aura Tropospheric Emissions Spectrometer (satellite borne instrument)
Twin Otter	Aircraft operated during CalNex by CIRPAS and NOAA
$\mu g\ m^{-3}$	micrograms per cubic meter
UT/LS	upper troposphere/lower stratosphere
VOC(s)	volatile organic compound
VOCR	volatile organic compound reactivity with OH
VSR	vessel speed reduction
W/m^2	watts per square meter
WD	weekday
WE	weekend
WP-3D	Lockheed WP-3D Orion Aircraft operated by NOAA
WRF	Weather Research and Forecasting
WSOC	water-soluble organic carbon

Summary of Platforms and Sites deployed for CalNex

For the fieldwork portion of CalNex, four instrumented aircraft and a research vessel were deployed, two major research sites in Pasadena and Bakersfield were established, networks of ozonesondes and radar wind profilers were operated, and the measurement program at Mt. Wilson was enhanced. Data from existing networks of air quality and meteorological measurements and satellite observations were incorporated into the analysis. Figure 2 summarizes the operation periods of the platforms and sites specifically deployed for CalNex. Appendix A gives details of these resources, including measurements made at each site and platform. Figures showing flight and ship tracks for the mobile platforms are included. Contact information and details for accessing data archives are also included.

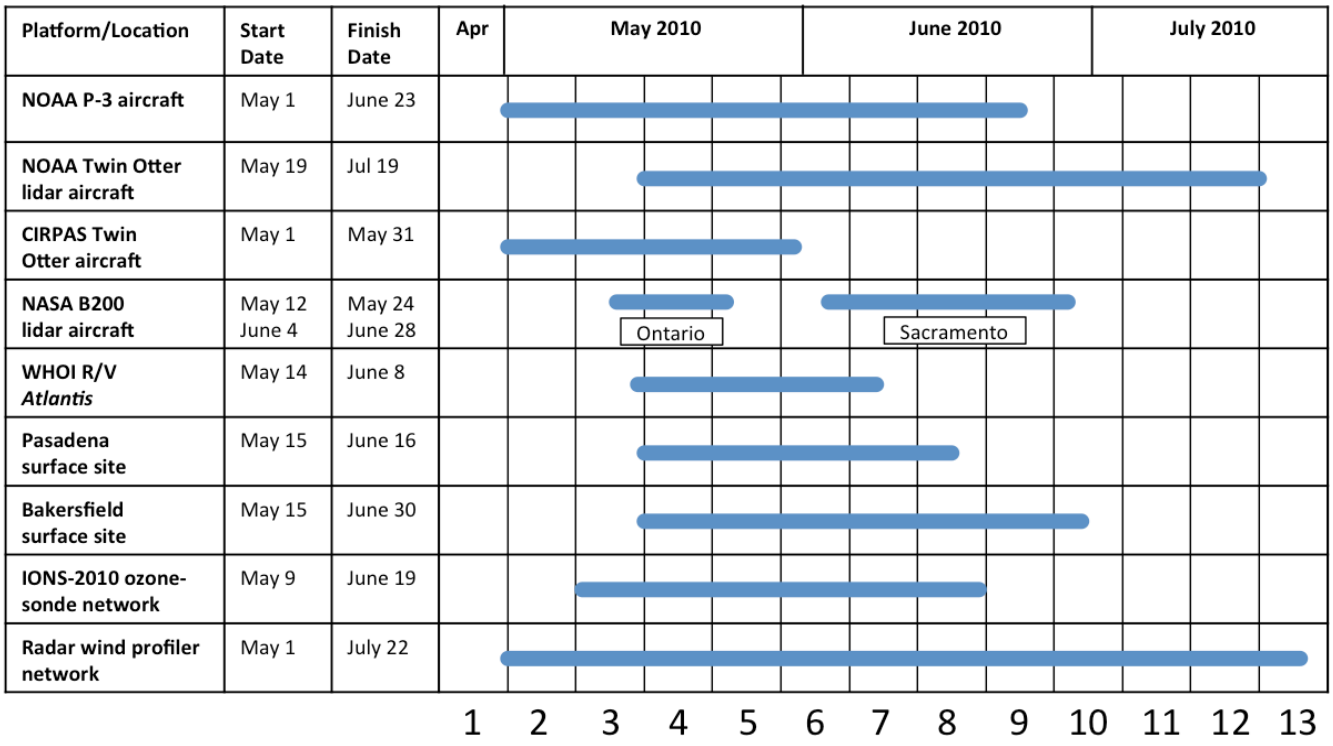

Figure 2. Operations schedule of CalNex 2010 mobile platforms, ground sites and instrument networks

Synthesis of Results - Meteorology and Atmospheric Climatology

Response to Question A

QUESTION A

How did the meteorology during CalNex compare to historical norms?

FINDING

***Finding A1*: May 2010 was cooler and wetter than normal, followed by more seasonal warm temperatures in June. In May deep upper level troughs moved into California bringing stratospheric intrusions that affected ozone concentrations in the State.**

Analysis: This material is taken from Ryerson et al. (2013)

Local land-sea breeze and mountain-valley circulations drive much of the pollutant transport in California [*Bao et al.*, 2008; *Langford et al.*, 2010; *Lu and Turco*, 1996]; however, synoptic-scale meteorology significantly influences both transport patterns and photochemical processing. Here we provide an overview of the climate and synoptic weather patterns during CalNex. *Fast et al.* [2012] provide an overview of the meteorology and transport during June 2010 when the Carbonaceous Aerosol and Radiative Effects Study (CARES) was conducted with an emphasis on the Sacramento Valley.

Spring 2010 was cooler and wetter than normal over most of California with frequent cold fronts and upper air disturbances. Fog was present frequently in the coastal areas and western Los Angeles basin and the monthly average temperature for the State during May was 2.3 °C below the long-term average of 13.0 °C (Figure A1; http://www.wrcc.dri.edu/monitor/cal-mon/). There were 62 new record low minimum temperatures and five record high maximum temperatures set in California during the month. These conditions followed the weakening El Niño, which dissipated during May as positive sea surface temperature (SST) anomalies decreased across the equatorial Pacific Ocean and negative SST anomalies emerged across the eastern half of the Pacific (http://www.cpc.ncep.noaa.gov).

The synoptic meteorology in May was dominated by a series of deep upper level troughs that moved off the Pacific Ocean into California on the 9th, 17th, 22nd, and 27th. Cold fronts associated with these systems brought low temperatures, high winds, and precipitation to many parts of the State. The first system brought up to 20 cm of snow to the central Sierra Nevada between Yosemite and Sequoia National Parks. Bishop, CA tied the all–time May low temperature of –4 °C on 11 May. The second system brought cold and rain to much of the San Joaquin Valley, with another 8-15 cm of snow to the Sierras. The third system brought more rain to the southern San Joaquin Valley, and led to record low temperatures at 22 locations across the State from Redding to Riverside on 23 May; Bishop tied the all–time May record low of –4 °C once again on that day, and the record lows were tied in both San Francisco and Sacramento. Storms associated with the 27-29 May trough brought more snow and thunderstorms to the southern Sierra Nevada and wind gusts in excess of 50 mph to the Tehachapi Mountains. Deep stratospheric intrusions associated with all four of these troughs were detected by IONS-2010 ozonesondes [*Cooper et al.*, 2011], and the NOAA WP-3D and Twin Otter aircraft [*Langford et al.*, 2012; *Lin et al.,* 2012].

Conditions became more seasonal in early June, which was slightly drier than average for most of California; the monthly mean temperature was 19.3 °C, only 0.1 °C higher than the long-term average. The weather patterns during the first week of June were dominated by the presence of a low-pressure system over the Gulf of Alaska and an upper-level high-pressure ridge over the southern half of the State. A weak upper level trough over northern California brought record precipitation to Crescent City on both 1 and 2 June (6 cm and 5 cm of rain, respectively) and slightly cooler temperatures to Sacramento and Bakersfield. The warm temperatures and subsiding air associated with the ridge led to the first prolonged ozone episode of the year in the Los Angeles basin, and the highest 8-h ozone concentrations measured in the State during 2010, 123 ppbv at Crestline on 5 June. Temperatures warmed to 27 °C (low 80s in °F) in downtown Los Angeles by 5 and 6 June, exceeding 36 °C (high 90s in °F) the central and southern San Joaquin Valley. Warming in the southern Sierras initiated rapid melting of the snowpack and afternoon cumulus formation in the San Joaquin Valley. A series of upper level lows in the Pacific Northwest kept the ridge from growing northward and produced strong winds over much of the State.

Temperatures fell over the southern half of the State as another upper-level trough moved into California off the Pacific on 9 June. This system developed into a cutoff low and spawned another tropopause fold with possible influence on surface ozone in southern California on 12 June [*Lin et al.,* 2012]. Cooler than normal temperatures persisted through 11 June with light rain over the southern Sierra Nevada and persistent high winds in the Tehachapi Mountains and west side of the San Joaquin Valley. Temperatures rose as high pressure followed the trough with near normal temperatures on 12 June; the first 37.8 °C (100 °F) day in Fresno occurred on 14 June, one week later than normal. However, two more upper level troughs on 15-17 and 21-23 June moderated the surface temperatures in the Central Valley through the third week of June, disrupting the local mountain-valley circulation patterns. The final trough brought a few showers to the central San Joaquin Valley and Southern Sierra Nevada during the morning of 25 June. A high-pressure ridge built up into California on 26 June as the trough passed through, with 38.3 °C observed in both Bakersfield and Fresno on 27 June, with Fresno tying the record high of 42.2 °C (108 °F) for the date on 28 June.

Most of the CalNex field operations had ceased by the end of June, but following its redeployment for a series of flights in the Sacramento and San Joaquin Valleys the NOAA Twin Otter returned to southern California from 30 June through 18 July. Although the July monthly mean temperature for the State was slightly above average, southern California remained cooler than average with frequent coastal fog that persisted into the afternoon. Temperatures were particularly low near the coast and Los Angeles Airport reached monthly record low maximum temperatures twice, with readings of 19 °C on 6 July followed by 18 °C on 8 July. The first six days of July 2010 were cooler than the first six days of January 2010 for Downtown Los Angeles, Los Angeles Airport, Long Beach Airport, Santa Barbara Airport, and Oxnard. San Diego also tied its lowest maximum temperature for July on the 8th with a reading of 64°F. This broke the daily record low maximum temperature of 65°F set in 1902. Temperatures along the coast increased on 13 July and remained several degrees above normal through 18 July.

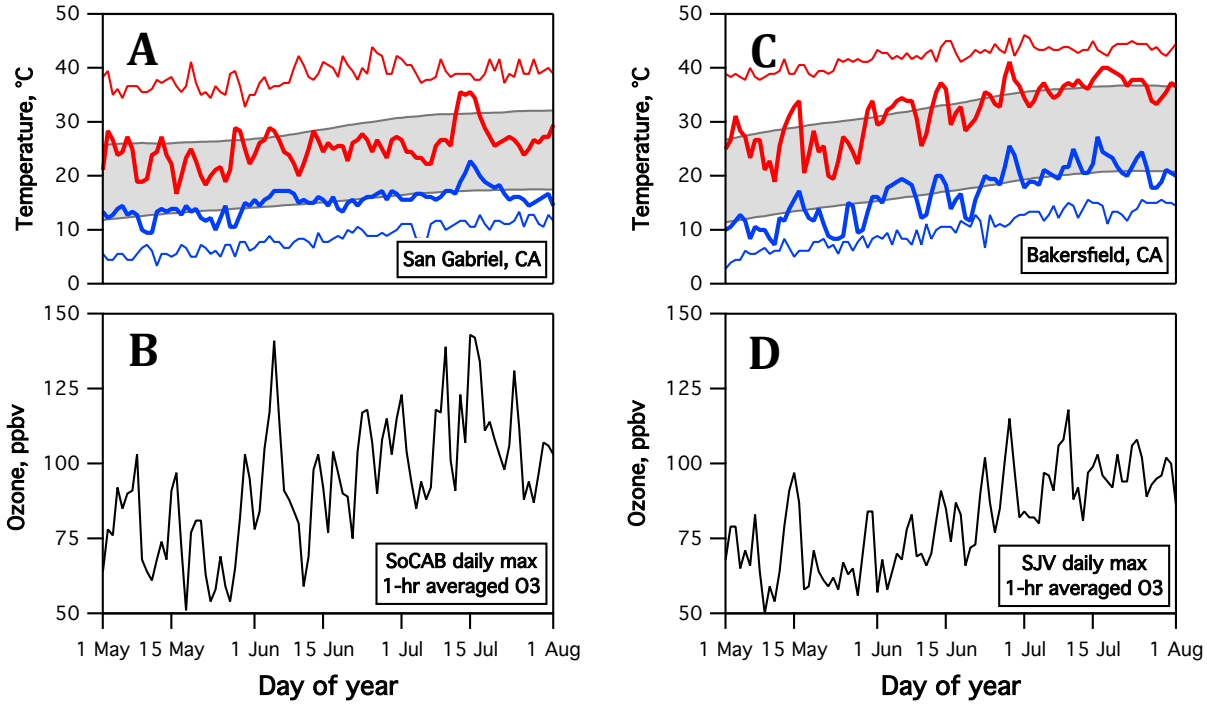

Figure A1. A) 2010 daily maximum (thick red line) and daily minimum (thick blue line) temperature data from a weather station near the CalNex ground site in Pasadena. Also shown are the record daily maximum (thin red line), record daily minimum (thin blue line) and average daily maximum and minimum (upper and lower bounds of grey shading) temperatures for 1979-2010. B) Daily 1-hour averaged ozone maxima in the air basin containing the Pasadena ground site, obtained from www.arb.ca.gov/aqmis2/aqdselect.php. C) As in A) using data from a weather station near the CalNex ground site in Bakersfield. D) As in B) using ozone data in the air basin containing the Bakersfield ground site.

References

Bao, J. W., S. A. Michelson, P. O. G. Persson, I. V. Djalalova, and J. M. Wilczak (2008), Observed and WRF-simulated low-level winds in a high-ozone episode during the Central California Ozone Study, *J. Appl. Meteorol. Climatol., 47*(9), 2372–2394.

Cooper, O. R., et al. (2011), Measurement of western U.S. baseline ozone from the surface to the tropopause and assessment of downwind impact regions, *J. Geophys. Res., 116*(D00V03), doi:10.1029/2011JD016095.

Fast, J. D., et al. (2012), Transport and mixing patterns over Central California during the carbonaceous aerosol and radiative effects study (CARES), *Atmos. Chem. Phys., 12*, 1759–1783, doi:10.5194/acp-12-1759-2012.

Langford, A. O., C. J. Senff, R. J. I. Alvarez, R. M. Banta, and R. M. Hardesty (2010), Long-range transport of ozone from the Los Angeles Basin: A case study, *Geophys. Res. Lett., 37*(L06807), doi:10.1029/2010GL042507.

Langford, A. O., J. Brioude, O. R. Cooper, C. J. Senff, R. J. Alvarez II, R. M. Hardesty, B. J. Johnson, and S. J. Oltmans (2012), Stratospheric influence on surface ozone in the Los Angeles area during late spring and early summer of 2010, *J. Geophys. Res., 117*(D00V06), doi:10.1029/ 2011JD016766.

Lin, M., A. M. Fiore, O. R. Cooper, L. W. Horowitz, A. O. Langford, H. Levy II, B. J. Johnson, B. Naik, S. J. Oltmans, and C. J. Senff (2012), Springtime high surface ozone events over the western United States: Quantifying the role of stratospheric intrusions, *J. Geophys. Res., 117* (D00V22), doi:10.1029/2012JD018151.

Lu, R., and R. P. Turco (1996), Ozone distributions over the Los Angeles Basin: Three-dimensional simulations with the SMOG model, *Atmos. Environ., 30*, 4155–4176.

Ryerson, T. B., et al. (2013), The 2010 California Research at the Nexus of Air Quality and Climate Change (CalNex) field study, *J. Geophys. Res. Atmos., 118*, 5830–5866, doi:10.1002/jgrd.50331.

Synthesis of Results - Meteorology and Atmospheric Climatology

Response to Question B

QUESTION B

How did the CalNex air quality measurements fit in the context of historical measurements?

BACKGROUND

Substantial efforts have been made to improve air quality throughout the U.S. and in California in particular. Ambient measurements over the past decades demonstrate that these efforts have resulted in very substantial reductions in a wide spectrum of air pollutants. This is a success that is perhaps not as widely appreciated as it should be by the general public. The CalNex field measurements provide a "snapshot" of current air quality, particularly in the South Coast Air Basin (SoCAB) and the San Joaquin Valley (SJV) that indicates continuing improvement. To provide a qualitative perspective of the dramatic progress made over the last five decades, Figure B1 shows a historical photograph that documents the visibility degradation that often occurred in the Los Angeles area; such conditions no longer occur. It is perhaps difficult to appreciate

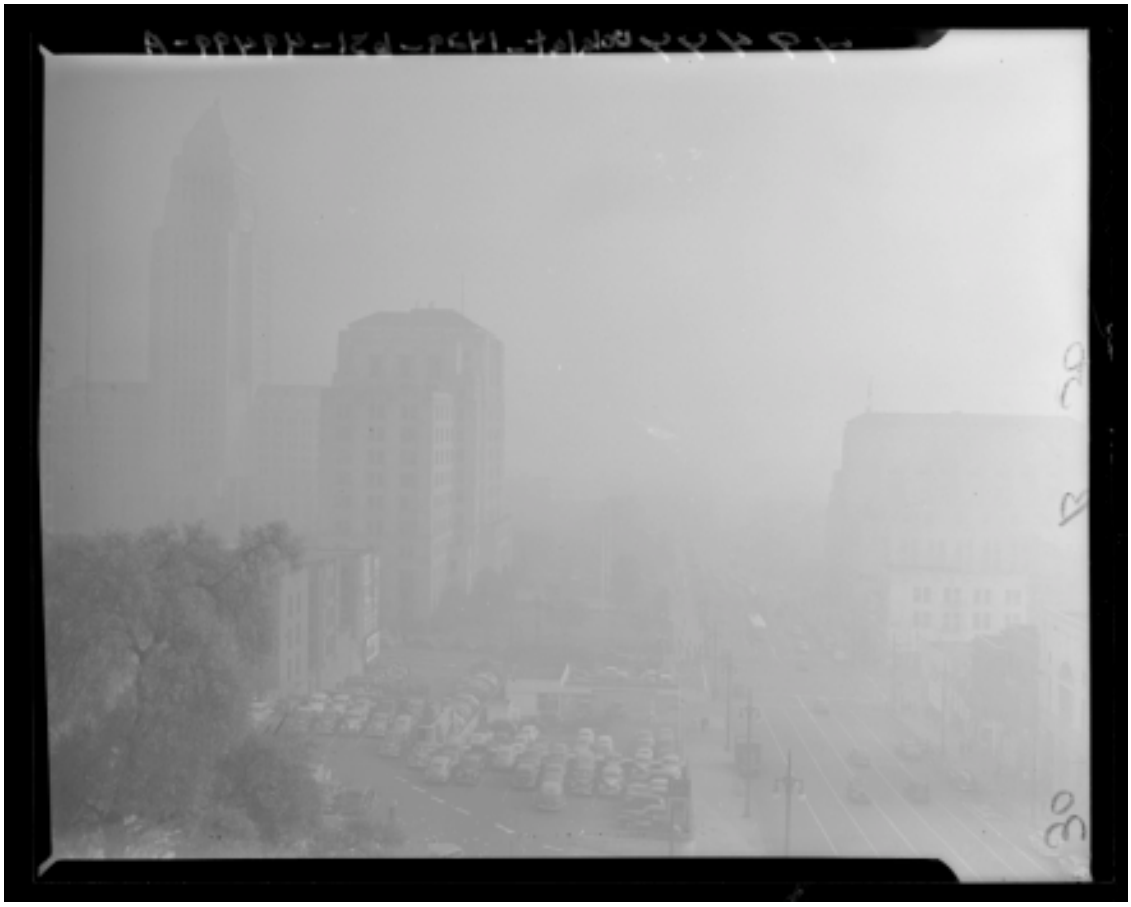

Figure B1. Photograph of the Los Angeles Civic Center area on January 5, 1948 showing a severe pollution episode. (*Photo: Los Angeles Times; Photographic Archive/UCLA*)

the improvement when it occurs over many decades. The Response to Question E quantifies the improvements in some particular air pollutants of concern.

Several CalNex analyses serve to place the CalNex datasets in a historical context, usually as the latest in a series of measurements that define the temporal evolution of air quality in California. *Warneke et al.* [2012] document that the mixing ratios of VOCs and CO have decreased in SoCAB by almost two orders of magnitude during the past five decades at an average annual rate of about 7.5% each year. This decrease has been accomplished despite approximately a factor of three increase in fuel sales during that time (see Figure G1 and associated discussion). *Pollack et al.* [2013] show that ambient concentrations of NO_X, ozone and other secondary photochemical products in SoCAB have also decreased at varying rates (see Figure E1 and associated discussion). *Pusede and Cohen* [2012] use sixteen years of observations of ozone, nitrogen oxides, and temperature at sites in SJV to show that, as emissions have decreased, photochemical O_3 production is transitioning to NO_X-limited chemistry in the southern and central parts of SJV, where O_3 violations are most frequent. *Thompson et al.* [2012] summarize optical properties measured at the Pasadena site during CalNex, and show that the 2010 aerosol optical densities were approximately five times lower than measured during the 1987 SCAQS field work [*Adams et al.,* 1990].

These results at least qualitatively demonstrate the major progress in PM control and resulting visibility improvement in the Los Angeles area in the last two decades, even though there were substantial differences between the SCAQS and the CalNex measurements. The SCAQS measurements were from a comparable season (i.e., 10 summer days during four months in 1987), but at a different site in Claremont CA. Most importantly, the sample treatment before measurement differed from that employed during CalNex [*Thompson et al.,* 2012].

FINDING

***Finding B1*: While nearly all atmospheric pollutants have decreased in California, ethanol is an exception because its use in gasoline has recently increased markedly. During CalNex ethanol was the VOC with the highest ambient concentrations in SoCAB. Acetaldehyde (an air toxic) is a secondary product of the atmospheric oxidation of ethanol, but its concentration has continued to decrease.**

The use of ethanol as a transportation fuel in the U.S. increased significantly from 2000–2009, and in 2010 nearly all gasoline contained 10% ethanol. In accordance with this increased use, atmospheric measurements of VOCs in SoCAB during CalNex were significantly enriched in ethanol compared to measurements in urban outflow in the Northeast U.S. in 2002 and 2004 [*de Gouw et al.,* 2012]. Mixing ratios of acetaldehyde, an atmospheric oxidation product of ethanol, decreased between 2002 and 2010 in Los Angeles. Previous work [e.g.*, Jacobson,* 2007] has suggested that large-scale use of ethanol may have detrimental effects on air quality. While no evidence for this has been identified in the U.S., this study indicates that ethanol has become a ubiquitous compound in urban air and that better measurements are required to monitor its increase and effects.

References

Adams, K.M., Davis, L.I., Japar, S.M., Finley, D.R. (1990), Real-time, in situ measurements of atmospheric optical absorption in the visible via photoacoustic spectroscopy - IV. Visibility degradation and aerosol optical properties in Los Angeles. *Atmos. Environ. 24A*, 605-610.

de Gouw, J. A., J. B. Gilman, A. Borbon, C. Warneke, W. C. Kuster, P. D. Goldan, J. S. Holloway, J. Peischl, and T. B. Ryerson (2012), Increasing atmospheric burden of ethanol in the United States, *Geophys. Res. Lett.*, *39*(L15803), doi:10.1029/2012GL052109.

Jacobson, M. Z. (2007), Effects of ethanol (E85) versus gasoline vehicles on cancer and mortality in the United States, *Environ. Sci. Technol., 41*, 4150–4157, doi:10.1021/es062085v.

Pollack, I. B., T. B. Ryerson, M. Trainer, J. A. Neuman, J. M. Roberts, and D. D. Parrish (2013), Trends in ozone, its precursors, and related secondary oxidation products in Los Angeles, California: A synthesis of measurements from 1960 to 2010, *J. Geophys. Res. Atmos., 118*, 5893–5911, doi:10.1002/jgrd.50472.

Pusede, S.E., and R.C. Cohen (2012), On the observed response of ozone to NO_X and VOC reactivity reductions in San Joaquin Valley California 1995–present, *Atmos. Chem. Phys., 12*, 8323–8339, www.atmos-chem-phys.net/12/8323/2012/doi:10.5194/acp-12-8323-2012

Thompson, J. E., P. L. Hayes, J. L. Jimenez, K. Adachi, X. Zhang, J. Liu, R. J. Weber, and P. R. Buseck (2012), Aerosol optical properties at Pasadena, CA during CalNex 2010, *Atmos. Environ.*, *55*, 190-200, doi:10.1016/j.atmosenv.2012.03.011.

Warneke, C., J. A. de Gouw, J. S. Holloway, J. Peischl, T. B. Ryerson, E. Atlas, D. Blake, M. Trainer, and D. D. Parrish (2012), Multi-year trends in volatile organic compounds in Los Angeles, California: five decades of improving air quality, *J. Geophys. Res.*, *117*(D00V17), doi:10.1029/2012JD017899.

Synthesis of Results - Meteorology and Atmospheric Climatology

Response to Question C

Question C

How do the CalNex air quality measurements in late spring and early summer relate to the peak ozone concentrations in summer and the peak PM2.5 concentrations in winter?

FINDINGS

***Finding C1*: The CalNex fieldwork was conducted primarily in May and June, 2010, but included some aircraft flights through mid-July. The measurements provide characterization of the photochemical environment in southern California, particularly in the SoCAB, during its most active period.**

***Finding C2*: The CalNex measurements cannot be used to characterize the peak PM2.5 concentrations observed in the Central Valley in winter. However, they do provide a guide for further studies of this important phenomenon.**

Analysis: D.D. Parrish, unpublished

In urban and rural areas of California O_3 concentrations are generally higher in summer; e.g., Figure C1 shows O_3 data from Crestline, a monitoring station in the SoCAB that often records the highest concentrations in the State, and from Arvin, a monitoring station that often records the highest concentrations in the southern SJV. On average the highest 8-h mean O_3 concentrations in the SoCAB were observed in July and August, with concentrations in June having greater variability (and a higher maximum) than in August. In the SJV, the highest O_3 is shifted to somewhat later in the year, with July, August and September exhibiting similar concentrations.

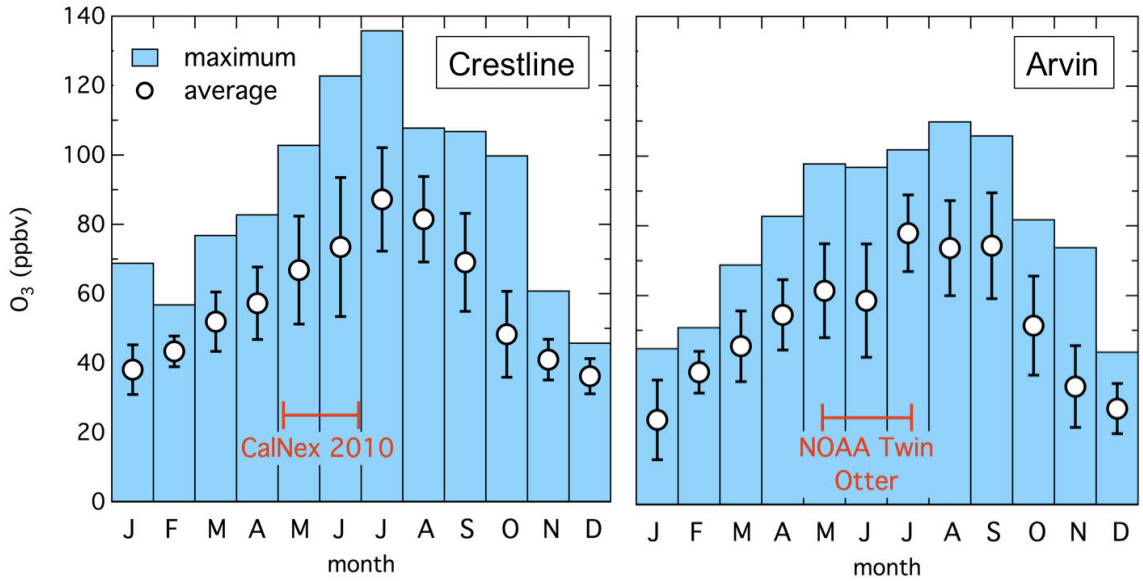

Figure C1. Monthly averages with standard deviations (symbols) and monthly maxima (bars) of daily maximum 8-hr ozone concentrations at the Crestline monitoring site in the SoCAB and the Arvin monitoring site in SJV for 2009-2011. The red bars indicate the time period of the majority of the CalNex fieldwork (left panel) and the NOAA Twin Otter deployment (right panel).

In contrast monthly mean as well as 24-hr average PM2.5 concentrations are at a maximum in winter in the Central Valley. Monthly mean PM2.5 does not vary greatly in Los Angeles, but peak 24-h PM2.5 tends to occur in the autumn and winter. Figure C2 reports PM2.5 data from urban areas in these two regions.

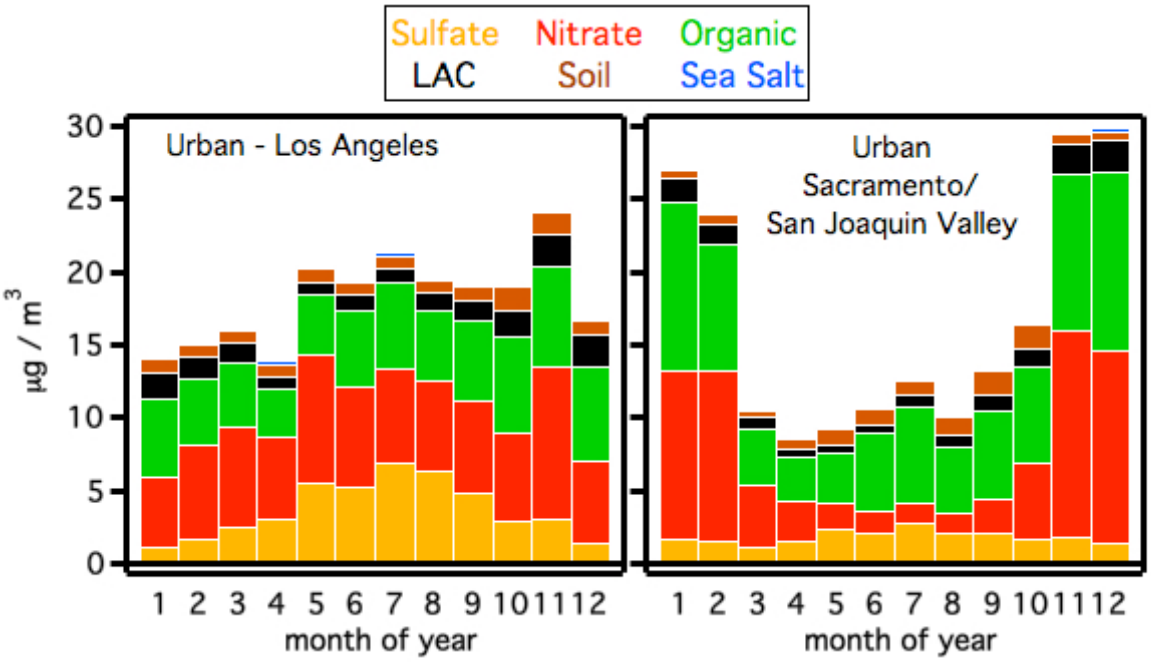

Figure C2. Comparison of monthly mean fine aerosol composition in California urban areas in 2005-2008 [*Hand et al.,* 2011]. The data are from US EPA's Speciated Trend (now Chemical Speciation) Network. "LAC" stands for light absorbing carbon.

The chosen focus of CalNex was on the photochemically active season; due to availability of platforms, most of the measurements on the airborne and ship platforms, as well as at the two major sites in Pasadena and Bakersfield were conducted in May and June, 2010, with the NOAA Twin Otter continuing operations until July 19 (see CalNex Operations Schedule on pg. 23).

Major photochemical episodes did occur during CalNex. In the SoCAB the maximum daily 8-hour O_3 average exceeded 75 ppbv on 5 of 31 days in May and 21 of 30 days in June. The highest maximum daily 8-hour O_3 concentration (123 ppbv) recorded in California during 2010 occurred at the Crestline site on June 5 (a Saturday). It is notable that at least one CalNex platform made measurements on the days when the four highest maximum daily 8-hour O_3 concentrations of 2010 occurred in the SoCAB. The Central Valley experienced lower O_3 concentrations. At the Arvin-Bear Mountain Blvd site during May and June, maximum daily 8-hour O_3 average exceeded 75 ppbv on 2 and 4 days, respectively, with a 90 ppbv maximum. The NOAA Twin Otter operated through July 19, and on 9 days in this period the Arvin site recorded maximum daily 8-hour O_3 average exceeding 75 ppbv, with a 93 ppbv maximum. The maximum 8-hour O_3 concentration in Kern County during 2010 was 107 ppbv, occurring on August 25 and September 2. The CalNex measurements do provide characterization of the photochemical environment in southern California, in the SoCAB during its most active period, but are perhaps less useful for this purpose in the San Joaquin Valley (SJV).

The late spring-early summer CalNex measurements provide characterization of PM2.5 in this season, but do not provide direct insight into the maximum PM2.5 episodes in SJV or the fall-

winter peak 24-hr PM2.5 concentrations in the SoCAB. However, the CalNex measurements do provide a guide for future research into PM2.5 maxima in both air basins. Figure C2 indicates that PM2.5 is dominated by organic matter and aerosol nitrate throughout the year in both air basins. CalNex provides a detailed characterization of these PM components during May and June. It will be useful to contrast the wintertime organic character with that measured in CalNex to determine if it is the same emissions and transformations that are responsible for this organic matter throughout the year. Aerosol nitrate is believed to be predominately ammonium nitrate (NH_4NO_3), which was characterized in SJV during CalNex (See Question I Response). The CalNex measurements demonstrate that there was a large excess of ammonia, and that NH_4NO_3 concentrations were limited by the availability of nitric acid in May and June. A similar situation is reasonably hypothesized to exist in winter, since the emissions of nitric acid precursors (i.e., NO_X) are not expected to be significantly larger, and conversion to nitric acid is not expected to be faster. Hence, the major reason for higher PM in winter is reasonably hypothesized to be less dilution due to a shallow boundary layer and slower advection in winter, which allows PM to accumulate the observed maximum concentrations. During January and February 2013 the NASA DISCOVER AQ (http://discover-aq.larc.nasa.gov/) field study was conducted in the Central Valley, and one of the goals of this study was to investigate these hypotheses.

References

Hand, J. L., S.A. Copeland, D.E. Day, A.M. Dillner, H. Indresand, W.C. Malm, C.E. McDade, C.T. Moore, M.L. Pitchford, B.A. Schichtel, and J. G. Watson (2011), Spatial and seasonal patterns and temporal variability of haze and its constituents in the United States—Report V. IMPROVE Reports. Available online: http://vista.cira.colostate.edu/improve/Publications/improve_reports.htm (accessed 02.15.13).

Synthesis of Results - Meteorology and Atmospheric Climatology

Response to Question D

QUESTION D

What were the global "background" concentrations observed during CalNex and how did they vary spatially and temporally?

BACKGROUND

The surface concentration of a pollutant at any given location can be considered, at least conceptually, to be the sum of that produced locally added to a "regional background" transported into the area. An important consideration for local O_3 and PM air quality is transport of these pollutants into a particular region from upwind regions or continents [e.g., *Dentener et al.,* 2011]. In California the transport issues for O_3 and PM are fundamentally different. The PM species of concern (see Figure C2) are emitted or produced close to source regions before being transported downwind. Long-range transport from Asia and other upwind continents is observed in the form of discrete plumes in the free troposphere with PM concentrations significantly greater than those usually encountered. These plumes often contain dust or smoke from large wild fires. Often such a plume can be directly attributed to a particular upwind source and, in favorable cases, particular plumes can be tracked in satellite data over periods of several days. The concept of a global or even regional background is not applicable to PM as many air masses arriving in California carry negligible PM concentrations. Nevertheless, plumes of transported PM can potentially affect California's air quality; for example *Jaffe et al.* [2003] report an episode when dust transported from Asia increased surface PM2.5 concentrations by up to 20 $\mu g/m^3$ over large regions of the U.S.

POLICY RELEVANCE
Emissions from within California are only partially responsible for exceedances of O_3 and PM air quality standards in the state. Transport of "background" (better referred to as "baseline") concentrations into California from over the Pacific Ocean can substantially contribute to local concentrations, even during exceedance episodes. Reliable and effective air quality modeling of O_3 and PM must accurately include the influence of baseline concentrations of PM, O_3, and its important precursors that are transported into the modeling domain.

In contrast, O_3 is a tropospheric species resulting from a complex manifold of sources and sinks. Injection from the stratosphere is a direct source. Ozone is also a secondary pollutant produced from precursor emissions such as CO, VOCs and NO_X. Production occurs not only close to source regions, but also continues during long-range transport due to photochemical production from transported precursors. Chemical and physical loss processes (dry and wet deposition, and reactions on aerosols) and mixing with air of different composition occur during transport. Air transported ashore along the California coast carries a complex mixture of ozone produced over time scales ranging from the previous few minutes to more than thirty days earlier, and from ozone precursors emitted from nearby ships or distant sources such as Asia or Europe. Thus, there are no clear source and receptor relationships. Ozone imported into California will include contributions from many anthropogenic and natural sources, importantly including the stratosphere. The spectrum of O_3 and its precursor concentrations in the air masses arriving at

California from over the Pacific generally defines the "background" concentrations that affect O_3 air quality in the State. However, this "background" is not "global" in the sense that this "background" is not uniform over the globe, and it is not a "natural background" as these concentrations have been strongly perturbed by anthropogenic influences. Here we use the term "baseline" to refer to these "background" concentrations, and take it to mean the concentrations measured in air masses transported into California that have not been influenced by local emissions or loss processes. The Responses to Questions O and T address some additional features of baseline O_3 entering California.

Recent studies have demonstrated that baseline O_3 flowing into California has been increasing since the 1980s both at the surface [*Parrish et al.,* 2009] and in the free troposphere [*Cooper et al.*, 2010], even as California's emissions of O_3 precursors have been decreasing. The increase in annual average baseline O_3 has been approximately 3 ppbv per decade from the mid-1980s (when measurements began) to the present. As a result baseline O_3 constitutes an increasing proportion of ambient concentrations when the NAAQS for O_3 is exceeded in California [*NRC*, 2009; *Dentener et al.*, 2011]. Hence, accurate treatment of lateral boundary conditions for regional air quality models, which are determined by these baseline concentrations, is increasingly important.

Ozone and PM are the two criteria pollutants whose baseline concentrations are of sufficient magnitude to have air quality significance in California. In addition, CO and peroxyacetyl nitrate (PAN) have sufficiently long lifetimes (at least in the upper troposphere for PAN) that transported concentrations can affect downwind photochemistry. CO and PAN are important because CO is an O_3 precursor and PAN is a reservoir species for NO_X, another O_3 precursor. As air warms during descent, possibly into the boundary layer of California, PAN decomposes to release NO_X, which can then enter the photochemical O_3 formation process. The variability of the baseline concentrations of these four species is great enough that the varying boundary conditions for each can significantly affect the results of regional air quality modeling. Methane is another important O_3 precursor whose transported concentrations affect photochemical O_3 formation; however the variability of its baseline concentrations is sufficiently small that boundary conditions are well represented by monthly mean concentrations measured at NOAA's baseline observatory at Trinidad Head CA; these data are available from http://www.esrl.noaa.gov/gmd/dv/data/.

Seasonally and interannually varying baseline concentrations entering California cannot be quantified based solely on the CalNex data sets. The following discussion relies upon other recent work in addition to the CalNex data.

FINDINGS

Finding D1: ***Baseline concentrations of pertinent air quality species have such large variability on time scales of days that average vertical profiles of baseline concentrations provide only poor quantification of boundary conditions for regional air quality modeling.***

Cooper et al. [2011] report the results from IONS-2010 (Intercontinental Chemical Transport Experiment Ozonesonde Network Study), the seven-site network (one in southern British Columbia and six in California) that launched near-daily ozonesondes between May 10 and June 19 during CalNex. To quantify the baseline ozone impacting California, four of the sites were positioned very close to the shore along a 960 km transect. Figure D1 shows vertical O_3 profiles

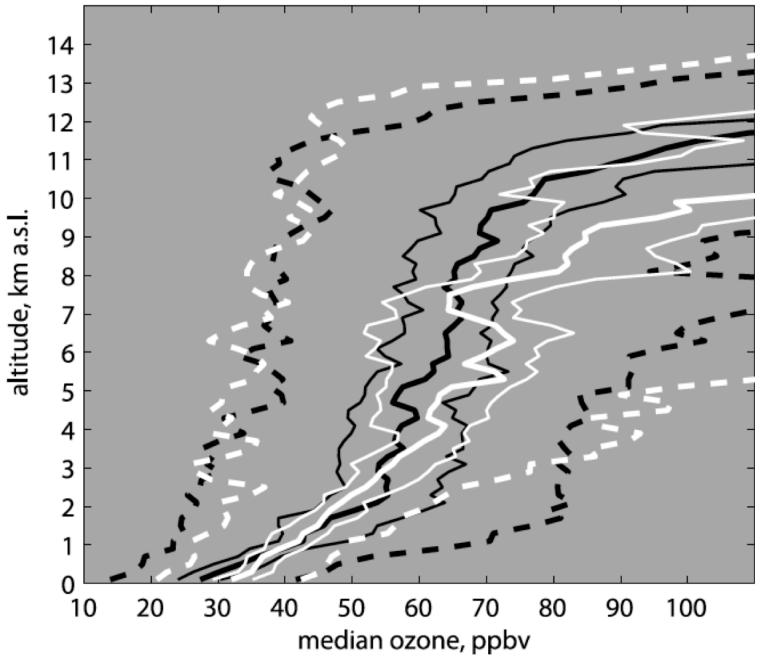

Figure D1. Ozone distributions above Trinidad Head, California for May–June 2004–2009 (black) and May–June 2010 (white) showing from left to right: 5th, 33rd, 50th, 67th and 95th ozone percentiles. (Reproduced from *Cooper et al.*, 2011).

measured at Trinidad Head CA during CalNex (white lines), and compares them with data collected during the previous years of operation (black lines). A notable feature of Figure D1 is the high variability of measured O_3 at all altitudes. For example, the 5th to 95th percentiles of the data span the range from < 20 to > 40 ppbv at the surface, and from ≈ 25 to > 80 ppbv at 2km altitude. *Parrish et al*. [2010] found that baseline O_3 transported in the lowest 2 km does impact the surface of the northern Sacramento Valley, so this variability in baseline O_3 must be incorporated into regional air quality modeling if it is to capture this important source of variability in observed surface ozone measurements.

The high variability of baseline O_3 is also reflected in the MOZAIC (Measurements of OZone, water vapor, carbon monoxide and nitrogen oxides by in service AIrbus airCraft) program [*Thouret et al.*, 2006] measurements along the U.S. west coast. Figure D2 shows cumulative probability distribution plots for O_3 and CO measurements on profiles (aircraft descents and ascents) over two airports. The variability of O_3 in Figure D2 is consistent with that shown in Figure D1. The variability of CO is lower with the 5th to 95th percentiles of the data between 2 and 10 km above Los Angeles spanning a range of approximately 55 to 135 ppbv in summer.

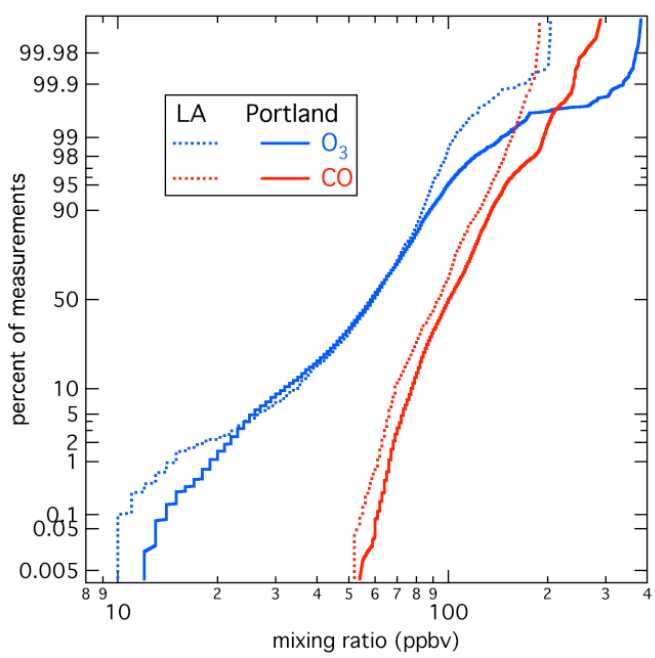

Pfister et al. [2011] combined in situ measurements collected during the June 2008 ARCTAS-CARB flights of the

Figure D2. Summertime probability distribution functions of CO (red lines) and O_3 (blue lines) measured between 2 and 10 km altitude by MOZAIC (http://mozaic.aero.obs-mip.fr) aircraft on descents into and ascents out off Portland, Oregon (PDX; solid lines) and Los Angeles, California (LAX; dotted lines) on the U.S. west coast. (Reproduced from *Dentener et al.*, 2011).

NASA DC-8 aircraft, data from the MOZAIC program and ozonesondes with satellite retrievals of carbon monoxide and ozone by the EOS Aura Tropospheric Emissions Spectrometer (TES) satellite. They report the mean and standard deviation of summertime baseline concentrations for O_3, CO and PAN synthesized from these measurements (Figure D3). These results also

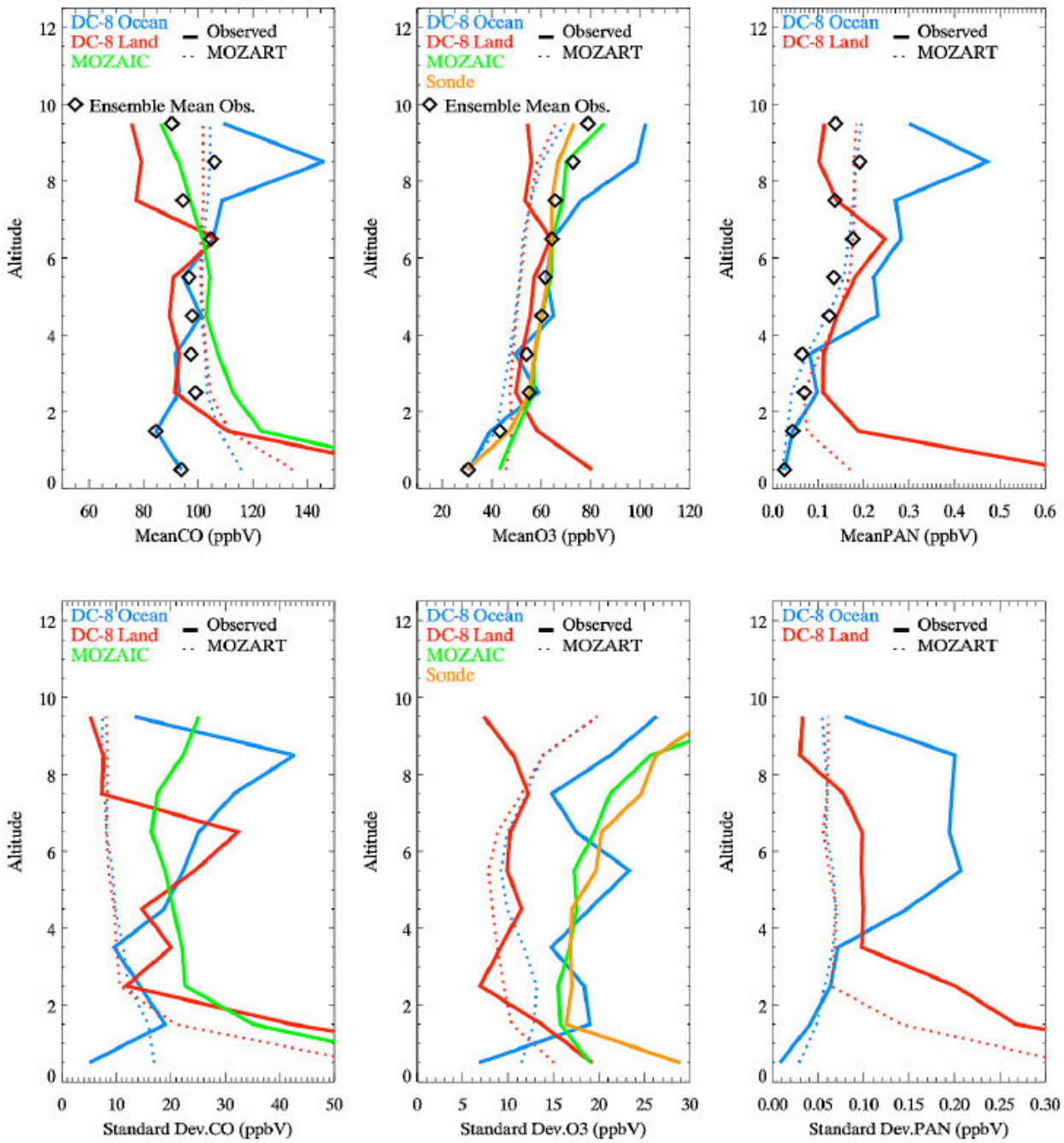

Figure D3. Mean and standard deviation of vertical profiles for CO, O_3 and PAN from four different data sets: DC8 over the ocean (blue), DC-8 over land (red), MOZAIC (green) and ozonesondes (orange). Observations are shown in thick solid lines, and model averages in dotted lines. The ensemble mean observed profile is denoted by symbols. For altitudes <2 km, the ensemble mean is derived from DC-8 over ocean and ozonesonde data only. Except for MOZAIC and sonde data, the data have been filtered to exclude California fire influence. (Reproduced from *Pfister et al.,* 2011).

indicate the large relative variability of these important gas phase species, including PAN. Included in Figure D3 are calculations of the concentrations along the NASA DC-8 aircraft flight tracks by the MOZART-4 global model, which is commonly used to provide boundary conditions for regional air quality simulations.

Finding D2: ***Along the California coast there is little indication of significant latitudinal gradient in average baseline concentrations of gas phase species important for air quality.***

The available evidence provides little indication of a significant average latitudinal gradient in baseline concentrations transported ashore along the west coast of California (coastal transect of sites indicated by line "1" in Figure D4b). The IONS-2010 measurements (Figure D4) indicate similar median ozone profiles below 4 km at the seven sites with only the inland site at Joshua Tree (JT) showing strong ozone enhancements above baseline. These enhancements are expected since the JT site receives outflow from the Los Angeles basin, and thus measurements there do not represent baseline conditions. Among the four coastal sites, there is a small latitudinal gradient of ozone below 1 km, with Point Sur (PS) and San Nicolas Island (SN) having 13% and 26% more ozone than Trinidad Head (TH), respectively (a statistically significant difference based on the total mass of ozone between 1025 and 900 hPa); Point Reyes (RY) has more ozone than TH by an insignificant 5%. The large variability in O_3 above 4 km in Figure 4 is likely due to different impacts of transport of stratospheric O_3 at the various sites. The CalNex period was a particularly active period for such stratospheric input [*Cooper et al.*, 2011]. The surface impact of these relatively high altitude O_3 enhancements is discussed in the response to Question O.

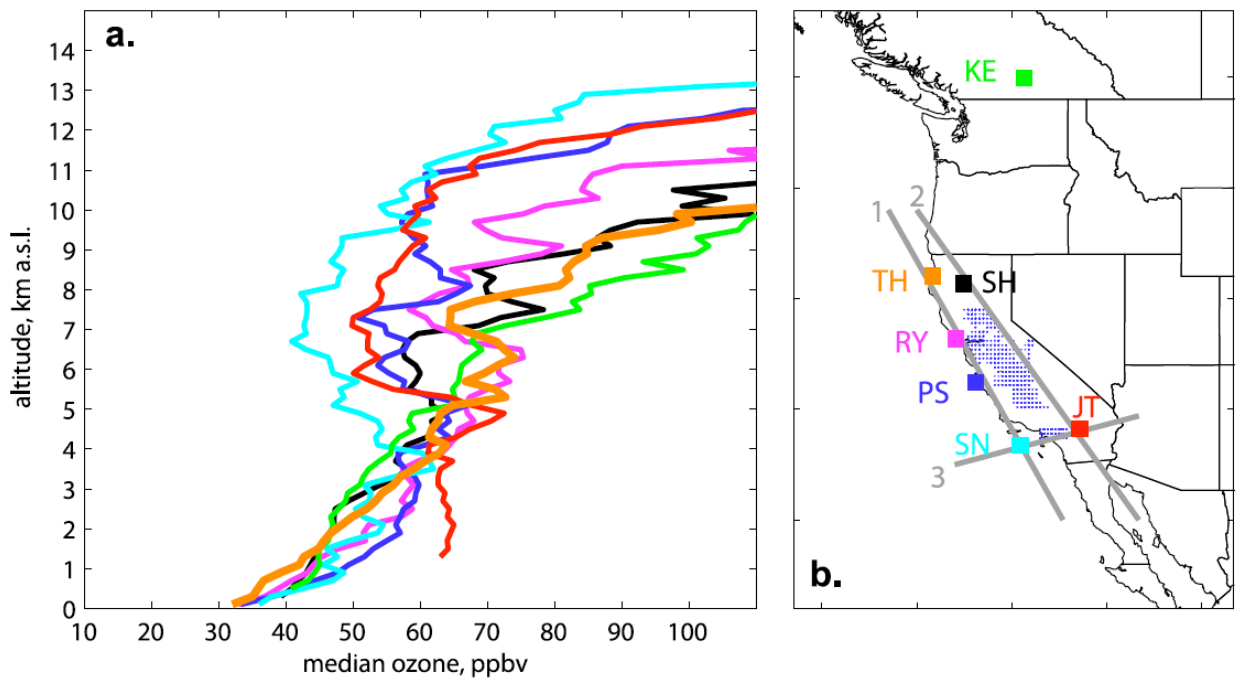

Figure D4. (a) Median ozone profiles above the IONS 2010 ozonesonde sites using all available profiles. Line colors correspond to the site label colors in Figure D4b. (b) Locations of the seven IONS 2010 ozonesonde sites. Gray transects indicate locations of the three ozone vertical cross sections with 1) representing the coastal baseline transect. (Figure reproduced from *Cooper et al*. [2011],

Figure D2 indicates generally similar O_3 and CO distributions in the 2-10 km altitude range at Portland OR and Los Angeles CA. Through most of the distribution CO is approximately 5 to 10 ppbv higher at Portland, with the upper 2 percentiles of the plumes enhanced by about 40 to 60 ppbv. Through most of the distribution, O_3 is nearly identical above the two cities. The O_3 differences at the lowest concentrations likely indicate greater tropical influence bringing lower O_3 concentrations to Los Angeles than Portland. The differences at the highest concentrations likely represent stronger stratospheric input at high altitudes above more northerly Portland, where the tropopause is lower; this pattern is consistent with the median IONS-2010 O_3 profiles shown in Figure 5 of *Cooper et al*. [2011].

Finding D3: ***Global chemical transport models (GTMs) capture a significant fraction of the temporal and spatial variability of the baseline concentrations, and hence can provide improved boundary conditions for regional air quality modeling.***

Pfister et al. [2011] show that global models can calculate time and space varying chemical boundary conditions that provide useful input to regional models for O_3, CO and PAN. Sensitivity simulations with a regional model with boundary conditions generated by a global model show that the temporal variability in the pollution inflow does impact modeled surface concentrations in California. However, the global model captured only about half of the observed free tropospheric variability, so inclusion of the varying boundary conditions likely still underestimates peak surface concentrations and the variability associated with long-range pollution transport.

As briefly discussed in the response to Question U, provision of lateral boundary conditions to a regional air quality model from a global model that included assimilation of upper-tropospheric satellite O_3 data did improve the correlation between observed and predicted ground-level ozone, but it also significantly increased the positive bias of the model. In contrast, the correlation between observed and predicted ground level-PM was negatively impacted by use of boundary conditions provided by the global model.

In summary, it is recognized that baseline concentrations of PM, O_3 and its precursors vary markedly in time and location. Thus, providing spatially and temporal varying lateral boundary conditions to regional air quality models is important for improving their performance. Some progress has been made toward achieving this goal through the use of global models, particularly with the incorporation of satellite data assimilation, but further work remains to be done before reliable procedures can implement this process on a routine basis.

References

Cooper, O. R., et al. (2011), Measurement of western U.S. baseline ozone from the surface to the tropopause and assessment of downwind impact regions, *J. Geophys. Res., 116*, D00V03, doi:10.1029/2011JD016095.

Cooper, O. R., et al. (2010), Increasing springtime ozone mixing ratios in the free troposphere over western North America, *Nature, 463*, 344–348, doi:10.1038/nature08708.

Dentener, F., T. Keating, and H. Akimoto (Eds.) (2011), *Hemispheric Transport of Air Pollution 2010: Part A: Ozone and Particulate Matter, Air Pollut. Stud., vol. 17*, United Nations, New York.

Jaffe, D., et al. (2003), The 2001 Asian Dust Events: Transport and Impact on Surface Aerosol Concentrations in the U.S., *EOS, Transactions American Geophysical Union*, *84*(46), 501-507.

National Research Council (NRC) (2009), *Global Sources of Local Pollution: An Assessment of Long-Range Transport of Key Air Pollutants to and From the United States,* 248 pp., Nat. Acad., Washington, D. C.

Parrish, D. D., D. B. Millet, and A. H. Goldstein (2009), Increasing ozone in marine boundary layer inflow at the west coasts of North America and Europe, *Atmos. Chem. Phys., 9*, 1303–1323, doi:10.5194/acp-9-1303-2009.

Parrish, D. D., K. C. Aikin, S. J. Oltmans, B. J. Johnson, M. Ives, and C. Sweeny (2010), Impact of transported background ozone inflow on summertime air quality in a California ozone exceedance area, *Atmos. Chem. Phys., 10*, 10,093–10,109, doi:10.5194/acp-10-10093-2010.

Pfister, G. G., D. Parrish, H. Worden, L. K. Emmons, D. P. Edwards, C. Wiedinmyer, G. S. Diskin, G. Huey, S. J. Oltmans, V. Thouret, A. Weinheimer and A. Wisthaler (2011) Characterizing summertime chemical boundary conditions for air masses entering the US West Coast, *Atmos. Chem. Phys., 11*, 1769–1790, 2011, doi:10.5194/acp-11-1769-2011.

Thouret, V., J.-P. Cammas, B. Sauvage, G. Athier, R. Zbinden, P. Nédélec, P. Simon, and F. Karcher (2006), Tropopause referenced ozone climatology and inter-annual variability (1994–2003) from the MOZAIC programme, *Atmos. Chem. Phys., 6*, 1033–1051, doi:10.5194/acp-6-1033-2006.

Synthesis of Results - Emissions

Response to Question E

QUESTION E

How effective have historical air pollution control efforts been? How effective have specific emission control measures been?

BACKGROUND

Substantial public resources have been expended to improve air quality throughout the U.S. and in California in particular. Ambient measurements demonstrate that these resources have resulted in very significant reductions in a wide spectrum of air pollutants. The following utilizes historical ambient pollutant measurements to document the long-term improvement of air quality in the SoCAB, and utilizes a specific CalNex investigation to demonstrate the efficacy of a recent pollution control measure.

POLICY RELEVANCE

When the public is asked to invest resources in air quality improvement, it is important to demonstrate that the policies implemented are effective in achieving their goals. Further, examination of long-term pollutant trends can guide us toward effective policy approaches.

In both California and the U.S., criteria air pollutants (i.e., those subject to regulation setting permissible ambient atmospheric levels) include both primary (i.e., directly emitted) and secondary (i.e., formed within the atmosphere) pollutants. The former include nitrogen oxides (NO_X), carbon monoxide (CO) and sulfur dioxide (SO_2) while the latter includes ozone (O_3). Particulate matter is a criteria air pollutant with both primary and secondary sources (see Response to Question N). Volatile organic compounds (VOCs) are not criteria pollutants, but their emissions from various sources are subject to regulation because they react in the atmosphere to create criteria pollutants. Finally, other secondary pollutants are of concern although not subject to specific regulation; two examples are peroxyacetyl nitrate (PAN), a species first identified as a component of Los Angeles smog that was a particularly important eye irritant [*Leighton,* 1961], and nitric acid (HNO_3), an important contributor to acid precipitation and a precursor to ammonium nitrate, which is an important component of PM. Both PAN and HNO_3 are atmospheric oxidation products of NO_X, while O_3 is a product of atmospheric photochemistry involving NO_X, VOCs and CO.

FINDINGS

***Finding E1*: The five decades of air pollution controls implemented in the SoCAB have produced remarkable improvement in air quality, with substantial reductions in both primary and secondary air pollutants.**

Pollack et al. [2013] show that decreases in O_3 concentrations observed in SoCAB over the past five decades are correlated with decreases in abundances of its precursors, NO_X, CO, and VOCs (Figure E1). Ozone precursors have been widely investigated and well characterized in the SoCAB with measurements dating back to 1960. *Pollack et al.* [2013] compiled an extensive SoCAB data set spanning 1960 to 2010 including ambient measurements from the CARB

surface monitoring network, mobile roadside monitors, ground-based field studies and chemically-instrumented research aircraft.

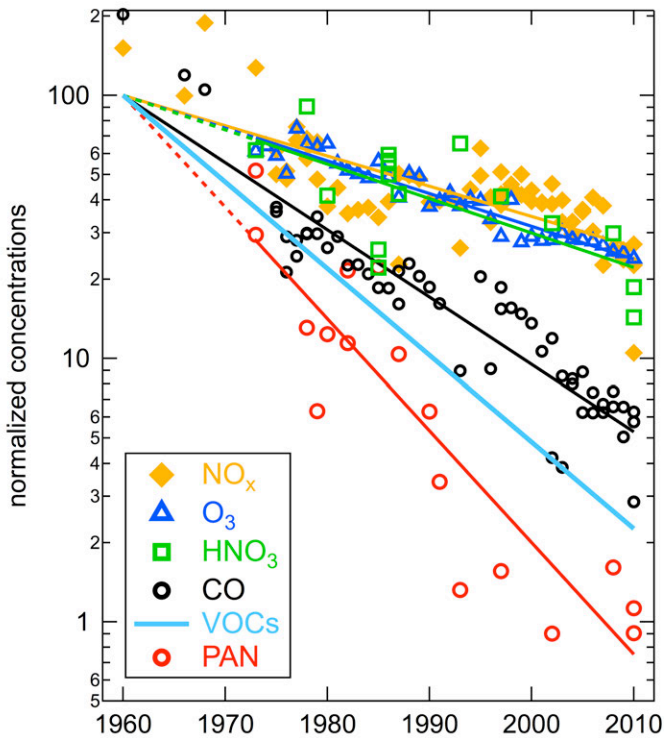

Figure E1. Long-term trends of ambient concentrations of primary (CO, VOCs and NO_X) and secondary (O_3, PAN, and HNO_3) pollutants in the SoCAB. The respective lines are linear least-squares fits to log-transformed data; these lines therefore define exponential decreases of the concentrations. The data are normalized so that the linear fits intersect 100 in the year 1960. Ozone data are annual maximum 8-hour averages for each year; other data are average concentrations for summertime weekdays. For clarity, only the linear fit to the VOC data is shown. All analyses and data are from *Pollack et al*. [2013].

Not all pollutants have decreased at the same rate in SoCAB. Of the primary pollutants, faster rates of decrease are observed in abundances of VOCs (7.3±0.7 % $year^{-1}$) and CO (5.7±0.3 % $year^{-1}$) than NO_X (2.6±0.3 % $year^{-1}$). The rate of decrease of O_3 (2.8±0.8 % $year^{-1}$) and HNO_3 (3.0±0.8 % $year^{-1}$) are statistically equivalent to that of NO_X, while PAN has decreased faster (9.3±1.1 % $year^{-1}$) than other secondary or primary pollutants. Progress has been much faster in reducing concentrations of PAN (a factor of 133 decrease over 50 years) compared to O_3 (a factor of 4.2 decrease over 50 years). Since PAN has been a compound of particular concern, air quality improvement should not be measured by the rate of decrease of O_3 concentrations alone.

***Finding E2*: By some measures, O_3 concentrations have decreased more slowly in the SJV than in the SoCAB. Although several factors likely contribute, the cause(s) and significance of this difference is ambiguous at this time.**

Analysis: M. Hiles and D.D. Parrish, NOAA

It is well established that emission controls implemented over the past decades have resulted in O_3 reductions that have varied between air basins (c.f., Figure 1 of the Introduction). Figure E2 compares the temporal evolution of four O_3 concentrations statistics between the SoCAB and the SJV. The faster decrease in absolute concentrations in the SoCAB is clear in all four statistical measures of O_3. It is notable that by 2011 the 25th percentile, median and 95th percentile concentrations were generally smaller in the SoCAB than in the SJV; only the maximum O_3 concentrations remained higher in the SoCAB. However, interpretation of the significance of this difference in the rates of decrease is ambiguous.

The solid lines in Figure E2 are least-square regression fits of the data sets to a function that assumes an exponential decrease in the O_3 concentrations with an approach to an asymptotic

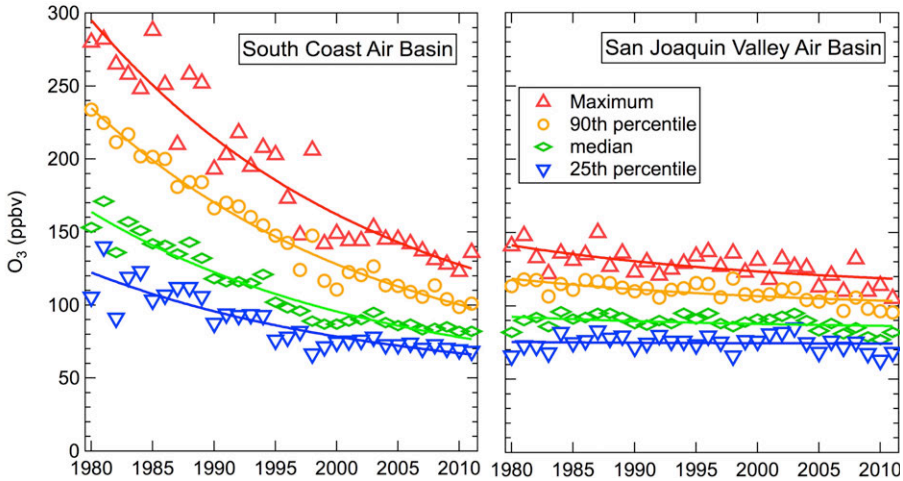

Figure E2. Comparison of the temporal evolution of four O_3 statistics between the SoCAB and the SJV. The data considered are the maximum daily 8-hr average O_3 concentration recorded at any site in the respective air basins on each day during each year's five-month (May - September) O_3 season. The statistics considered are the yearly maximum, 90th percentile, median and 25th percentile of these data. The solid lines indicate least-squares regression fits to the respective data sets.

baseline concentration that is closely related to the policy relevant background (PRB) O_3 (see discussion in the Response to Question D). Within the SoCAB, fits to all four statistics suggest exponential decreases with an average time constant of 23.5 years, which corresponds to a decrease in the California enhancement of O_3 above the baseline concentrations of 4.2 % year^{-1}. This is a somewhat larger rate of decrease than the 2.8±0.8 % year^{-1} derived above in Finding E1 for the SoCAB. Here it is assumed that O_3 will eventually approach the baseline value, which is neglected in the Finding E1 analysis. The derived asymptote concentrations for the three smaller O_3 statistics average 46 ppbv, which is consistent with the upper end of the near-surface baseline O_3 concentrations transported into California as discussed in the Response to Question D.

Similar fits to the SJV data are much less certain; they are consistent with two contrasting interpretations. First, it can be assumed that the exponential time constant of 23.5 years found for the SoCAB can be directly applied to the SJV; this is perhaps reasonable, since emission control efforts have been implemented simultaneously in both basins. (The SJV curves in Figure E2 are based on this assumption.) In this case the difference between air basins is solely due to significantly larger baseline O_3 concentrations in SJV than in the SoCAB. Second, it can be assumed that the baseline O_3 concentrations derived for the SoCAB can be directly applied to the SJV; this is perhaps reasonable, since in the absence of anthropogenic emissions, the same baseline (or PRB O_3) could be present in both air basins. (The SJV curves based on this assumption are statistically indistinguishable from those in Figure E2.) In this case the difference between air basins is solely due to longer time scales for the exponential decrease, on average on the order of 100 years, in SJV. It may be that both larger baseline O_3 concentrations and slower reductions in the anthropogenic O_3 contribution accounts for the slower reduction of O_3 concentrations in the SJV compared to the SoCAB.

***Finding E3*: Compliance of marine vessels with the California fuel quality regulation and participation in the vessel speed reduction program yield the expected reduction in emissions of SO_2, and also provide substantial reductions in emissions of carbon dioxide and primary PM.**

CalNex studies have reported the speed dependence of emissions from a vessel burning low-sulfur fuel [*Cappa et al.,* 2013] and from a vessel during a switch from high- to low-sulfur fuel

[*Lack et al.*, 2011]. These analyses showed that speed reductions led to significant reductions in primary emissions of all species per kilometer traveled, by a factor of two or more. Further, *Lack et al.* [2011] used a wide variety of chemical and aerosol measurements from the NOAA WP-3D aircraft and the Research Vessel *Atlantis* to quantify differences in actual emissions from a single ship observed underway prior to, during, and after switching between high– and low–sulfur fuel. That analysis noted additional reductions in emissions as a result of burning low-sulfur fuel: both SO_2 and particulate sulfate decreased by more than 90%, and particulate organic matter by decreased by 73% (Figure E3).

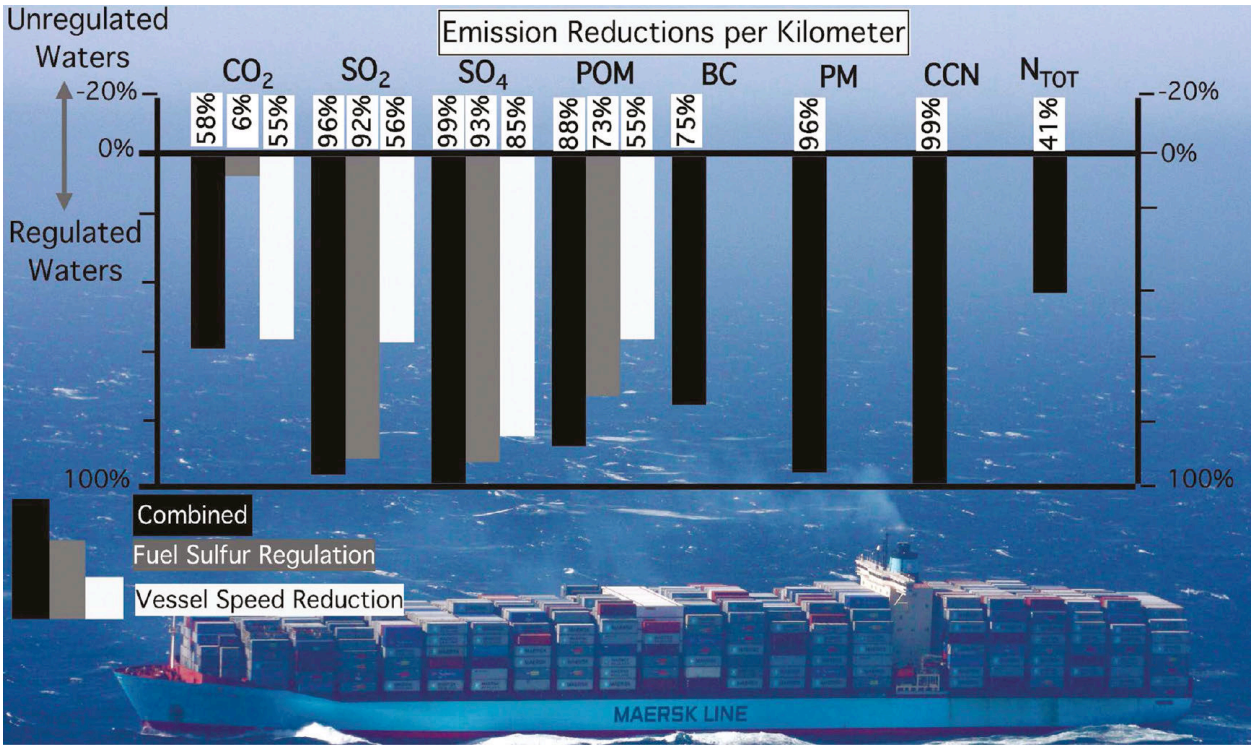

Figure E3. Emissions reductions (per km of travel) from the *Margrethe Maersk* vessel as a result of the State of California fuel sulfur regulation (gray), vessel speed reduction program (white) and combined (black). (Figure from *Lack et al*. [2011])

References

Cappa, C. D., et al. (2013), The influence of operating speed on gas and particle–phase shipping emissions: results from the NOAA Ship *Miller Freeman*, *J. Geophys. Res. Atmos., (in preparation)*.

Lack, D. A., et al. (2011), Impact of fuel quality regulation and speed reductions on shipping emissions: Implications for climate and air quality, *Environ. Sci. Technol., 45, 9052–9060, doi:10.1021/es2013424*.

Leighton, P. A. (1961), *Photochemistry of Air Pollution*, Academic Press, New York.

Pollack, I.B., T. B. Ryerson, M. Trainer, J.A. Neuman, J.M. Roberts and D.D. Parrish (2013), Trends in ozone, its precursors, and related secondary oxidation products in Los Angeles, California: A synthesis of measurements from 1960 to 2010, *J. Geophys. Res. Atmos., 118*, 5893–5911, doi:10.1002/jgrd.50472.

Synthesis of Results - Emissions

Response to Question F

QUESTION F

Are emission inventory estimates for air pollutants and climate forcing agents accurate? Are there under- or over-estimated emissions or even missing emission sources in the emission inventories?

BACKGROUND

Top-down assessment of emissions inventories is a major focus of analysis of the CalNex data sets. Measured atmospheric concentrations in source regions can provide critical assessments of the emissions of the measured species. These assessments test the bottom-up approach used in inventory tabulations and establish benchmarks for relative emissions changes over time in response to control strategies. Several analyses of CalNex data have used top-down emissions assessment approaches to help quantify inventories of greenhouse gases and precursors of ozone and aerosols.

POLICY RELEVANCE

Our ability to understand air quality degradation and changing climate is based upon a wide array of atmospheric models that treat transport, composition, chemical transformations and other atmospheric processes. Policy decisions are guided by the results of these models. Emission inventories are one of the essential components of models, providing the location, magnitude, and composition of relevant chemical species. Changing emissions (e.g., amount, composition, timing of release, etc.) is the only means available to implement policy. To effectively apply this tool requires accurate knowledge of emission sources and magnitudes, information provided by the emission inventories.

Emissions of greenhouse gases from California, when averaged over the 2002-2004 period, account for 2% of the global total [*CARB*, 2008]. The provisions in the California Global Warming Solutions Act of 2006 call for regulations to reduce emissions by 2020 to levels equivalent to those estimated for 1990 (equivalent to a 10 to 15% reduction from the 2002-2004 average by 2020). Implementation requires the State to establish a GHG inventory and evaluate emissions reduction progress against this inventory baseline. Anthropogenic CO_2 is emitted primarily from combustion processes; its annually-averaged emissions account for 86% of the calculated 100-year global warming potential (GWP) and thus dominate the CARB inventory of directly emitted greenhouse gases [*CARB*, 2011] (Figure F1). The ubiquity of anthropogenic CO_2 emission sources, coupled with significant diurnal variability in biospheric CO_2 sources and sinks, complicates accurate top-down assessments of CO_2 emissions based on atmospheric measurements. CH_4 emissions account for 7% of the total GWP in the 2009 California annual inventory [*CARB*, 2011] (Figure F1). This inventory apportions total CH_4 emissions as 56% from enteric fermentation and manure management (primarily dairy cattle), 21% from landfills, 11% from the combined emissions of wastewater treatment, oil and gas development, rice cultivation, and vehicular traffic sources, and 12% from sources listed as "other". The variety of source types leads to significant spatial and temporal heterogeneity of CH_4 emissions in

California. N_2O emissions account for approximately 3% of the total GWP in the California annual inventory (Figure F1); the largest anthropogenic emissions in California are thought to be from agriculture, primarily synthetic fertilizer use and dairy cattle, both predominately located in the Central Valley. Halocarbons (the sum of CFCs, HCFCs, HFCs, and other halogenated gases) account for 3% of the annual GWP of inventoried California emissions. Emissions of all these greenhouse gases have been assessed from the CalNex data.

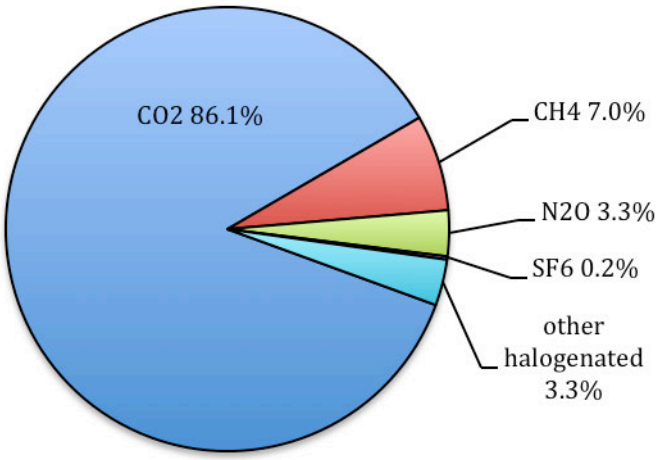

Figure F1. CO_2–equivalent radiative forcing estimated from the 2009 inventory of California greenhouse gas emissions [*CARB*, 2011]. Figure reproduced from *Ryerson et al*. (2013).

Ozone precursors include carbon monoxide (CO), volatile organic compounds (VOCs) and oxides of nitrogen (NO_X). Other emissions that lead to air quality degradation are particulate matter (PM) including black carbon (BC) and PM precursors including ammonia (NH_3) and sulfur dioxide (SO_2), as well as VOCs and NO_X. Aspects of the emissions of all of these precursor species have also been assessed from the CalNex data.

The CalNex fieldwork was conducted in 2010, so ideally emission inventory assessments would be based upon inventories for the year 2010. However, at the time that the assessments were conducted, 2008 inventories generally were the most recent available, and therefore were used for comparisons. The 2010 inventories are generally slightly different, so for purposes requiring very precise comparisons, this difference should be taken into account.

FINDINGS

***Finding F1*: CO_2 emissions for the SoCAB estimated by an observation-based mesoscale inverse modeling technique agree with emission estimates by CARB. Both of these estimates are higher by 15 to 38% than that in the Vulcan inventory of North American CO_2 emissions.**

Brioude et al. [2013] present top-down estimates of anthropogenic CO_2 surface emissions using a Lagrangian model in combination with three different WRF model meteorological configurations, driven by CO_2 measurements from NOAA WP-3D aircraft flights during CalNex, as well as one flight in 2002. Within the uncertainties of these estimates, CO_2 emissions in SoCAB did not change significantly with day of week (increase of 7 ± 14% on weekends) or between 2002 and 2010 (decrease of 4 ± 10%). Assuming that the CalNex results can be extrapolated to total annual anthropogenic emissions, 183±18 Tg CO_2 yr^{-1} is estimated for the SoCAB. This estimate agrees well with the estimate of 180 Tg yr^{-1} derived by *Peischl et al.*

[2013] from the CARB statewide greenhouse gas inventory for 2009, but is 15 to 38% higher than the widely used Vulcan inventory [http://vulcan.project.asu.edu/, *Gurney et al.*, 2009].

***Finding F2a*: Total methane emissions for the SoCAB have been consistently underestimated by inventories. CalNex analyses implicate larger-than-expected CH_4 emissions from the oil and gas sector in Los Angeles as the emissions missing from current inventories.**

Analysis: This material is taken from Ryerson et al. (2013).

Ground-based Fourier transform spectrometer (FTS) measurements of atmospheric column abundances of CH_4 above Pasadena, CA in 2007 and 2008 [*Wunch et al.*, 2009] had suggested that a significant source of CH_4, up to one half of the derived total of 0.6 Tg/yr, was unaccounted for in the CARB emission inventory for the heavily urbanized SoCAB. Following these studies *Wennberg et al.* [2012], *Santoni et al.* [2013] and *Peischl et al.* [2013] analyzed CalNex ground and airborne data and separately concluded that CH_4 sources continue to be significantly underestimated in the current inventory for the Los Angeles basin. *Wennberg et al.* [2012] note that atmospheric CH_4 enhancement ratios to ethane (C_2H_6) are similar to those in natural gas supplied to the basin in both 2008 and in 2010, and concluded that leakage from the natural gas distribution infrastructure in the basin is the most likely source of excess atmospheric CH_4. Their study did not rule out natural gas seeps or industrial emissions as significant potential sources. *Peischl et al.* [2013] examine CH_4 enhancement ratios to C_2 through C_5 alkanes (ethane, propane, and the isomers of butane and pentane, Figure F2) and utilized the geographic distribution of airborne samples taken during CalNex to exclude traffic, dairy feedlots, landfills, and wastewater treatment plants as significant sources of the unaccounted CH_4 emissions in the LA basin. They attribute the missing methane to leaks from natural gas extraction, production, and distribution, based on the observed correlations with the light alkanes. *Santoni et al.* [2013] use an inverse model constrained by the WP-3D aircraft data and calculate emissions in the LA basin of 0.39 Tg CH_4/year, consistent with an assumed leak rate of 2.5% from the natural gas delivery infrastructure in the basin. Thus, these CalNex analyses implicate larger-than-expected CH_4 emissions from the oil and gas sector in Los Angeles as the emissions missing from the inventory, but differ on the root cause. Spatially-resolved measurements in Los Angeles, possibly including CH_4 stable isotope data [*Townsend-Small et al.*, 2012] both in atmospheric samples and in direct samples of potential source emissions, are needed for more detailed identification and attribution of the excess CH_4 that appears to be a consistent feature of Los Angeles' atmosphere.

***Finding F2b*: Methane emissions from landfills and dairies in the SoCAB are accurately estimated in the inventories developed by CARB.**

From crosswind plume transects flown by the NOAA P-3 aircraft downwind of the two largest landfills in the basin, *Peischl et al.* [2013] determined that CH_4 fluxes are consistent with the 2008 CARB GHG inventory values, which total 164 Gg CH_4/yr emitted from all landfills in the South Coast Air Basin. NOAA P-3 aircraft data were also used to estimate CH_4 emission fluxes from Chino-area dairies in the eastern L.A. basin. Flux estimates from these dairies ranged from 24 ± 12 to 87 ± 44 Gg CH_4/yr, and the average flux (49 ± 25 Gg CH_4/yr) is statistically consistent with a revised bottom-up inventory (31.6 Gg CH/yr,) derived from the methods compiled by *Salas et al.* [2008], and with another previous inventory estimate of (76 Gg CH/yr,) [*Wennberg et al.*, 2012]. The aircraft-based flux determinations do vary by more than a factor of three, which is outside the expected uncertainties of the estimates. This variation suggests

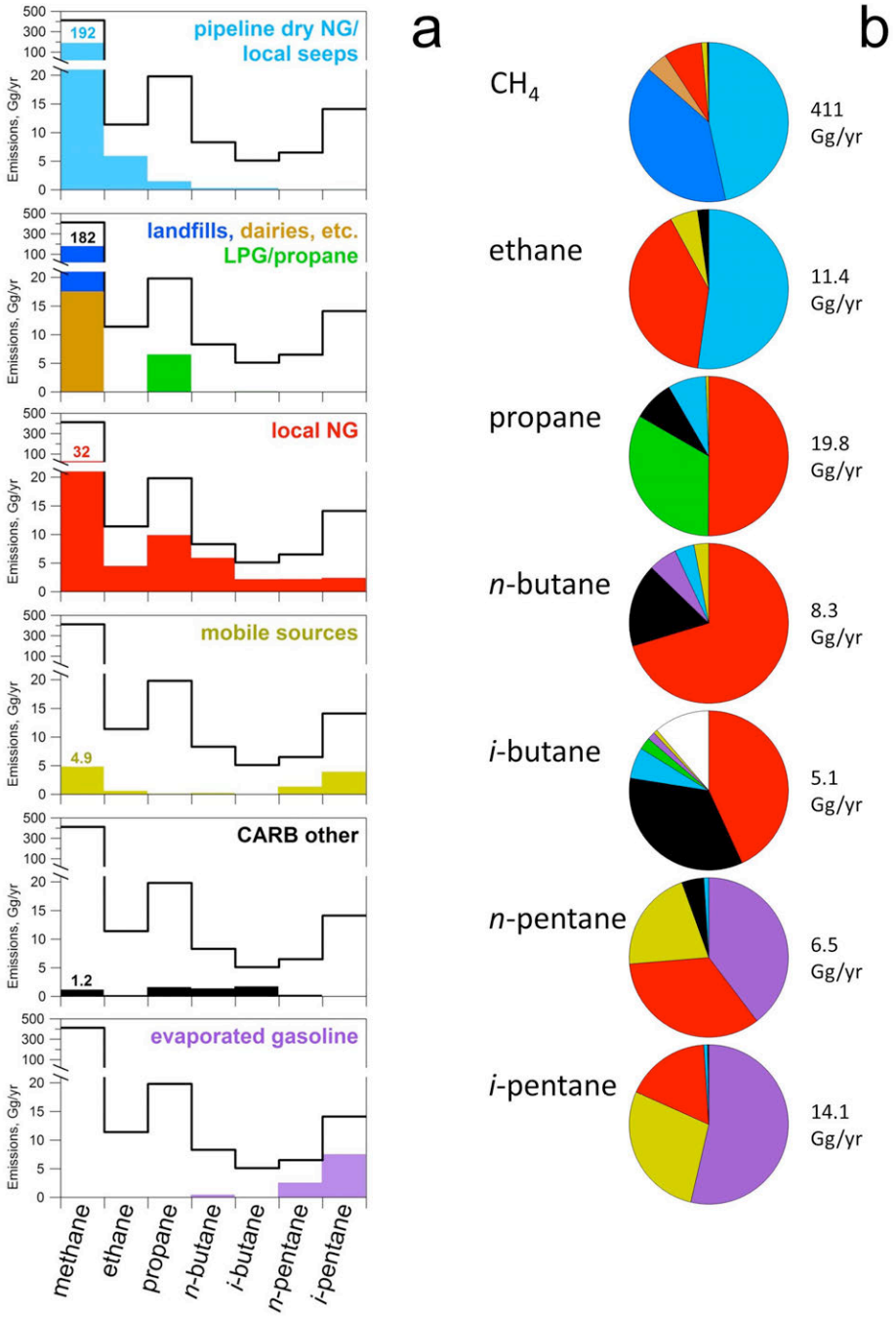

Figure F2. a) Estimate of seven hydrocarbon emissions from six sources in the SoCAB. The thick black line represents the estimated total annual emission for each of seven alkanes (CH_4 and C_2–C_5). The colored bars represent the fraction of the total contributed by each of the six sources. CH_4 emissions are written above the bar. **b)** Pie charts for the data in (a) showing the relative contributions from each source for each alkane, colored as in (a). The white region in the *i*-butane pie chart represents the 11% shortfall between the source attribution and the estimated total emissions. The total emission of each alkane in the SoCAB is given to the right of each pie chart. (Figure taken from *Peischl et al*. [2013]).

real day-to-day variability in the dairy CH_4 fluxes, which may be associated with manure management practices. Further investigation of this variability may provide guidance for reducing these CH_4 emissions.

***Finding F2c*: Annual average methane emissions from rice agriculture are factors of 2 to 3 greater than in the CARB inventory.**

Data from two flights of the NOAA P-3 aircraft in CalNex were used to investigate the spatial consistency of CH_4 emissions from rice paddies during the growing season in the Sacramento Valley [*Peischl et al.*, 2012]. This paper demonstrated that rice emissions dominated other potential sources of CH_4 in the region, including oil and gas development, dairy farms, and wastewater treatment facilities. The analysis showed that earlier long-term measurements of CH_4 and CO_2 at a single paddy [*McMillan et al.*, 2007] were generally representative of emissions from rice cultivation throughout the Sacramento Valley in California. *Peischl et al.* [2012] further note the annual average CH_4 emissions from rice in *McMillan et al.* [2007] are factors of 2 to 3 greater than in the CARB annual inventory, and attribute this inventory discrepancy to the lack of accounting for changes in residual crop management following a 2001 ban on most rice straw burning in the Sacramento Valley. Inverse modeling results reported by *Santoni et al.* [2013] are also consistent with a low bias, by about a factor of three, in the CARB inventory of CH_4 emissions from rice in the Sacramento Valley.

***Finding F3*: Analyses of CalNex nitrous oxide measurements suggest that inventory improvements are needed to correct a potential low bias and improve the spatial and seasonal patterns of emissions.**

Xiang et al. [2012] used a 3-D mesoscale meteorological model coupled with a Lagrangian particle dispersion model to link N_2O concentrations observed from the P-3 aircraft to source emission areas, and concluded that fertilizer application in the Central Valley was the largest source of N_2O during the study period. High-resolution surface emission maps derived from their inversion analysis showed a different spatial pattern of N_2O emissions in the Central Valley than expected from the EDGAR 4.0 inventory. This conclusion is consistent with a recent inverse modeling study based on long-term tall tower N_2O observations [*Miller et al.*, 2012] of agricultural N_2O emissions derived using top-down methods.

The global total of N_2O emissions is thought to be well known; however, individual source terms in inventories are uncertain. The potential low bias in agricultural N_2O inventories, potentially coupled with poor spatial [*Xiang et al.*, 2012] and seasonal [*Miller et al.*, 2012] representations, may handicap scientifically sound GHG emissions control strategies and ozone layer protection based on N_2O emissions reductions. These uncertainties further complicate accurate projections of future N_2O emissions under potential climate mitigation or adaptation strategies. These conclusions suggest that improved quantification of agricultural N_2O sources in California may help the State meet the GHG reduction timelines spelled out in AB32.

***Finding F4*: Top-down assessments of anthropogenic halocarbon emissions are generally consistent with the CARB emission inventory.**

Halocarbon emissions patterns, trends, and seasonality in California have been previously reported [*Barletta et al.*, 2011; *Gentner et al.*, 2010]. These compounds were measured at a variety of sites during CalNex (Appendix A). *Barletta et al.* [2013] used whole-air samples acquired in the Central Valley and the Los Angeles basin from the NOAA WP-3D flights during

CalNex to show that the 2008 CARB inventory is generally consistent with their top-down assessment of anthropogenic emissions of halocarbons HFC-134a, HFC-152a, HCFC-22, HCFC-124, HCFC-141b, and HCFC-142b in California.

***Finding F5*: Top-down assessments of the CO emissions in 2010 are within 15% of the CARB 2008 emission inventory.**

The top-down method of *Brioude et al.* [2013] discussed in Finding F1 also provided estimates of anthropogenic CO emissions based on NOAA P-3 aircraft flights. These estimates are within 15% of the CARB 2008 inventory for both LA County and the SoCAB, but average about 40% lower than EPA's NEI 2005 inventory [*US Environmental Protection Agency*, 2010]. Urban CO concentrations are dominated by on-road emissions from gasoline-fueled passenger vehicles and have been steadily decreasing over time throughout the U.S. [*Parrish et al.*, 2002] in response to control strategies. CO in California shows a similar trend, recently demonstrated by a study using atmospheric CO measurements and the radiocarbon composition of tree rings in the Los Angeles basin as a record of atmospheric CO_2 from fossil fuel [*Djuricin et al.*, 2010]. Since the emissions of CO over time are thought to be accurately known, CO serves as a conserved tracer, a utility that has been exploited in several CalNex studies to calculate mass emissions of other species of interest, either co-emitted with CO [*Barletta et al,* 2013; *Pollack et al., 2012*; *Warneke et al.*, 2012] or emitted from different sources but sufficiently mixed following emission such that their atmospheric variability becomes correlated with CO [*Nowak et al.*, 2012; *Peischl et al.*, 2013; *Peischl et al.*, 2012].

***Finding F6*: Top-down assessments of NO_X emissions are in general agreement with the CARB emission inventory.**

McDonald et al. [2012] use a fuel-based approach to estimate NO_X emissions from gasoline and diesel-powered on-road vehicles in the SoCAB and the SJVAB (Figure F3) as well as for California and the entire nation from 1990 to 2010. They compare their results with emission inventories, including EMFAC. To quantify total NO_X emissions, the on-road emission estimates were combined with estimates for other anthropogenic sources and compared with satellite and ground-based observations.

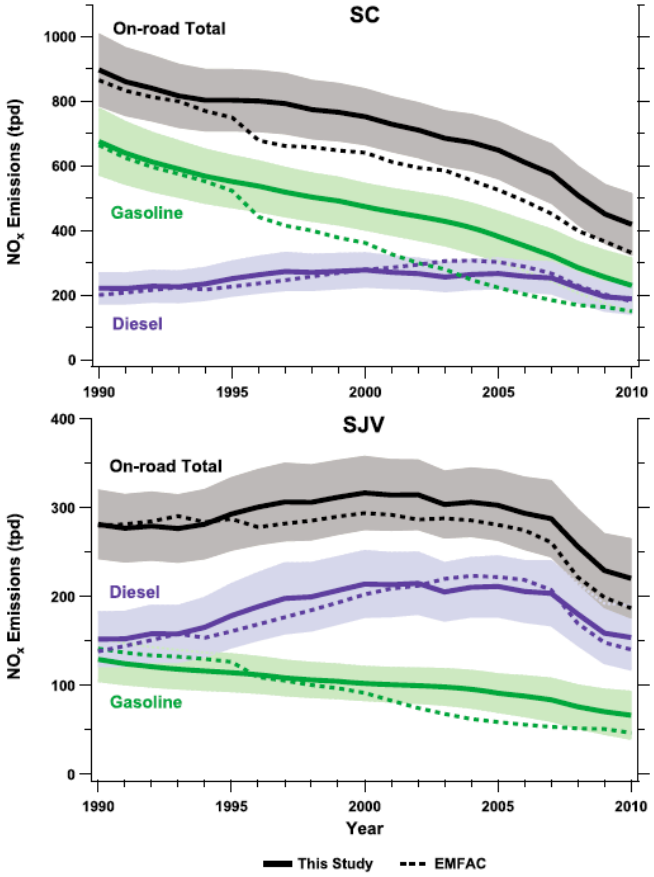

Figure F3. Trends in NO_X emissions from on-road vehicles in the South Coast Air Basin (SC) and SJV. Shaded areas represent uncertainties of estimates. Dotted lines show estimates from EMFAC (Figure taken from *McDonald et al*. [2013]).

Growth in on-road diesel fuel consumption outpaced that of gasoline from 1990 to 2007, followed by a decrease in the consumption of both, which is attributed to the economic downturn. The ratio of NO_X emission factors for heavy-duty diesel versus light-

duty gasoline engines grew from ~3 in 1990 to ~8 in 2010, which is attributed to the near universal deployment of catalytic converters on gasoline engines. In contrast, NO_X emission factors for heavy-duty diesel trucks showed little change during the 1990s, and have decreased only gradually since then. The NO_X emission changes shown in Figure F3 result from the combination of changing fuel consumption, both in total amount and apportionment between gasoline and diesel, and the NO_X emission factors. The impact of the economic recession after 2007 is clear in the estimated NO_X emissions.

The top-down method of *Brioude et al*. [2013] discussed in Finding F1 also provided estimates of anthropogenic NO_X emissions based on NOAA WP-3D aircraft flights. Their observation-based estimate for NO_X emissions in Los Angeles County in 2010 is lower than the CARB 2008 inventory by 6% on weekdays and 17% during weekends, differences within the uncertainty range of their inversion method. In the entire SoCAB region, a similar difference was seen on weekdays, but only a 2% difference during weekends. However, their derived spatial distribution of NO_X emissions in SoCAB was significantly different from the CARB 2008 inventory. The NEI 2005 inventory did not compare as well with the results of *Brioude et al*. [2013], which were lower by 32%±10% in LA County and by 27%±15% in the SoCAB than in the NEI 2005 inventory.

Weekday-weekend NO_X emissions differences, and their trends over time, are documented from 1990 through the CalNex study in 2010 [*Pollack et al.,* 2012]. Pollack *et al.* [2012] used ambient measurements to show significant weekend decreases of the NO_X to CO emission ratio, between one-third to one-half of the characteristic weekday ratio, have been a consistent feature of the South Coast Air Basin since at least the mid-1990s.

***Finding F7*: Top-down assessments of VOC emissions of measured species indicate some discrepancies with inventories, but they are not sufficiently large to appreciably affect results of air quality modeling. However, an important, temperature-dependent source of unidentified VOC species is missing from inventories in the SJV.**

Borbon et al. [2013] used the CalNex Pasadena ground site data to derive top-down emissions estimates of many VOCs relative to CO and acetylene in vehicular exhaust; they find that individual VOC to CO emission ratios can disagree by with the ratios derived from emission inventories, but the disagreements are not sufficiently large to appreciably affect results of air quality modeling (see discussion in response to Question G). *de Gouw et al.* [2012] used the CalNex measurements to show that ethanol has become significantly enriched in U.S. urban atmospheres in the last decade due to its increasing use as a biofuel amendment to gasoline (see discussion in response to Question B). *Pusede and Cohen* [2012] and *Pusede et al.* [2013] have identified an important, temperature source of VOCs. For the most part, these species are not measured, but they do contribute significantly to the photochemical reactivity in that area. This source is discussed more fully in the Response to Question J.

***Finding F8*: Measurements at the Bakersfield site have been used to assess the magnitude, composition and spatial distribution of emissions from petroleum and dairy operations and other agricultural activities in the SJV.**

Gentner et al. [2013a,b] use Bakersfield measurements and other data to assess the magnitude and composition of emissions from petroleum and dairy operations and other agricultural activities in the SJV. They present evidence for large sources of 1) paraffinic hydrocarbons from petroleum extraction/processing operations, notably including a wide range of branched and cyclic alkanes, 2) oxygenated compounds from dairy (and other cattle) operations, and 3) terpenoids and other biogenic compounds from agricultural crops. In SJV, the mass of biogenic emissions from agricultural crops during the summer and the potential ozone and secondary organic aerosol formation from these emissions are on the same order as anthropogenic emissions from motor vehicles.

Gentner et al. [2013a] also developed a statistical, meteorologically-based modeling method to assess the spatial distribution of emissions in the SJV. For example, Figure F4 shows the derived spatial emissions of methane compared with the location of dairies, which *Gentner et al.* [2013a] find to be the primary source of methane in the SJV.

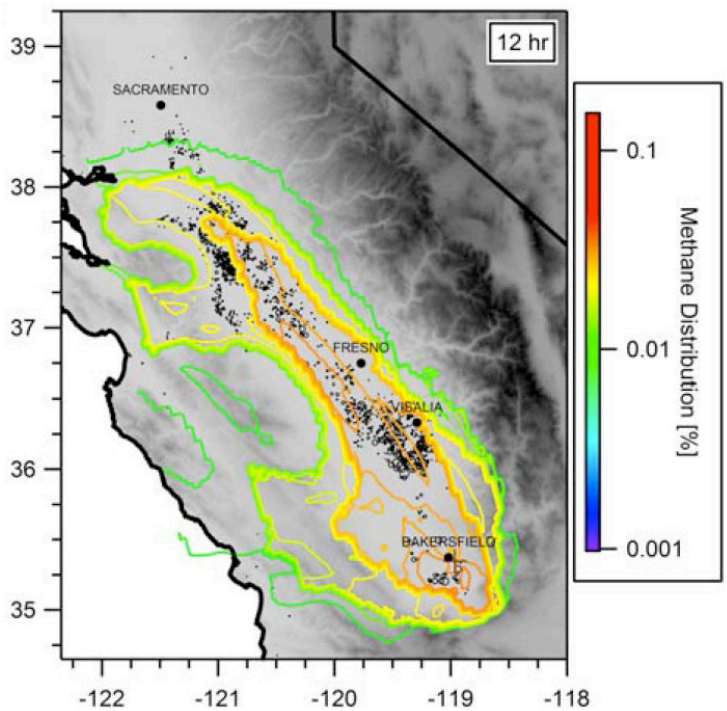

Figure F4. Statistical distribution of emissions of methane in the SJV shown as colored contours for an assumed 12-hour footprint. Black dots mark the location of dairies.

References

Barletta, B., P. Nissenson, S. Meinardi, D. Dabdub, F. S. Rowland, R. A. VanCuren, J. Pederson, G. S. Diskin, and D. R. Blake (2011), HFC-152a and HFC-134a emission estimates and characterization of CFCs, CFC replacements, and other halogenated solvents measured during the 2008 ARCTAS campaign (CARB phase) over the South Coast Air Basin of California, *Atmos. Chem. Phys.*, *11*, 2655-2669, doi:10.5194/acp-11-2655-2011.

Barletta, B. et al. (2013), Emission estimates of HCFCs and HFCs in California from the 2010 CalNex study, *J. Geophys. Res. Atmos., 118*, 2019–2030, doi:10.1002/jgrd.50209.

Borbon, A., et al. (2013), Emission ratios of anthropogenic volatile organic compounds in northern mid-latitude megacities: Observations versus emission inventories in Los Angeles and Paris, *J. Geophys. Res. Atmos., 118,* 2041–2057, doi:10.1002/jgrd.50059.

Brioude, J., et al. (2013), Top-down estimate of surface flux in the Los Angeles Basin using a mesoscale inverse modeling technique: Assessing anthropogenic emissions of CO, NO_x and CO_2 and their impacts, *Atmos. Chem. Phys.*, *13*, 3661-3677, doi:10.5194/acp-13-3661-2013.

CARB (2008), Climate Change Scoping Plan: A Framework for Change, pursuant to AB 32, the California Global Warming Solutions Act of 2006, report, 133 pp., available at: http://www.arb.ca.gov/cc/scopingplan/document/adopted_scoping_plan.pdf

CARB (2011), California Greenhouse Gas Emission Inventory: 2000–2009, report, 32 pp., available at: http://www.arb.ca.gov/cc/inventory/pubs/reports/ghg_inventory_00-09_report.pdf.

de Gouw, J. A., J. B. Gilman, A. Borbon, C. Warneke, W. C. Kuster, P. D. Goldan, J. S. Holloway, J. Peischl, and T. B. Ryerson (2012), Increasing atmospheric burden of ethanol in the United States, *Geophys. Res. Lett., 39*(L15803), doi:10.1029/2012GL052109.

Djuricin, S., D. E. Pataki, and X. Xu (2010), A comparison of tracer methods for quantifying CO_2 sources in an urban region, *J. Geophys. Res. Atmos.*, *115*(D11303), doi:10.1029/2009JD012236.

Gentner, D. R., A. M. Miller, and A. H. Goldstein (2010), Seasonal variability in anthropogenic halocarbon emissions, *Environ. Sci. Technol.*, *44*(14), 5377-5382, doi:10.1021/es1005362.

Gentner, D.R., et al. (2013a), Emissions of organic carbon and methane from petroleum and dairy operations in California's San Joaquin Valley, *Atmos. Chem. Phys. Disc., 13*, 28225-28278.

Gentner, D.R., E. Ormeno, T.B. Ford, S. Fares, R. Weber, J.H. Park, J.F. Karlik, A.H. Goldstein (2013b) Emissions of Terpenoids, Benzenoids, and Other Biogenic Gas-phase Organic Compounds from Agriculture and their Potential Implications for Air Quality, *Atmos. Chem. Phys. Disc., 13*, 28343-28393.

Gurney, K. R., Mendoza, D. L., Zhou, Y., Fischer, M. L., Miller, C. C., Geethakumar, S., and de la Rue du Can, S. (2009), High resolution fossil fuel combustion CO2 emission fluxes for the United States, *Environ. Sci. Technol., 43,* 5535–5541, doi:10.1021/es900806c.

McDonald, B. C., T. R. Dallmann, E. W. Martin, and R. A. Harley (2012), Long-term trends in nitrogen oxide emissions from motor vehicles at national, state, and air basin scales, *J. Geophys. Res. Atmos.*, 117, D00V18, doi:10.1029/2012JD018304.

McMillan, A. M. S., M. L. Goulden, and S. C. Tyler (2007), Stoichiometry of CH_4 and CO_2 flux in a California rice paddy, *J. Geophys. Res. Atmos.*, *112*(G01008), doi:10.1029/2006JG000198.

Miller, S. M., et al. (2012), Regional sources of nitrous oxide over the United States: Seasonal variation and spatial distribution, *J. Geophys. Res. Atmos.*, *117*(D06310), doi:10.1029/2011JD016951.

Nowak, J. B., J. A. Neuman, R. Bahreini, A. M. Middlebrook, J. S. Holloway, S. A. McKeen, D. D. Parrish, T. B. Ryerson, and M. Trainer (2012), Ammonia sources in the California South Coast Air Basin and their impact on ammonium nitrate formation, *Geophys. Res. Lett., 39*(L07804), doi:10.1029/2012GL051197.

Parrish, D. D., M. Trainer, D. Hereid, E. J. Williams, K. J. Olszyna, R. A. Harley, J. F. Meagher, and F. C. Fehsenfeld (2002), Decadal change in carbon monoxide to nitrogen oxide ratio in U.S. vehicular emissions, *J. Geophys. Res. Atmos.*, *107*(D12), doi:10.1029/2001JD000720.

Peischl, J., et al. (2012), Airborne observations of methane emissions from rice cultivation in the Sacramento Valley of California, *J. Geophys. Res. Atmos.*, *117*, D00V25, doi:10.1029/2012JD017994.

Peischl, J., et al. (2013), Quantifying sources of methane using light alkanes in the Los Angeles basin, California*, J. Geophys. Res. Atmos., 118*, 4974–4990, doi:10.1002/jgrd.50413.

Pollack, I. B., et al. (2012), Airborne and ground-based observations of a weekend effect in ozone, precursors, and oxidation products in the California South Coast Air Basin, *J. Geophys. Res. Atmos., 117*, D00V05, doi:10.1029/2011JD016772.

Pusede, S. E., and R. C. Cohen (2012), On the observed response of ozone to NOx and VOC reactivity reductions in San Joaquin Valley California 1995–present, *Atmos. Chem. Phys.*, *12*, 8323–8339, doi:10.5194/ acp-12-8323-2012.

Pusede, S. E., et al. (2013), On the temperature dependence of organic reactivity, ozone production, and the impact of emissions controls in San Joaquin Valley California, *Atmos. Chem. Phys. Disc*, *13*, 28511–28560, doi:10.5194/acpd-13-28511-2013.

Ryerson, T. B., et al. (2013), The 2010 California Research at the Nexus of Air Quality and Climate Change (CalNex) field study, *J. Geophys. Res. Atmos., 118*, 5830–5866, doi:10.1002/jgrd.50331.

Salas, W. A., et al. (2008), Developing and Applying Process-Based Models for Estimating Greenhouse Gas and Air Emission From California Dairies, *California Energy Commission, PIER Energy-Related Environmental Research*, *CEC-500-2008-093*, http://www.energy.ca.gov/2008publications/CEC-500-2008-093/CEC-500-2008-093.PDF.

Santoni, G. W., et al. (2014), California's methane budget derived from CalNex WP-3 aircraft observations and a Lagrangian transport model, *J. Geophys. Res. Atmos.,* (submitted).

Townsend-Small, A., S. C. Tyler, D. E. Pataki, X. Xu, and L. E. Christensen (2012), Isotopic measurements of atmospheric methane in Los Angeles, California, USA: Influence of "fugitive" fossil fuel emissions, *J. Geophys. Res. Atmos.*, *117*(D07308), doi:10.1029/2011JD016826.

US Environmental Protection Agency (2010), Technical support document: Preparation of emissions inventories for the Version 4, 2005-based platform, report, Washington, DC, 73 pp., available at: http://www.epa.gov/airquality/transport/pdfs/2005 emissions tsd 07jul2010.pdf.

Warneke, C., J. A. de Gouw, J. S. Holloway, J. Peischl, T. B. Ryerson, E. Atlas, D. Blake, M. Trainer, and D. D. Parrish (2012), Multi-year trends in volatile organic compounds in Los Angeles, California: five decades of improving air quality, *J. Geophys. Res., 117,* (D00V17), doi:10.1029/2012JD017899.

Wennberg, P. O., et al. (2012), On the sources of methane to the Los Angeles atmosphere, *Environ. Sci. Technol., 46*, 9282-9289, doi:10.1021/es301138y.

Wunch, D., P. O. Wennberg, G. C. Toon, G. Keppel-Aleks, and Y. G. Yavin (2009), Emissions of greenhouse gases from a North American megacity, *Geophys. Res. Lett., 36*(L15810), doi:10.1029/2009GL039825.

Xiang, B., et al. (2013), Nitrous oxide (N_2O) emissions from California based on 2010 CalNex airborne measurements, *J. Geophys. Res. Atmos., 118*, 2809–2820, doi:10.1002/jgrd.50189.

Synthesis of Results - Emissions

Response to Question G

QUESTION G

Do the VOC measurements provide any new insights into emission sources?

BACKGROUND

Patterns of measured ambient concentrations of VOCs provide indications of the important emission sources of these species to the atmosphere. There have been a wide variety of source apportionment techniques applied to data sets of VOC measurements in attempts to determine the VOC sources responsible for those ambient concentrations. However, many of these techniques give questionable results since reactions of VOCs within the atmosphere change the concentration patterns from those emitted [*Yuan, et al*., 2012]. *Parrish et al*. [2009] identify similarities in the VOC emission patterns in urban areas throughout the world and suggest that in all urban areas, including Los Angeles, VOC emissions are dominated by mobile emission sources. Emissions from industrial processes and use of consumer products and biogenic emissions are additional sources that may be important in some urban areas.

POLICY RELEVANCE

Effective policies for improving air quality require accurate knowledge of emission sources of important VOC precursors of ozone and aerosols. Ambient VOC measurements can help to identify and quantify specific VOC sources (e.g., use of a particular solvent) that may be cost-effective control targets.

FINDINGS

***Finding G1*: Ambient VOC concentrations in the SoCAB have decreased by a factor of approximately 50 in the past five decades, but the ambient relative concentrations have remained remarkably constant, indicating that mobile emissions have remained the predominant source over this entire period.**

Warneke et al. [2012] summarize ambient VOC measurements in the SoCAB from 1960-2010 (Figure G1); they find that concentrations decreased by a factor of approximately 50 over that period, despite an approximate three-fold increase in fuel sales in the region. During these five decades the relative concentrations among the VOCs have remained remarkably constant, which is attributed to continuing dominance of mobile emissions, particularly the on-roadway vehicle fleet, throughout this period. This constant VOC pattern persisted through the introduction of catalytic convertors in exhaust systems and also reformulated and oxygenated gasoline. There are some exceptions to this consistency. The relative concentrations of the light alkanes (ethane, propane) have increased to the point that by 2010 they have the highest concentrations of the species plotted in Figure G1. This change is attributed to the growing relative importance of natural gas emissions in the SoCAB (see discussion in Finding F2a). *Pollack et al.* [2013] also note that concentrations of the biogenic hydrocarbon isoprene have not changed significantly over the last two decades.

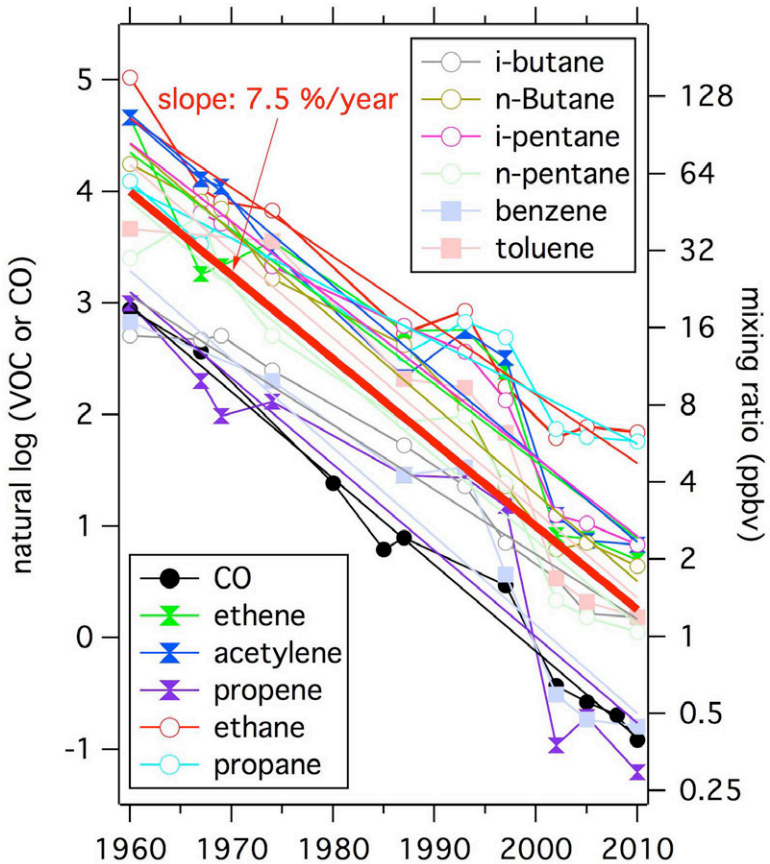

Figure G1. Typical mixing ratios estimated from published data from various field campaigns conducted near downtown Los Angeles together with linear fits to the logarithm of the data the left axis. The solid red line indicates a 7.5%/year decrease, which equates to a 98% reduction in concentrations during the last 50 years. Figure reproduced from *Warneke et al*. (2012).

Similar anthropogenic VOC concentrations patterns are observed in urban areas throughout North America and in Asia [*Parrish et al.,* 2009] and in Europe [*Borbon et al.,* 2013]. Deviations from the common pattern can lead to conclusions regarding important characteristics of local sources. For example, *Borbon et al.* [2013] compared ambient VOC concentrations in France to those observed in the SoCAB during CalNex. They found that the emission ratios for C7–C9 aromatics in Paris are higher by a factor of 2–3 compared to the U.S. and other French and European Union urban areas, and traced the cause to the greater aromatic content of gasoline sold in the Paris region. A second example is ambient ethanol concentrations in the SoCAB, which have greatly increased in recent years due to the rapid increase in the ethanol content of gasoline (see more discussion in Finding B1.)

***Finding G2*: The individual VOC to CO emission ratios observed in the SoCAB can disagree by a factor of four or more with the ratios derived from NEI 2005 and CARB 2008 emission inventories. The agreement is particularly poor for oxygenated VOCs. Nevertheless, the difference between measurements and inventory in terms of the overall OH reactivity is within 15% of that from the CARB inventory, and the potential to form secondary organic aerosols (SOA) agrees within 35%.**

The urban emission ratios (ERs) of individual VOCs relative to CO generally agree within a factor of four (4) in the SoCAB (Figure G2a). The inventory ERs generally fall below the 1:1 line, particularly for the NEI 2005 [*US Environmental Protection Agency*, 2010], which is consistent with the inventory overestimate of CO emissions discussed in Finding F5. When comparing the ERs relative to acetylene (Figure G2b) and differences between the NEI 2005 inventory and observations are reduced by a factor of two (2) for most of the compounds. Figure G2c reports the ERs relative to CO color-coded by the VOC groups. The largest discrepancies are for the three oxygenated VOCs (OVOCs) specifically identified in the figure.

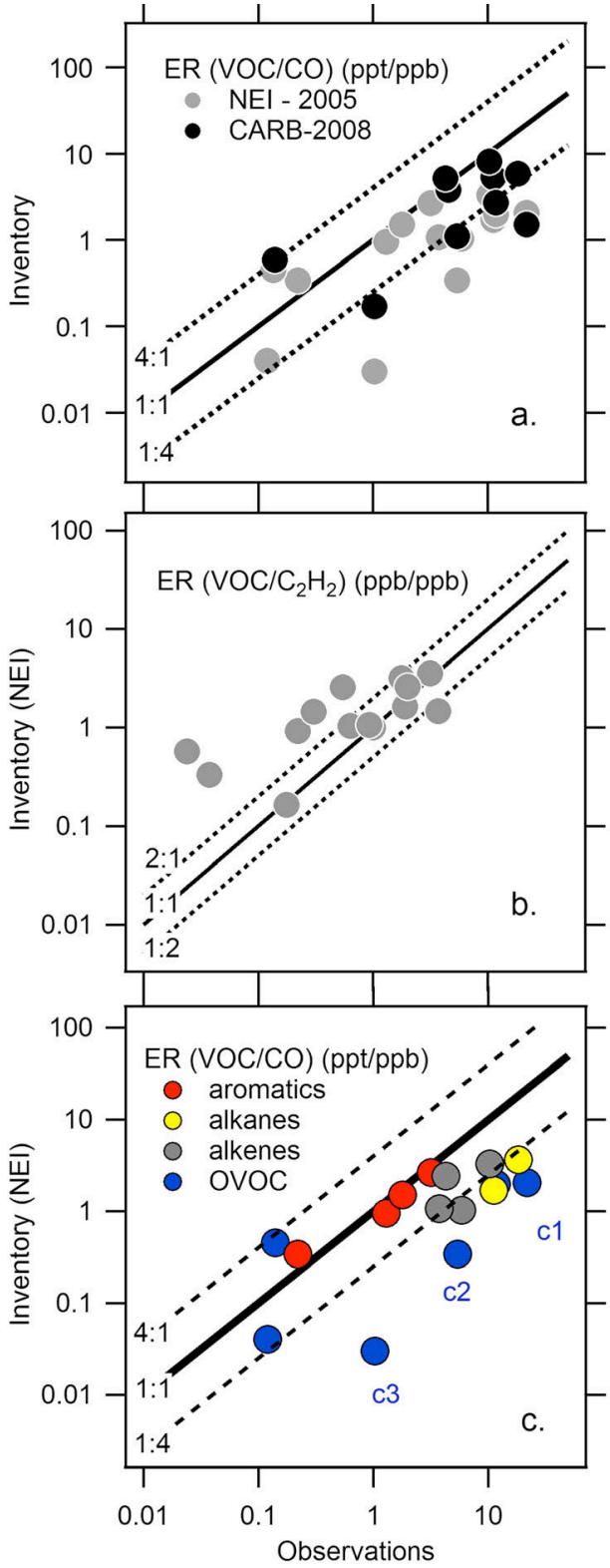

Figure G2. Comparison of measured emission ratios of VOCs relative to CO in a) and c) and to acetylene in b) versus the same ratios in two VOC emission inventories (NEI 2005 and CARB 2008) for the SoCAB. Abbreviations identifying specific species in panel c) are: c1, methanol; c2, acetaldehyde; and c3, benzaldehyde. Figure reproduced from *Borbon et al*. [2013].

Two metrics can be used to test how well the emission database reproduces the potential of sampled air masses to form ozone and secondary organic aerosol (SOA): 1) OH reactivity and 2) SOA formation potential. The OH reactivity is calculated by multiplying each compound's concentration by its OH rate coefficient, and summing over all individual VOCs included in the comparison (although this comparison is limited by the speciation in the inventory). Despite the large discrepancies between the individual ERs (Figure G2), the overall OH reactivity of the measured VOCs and the reactivity of the same compounds in the regional emission database per molecule of CO emitted agree within 15% (Figure G3, left panels) for the CARB 2008 inventory, but is in significantly greater disagreement with the NEI 2005 inventory. The OH reactivity is dominated by contributions from alkenes and aromatics, which are both well represented by the CARB 2008 inventory. The underestimate of OVOCs by the inventory primarily accounts for the underestimate of the total OH reactivity.

The secondary organic aerosol potential (SOAP) reflects the ability of each organic compound to form SOA on an equal mass emitted basis relative to toluene set to 100. As a class, the aromatics exhibit the greatest propensity to form SOA. The potential of SoCAB anthropogenic VOC emissions to form SOA (Figure G3, right panels) shows good agreement for the aromatics with an underestimate for the OVOCs, in this case primarily benzaldehyde.

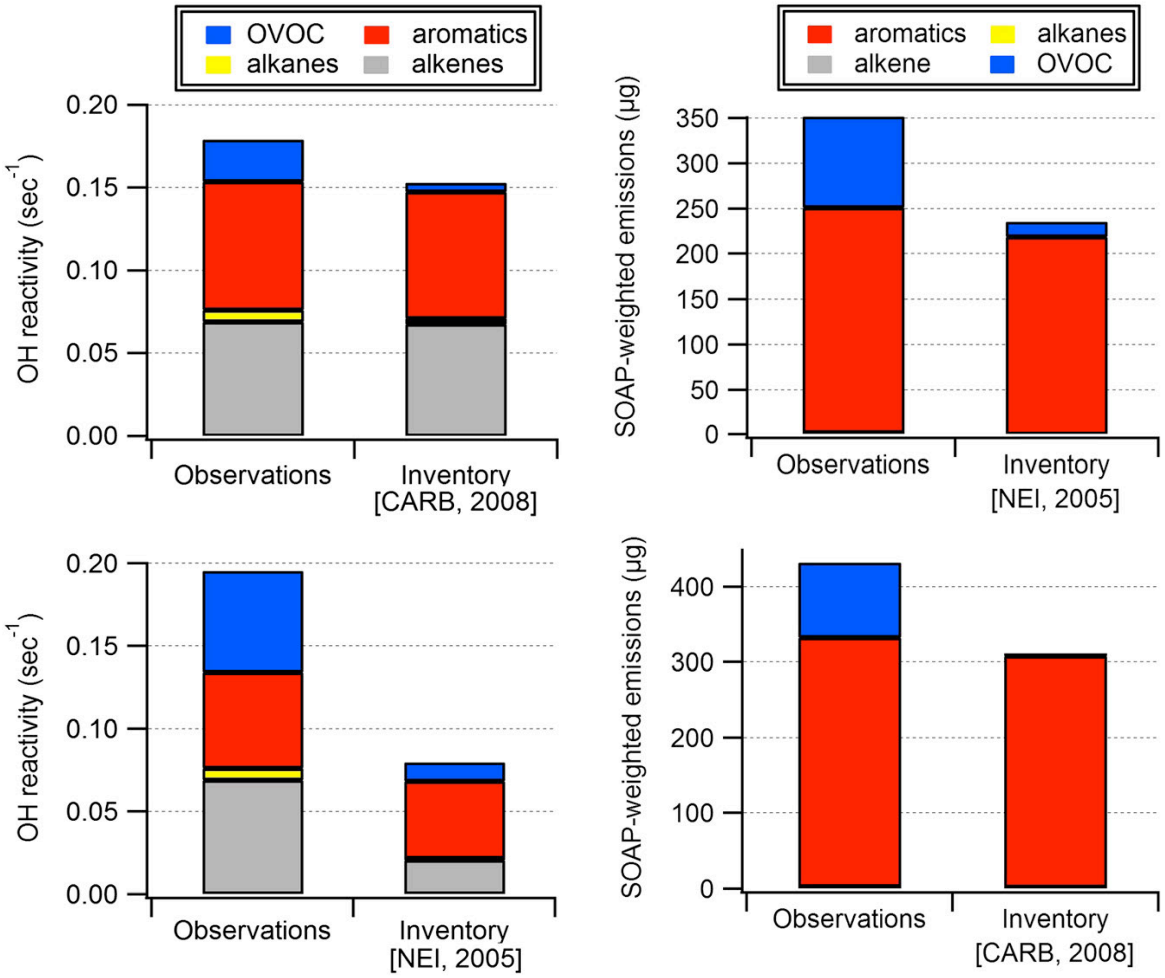

Figure G3. Sum of VOC reactivity with OH (left panel) and secondary organic aerosol formation potential (SOAP) (right panel) calculated from the emission ratios of anthropogenic VOCs and a CO enhancement of 100 ppb in the Los Angeles basin. Observed reactivity and SOAP (left-hand bars) are compared with the different emission database results (right-hand bars). The number and nature of the VOCs used in the comparisons are different depending on the speciation available in each inventory. Figure reproduced from *Borbon et al*. [2013].

***Finding G3*: Ambient benzene concentrations in the SoCAB have decreased more rapidly than concentrations of other VOCs, which is primarily attributed to efforts to remove benzene from gasoline due to its recognized toxicity.**

In the early 1990s, California implemented its Reformulated Gasoline Program. One goal of this program was to reduce the amount of benzene in gasoline, as it is a recognized air toxic contaminant. From 1960 to 2010, ambient benzene concentrations have decreased about twice as much (by a factor of ≈ 65) as the concentrations of other aromatics (factors of ≈ 32 and ≈ 37 for toluene and ethylbenzene, respectively). This difference is believed to reflect a success of California's Reformulated Gasoline Program, and is consistent with nationwide changes documented by *Fortin et al*. [2005].

References

Borbon, A., et al. (2013), Emission ratios of anthropogenic volatile organic compounds in northern mid-latitude megacities: Observations versus emission inventories in Los Angeles and Paris, *J. Geophys. Res. Atmos., 118,* 2041–2057, doi:10.1002/jgrd.50059.

CARB (2008), available at http://www.arb.ca.gov/ei/maps/basins/abscmap.htm.

Fortin, T.J., B.J. Howard, D.D. Parrish, P.D. Goldan, W.C. Kuster, E.L. Atlas, and R.A. Harley (2005), Temporal changes in U.S. benzene emissions inferred from atmospheric measurements, *Environ. Sci. Technol., 39,* 1403-1408.

Parrish, D.D., W.C. Kuster, M. Shao, Y. Yokouchi, Y. Kondo, P.D. Goldan, J.A. de Gouw, M. Koike and T. Shirai (2009), Comparison of air pollutant emissions among mega-cities, *Atmos. Environ., 43*, 6435-6441.

Pollack, I. B., T. B. Ryerson, M. Trainer, J. A. Neuman, J. M. Roberts, and D. D. Parrish (2013), Trends in ozone, its precursors, and related secondary oxidation products in Los Angeles, California: A synthesis of measurements from 1960 to 2010*, J. Geophys. Res. Atmos., 118*, 5893–5911, doi:10.1002/jgrd.50472.

US Environmental Protection Agency (2010), Technical support document: Preparation of emissions inventories for the Version 4, 2005-based platform, report, Washington, DC, 73 pp., available at: http://www.epa.gov/airquality/transport/pdfs/2005 emissions tsd 07jul2010.pdf.

Warneke, C., J. A. de Gouw, J. S. Holloway, J. Peischl, T. B. Ryerson, E. Atlas, D. Blake, M. Trainer, and D. D. Parrish (2012), Multi-year trends in volatile organic compounds in Los Angeles, California: five decades of improving air quality, *J. Geophys. Res., 117,* (D00V17), doi:10.1029/2012JD017899.

Yuan, B., et al. (2012), Volatile organic compounds (VOCs) in urban air: How chemistry affects the interpretation of positive matrix factorization (PMF) analysis, *J. Geophys. Res., 117,* D24302, doi:10.1029/2012JD018236.

Synthesis of Results - Emissions

Response to Question H

QUESTION H

Can emission estimates from area sources be improved with the CalNex measurements?

BACKGROUND

In general, area sources are defined as all stationary sources of air pollutants that are not identified as major point sources. This category excludes large industrial and power generation point sources, vehicle fleets, and natural sources, but includes all other sources. Though emissions from individual area sources are often relatively small, collectively their emissions can be of concern - particularly where large numbers of sources are located in heavily populated areas. Area sources thus include many broad categories of industrial, commercial and agricultural facilities.

POLICY RELEVANCE

The highly variable distribution, both spatially and temporally, of many pollutants makes estimates of their emissions from area sources some of the most uncertain in the inventory. Observation-based constraints on the quantification of these emissions are particularly valuable for improving the accuracy of emission inventories, and hence the reliability of modeling based upon these inventories.

Some area source emissions have already been discussed in the response to Question F. These emissions include methane and other small alkanes from the natural gas distribution system and oil and gas production in the SoCAB (see Finding F2a), methane from landfills and dairies in the SoCAB (see Finding F2b), methane and nitrous oxide from agricultural activities in the Central Valley (see Findings F2c and F3), and halocarbon emissions in the SoCAB (see Finding F4).

FINDINGS

***Finding H1*: Gaseous elemental mercury emissions from a variety of California sources were estimated, and these estimates generally agreed with inventoried emissions. An exception is that emissions from the Los Angeles urban area were much larger than those in the inventory; reemission of mercury accumulated over the industrialized history of Los Angeles could account for this discrepancy.**

Weiss-Penzias et al. [2013] measured gaseous elemental mercury (GEM) in the atmosphere during the R/V *Atlantis* cruise between San Diego and San Francisco. GEM was quantified in urban outflow, the Port of Los Angeles and associated shipping lanes, areas of high primary productivity in coastal upwelling, the San Francisco Bay, and the Sacramento ship channel. Mean GEM for the whole cruise was 1.41±0.20 ng m^{-3}, indicating that background concentrations were predominantly observed. When Los Angeles urban outflow was sampled, GEM displayed significantly higher concentrations that correlated with CO. Given the inventoried CO emissions for the region, the correlation slope suggests a LA urban GEM source of 1500 kg annually, which is about a factor of 10 larger than the total mercury emissions form

the SoCAB estimated by the 2008 California Air Resources Board inventory. A contributing factor to this disagreement could be reemission of GEM from land and vegetation surfaces of anthropogenic mercury accumulated over the industrialized history of Los Angeles. Although experimental studies of GEM reemission are sparse, models suggest that reemission is important globally, making an atmospheric contribution of a similar magnitude as emissions from primary anthropogenic sources [*Selin et al.*, 2007].

The emissions plume from a local waste incinerator in the Port of Long Beach was sampled several times by the R/V *Atlantis*. GEM emissions estimated from these plume encounters varied widely, suggesting that mercury-containing material was variable in the waste stream at this facility. An encounter with a plume from a large cargo ship allowed the estimation of GEM emissions from ocean ships worldwide of roughly 14 Mg y^{-1}, which is a minor contributor to global emissions (< 1% global anthropogenic sources), but may be an important local source in ports. GEM concentrations in the Carquinez Straits, where many large oil refineries are located, were rarely significantly above background concentrations. In an area where observed NO_X to SO_2 ratios indicated impacts from refinery emissions, the observed GEM concentrations were less than those predicted based on the 2008 California Air Resources Board inventory, indicating that GEM emissions may have been reduced.

In a region north of Monterey Bay known for upwelling and high primary productivity, GEM was positively correlated with dimethyl sulfide (DMS) in seawater and the atmosphere. Using the observed GEM/DMS relationship and an estimate of the DMS flux in areas of high primary productivity, a flux of GEM of 0.017 ± 0.009 μmol m^{-2} d^{-1} was estimated. This flux is on the upper end of previously reported GEM ocean-air fluxes, suggesting that more data are needed to understand the potential for extremely high GEM fluxes in regions affected by coastal upwelling.

References

Selin, N. E., D. J. Jacob, R. J. Park, R. M. Yantosca, S. Strode, L. Jaeglé, and D. Jaffe (2007), Chemical cycling and deposition of atmospheric mercury: Global constraints from observations, *J. Geophys. Res., 112*, D02308, doi:10.1029/2006JD007450.

Weiss-Penzias, P. S., E. J. Williams, B. M. Lerner, T. S. Bates, C. Gaston, K. Prather, A. Vlasenko, and S. M. Li (2013), Shipboard measurements of gaseous elemental mercury along the coast of Central and Southern California. *J. Geophys. Res. Atmos., 118*, 208–219, doi:10.1029/2012JD018463.

Synthesis of Results - Emissions

Response to Question I

QUESTION I

What are the relative roles and impacts of NH_3 emissions from motor vehicles and dairy farms?

BACKGROUND

Ammonium nitrate (NH_4NO_3) aerosol is a major, and often the primary, contributor to atmospheric PM2.5 concentrations in California. It is semi-volatile and continuously partitions between the gas and aerosol phase. The distribution of total ammonium ($NH_3 + NH_4^+$) and total nitrate ($NO_3^- + HNO_3$) between the gas and aerosol phases is sensitive to meteorological factors such as temperature and relative humidity. Major sources of ammonia in California are livestock operations including dairies, agricultural fertilizers, waste management facilities, and motor vehicles, while HNO_3 is an oxidation product of NO_X, primarily emitted by mobile sources.

POLICY RELEVANCE

PM2.5 currently exceeds ambient air quality standards in California. Development of effective strategies for controlling the nitrate contribution to PM2.5 depends upon determining whether available NH_3 or HNO_3 limits the amount of NH_4NO_3 that can be formed, and what are the major sources of the limiting reactant.

FINDINGS

***Finding I1*: Within the SoCAB, conditions observed downwind of the dairy facilities were always thermodynamically favorable for NH_4NO_3 formation due to high NH_3 mixing ratios from those concentrated sources. Although automobile emissions of NH_3 within the basin were of approximately the same magnitude as the dairies, they were more dispersed and thus generated lower NH_3 mixing ratios. However, they are sufficiently high that they can thermodynamically favor NH_4NO_3 formation. Reducing the dairy NH_3 emissions would have a larger impact on reducing SoCAB NH_4NO_3 formation than would reducing automobile NH_3 emissions.**

Nowak et al. [2012] used airborne measurements from the NOAA WP-3D to quantify NH_3 emissions from both automobile and dairy facility sources in the LA basin. This analysis compared these two emission sources to state and federal emission inventories, and assessed the impact of these NH_3 sources on particulate ammonium nitrate (NH_4NO_3) formation. The estimated NH_3 emissions from automobiles (62±24 metric tons per day) were similar in magnitude to those from the dairy facilities (estimates from two flights were 33±16 and 176±88 metric tons per day). CARB's 2012 PM2.5 SIP inventory shows significantly lower NH_3 emission estimates for the SoCAB: 19 metric tons per day from on-road vehicles and 12 metric tons per day for dairies. It must be noted that the CARB estimate for dairy emissions are based on a winter emission factor; a summer emission factor would probably yield higher estimates. The high emission rates from the spatially concentrated dairy facilities led to a larger impact on NH_4NO_3 particle formation, with the calculated gas-particle equilibrium favoring the particle phase in plumes downwind of the dairy facilities (points above black line in Figure I1). This

paper suggested that NH_3 control strategies addressing dairy rather than automobile emissions would have the larger effect on reducing particulate NH_4NO_3 formation in the Los Angeles basin.

To simulate atmospheric concentrations of gas- and aerosol-phase species in the SoCAB during the CalNex study period, *Ensberg et al.* [2013] applied a detailed CMAQ three-dimensional chemical transport model with boundary conditions extracted from a nested global-scale GEOS-Chem model. Comparison of the simulation with observations at ground sites and from aircraft corroborated the conclusions of *Nowak et al.* [2012], but also showed that NH_3 mixing ratios can be under-predicted by factors as high as 100 to 1000. Severe under-prediction of NH_3 emissions from dairy facilities is identified as the dominant source of measurement/model disagreement in the eastern Los Angeles basin.

The cause of the day-to-day variability in dairy farm NH_3 emissions seen in the two P-3 flights [*Nowak et al.*, 2012] is not fully understood. Understanding variability of the magnitude suggested by the WP-3D data may result in an improved ability to address NH_3 emissions, and thus particulate ammonium nitrate formation in the LA basin, via dairy farm management practices. These sources may be a good target for a longer-term, ground-based emissions monitoring effort to better quantify and understand the drivers for such variability. *Ensberg et al.* [2013] suggest that adding gas-phase NH_3 measurements and size-resolved measurements, up to 10 μm, of nitrate and various cations (e.g. Na^+, Ca^{2+}, K^+, Mg^{2+}) to routine monitoring stations in the L.A. basin would greatly facilitate interpreting day-to-day fluctuations in fine and coarse inorganic aerosol.

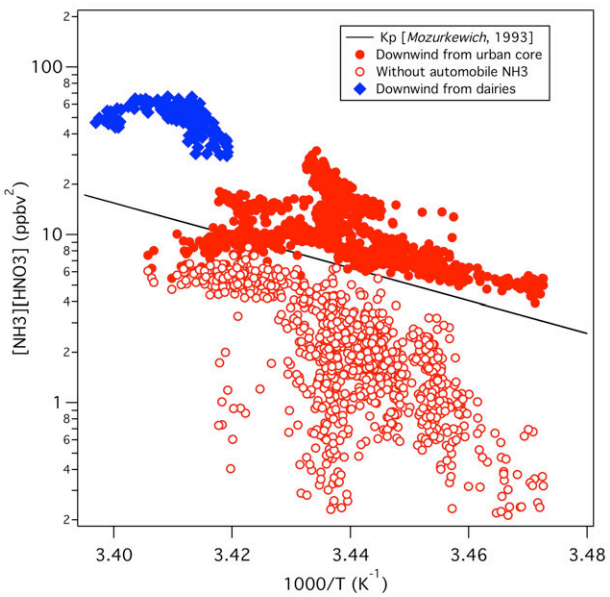

Figure I1. The theoretical solid NH_4NO_3 dissociation constant (K_p) (black line), the observed urban core NH_3 and HNO_3 partial pressure product (solid circles), the estimated urban core NH_3 and HNO_3 partial pressure product without automobile NH_3 emissions (open circles), and the observed NH_3 and HNO_3 partial pressure product in the dairy plumes (blue diamonds) for the 14 May flight plotted as a function of ambient temperature. Formation of particulate NH_4NO_3 is favored when points are above the line, and the gas-phase NH_3 and HNO_3 when points are below the line. The range of the abscissa corresponds to 14 °C on the right and 22 °C on the left.

***Finding I2a*: Within the San Joaquin Valley, despite large concentrations of NH_3 (often many 100's of ppbv) associated with dairies, measured NH_4NO_3 concentrations were relatively low (≤ 4 μg/m^3) due to low HNO_3 concentrations resulting from low NO_X emissions.**

***Finding I2b*: Preliminary results indicate that within the San Joaquin Valley, NH_3 emissions could be underestimated in inventories by about a factor of three.**

Analysis: J.B. Nowak (presentation at ACS National Meeting, August 2012, Philadelphia)

A limited number of WP-3D flights in the Central Valley during CalNex provided an initial look at NH_3 emissions and subsequent NH_4NO_3 formation in the spring (i.e., May). Figure I2 presents the observed concentrations of the NH_4NO_3 precursors, NH_3 and HNO_3. NH_3 concentrations were much higher (up to 100's of ppbv) in the San Joaquin Valley (SJV) than in SoCAB, but NH_4NO_3 concentrations were not particularly elevated (maximum ~ 4 $\mu g/m^3$), and were lower than the maximum concentrations observed in SoCAB (~ 11 $\mu g/m^3$). The concentrations of NH_4NO_3 formed were limited by relatively small NO_X emissions in SJV, and by the magnitude of NH_3 emissions in SoCAB.

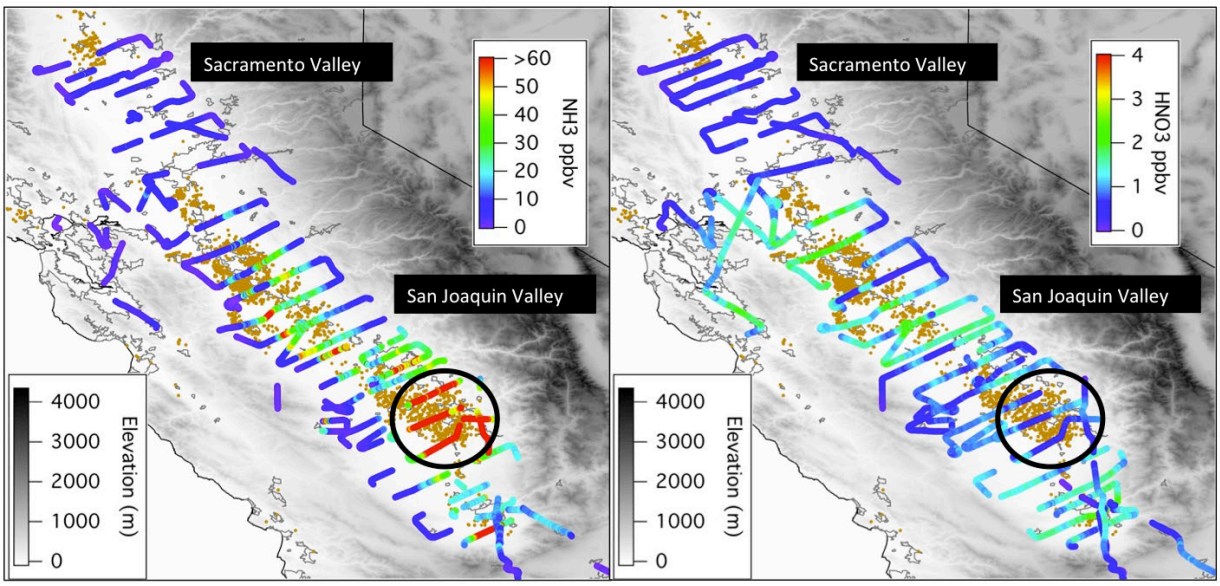

Figure I2. Flight tracks of the NOAA WP-3D aircraft in the Central Valley within the planetary boundary layer during CalNex (May 7, 11, and 12). The color-coding indicates the measured ammonia (left panel) and nitric acid (right panel) mixing ratios. The small orange circles indicate livestock facilities.

Measurements from the Bakersfield surface site are generally consistent with the WP-3D aircraft results [*Murphy*, 2012]. The NH_3 concentrations and the $(NH_3 + NH_4^+)/NO_Y$ ratio were much higher than seen in the SoCAB, and NH_3 sources were clearly dominated by area emissions from agricultural activities. The correlation between NH_3 and CO was weak indicating a relatively small contribution of mobile NH_3 emissions in the SJV.

The May 12, 2010 flight in the northern San Joaquin Valley was conducted under suitable meteorological conditions (relatively constant northwesterly winds and a well defined, stable boundary layer) to allow a preliminary estimate of the total ammonia emissions from the region. Figure I3 indicates the flight track and measured ammonia concentrations. The ammonia flux at each crosswind transect (indicated in Figure I3a) was calculated from the product of the wind speed, boundary layer depth, and integrated ammonia concentration. Figure I3b shows the increasing NH_3 flux as air moves downwind over the emission region. The total ammonia flux measured from the area enclosed by the blue rectangle in Figure I3a is ~ 550 metric tons/day, which is a factor of ~3 larger than the integrated emissions from inventories (118 and 170 metric tons/day from the NEI 2005 and CARB-ARCTAS 2008 inventories, respectively). Care must be

taken in interpreting this comparison, as the measurements represent a single springtime, mid-day period, and thus cannot account for seasonal or diurnal variations.

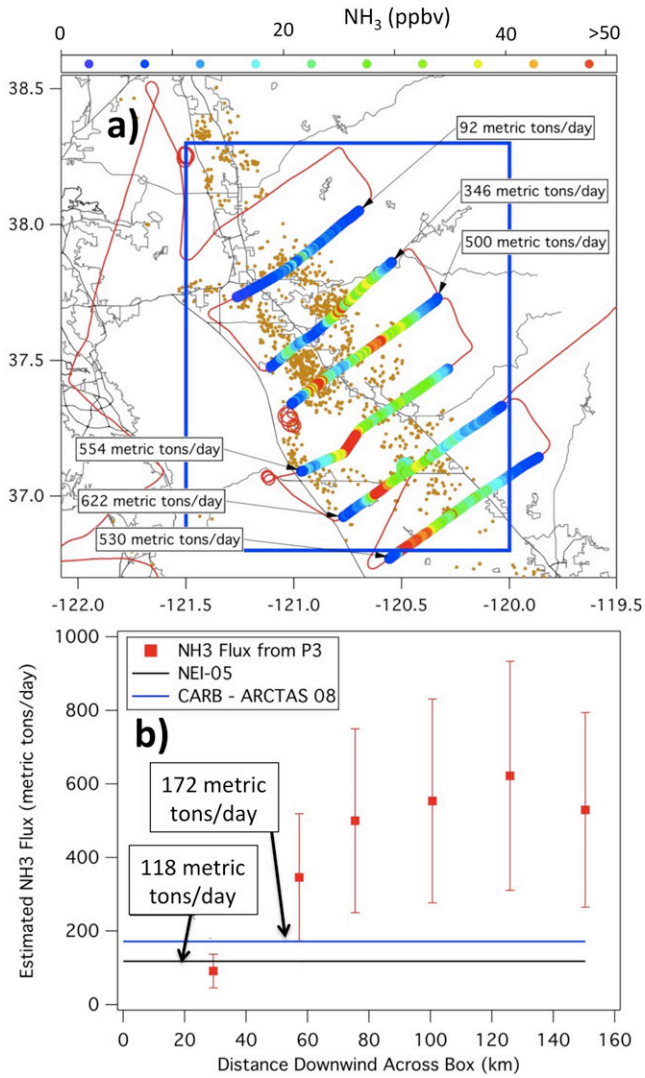

Figure I3. a) Flight track of the NOAA WP-3D aircraft in the northern San Joaquin Valley within the planetary boundary layer on May 12. The color-coding indicates the measured NH_3 concentrations. The small orange circles indicate livestock facilities. The NH_3 flux measured on each transect is indicated. **b)** The measured NH_3 flux as a function of downwind distance compared to the total emissions integrated over the blue rectangle indicated in a) from two emissions inventories.

***Finding I3*: Within the San Joaquin Valley, the large concentrations of NH_3 enhance SOA formation in the atmosphere, likely due to reactions between NH_3 and carboxylic acids.**

Zhao et al. [2013a] have shown that SOA production from phthalic acid can be substantially increased by reactions with NH_3 forming ammonium salts that have much lower volatility, favoring their partitioning into OA. PMF analysis of organic species, including phthalic acid as an organic tracer, also implies that these reactions between NH_3 and carboxylic acids play a significant role in SOA formation [Zhao et al., 2013b]. Reducing the emissions of pollutants involved in these pathways of gas-to-particle partitioning, such as ammonia and organic precursors, are expected to lead to reductions in OA concentrations. However, the potential effectiveness of the reduction in SOA concentrations by controlling ammonia requires further investigation. For example, the reduction in NH_3 emissions would also lead to an increase of aerosol, acidity, which subsequently could enhance the SOA formation from particle-phase reactions.

References

Ensberg, J. J., et al. (2013), Inorganic and black carbon aerosols in the Los Angeles Basin during CalNex, *J. Geophys. Res. Atmos., 118*, doi:10.1029/2012JD018136.

Murphy, J., (2012), personal communication, University of Toronto.

Nowak, J. B., J. A. Neuman, R. Bahreini, A. M. Middlebrook, J. S. Holloway, S. A. McKeen, D. D. Parrish, T. B. Ryerson, and M. Trainer (2012), Ammonia sources in the California South Coast Air Basin and their impact on ammonium nitrate formation, *Geophys. Res. Lett., 39*, L07804, doi:10.1029/2012GL051197.

Zhao et al. (2013a), Insights into Secondary Organic Aerosol Formation Mechanisms from Measured Gas/Particle Partitioning of Specific Organic Tracer Compounds, *Environ. Sci. & Tech.*, doi:10.1021/es304587x.

Zhao, Y., et al. (2013b), Sources of organic aerosol investigated using organic compounds as tracers measured during CalNex in Bakersfield, *J. Geophys. Res. Atmos., 118*, doi:10.1002/jgrd.50825.

Synthesis of Results - Emissions

Response to Question J

QUESTION J

Are there significant differences between emissions in the San Joaquin Valley Air Basin (SJVAB) and the South Coast Air Basin (SoCAB)?

BACKGROUND

By some metrics, the improvement of air quality in the SoCAB has been faster than in the SJVAB (e.g., see Figure 1 in the Introduction). One possible cause of this difference may be due to a different mix of emissions between the two regions.

POLICY RELEVANCE
Most mobile source emission controls are applied uniformly across California. However, there are indications that the response of pollutant concentrations to these emission controls may differ among regions of the State. When there are important regional differences in emissions, then regional/local emphasis of area and stationary emission controls may more effectively reduce pollutant concentrations.

FINDINGS

***Finding J1*: NO_X emissions from the on-road vehicle fleet have decreased more rapidly in the SoCAB than in the SJVAB.**

McDonald et al. [2012] show that total NO_X emissions from gasoline and diesel-powered on-road vehicles in the SoCAB and the SJVAB have differed in their time response between 1990 and 2010 (Figure J1, also included in this report as Figure F3). In the SoCAB, NO_X emissions decreased continuously by more than a factor of 2 through the period, while in the SJV NO_X emissions initially increased, reaching a peak near 2000, and only dropping below the 1990 level at the start

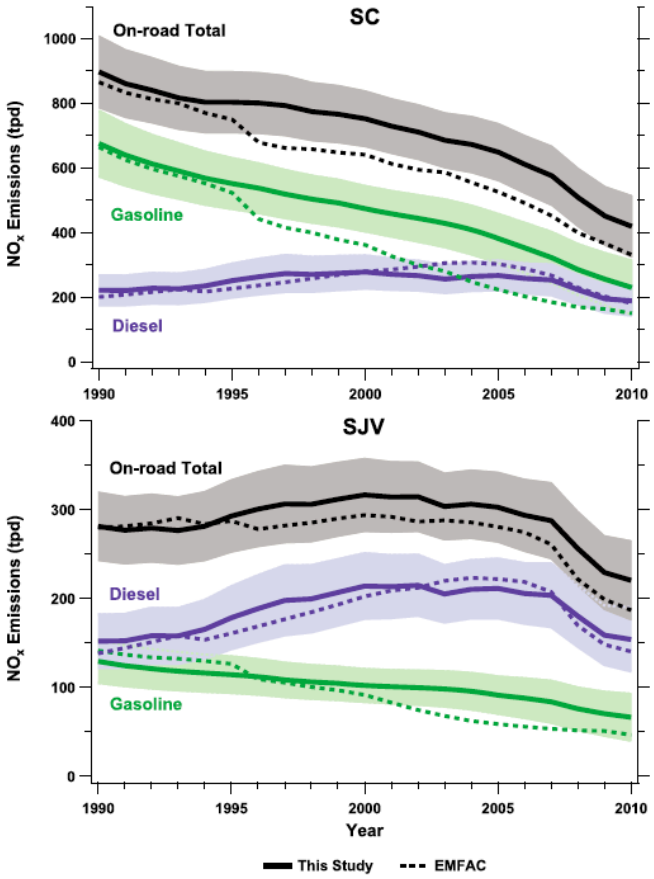

Figure J1. Trends in NO_X emissions from on-road vehicles in the South Coast Air Basin (SC) and the SJV. Shaded areas represent uncertainties of estimates. Dotted lines show estimates from EMFAC (Figure taken from *McDonald et al*. [2012]).

of the recession in 2008. This is largely caused by differences in the vehicle fleet mixes, with diesel vehicles being more common in the SJV than in the SoCAB (~25% vs. 15% of total fuel sold, respectively). The time variation of the emissions from these two vehicle classes has differed markedly in California. Diesel NO_X emissions increased between 1990 and 1997, stabilized between 1997 and 2007, and decreased since 2007, while gasoline NO_X emissions decreased steadily, by 65% overall between 1990 and 2010. A secondary cause of this regional difference is a slower decrease of NO_X emissions from gasoline vehicles due to a larger percentage population increase in the SJVAB than in SoCAB.

***Finding J2*: There is evidence that temperature dependent VOC emissions from an unidentified source, perhaps associated with agricultural activities and petroleum operations, are important in the SJVAB but absent in the SoCAB.**

Analysis of historical data from the SJVAB [*Pusede and Cohen,* 2012; *Pusede et al.,* 2013] shows that the NO_X versus VOC sensitivity of the O_3 photochemistry changes markedly with ambient temperature, becoming much more NO_X sensitive on the hottest days, which are also the days that lead to most O_3 exceedances in this air basin. CalNex measurements from the Bakersfield site (Figure J2) have been analyzed to identify the cause of this change in photochemical regime as a particular VOC source that is rich in oxygenated VOCs [*Pusede et al.,* 2013]. The temperature dependence of the ambient concentrations of some oxygenated VOCs (Figure J2a illustrates one example) provides some of the support for this identification; their rapid increase with temperature provides more photochemical fuel and larger VOC to NOx ratios on hot days. In addition, the measured reactivity of OH radicals with VOCs (an indication of the photochemical regime) shows a similar rapid increase with temperature (Figure J2b). Notably, at lower temperatures, the measured OH reactivity agrees with that calculated from the measured VOC concentrations, indicating that all VOCs important for O_3 production at

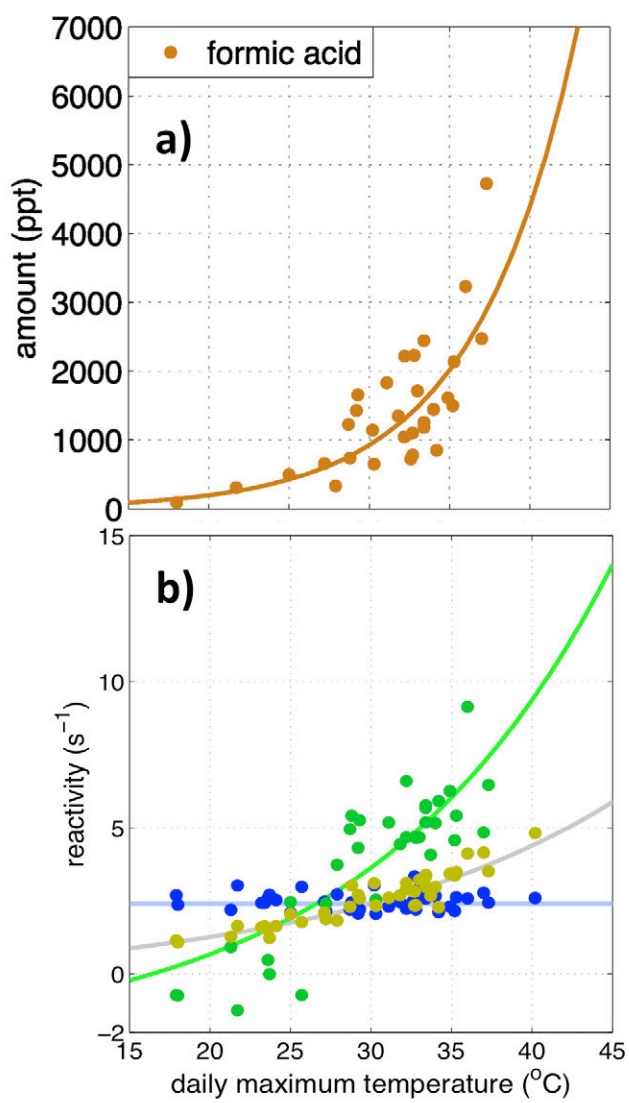

Figure J2. Temperature dependence of: **a)** formic acid concentrations, and **b)** reactivity of organic compounds with OH radicals at the Bakersfield site during CalNex 2010. Panel **b)** shows daily average reactivity (with fits) for sum of temperature-independent organic species (blue), sum of temperature-dependent organic species (yellow), and the directly measured OH reactivity with the contributions from inorganic and temperature-independent organic species subtracted (green). Panel **a)** taken from *Cohen et al*., [2013], and panel **b)** adapted from *Pusede et al*. [2013].

those temperatures are measured. However, at higher temperatures the measured VOCs can account for only about half of the measured OH reactivity, pointing to the importance of unmeasured VOCs. The reactivity contribution of these unmeasured VOCs is equal to the difference between the green and yellow fits in Figure J1b.

The measured reactivity of OH radicals with VOCs behaves very differently in the SoCAB compared to the SJV (Figure J2) as evidenced by the measurements from the Pasadena ground site [*Stevens*, 2013]. First, at all temperatures the measured OH reactivity agrees well (generally about 20% greater) with that calculated from the measured VOC concentrations, and second the relatively small difference between the measured reactivity and that calculated from the measured VOC concentrations does not vary significantly with temperature. Evidently the important, temperature dependent source of VOC emissions in the SJV is not present in the SoCAB.

The source of the oxygenated VOCs in the SJV has not been firmly established. The intense agricultural activity in the SJVAB that is not present in the SoCAB may indicate that this source leads to a significant difference in emissions between the air basins. However, our understanding of the source of these species is not sufficient to design a strategy aimed at controlling these VOC emissions in the southern SJVAB. Thus, NO_X controls are currently the only option for reducing high temperature violations of the O_3 standard in the SJVAB. The analysis of *Pusede and Cohen* [2012] and *Pusede et al.* [2013] indicates that such NO_X controls would be effective. Indeed, they conclude that widespread NO_X reductions are approaching the point where O_3 reductions throughout the entire SJVAB will be a direct consequence of NO_X emission reductions. The effectiveness has been and will be dependent on temperature; at the highest temperatures, where violations of state and federal standards are most frequent, NO_X controls will be most effective.

Gentner et al. [2013a] find that at Bakersfield, petroleum and dairy operations each comprised 22-23% of anthropogenic non-methane organic carbon and were each responsible for ~12% of potential precursors to ozone, but their impacts as potential SOA precursors were estimated to be minor. A rough comparison with the *CARB* [2010] emission inventory supports the quantification of the relative emissions of reactive organic gases provided by the inventories. The SoCAB does receive emissions from oil and gas production [*Peischl, et al.,* 2013], but of a much smaller magnitude. *Gentner et al.* [2013b] find that the mass of biogenic emissions from agricultural crops during the summer and the potential ozone and secondary organic aerosol formation from these emissions are on the same order as anthropogenic emissions from motor vehicles.

***Finding J3*: The relative amounts of ammonia and NO_X emissions are such that formation of ammonium nitrate aerosol (the major component of PM2.5 during many exceedance episodes) is ammonia-limited in the SoCAB and NO_X-limited in the SJVAB.**

Analysis: This material is taken from Nowak et al. (2012a,b).

As fully discussed in the Response to Question I, the relatively large NO_X emissions from the vehicle fleet and the relative small ammonia emissions from dairies and vehicles in the SoCAB causes the formation of ammonium nitrate aerosol to be NH_3-limited. In the SJVAB, the intense agricultural activities and smaller vehicle emissions causes the relative emission magnitudes to be reversed so that the formation of ammonium nitrate aerosol is NO_X-limited.

References

Cohen, R. C., et al. (2013), SJV Air Quality: Insights from CalNex 2010, ARB Chair's Research Seminar, 22 April 2013 (http://www.arb.ca.gov/research/seminars/cohen3/cohen3.pdf).

Gentner, D.R., et al. (2013a), Emissions of organic carbon and methane from petroleum and dairy operations in California's San Joaquin Valley, *Atmos. Chem. Phys. Disc., 13*, 28225-28278.

Gentner, D.R., E. Ormeno, T.B. Ford, S. Fares, R. Weber, J.H. Park, J.F. Karlik, A.H. Goldstein (2013b), Emissions of Terpenoids, Benzenoids, and Other Biogenic Gas-phase Organic Compounds from Agriculture and their Potential Implications for Air Quality, *Atmos. Chem. Phys. Disc., 13*, 28343-28393.

McDonald, B. C., T. R. Dallmann, E. W. Martin, and R. A. Harley (2012), Long-term trends in nitrogen oxide emissions from motor vehicles at national, state, and air basin scales, *J. Geophys. Res.*, *117*, D00V18, doi:10.1029/2012JD018304.

Nowak, J. B., J. A. Neuman, R. Bahreini, A. M. Middlebrook, J. S. Holloway, S. A. McKeen, D. D. Parrish, T. B. Ryerson, and M. Trainer (2012a), Ammonia sources in the California South Coast Air Basin and their impact on ammonium nitrate formation, *Geophys. Res. Lett., 39*, L07804, doi:10.1029/2012GL051197.

Nowak, J. B. (2012b), Ammonia Emissions from Agricultural Sources and their Implications for Ammonium Nitrate Formation in California, presentation at ACS National Meeting, August 2012, Philadelphia, PA.

Peischl, J., et al. (2013), Quantifying sources of methane using light alkanes in the Los Angeles basin, California, *J. Geophys. Res. Atmos., 118*, 4974–4990, doi:10.1002/jgrd.50413.

Pusede, S. E., and R. C. Cohen (2012), On the observed response of ozone to NOx and VOC reactivity reductions in San Joaquin Valley California 1995–present, *Atmos. Chem. Phys.*, *12*, 8323–8339, doi:10.5194/ acp-12-8323-2012.

Pusede, S. E., et al. (2013), On the temperature dependence of organic reactivity, ozone production, and the impact of emissions controls in San Joaquin Valley California, *Atmos. Chem. Phys. Disc*, *13*, 28511–28560, doi:10.5194/acpd-13-28511-2013.

Stevens, P., (2013), personal communication, Indiana University.

Synthesis of Results - Emissions

Response to Question K

QUESTION K

What are the significant sources of sulfur in southern California that contribute to enhanced sulfate ($SO_4^=$) concentrations in SoCAB?

Sulfate constitutes a significant fraction of ambient PM2.5 concentrations in the SoCAB, an air basin that exceeded the NAAQS on an estimated 8 to 19 days in each of the years 2008-2012. The sulfate contribution is particularly large in summer in the SoCAB (see Figure C2).

POLICY RELEVANCE
Due to ongoing control efforts, SO_X emissions and corresponding sulfate concentrations have decreased in the SoCAB. An understanding of Southern California's remaining sulfur sources is necessary to formulate effective policies to further reduce this PM2.5 constituent.

California has made substantial efforts to reduce sulfur emissions from point sources, from the on-road vehicle fleet by reducing the sulfur content of gasoline and diesel fuel, and from commercial marine vessels by requiring use of low-sulfur fuel and low-speed operation within Regulated California Waters (up to 24 nautical miles of the California coastline). The 2008 CARB emission inventory estimates that total SO_X emissions in the SoCAB decreased from 51.2 tons in 2000 to 38.0 tons in 2008.

During CalNex, sulfur dioxide (SO_2, the primary sulfur species emitted by anthropogenic sources) and dimethylsulfide (DMS, a major sulfur species released by natural sources) were measured throughout the SoCAB by the WP-3D aircraft and at the Pasadena ground site; the R/V *Atlantis* also measured SO_2 in California ports and coastal waters.

FINDINGS

***Finding K1*: No significant sources of sulfur beyond those included in the CARB inventory could be identified from the CalNex 2010 data.**

The measurements in Figure K1 illustrate emissions from the two major SO_2 source classes impacting the SoCAB that could be identified from the CalNex 2010 data: point source industrial emissions in the vicinity of the Port of Long Beach and commercial marine vessels. Although it is not possible to quantify the Long Beach point source emissions from the WP-3D aircraft data, it is clear that the emissions in 2010 were significantly reduced from those observed in 2002, qualitatively consistent with the reductions included in the CARB inventory. The ship emission data included in Figure K2 are those collected by the WP-3D reported by *Lack et al.* [2011] while the marine vessel was operating on high sulfur fuel. The slope of the line (10.6 ± 0.5 ppbv SO_2 / ppmv CO_2) is consistent with the 3.1% sulfur fuel content reported by the vessel. These emissions represent marine vessel operation outside of the Regulated California Waters. When the vessel switched to low-sulfur fuel and low-speed operation, sulfur emissions dropped by 96% [*Lack et al.,* 2011], indicating that the marine vessel regulations are highly effective.

Within the urban areas of the SoCAB, it was not possible to identify and quantify emissions from the on-road vehicle fleet. At the Pasadena ground site, both surface measurements and DOAS measurements at elevated altitudes through the boundary layer [*Ryerson et al.,* 2013] generally found low concentrations (average ± standard deviation = 0.3 ± 0.3 ppbv), with only occasional peaks increasing to a maximum of 3.4 ppbv. Any on-road vehicle emissions could not be differentiated from small contributions from point source plumes transported to Pasadena from industrial facilities or marine vessels.

DMS emissions from oceanic sources do not make a significant contribution to the sulfate burden in the SoCAB. DMS measurements at Pasadena were very low (average ± standard deviation = 0.010 ± 0.016 ppbv, with a maximum of 0.13 ppbv). The WP-3D aircraft measured within the SoCAB and over coastal waters, but did not encounter any concentrations greater than 0.4 ppbv. With a lifetime on the order of a day, the DMS contribution to the SoCAB sulfate burden cannot be large (average roughly estimated as less than 0.1 $\mu g/m^{-3}$).

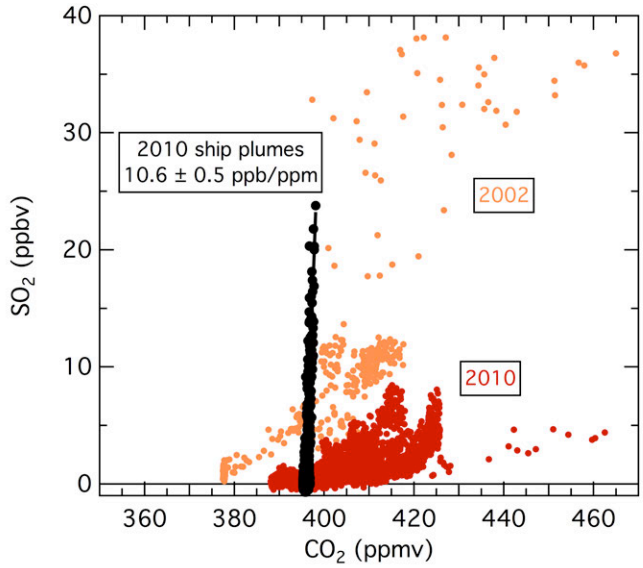

Figure K1. Dependence of SO_2 on CO_2 in the Long Beach area and in offshore ship plumes. The WP-3D aircraft collected the Long Beach data during a single flight in 2002 (orange symbols) and four flights in 2010 (red symbols). The ship plume data (black symbols) were collected in the ship emission study reported by *Lack et al*. [2011] outside Regulated California Waters. The black line indicates the linear least squares fit to the ship plume data, with the slope annotated. (Figure from *J. Holloway*, NOAA)

References

Lack, D. A., et al. (2011), Impact of fuel quality regulation and speed reductions on shipping emissions: Implications for climate and air quality, *Environ. Sci. Technol., 45*, 9052–9060, doi:10.1021/es2013424.

Ryerson, T.B., et al. (2013), The 2010 California Research at the Nexus of Air Quality and Climate Change (CalNex) field study, *J. Geophys. Res. Atmos., 118*, 5830–5866, doi:10.1002/jgrd.50331.

Synthesis of Results - Emissions

Response to Question L

QUESTION L

What is the impact of biogenic emissions, especially in foothills of the Sierra Nevada?

BACKGROUND

On a global scale, emissions of VOCs from vegetation are estimated to be an order of magnitude greater than those anthropogenic sources [*Guenther et al.,* 1995]. In forested rural environments [*Trainer et al.,* 1987] and even in some urban areas [*Chameides et al.,* 1988], biogenic VOCs have been shown to dominate over anthropogenic VOCs in photochemical O_3 production. They are also thought to play a major role in SOA formation, a role that may involve interaction between biogenic VOCs and anthropogenic NO_X emissions [e.g., *Hoyle et al.*, 2011].

Quantifying the impact of biogenic species on O_3 and SOA production is difficult because the emissions are highly variable, dependent upon vegetation density and plant species as well as a variety of meteorological parameters including temperature, sunlight intensity and drought stress. Up to the present time, isoprene (primarily from deciduous vegetation) and monoterpenes (primarily from coniferous trees) are the biogenic species that have received the most attention in atmospheric chemistry research, but it is suspected that there are many more biogenic species whose emissions may be important [e.g., *Goldstein and Galbally*, 2007], including those from agricultural sources [e.g., *Fares et al.*, 2012].

POLICY RELEVANCE

Biogenic emissions of VOCs represent a natural source of fuel for photochemical production of O_3 and SOA formation, a source that largely cannot be regulated. It is important to quantify the emissions and the roles of these VOCs in order to accurately evaluate the effectiveness of policy-mandated reductions of emissions of anthropogenic VOCs and NO_X.

FINDINGS

***Finding L1a*: Photochemical O_3 formation in the SoCAB is dominated by anthropogenic VOCs rather than biogenic VOCs; this was true in 2010 despite very substantial reductions in anthropogenic VOC emissions over past decades.**

***Finding L1b*: Considering only the individually measured VOCs, photochemical O_3 formation in the SJVAB is also dominated by anthropogenic VOCs. However, on the hotter days in the SJVAB there is evidence that additional VOCs make an important contribution to O_3 formation, and this contribution well may be of biogenic origin.**

The OH reactivity of organic species provides a measure of the O_3 photochemical formation potential of ambient pollutant concentrations. Figure L1 compares the OH reactivity for species measured at the Pasadena and Bakersfield sites during CalNex 2010. Considering all species (with all VOCs considered together), the relative contributions of the different species (left

panels in Figure L1) are quite similar at the two sites, although the median total reactivity was about 60% higher in Pasadena.

The measured biogenic VOCs (green segments in the four plots to the right) account for a relatively small and similar fraction of the total organic OH reactivity at each site (12-16%). However, at Pasadena, the biogenic contribution peaked at midday (upper right panel in Figure L1), when O_3 production is at its maximum, while at Bakersfield the biogenic contribution remained approximately constant throughout the day and night (lower right panel in Figure L1). Thus, the directly measured biogenic species make a larger contribution to photochemical O_3 production at the Pasadena site compared to the Bakersfield site. However it is important to consider the difference between the total, directly measured OH reactivity at the Bakersfield site and the reactivity calculated from the sum of the individually measured VOCs. *Pusede and Cohen* [2012] and *Pusede et al.* [2013] show that there is a large contribution to total VOC reactivity due to unmeasured VOCs, especially on the hotter days (see more detailed discussion in the Response to Question J). If these unmeasured species are of biogenic origin, such as dairy emissions or other biogenic sources, then the importance of biogenic VOCs would be underestimated by the analysis in Figure L1. Importantly, at Pasadena a similar difference was not observed between total OH reactivity and that calculated from the individually measured VOCs.

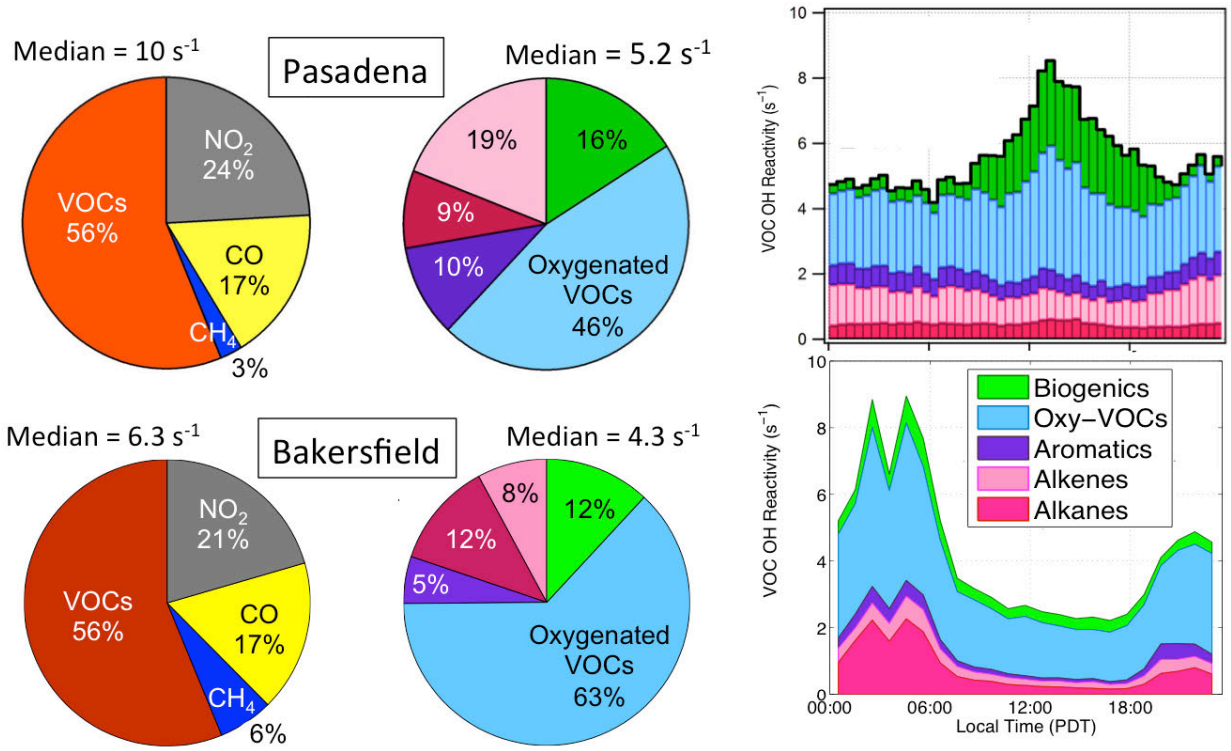

Figure L1. OH reactivity for all species (left) and organic species only (middle) at the Pasadena (top) and Bakersfield (bottom) sites, based on the median measured concentrations throughout the day. The diurnal variability of the VOC reactivity and its speciation is shown on the right. The color code for the VOC species are annotated in lower right panel. Biogenic species include isoprene, MVK and MACR. Oxygenated species include ethanol, formaldehyde and acetaldehyde; the latter two may include a contribution produced from the oxidation of isoprene. (Figure from *J. Gilman, NOAA and S. Pusede, Univ. Cal., Berkeley*)

***Finding L2*: Biogenic VOCs play significant roles in SOA formation in the Central Valley during both daytime and nighttime; the different processes important during light and dark periods both involve interactions between biogenic VOCs and anthropogenic emissions.**

Rollins et al. [2012] identified substantial secondary organic aerosol (SOA) production at night at the Bakersfield site. SOA was produced from the reaction of the NO_3 radical (a nighttime oxidation product of anthropogenic NO_X emissions) with unsaturated VOCs of biogenic origin. At this site, SOA concentrations peaked during the night, a situation different from most urban areas, which experience daytime SOA maxima. This analysis of *Rollins et al.* [2012] is discussed more completely in Finding N4.

Research conducted as part of the Carbonaceous Aerosols and Radiative Effects Study (CARES) field campaign has identified enhanced SOA formation during daytime in the transported Sacramento plume, when the anthropogenic emissions mixed with isoprene-rich air in the Sierra Nevada foothills [*Setyan et al.*, 2012; *Shilling et al.,* 2013]. These results indicate that the presence of anthropogenic emissions increase SOA formation from biogenic VOCs.

Two studies [*Liu et al.*, 2012; *Zhao et al.,* 2013] based upon different instrumental measurement techniques and utilizing different analysis approaches reach similar conclusions regarding sources of organic aerosol (OA) at the Bakersfield site. SOA accounts for 70-90% of the OA, while the SOA formed from biogenic VOCs account for only about ~10% of the total OA. This biogenic contribution is a maximum at night, consistent with the conclusions of *Rollins et al.* [2012].

Both the nighttime mechanism in the southern SJV and the daytime mechanism in the Sacramento plume produce significant amounts of SOA, but it has not yet been possible to provide a budget of the contributions of different VOC sources to the atmospheric burden of SOA. Development of such a budget must account for the interactions of biogenic VOCs with anthropogenic emissions. However, as pointed out by *Rollins et al.* [2012], it is clear that reductions in NOx emissions are expected to reduce the concentration of organic aerosol, at least in Bakersfield and the southern SJV region.

***Finding L3*: Biogenic VOCs play a significant, but minor role in SOA formation in the SoCAB.**

Several lines of reasoning indicate that biogenic VOCs make a significant but minor contribution to SOA formation in the SoCAB. First, Figure L1 shows that biogenic VOCs account for only a small fraction of total organic OH reactivity, and oxidation of the species responsible for the reactivity (isoprene, MVK and MACR) are generally believed to have small yields of SOA. Second, glyoxal is believed to be an important secondary product of biogenic VOC oxidation that is particularly important for SOA formation. However, *Washenfelder et al.* [2011] show that glyoxal contributes no more than 0.2 $\mu g\ m^{-3}$ or 4% of the SOA mass at the Pasadena site in the SoCAB. *Williams et al.* [2010] present an analysis of SOA measurements from the 2005 Study of Organic Aerosol at Riverside (SOAR). They find that the predominant source of SOA appears to be from the oxidation of anthropogenic precursor gases, but that one SOA component had contributions from oxygenated biogenics. *Hayes et al.* [2013] analyze SOA sources at the Pasadena site during CalNex, and find that biogenic sources do influence the measured OA. They also note that ^{14}C measurements for selected days during CalNex show that

in the early morning hours when low-volatility oxygenated organic aerosol (LV-OOA) is dominant (compared to other OA components and elemental carbon), about 50% of total carbon is non-fossil (e.g., from modern presumably biogenic sources) [P. Zotter et al., manuscript in preparation; *Bahreini et al.,* 2012]. However, the mass of the non-fossil aerosol component does not increase during the day when SOA is primarily formed in the SoCAB.

References

Bahreini, R., et al. (2012), Gasoline emissions dominate over diesel in formation of secondary organic aerosol mass, *Geophys. Res. Lett., 39*, L06805, doi:10.1029/2011GL050718.

Chameides, W. L., et al. (1988), The role of biogenic hydrocarbons in urban photochemical smog: Atlanta as a case study, *Science, 241*, 1473–1475.

Fares, S., J-H. Park, D.R. Gentner, R. Weber, E. Ormeño, J. Karlik, and A.H. Goldstein (2012), Seasonal cycles of biogenic volatile organic compound fluxes and concentrations in a California citrus orchard, *Atmos. Chem. Phys.*, 12, 9865-9880, doi:10.5194/acp-12-9865-2012.

Goldstein, A. H., and I. E. Galbally (2007), Known and unexplored organic constituents in the earth's atmosphere, *Environ. Sci. Technol., 41*(5), 1514-1521.

Guenther, A., et al. (1995), A Global Model of Natural Volatile Organic Compound Emissions, *J. Geophys. Res. Atmos., 100,* 8873–8892.

Hayes, P. L., et al. (2013), Organic aerosol composition and sources in Pasadena, California during the 2010 CalNex campaign*, J. Geophys. Res. Atmos., 118*, 9233–9257, doi:10.1002/jgrd.50530.

Hoyle, C. R., et al. (2011), A review of the anthropogenic influence on biogenic secondary organic aerosol *Atmos. Chem. Phys., 11*, 321–343.

Liu, S., et al. (2012), Secondary organic aerosol formation from fossil fuel sources contribute majority of summertime organic mass at Bakersfield, *J. Geophys. Res.*, *117*, D00V26, doi:10.1029/2012JD018170.

Pusede, S. E., and R. C. Cohen (2012), On the observed response of ozone to NO_X and VOC reactivity reductions in San Joaquin Valley California 1995–present, *Atmos. Chem. Phys.*, *12*, 8323–8339, doi:10.5194/ acp-12-8323-2012.

Pusede, S. E., et al. (2013), On the temperature dependence of organic reactivity, ozone production, and the impact of emissions controls in San Joaquin Valley California, *Atmos. Chem. Phys. Disc*, *13*, 28511–28560, doi:10.5194/acpd-13-28511-2013.

Rollins, A. W., E. C. Browne, K.-E. Min, S. E. Pusede, P. J. Wooldridge, D. Gentner, A. H. Goldstein, S. Liu, D. A. Day, L. M. Russell, and R. C. Cohen (2012), Evidence for NOx Control over Nighttime SOA Formation, *Science, 337*, 1210-1212, doi:10.1126/science.1221520.

Setyan, A., et al. (2012), Characterization of submicron particles influenced by mixed biogenic and anthropogenic emissions using high-resolution aerosol mass spectrometry: results from CARES, *Atmos. Chem. Phys., 12*, 8131-8156, doi:10.5194/acp-12-8131-2012.

Shilling, J. E., et al. (2013), Enhanced SOA formation from mixed anthropogenic and biogenic emissions during the CARES campaign, *Atmos. Chem. Phys., 13*, 2091-2113, doi:10.5194/acp-13-2091-2013.

Trainer, M., E. J., Williams, D. D., Parrish, M. P., Buhr, E. J., Allwine, H. H., Westberg, F. C., Fehsenfeld, and S. C. , Liu, (1987), Models and observations of the impact of natural hydrocarbons on rural ozone, *Nature, 329*, 705–707.

Washenfelder, R. A., et al. (2011), The glyoxal budget and its contribution to organic aerosol for Los Angeles, California, during CalNex 2010, *J. Geophys. Res. Atmos., 116*, D00V02, doi:10.1029/2011JD016314.

Williams, B. J., A. H. Goldstein, N. M. Kreisberg, S. V. Hering, D. R. Worsnop, I. M. Ulbrich, K. S. Docherty, and J. L. Jimenez (2010), Major components of atmospheric organic aerosol in southern California as determined by hourly measurements of source marker compounds, *Atmos. Chem. Phys.,10* (23), 11577-11603.

Zhao, Y., et al. (2013), Sources of organic aerosol investigated using organic compounds as tracers measured during CalNex in Bakersfield, *J. Geophys. Res. Atmos., 118*, 11388–11398, doi:10.1002/jgrd.50825.

Synthesis of Results - Climate Processes/Transformation

Response to Question M

QUESTION M

How does the atmospheric chemistry vary spatially and temporally?

BACKGROUND

California has a great diversity of lands, from seashore to high mountains, from densely populated urban areas through sparsely populated rural areas to wilderness areas, and from rich agricultural areas to deserts. A great spatial variation in the emissions of reactive species to the atmosphere accompanies this diversity of land types and uses. Within all of these areas, these emissions vary widely on time scales of hours with changing solar radiance, days as synoptic scale meteorological systems pass, days of the week in response to human activities, seasons (with all of the accompanying changes in temperature, humidity, vegetation activity, etc.), years in response to interannual variability, and decades in response to changing climate. These spatial and temporal variations influence the chemical processing of pollutants in the atmosphere.

POLICY RELEVANCE

Developing effective policies for air quality improvement in California is challenging, as they must account for the spatial and temporal variation in emissions and atmospheric chemistry. Further, our knowledge of this chemistry and its variation is incomplete, but continually advancing. The CalNex study has added to this knowledge of atmospheric processes, which can help guide and increase confidence in policy development.

Temporally, the CalNex field study provides only a single point on annual to decadal time scales, and so the results represent the particular conditions of 2010 within the uncertainties of interannual variations and changing climate. Some aspects of the relationship of the CalNex measurements to those of earlier years and decades are discussed in the responses to Questions A, B and E. The CalNex sampling season was late spring to early summer and the results are directly relevant to that season only; how the results relate to other seasons is addressed in the response to Question C. The CalNex field study was primarily limited to two months, May and June 2010, with most platforms and sites active for only a portion of that period. Hence, statistical sampling of the synoptic scale meteorological and weekly scale changes is limited in the CalNex results; the response to Question P addresses temporal variations on a weekly time scale. In this response we primarily examine variations in atmospheric chemistry over a diurnal period.

Spatially, the CalNex field study focused on southern California, particularly the SoCAB and the SJV, where the two major field sites were established. The mobile platforms (four aircraft and a research vessel) the CalNex supersites, and California's statewide monitoring networks allowed some of California's spatial variability to be probed. For example, the NOAA WP-3D aircraft conducted several flights into the Sacramento Valley and SJV, and the Research Vessel Atlantis sailed up the coast from Los Angeles to San Francisco, and up the Sacramento River to

Sacramento. Appendix A provides details of the air quality networks and mobile platform deployments.

In the response to this question, we concentrated on two areas where the CalNex results have significantly advanced our understanding of atmospheric chemistry: nighttime atmospheric processing and the relative contributions of different radical sources to photochemistry during the day. Other advances in our understanding of atmospheric chemistry and its spatial variability include the formation of secondary organic aerosols (see Response to Question N), and what has been learned from studies of the ozone weekend effect (see Response to Question P).

In the ambient atmosphere, the NO_3 radical is formed when NO_2 (one of the components of NO_X) reacts with O_3. NO_3 only accumulates to significant concentrations at night because during the day it is rapidly photolyzed by sunlight and reacts with NO to reform NO_2. NO_3 is an important species because it reacts rapidly with unsaturated VOCs and because it can combine with NO_2 to form N_2O_5, which is potentially a source for nitrate aerosol and a sink for NO_X when it is incorporated into particulate matter. If that particulate matter contains significant chloride ion (e.g., from sea salt aerosol), N_2O_5 can release $ClNO_2$, which can then accumulate in the nighttime atmosphere. $ClNO_2$ is important because at sunrise it photolyzes to release NO_2 and produce a chlorine atom; thus, NO_2 is returned to the NO_X reservoir where it can take part in daytime photochemistry and chlorine atoms are radicals that can help to drive that photochemistry.

Radicals formed by sunlight are the active agents that drive atmospheric photochemistry. Traditional photochemical modeling considers photolysis of O_3 (with subsequent reaction of the $O(^1D)$ product with water) and photolysis of carbonyls, particularly formaldehyde, as the primary radical sources. Photolysis of $ClNO_2$, formed during the night as outlined above, and photolysis of nitrous acid (HONO) are also radical sources that can affect daytime photochemistry. HONO can be directly emitted (e.g., from on-road vehicles) and is also formed from NO_2 and water in the ambient environment.

FINDINGS

***Finding M1*: Nighttime atmospheric chemistry plays multiple important air quality roles including interconversion of reactive oxidized nitrogen species, formation of gas phase chlorine species, and formation of aerosol nitrate. It is important that these processes are accurately included in the air quality models from which air quality policy and regulations are generally developed.**

In-situ measurements of NO_3, N_2O_5, $ClNO_2$, aerosol chloride and relevant ancillary species were made at the Pasadena ground site and/or aboard the NOAA WP-3D aircraft (a comprehensive list of measurements is included in Appendix A) to better understand the complex interaction between emissions, chemistry, and transport that determines the balance between sources and sinks of the highly reactive nocturnal nitrogen oxides. Measurements of N_2O_5, $ClNO_2$, molecular chlorine (Cl_2), and aerosol chloride (Cl^-) on the *Atlantis* provided additional key data with which to examine chemistry involving N_2O_5-mediated chlorine release from aerosol particles. In-situ $ClNO_2$, aerosol chloride, and long-path DOAS measurements of NO_3, NO_2, and O_3 were made from the Pasadena site to simultaneously constrain the chemistry, as well as the vertical distribution of the nocturnal nitrogen oxides.

Meilke et al. [2013] concluded from the Pasadena ground site data that nocturnal nitrogen oxides constitute a significant reservoir for NO_X at night, with $ClNO_2$ alone contributing 21% on average to the total budget of NO_X oxidation products measured at the site during the CalNex study. They further calculated that photolysis of $ClNO_2$ during the study added a median of 0.8 ppbv of Cl radicals and NO_2 to the Pasadena boundary layer following sunrise. Stable isotopic measurements of aerosol nitrate made from the R/V *Atlantis* suggested significant differences in aerosol sources to the inshore marine boundary layers of the southern and central coasts of California [*Vicars et al.,* 2013]. This analysis concluded that nocturnal nitrogen oxide chemistry in continental outflow is an important source of aerosol nitrate to the South Coast marine layer, while daytime oxidation of NO_2 by the hydroxyl radical (OH) was the principal source for aerosol nitrate in the Central Coast marine layer. *Hayes et al.* [2013] noted the sea salt aerosol measured at the Pasadena ground site was substantially depleted in chloride due to atmospheric processing, presumably in part due to nocturnal oxidation chemistry involving reactive uptake of N_2O_5; they further noted a parallel increase in supermicron aerosol nitrate. *Young et al.* [2012] used altitude profiles from the NOAA P-3 aircraft to report the first vertically-resolved measurements of $ClNO_2$, and noted different source terms led to very different vertical profiles of $ClNO_2$ and HONO after dark.

Measurements inland at the Bakersfield ground site during CalNex showed that roughly 30% of nighttime increases in organic particle mass were due to particulate organic nitrates (p∑ANs) [*Rollins et al.*, 2012], demonstrating that their production after dark via NO_3–initiated chemistry was a major source of SOA mass. These results are described in more detail in the response to Question N.

***Finding M2*: $ClNO_2$ and HONO are significant primary radical sources in SoCAB, particularly in early morning when they were the dominant radical source near the surface between sunrise and 09:00 PDT. However, it is important that vertical gradients of radical precursors be taken into account in radical budgets, particularly with respect to HONO.**

Young et al. [2012] used the Pasadena ground site measurements to construct a primary radical budget (Figure M1), and showed that contributions from HONO photolysis would be overestimated without proper accounting for significant decreases in the vertical, due to its strong surface source. At ground level, total daytime radical formation calculated from nighttime-accumulated HONO and $ClNO_2$ was about the same for the two radical sources. Incorporating the different vertical distributions by integrating through the boundary and residual layers demonstrated that nighttime-accumulated $ClNO_2$ produced nine times as many radicals as nighttime-accumulated HONO. A comprehensive radical budget at ground level demonstrated that nighttime radical reservoirs accounted for 8% of total radicals formed and that they were the dominant radical source between sunrise and 09:00 Pacific daylight time (PDT). Importantly, these data show that vertical gradients of radical precursors must be taken into account in radical budgets, particularly with respect to HONO.

Radicals that are formed in early morning can contribute to radical propagation through the formation of O_3 early in the day, which will act as a radical source, via O_3 photolysis, to produce more O_3 later in the day. Thus, early morning radical sources may have an overall greater impact on chemistry that occurs throughout the day. It should be noted that photolysis of $ClNO_2$ produces chlorine atoms, while photolysis of HONO produces hydroxyl radicals. The impacts of these two radicals are not equal, as they react differently with VOCs, affecting their propensity to form O_3 and aerosols. For example, Cl radicals are reactive toward all VOC classes, including alkanes, whereas aromatics, oxygenates, and alkenes tend to dominate OH reactivity. Thus, the

absolute number of radicals produced by each nighttime radical reservoir may not represent their full atmospheric influence. A complete comparison of Cl to OH requires consideration of the particular VOC mixture, its variation over time, and the relative reactivity of each radical. Further, it is noted that recent observations of daytime HONO concentrations have indicated that additional daytime sources must exist with a rate of formation more rapid than the nighttime source, though the mechanism for these sources remains highly uncertain. This daytime source would increase the HONO contribution to primary radical formation.

Riedel et al. [2012] used data from the R/V *Atlantis* to show that photolysis of $ClNO_2$ following sunrise dominates the morning-time source of reactive Cl atoms. They noted that Cl atoms from $ClNO_2$ photolysis dominate the early-morning oxidation of alkanes in the polluted coastal marine boundary layer, resulting in increased O_3 production in the LA basin. Full 3-dimensional chemical-transport modeling incorporating the CalNex $ClNO_2$ observations has not been published to date. Earlier results using the CMAQ model suggest that chemistry involving $ClNO_2$ could increase monthly mean 8-hour O_3 averages in Los Angeles by 1-2 ppbv, but could cause larger increases, up to 13 ppbv of O_3, in isolated episodes [*Sarwar et al.*, 2012].

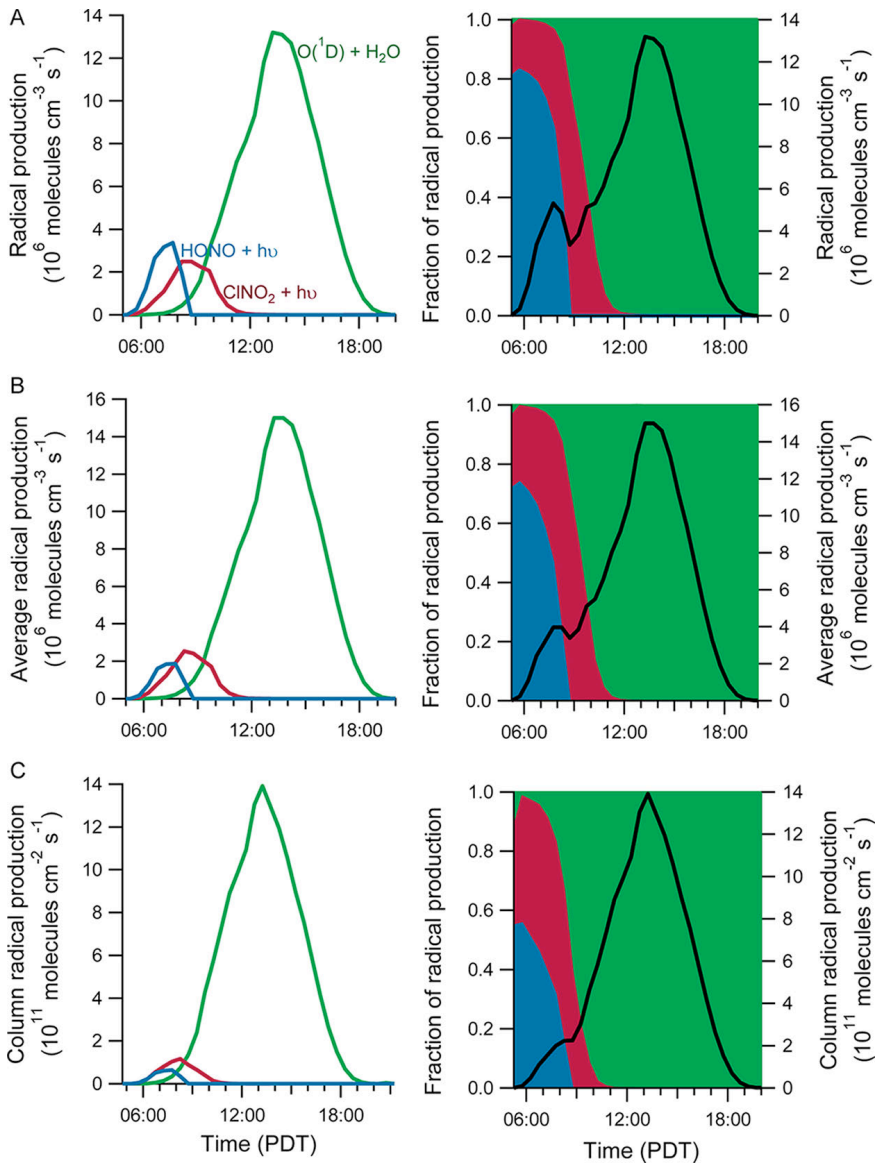

Figure M1. Comparison of absolute and fractional radical production for HONO photolysis (blue), $ClNO_2$ photolysis (red), reaction of $O(^1D)$ plus water (green), and total radical production of the three processes (black) under different conditions: (A) ground level (10 m); (B) average through the boundary layer; and (C) integrated through the boundary and residual layers. (*Figure reproduced from Young et al., 2012*)

Gas-phase chlorine chemistry was recently added to the SAPRC07 chemical mechanism, which is used in regional air quality models. However, the default versions of air quality models like CMAQ, do not include the $ClNO_2$ formation from aqueous phase chemistry involving N_2O_5. The findings above confirm the importance of including these chemical processes in future model development and applications in California.

***Finding M3*: The propensity of Cl for radical propagation yielding second-generation OH radicals indicates that the relative contributions of Cl and OH to tropospheric oxidation are not accurately captured through simple radical budgets.**

Young et al. [2013] used a box model constrained by observations at the Pasadena site to examine Cl and OH chemistry as a function of NO_X and secondary radical production. The model results show that second-generation OH production resulting from Cl oxidation of VOCs is strongly influenced by NO_X, and that this effect can greatly amplify the importance of Cl as a primary oxidant.

References

Hayes, P. L., et al. (2013), Organic aerosol composition and sources in Pasadena, California during the 2010 CalNex campaign, *J. Geophys. Res. Atmos., 118*, 9233–9257, doi:10.1002/jgrd.50530.

Mielke, L. H., et al. (2013), Heterogeneous formation of nitryl chloride and its role as a nocturnal NO_x reservoir species during CalNex-LA 2010, *J. Geophys. Res. Atmos., 118*, doi:10.1002/jgrd.50783.

Riedel, T. P., et al. (2012), Nitryl chloride and molecular chlorine in the coastal marine boundary layer, *Environ. Sci. Technol., 46*, 10463-10470, doi:10.1021/es204632r.

Rollins, A. W., et al. (2012), Evidence for NO_X control over nighttime SOA formation, *Science*, *337*(6099), 1210-1212, doi:10.1126/science.1221520.

Sarwar, G., H. Simon, P. Bhave, and G. Yarwood (2012), Examining the impact of heterogeneous nitryl chloride production on air quality across the United States, *Atmos. Chem. and Phys.*, *12*, 6455-6473, doi:10.5194/acp-12-6455-2012.

Vicars, W. C., et al. (2013), Spatial and diurnal variability in reactive nitrogen oxide chemistry as reflected in the isotopic composition of atmospheric nitrate: Results from the CalNex 2010 field study, *J. Geophys. Res. Atmos., 118*, doi:10.1002/jgrd.50680.

Young, C. J., et al. (2012), Vertically resolved measurements of nighttime radical reservoirs in Los Angeles and their contribution to the urban radical budget, *Environ. Sci. Technol*, *46*, 10965-10973, doi:10.1021/es302206a.

Young, C.J., et al. (2013), Evaluating the role of chlorine in tropospheric oxidation using observations and models in a coastal, urban environment, *Atmos. Chem. Phys. Discuss., 13,* 13685-13720.

Synthesis of Results - Climate Processes/Transformation

Response to Question N

QUESTION N

What are the major contributors to secondary organic aerosol (SOA)? What are the relative magnitudes of SOA compared with primary organic aerosols in different areas?

BACKGROUND

In many environments, including California as exemplified in Figure N1, organic aerosol (OA) composes a large fraction (~50%) of the submicron aerosol mass (PM1) in the troposphere. This is true in all seasons (c.f., Figure C2), although the OA contribution is less in winter at many sites. The sources, composition, and chemical processing of OA are not well-understood. Generally, OA is composed of thousands of individual compounds that are either directly emitted into the atmosphere ('primary' OA or 'POA') or are formed though chemical reactions involving gas phase precursors ('secondary' OA or 'SOA'). The multiple sources and complexity of molecular composition represent major challenges for understanding and predicting OA properties. During CalNex extensive investigations of OA were conducted at the Pasadena and Bakersfield ground sites, aboard the NOAA WP-3D and CIRPAS Twin Otter aircraft, and aboard the R/V *Atlantis*.

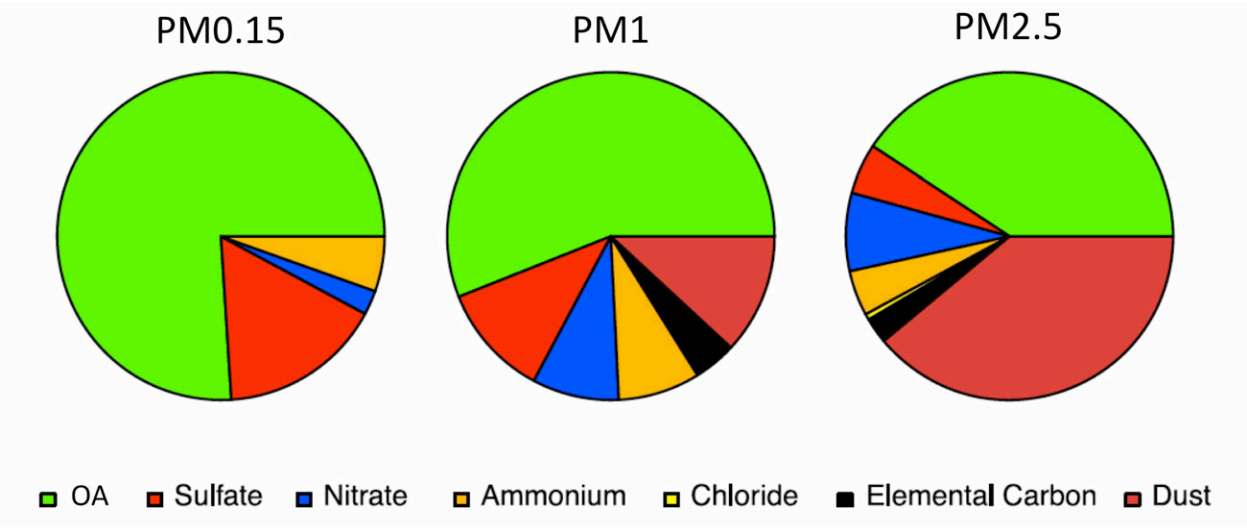

Figure N1. Average composition of PM0.15, PM1, and PM2.5 measured at Bakersfield during CalNex [Figure modified from *Liu et al.,* 2012].

POLICY RELEVANCE

Many areas of California do not attain health-based ambient air quality standards for PM2.5. Organic aerosol is a major contributor to ambient PM2.5 concentrations. To effectively address the reduction of this contribution, it is necessary to identify the emission sources responsible for primary organic aerosol, determine the processes that form SOA, and identify the emission sources of the precursors of this SOA.

Caution must be exercised when comparing the CalNex aerosol measurements made for research

purposes with regulatory measurements of PM2.5. Most of the CalNex research measurements are of sub-micron (PM1) aerosol. Comparisons of PM1 and PM2.5 measurements at Pasadena [*Jimenez et al.*, 2013] indicate that less than about 20% of the OA mass and negligible sulfate mass is above 1 µm, but that a substantial amount of nitrate mass (about 35%) is present above 1 µm. The super-micron nitrate is at least partially composed of sodium nitrate from chemical aging of sea salt by nitric acid, although some super-micron ammonium nitrate may be present as well. In addition, there are systematic differences between PM2.5 measured by air quality networks and by research instrumentation. These differences arise at least partially from loss of semi-volatile components of PM2.5, such as NH_4NO_3 and OA components [e.g., *Tortajada-Genaro and Borrás,* 2011]. Consequently the OA contribution found in research measurements is often larger than that found with regulatory air quality monitoring methods.

FINDINGS

***Finding N1*: SOA contributions to OA at Pasadena could be identified from 1) their diurnal cycles and their correlations with photochemical ozone production, and 2) an increase in SOA concentration with increasing photochemical processing of urban air.**

At the Pasadena site the total organic contribution was 41% of total sub-micron aerosol mass. Analysis of ambient aerosol by AMS (aerosol mass spectrometer) provides an effective means to quantify various contributions to this organic fraction. Five contributions to OA were identified from the Pasadena data set. The two oxygenated OA (OOA) contributions were identified as SOA (SV-OOA and LV-OOA). Figure N2 shows the total measured SOA and total

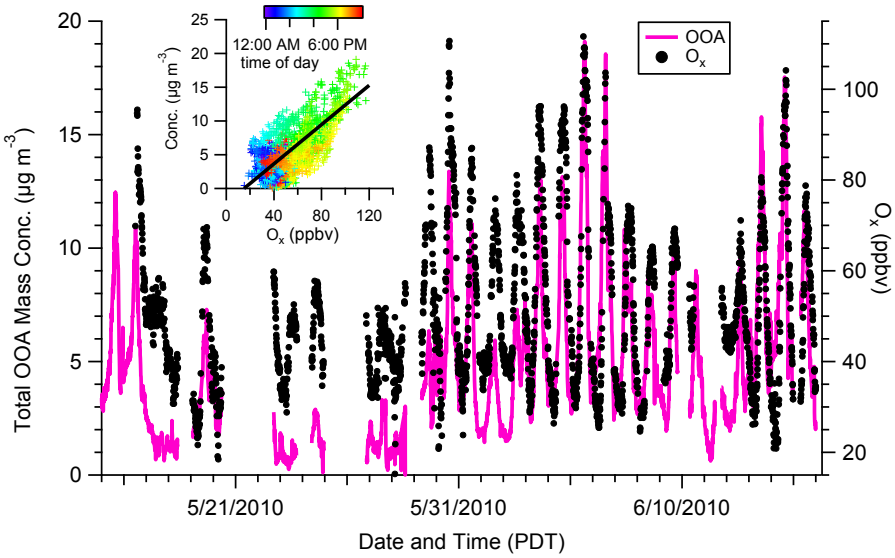

Figure N2. Time series for OOA (the sum of SV-OOA and LV-OOA), and O_X (the sum of O_3 and NO_2). **(Inset)** Correlation plot of OOA versus O_X with linear fit and colored by time-of-day. The best-fit slope is 0.146 (R^2 = 0.53). [Figure from *Hayes et al.*, 2013].

photochemical ozone produced (approximated by O_X, the sum of the measured O_3 and NO_2 to account for O_3 lost through reaction with NO emitted by local sources) at the Pasadena site during the CalNex study. The measured SOA and O_X follow similar diurnal cycles (R^2 = 0.53), with afternoon maxima indicating that photochemical processes in the atmosphere form both. The magnitude of the SOA and O_X maxima are also correlated, each depending upon the changing photochemical environment. The correlation between the two species is stronger during the more polluted periods of high OOA concentration in June (R^2 = 0.72 for the June 2nd through 6th). At the Pasadena site the regression slope for OOA versus O_x is 0.146±0.001 µg m^{-3} ppbv^{-1} (Figure N2 inset). The slopes of identical analyses for Riverside, CA and Mexico City

(0.142±0.004 and 0.156±0.001 μg m^{-3} $ppbv^{-1}$, respectively) are similar to the Pasadena ground site. This similarity suggests similar SOA and O_x formation chemistries on average, in these different urban environments.

To evaluate the timescales and efficiency of SOA formation in Pasadena, the evolution of OA relative to CO (OA/ΔCO) as a function of photochemical age is plotted in Figure N3. Here ΔCO is the CO concentration enhancement above its background concentration, which is taken as 105 ppbv based on CO measurements taken aboard the NOAA WP-3D aircraft off the LA coastline. The CO enhancement is assumed to be a conservative tracer of urban combustion emissions that are also a source of aerosols and aerosol precursors, and thus, normalizing the OA concentration to CO will remove the effect of dilution. The photochemical age is a semi-quantitative measure of the degree of photochemical processing of a sampled air mass. For the air masses sampled at the Pasadena site, photochemical age was calculated by two different methods. First, using the ratio of 1,2,4-trimethylbenzene to benzene, and second, by defining the photochemical age as $-\log_{10}(NO_X/NO_Y)$. Both photochemical ages were calculated using a standard OH radical concentration of 1.5 x 10^6 molecules cm^{-3}. For reference, the daily OH radical concentrations averaged for the whole campaign at the Pasadena site was 1.3 x 10^6 molecules cm^{-3}. The diurnal cycles of the two photochemical age estimates show generally good agreement.

In Figure N3, the Pasadena OA/ΔCO increases markedly with photochemical age, a clear indication of SOA production during photochemical processing of urban air within the Los Angeles basin. The Pasadena results follow the upper limit of the range of values previously reported for Mexico City and the northeastern United States (grey region in the figure), which suggests a common, dominant source of SOA precursors in these urban areas. The inset in Figure N2 shows the variation with photochemical age of the five contributors to OA identified in the analysis of the Pasadena AMS data. Both of the contributions identified as SOA (SV-OOA and LV-OOA) increase with photochemical age, while the other three contributors remain constant, which is consistent with their identification as POA contributions from different sources.

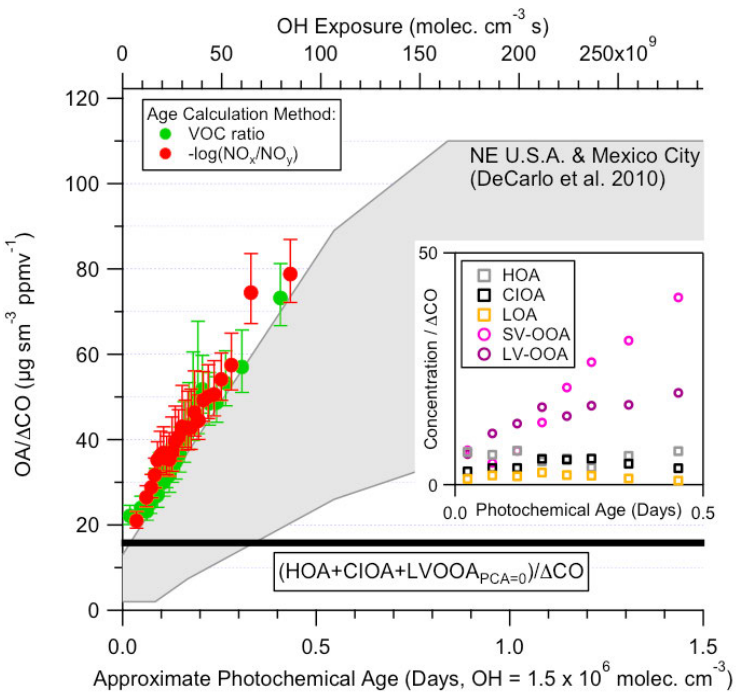

Figure N3. Evolution of OA/ΔCO versus photochemical age at the Pasadena site during CalNex. The measured ratios are averaged into 25 bins according to photochemical age. The enhanced CO (ΔCO) is the ambient CO minus the estimated background CO (105 ppbv). Error bars representing the uncertainty in the ratio are shown. The gray region represents the evolution of OA/ΔCO observed in the northeastern United States and the Mexico City area. The black horizontal line is the ratio of (HOA + CIOA + 'background LVOOA') to ΔCO. **Inset:** Evolution of the OA component concentrations normalized to ΔCO versus photochemical age. Data are binned according to photochemical age. [Figure from *Hayes et al.,* 2013].

***Finding N2*: Averaged over the entire CalNex study, the 24-hour average SOA contributions to total OA in PM1 at the Pasadena (≈ 66%) and Bakersfield (≈ 72%) sites were about two to three times that of primary organic aerosols.**

Figure N4 shows the diurnal cycle of the five aerosol components identified at the Pasadena site. *Hayes et al*. [2013] take the total of the two OOA components as a surrogate for SOA, and the sum of HOA, CIOA, and LOA is taken as a surrogate for POA. On average the total OA mass for the measurement period is composed of 66% OOA (SV-OOA + LV-OOA), a percentage that lies between that observed for a selection of 'urban' and 'urban downwind' sites [*Zhang et al*., 2007]. This percentage is also similar to previous results from measurements based in Pasadena; *Hersey et al*. [2011] reported that, during the PACO campaign in May/June 2009, 77% of OA was classified as OOA, and *Turpin et al*. [1991] reported that SOA contributed roughly half of the OA mass during the summer of 1984.

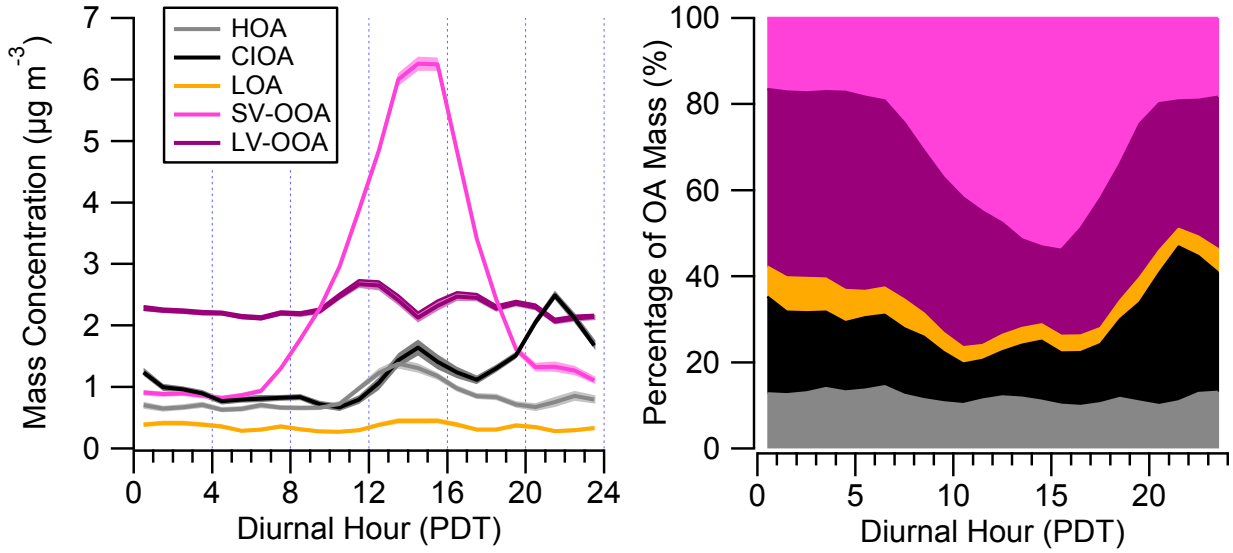

Figure N4. Diurnal profiles of the SOA components in concentrations (left) and by percent mass (right) at the Pasadena site. Shaded regions in left panel indicate uncertainties calculated using a bootstrapping technique. [Figure from *Hayes et al.,* 2013].

Research conducted at the Bakersfield site provides a great deal of detailed information regarding SOA formation in the SJV. *Liu et al.* [2012] and *Zhao et al.* [2013a] present source apportionment analyses of the OA at Bakersfield that are similar to that for Pasadena illustrated in Figure N4. Notably these two analyses consider different data collected by independent instruments, and reach highly consistent conclusions. *Zhao et al.* [2013a] find that SOA contributed on average 72% of measured OA at Bakersfield. *Ahlm et al.* [2012] find that SOA formation dominates particle growth during daytime, with sulfate generally providing only a minor contribution. The mass of particles smaller than 150 nm showed a strong correlation with gas-phase OVOCs (formaldehyde, glyoxal, formic acid and oxalic acid) of largely photochemical origin, indicating the secondary origin of the OA. *Chan et al.* [2013] indicate that semi-volatile branched alkanes are particularly important precursors of SOA. *Zhao et al.* [2013b] identify the important SOA contribution from reactions of carboxylic acids, which are phtotochemical oxidation products of VOCs, with ammonia, a species found in high concentrations due to the large agricultural emissions of the SJV; this work is discussed more fully in Finding I3. *Gentner et al*. [2013] conclude that the potential for SOA formation from

agricultural crop emissions is of the same order as that from anthropogenic emissions from motor vehicles.

***Finding N3*: At the Bakersfield site, most nighttime SOA formation is due to the reaction of the NO_3 radical (a product of anthropogenic NO_X emissions) with unsaturated, primarily biogenic VOCs.**

Instruments at the Bakersfield site measured the total alkyl and multifunctional nitrates in the aerosol phase (pΣAN) as well as total OA and many aerosol precursors, including a wide suite of VOCs. OA concentrations exceeding 10 μg/m^3 were frequently observed at night. The pΣAN and pΣAN/OA ratio were observed to increase at night (Figure N5), which suggests not only that NO_3 chemistry is important for SOA production at night, but also that the organic nitrate tracers of this chemistry contribute appreciably to the total OA. Over the 5-hour time period after sunset (18:30 to 23:30), the average total OA increase was 1.54 μg/m^3. The added mass of nitrate functional groups alone accounted for 0.13 μg/m^3 (8.4%) of this total mass. That this ratio increased continuously for five hours after sunset (a period of predominately northwesterly winds) while Bakersfield is only 1 to 2 hours upwind suggests that the production process has somewhat of a regional character.

Rollins et al. [2012] further interpret the observed relationship of particulate organic nitrates with NO_2 measured at the site, and suggest that this major source of particulate mass would be effectively addressed by targeted NO_X emissions reductions in the Central Valley. While the carbon source of this newly quantified nighttime source can be biogenic in origin, the product SOA must be considered anthropogenic, since its formation is critically dependent on anthropogenic NO_X emissions driving the NO_3 radical chemistry after dark.

From the nitrate content of the aerosol, *Rollins et al*. [2012] calculate that 27 to 40% of the OA growth was due to molecules with nitrate functionalities. This fraction of OA molecules that are nitrates is similar to the nitrate yields from a number of NO_3 plus biogenic VOC reactions. Thus, these numbers do not preclude all of the nighttime SOA production, including non-nitrates, being a result of NO_3 chemistry.

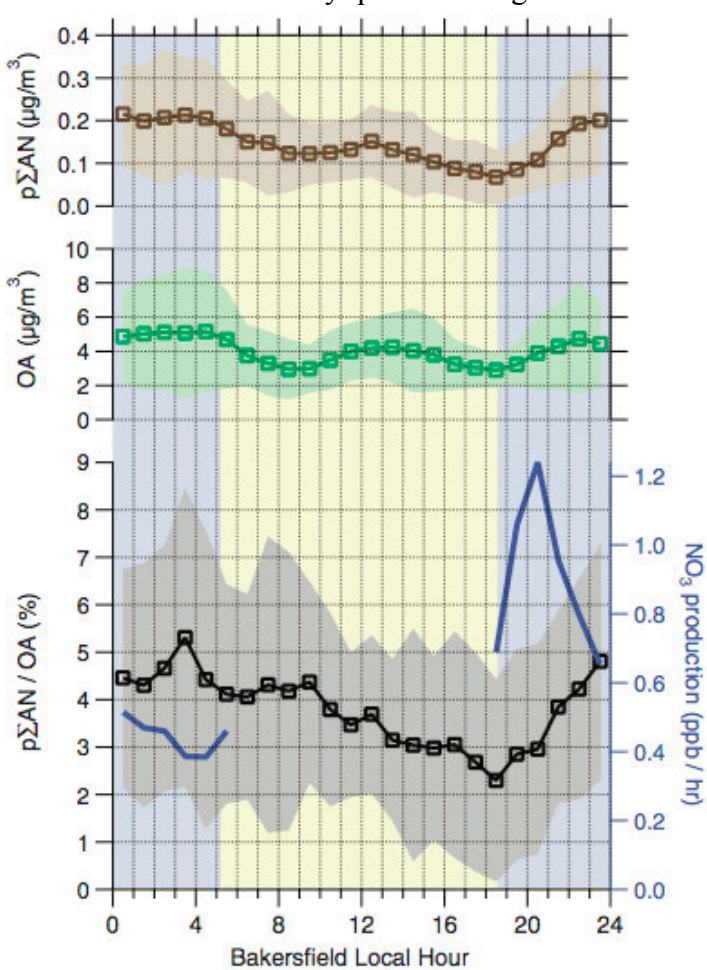

Figure N5. Diurnal trends (means with ±1σ ranges in shading) in pΣAN (brown), OA (green), pΣAN/OA (black), and NO_3 production rate (blue). Blue shading indicates nighttime, and yellow indicates daytime. [Figure from *Rollins et al*., 2012]

***Finding N4*: Analysis of ambient OA measurements in SoCAB indicate that gasoline emissions dominate over diesel in formation of secondary organic aerosol mass; however, an analysis (based on liquid fuel composition) indicated that diesel dominates over gasoline for the formation of SOA in the southern SJV.**

On weekends compared to weekdays, daily total heavy-duty diesel truck traffic decreases in the SoCAB, but light-duty gasoline vehicle traffic remains relatively constant (although the spatial and temporal patterns change). As a consequence, NO_X and black carbon emissions decrease by almost 50%, while CO and VOCs, which are predominantly from gasoline exhaust, remain nearly constant (see *Pollack, et al.*, [2012] and discussion in response to Question P). However, *Bahreini et al.* [2012] show that concentrations of OA do not significantly decrease on weekends. Two separate top-down analyses of CalNex data utilized the lack of a weekend effect in OA mass in the Los Angeles basin, under the assumption that vehicular emissions dominate urban SOA, to conclude that gasoline emissions dominate over diesel emissions in the formation of SOA [*Bahreini et al.*, 2012; *Hayes et al.,* 2013], providing support for SOA control strategies that target gasoline-fueled vehicular emissions. However, a bottom-up approach using detailed fuel chemical composition information, estimates of the SOA formation potential of individual species, and regional fuel sales data [*Gentner et al.*, 2012] concluded that diesel fuel is responsible for 60-90% of the SOA, depending on the diesel fraction of total fuel sales (ranging in California from ~10% in some urban areas to ~30% in some rural areas). A resolution of the contradiction between these studies may be provided by smog chamber studies of SOA formation from evaporated gasoline and diesel fuel and from exhaust from these two classes of vehicles. *Chirico et al.* [2010] find very little primary or secondary OA from diesel engines, at least when equipped with a diesel oxidation catalyst and diesel particulate filter. *Gordon et al.* [2013] find that the SOA formed from exhaust of newer gasoline vehicles, greatly exceeds that formed from vaporized gasoline, and conclude that the mix of organic vapors emitted by newer vehicles appear to be more efficient (higher yielding) in producing SOA than the emissions from older vehicles. This suggests that while tighter emission standards are clearly reducing primary PM emissions from light duty gasoline vehicle exhaust, they may not be as effective at reducing SOA formation. ARB is now investigating this issue for Super ultra-low emission vehicles, which were not a focus of the work cited above.

References

Ahlm, L., et al. (2012), Formation and growth of ultrafine particles from secondary sources in Bakersfield, California, *J. Geophys. Res., 117*, D00V08, doi:10.1029/2011JD017144.

Bahreini, R., et al. (2012), Gasoline emissions dominate over diesel in formation of secondary organic aerosol mass, *Geophys. Res. Lett.*, *39*(L06805), doi:10.1029/2011GL050718.

Chan, A. W. H., et al. (2013), Detailed chemical characterization of unresolved complex mixtures in atmospheric organics: Insights into emission sources, atmospheric processing, and secondary organic aerosol formation, *J. Geophys. Res. Atmos., 118*, 6783–6796, doi:10.1002/jgrd.50533.

Chirico, R., et al. (2010) Impact of aftertreatment devices on primary emissions and secondary organic aerosol formation potential from in-use diesel vehicles: results from smog chamber experiments, *Atmos. Chem. Phys.*, *10*, 11545–11563, doi:10.5194/acp-10-11545-2010

DeCarlo, P. F., et al. (2010), Investigation of the sources and processing of organic aerosol over the Central Mexican Plateau from aircraft measurements during MILAGRO, *Atmos. Chem.*

Phys., *10*(12), 5257-5280.

Gentner, D. R., et al. (2012), Elucidating secondary organic aerosol from diesel and gasoline vehicles through detailed characterization of organic carbon emissions, *Proc. Natl. Acad. Sci., 109*(45), 18318-18323, doi:10.1073/pnas.1212272109.

Gentner, D.R., E. Ormeno, T.B. Ford, S. Fares, R. Weber, J.H. Park, J.F. Karlik, A.H. Goldstein (2013) Emissions of Terpenoids, Benzenoids, and Other Biogenic Gas-phase Organic Compounds from Agriculture and their Potential Implications for Air Quality, *Atmos. Chem. Phys. Disc., 13*, 28343-28393.

Gordon, T.D. (2013), Secondary Organic Aerosol Formed from Gasoline Powered Light Duty Vehicle Exhaust Dominates Primary Particulate Matter Emissions, *manuscript in preparation.*

Hayes, P.L., et al. (2013), Aerosol Composition and Sources in Los Angeles during the 2010 CalNex Campaign, *J. Geophys. Res.-Atmos.*, *118*, 9233–9257, doi:10.1002/jgrd.50530..

Hersey, S. P., J. S. Craven, K. A. Schilling, A. R. Metcalf, A. Sorooshian, M. N. Chan, R. C. Flagan, and J. H. Seinfeld (2011), The Pasadena Aerosol Characterization Observatory (PACO): chemical and physical analysis of the Western Los Angeles basin aerosol, *Atmos. Chem. Phys.*, *11*(15), 7417-7443.

Jimenez, J.-L., W.H. Brune, P.L. Hayes, A.M. Ortega and M.J. Cubison (2013), Characterization of Ambient Aerosol Sources and Processes during CalNex 2010 with Aerosol Mass Spectrometry, Final Report Contract 08-319, California Air Resources Board.

Liu, S., et al. (2012), Secondary organic aerosol formation from fossil fuel sources contribute majority of summertime organic mass at Bakersfield, *J. Geophys. Res.*, 117, D00V26, doi:10.1029/2012JD018170.

Pollack, I.B., et al. (2012), Airborne and ground-based observations of a weekend effect in ozone, precursors, and oxidation products in the California South Coast Air Basin, *J. Geophys. Res.*, *117,* D00V05, doi:10.1029/2011JD016772.

Rollins, A. W., E. C. Browne, K.-E. Min, S. E. Pusede, P. J. Wooldridge, D. Gentner, A. H. Goldstein, S. Liu, D. A. Day, L. M. Russell, and R. C. Cohen (2012), Evidence for NO_X Control over Nighttime SOA Formation, *Science, 337*, 1210-1212, doi:10.1126/science.1221520.

Tortajada-Genaro, L.-A., and E. Borrás (2011), Temperature effect of tapered element oscillating microbalance (TEOM) system measuring semi-volatile organic particulate matter, *J. Environ. Monit., 13*, 1017-1026.

Turpin, B. J., J. J. Huntzicker, S. M. Larson, and G. R. Cass (1991), Los-Angeles Summer Midday Particulate Carbon - Primary And Secondary Aerosol, *Environ. Sci. Technol.*, *25*(10), 1788-1793.

Zhang, Q., et al. (2007), Ubiquity and Dominance of Oxygenated Species in Organic Aerosols in Anthropogenically-Influenced Northern Hemisphere Mid-latitudes, *Geophys. Res. Lett.*, *34*, L13801.

Zhao, Y., et al. (2013a), Sources of organic aerosol investigated using organic compounds as tracers measured during CalNex in Bakersfield, *J. Geophys. Res. Atmos., 118*, doi:10.1002/jgrd.50825.

Zhao et al. (2013b), Insights into Secondary Organic Aerosol Formation Mechanisms from Measured Gas/Particle Partitioning of Specific Organic Tracer Compounds, *Environ. Sci. & Tech.*, doi:10.1021/es304587x.

Synthesis of Results - Climate Processes/Transformation

Response to Question O

QUESTION O

How do layers of enhanced ozone concentrations form aloft and how do they impact ground-level ozone concentrations?

BACKGROUND

Compared to surface concentrations, layers of enhanced ozone concentrations aloft are quite common over most areas of the Earth [e.g., *Newell et al.,* 1999]. The troposphere is filled with such layers for two reasons. First, ozone concentrations on average increase with altitude from the surface through the depth of the troposphere up to the tropopause, which marks the bottom of the stratosphere. (Ozone concentrations increase much more rapidly still with increasing altitude in the lower stratosphere.) Second, above the convective boundary layer (CBL, the near surface layer of the troposphere that is rapidly mixed by surface-based convection), the troposphere is quite stable, limiting vertical mixing. Vertical wind shear causes air at different altitudes to move in different directions, much as a deck of cards can slide horizontally with respect to each other. This transport effectively produces atmospheric layers. As a result of differing sources and sinks of O_3 among the layers, different O_3 concentrations generally mark different layers.

Following sunrise, solar heating of the Earth's surface causes the CBL to grow through turbulent mixing, thereby mixing higher atmospheric layers to the surface. On average, in unpolluted regions, this mixing down of higher layers increases surface O_3 concentrations. Even in polluted regions (e.g., the Los Angeles basin) where the surface layer often has O_3 concentrations exceeding those in near-surface layers aloft, the growth of the CBL and the concomitant mixing of air from aloft will yield a higher net O_3 concentration within the growing CBL than would mixing of an equal amount of clean air from near the surface (e.g., inflow from the marine boundary layer over the Pacific Ocean in the case of Los Angeles basin). The entrainment of layers aloft will have a greater impact in locations where the CBL typically grows to higher altitudes, e.g. in inland air basins compared to coastal air basins where the more pronounced marine influence limits CBL growth.

POLICY RELEVANCE

Mixing of air layers aloft that contain enhanced O_3 concentrations down to the surface can increase surface concentrations within an air basin. This O_3 source is potentially not subject to local controls. Understanding the origin and impact of this down-mixing of O_3 is important for formulating effective air quality control policies. Further, if a particular episode can be shown to originate from mixing down of an elevated layer containing O_3 of stratospheric origin, it may be excluded from regulatory determinations related to violations of the U.S. NAAQS, since these naturally occurring "exceptional events" are not controllable by state agencies [*U.S. EPA*, 2007].

The response to this question discusses some of the evidence for the formation of layers of enhanced O_3 and the mechanism by which they impact ground-level O_3 concentrations. The Response to Question T quantifies the magnitude of this impact.

FINDINGS

***Finding O1*: Layers of enhanced O_3 concentrations aloft over California reflect the interleaving of layers of air affected by differing O_3 sources. Enhanced O_3 concentrations arise from decent of upper tropospheric air with O_3 of stratospheric origin, long-range transport of anthropogenic emissions (e.g., from Asia), and lofted aged regional pollution (e.g., from California urban areas).**

Several CalNex modeling and measurement studies investigated the vertical structure of O_3 concentrations above California, and identified layers of enhanced O_3. Figure O1 shows one example when an atmospheric layer with O_3 of stratospheric origin at concentrations greater than 100 ppbv was transported to within 1 km of the surface. This layer was being actively entrained into the CBL at the time of the sonde measurement [*Langford et al.,* 2012].

Neuman et al. [2012] studied the chemical composition, origin, and transport of air upwind and over Los Angeles, California, using measurements of carbon monoxide (CO), O_3, reactive nitrogen species and meteorological parameters from the WP-3D aircraft during CalNex. Measurements in 32 vertical profiles were used to characterize air masses in the free troposphere over the LA basin, in order to determine the source of enhanced O_3 observed above the CBL. Four primary air mass influences were observed regularly between approximately 1 and 3.5 km altitude: descent of upper tropospheric air carrying O_3 of stratospheric origin, long-range transport of anthropogenic emissions (e.g., from Asia), lofting of aged regional emissions (i.e., from California), and lofting of marine air. The first three air mass types accounted for 89% of the free troposphere observations, each with similarly enhanced average (± 1 standard deviation) O_3 concentrations: 71 (±8) ppbv in upper tropospheric air, 69 (±6) ppbv in air affected by long-range emission transport, and 65 (±4) ppbv in air with aged regional emissions. Marine air had lower average O_3 concentrations: 53 (±10) ppbv. *Langford et al.* [2010] provide detailed documentation of one episode of lofting of aged regional pollution when a layer with O_3 concentrations in excess of 100 ppbv was observed at an altitude of about 4 km above the Los Angeles basin.

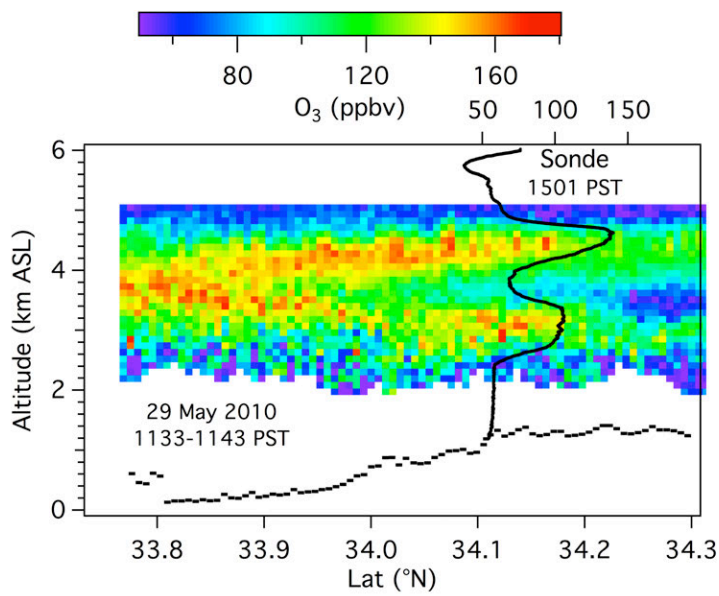

Figure O1. Latitude-height curtain plot of ozone measured along a N-S transect ~10 km west of Joshua Tree National Park by the airborne ozone lidar aboard the NOAA Twin Otter aircraft. The solid black curve shows the concentration profile observed by the ozonesonde. The dashed line along the bottom shows the surface elevation. (Figure based on *Langford et al,* 2012.)

It is useful to note that O_3 concentrations in layers from two of the three sources of enhanced O_3 are expected to have evolved over the past decades above California. Emissions of O_3 precursors have decreased substantially in California (see Response to Question E), but increased in Asia

[e.g., *Ohara et al.,* 2007]. Consequently, it is expected that O_3 enhancements in layers of lofted regional emissions have decreased markedly, while they have increased in layers affected by long-range transport from Asia.

***Finding O2*: Layers of enhanced ozone concentrations aloft are entrained into the convective boundary layer throughout California, thereby enhancing surface level ozone concentrations.**

Neuman et al. [2012] examined correlations between O_3 and CO and between O_3 and nitric acid from WP-3D aircraft observations over the Los Angeles basin. These correlations demonstrate that mixing of three different air masses affect O_3 concentrations across the LA basin: clean marine air with low concentrations of all three species, dry air with increased O_3 and decreased CO characteristic of the upper troposphere, and photochemically-processed Los Angeles basin air with enhanced O_3, CO and nitric acid. This observation-based study is complemented by studies that incorporate both measurements and model calculations.

Langford et al. [2012] utilized principal component analysis (PCA) to quantify the influence of air from the upper troposphere/lower stratosphere (UT/LS) on surface O_3; they find that ~13% of the variance in the maximum daily 8-hour average O_3 between May 10 and June 19, 2010 was associated with changes of 2–3 day duration linked to the passage of upper-level troughs. Vertical profiles of O_3 measured by balloon-borne instruments above Joshua Tree National Park and by airborne lidar over the Los Angeles basin (see Figure O1) show that these changes coincided with the appearance of intrusions descending from the UT/LS to just above the CBL over southern California. The Lagrangian particle dispersion model FLEXPART reproduced most of these intrusions, and supports the conclusion from the PCA that significant transport to the surface of UT/LS air did occur.

To explore baseline O_3 (i.e., O_3 not affected by local and regional emissions) entering California throughout the latitude expanse of the State, an ozonesonde network was implemented during spring 2010, including four launch sites along the California coast. *Cooper et al.* [2011] determined that the vertical and latitudinal variation in free tropospheric baseline O_3 is partly explained by polluted and stratospheric air masses descending along the west coast. Above 3 km altitude, the dominant pollution sources of O_3 precursors were China and international shipping, while international shipping was the greatest source below 2 km. Within California, the major surface impact of baseline O_3 transported ashore above 2 km is on the high elevation terrain of eastern California. Baseline O_3 below 2 km has its strongest impact on the low elevation sites throughout the State.

Analysis of ozonesondes, lidar, and surface measurements over the western U.S. from April to June 2010 show that a global high-resolution (~50 x ~50 km^2) chemistry-climate model (GFDL AM3) successfully reproduced the observed sharp O_3 gradients above California, including the interleaving and mixing of Asian pollution and stratospheric air associated with complex interactions of mid-latitude cyclone air streams. The model results show that from April to June 2010 thirteen stratospheric intrusions enhanced total daily maximum 8-hour average (MDA8) O_3 at surface sites [*Lin et al.,* 2012a]. O_3 due to long-range transport of anthropogenic emissions from Asia was also identified in the CalNex data set and quantified in the model simulations [*Lin et al.*, 2012b]. Asian pollution descends behind cold fronts. The maximum O_3 enhancement from Asian pollution occurs at about 2 km AGL over the southwestern U.S., including the densely populated Los Angeles basin. This layer can be entrained into the CBL and impact surface concentrations.

Although the higher spatial resolution of the model utilized by *Lin et al.* [2012a;b] improved model performance over earlier model calculations, concern remains that the model does not perform as well as desired over California with its complex meteorology and terrain. Their work has significantly increased our understanding of upper level impacts on surface O_3 in the southwest U.S. However, because of the difficulty of modeling California (especially in coastal areas such as the Los Angeles basin), the model-derived impacts of upper-level O_3 sources are better interpreted heuristically than quantitatively.

References

Cooper, O. R., et al. (2011), Measurement of western U.S. baseline ozone from the surface to the tropopause and assessment of downwind impact regions, *J. Geophys. Res., 116*, D00V03, doi:10.1029/2011JD016095.

Langford, A. O., C. J. Senff, R. J. Alvarez II, R. M. Banta, and R. M. Hardesty (2010), Long−range transport of ozone from the Los Angeles Basin: A case study, *Geophys. Res. Lett., 37*, L06807, doi:10.1029/2010GL042507.

Langford, A. O., J. Brioude, O. R. Cooper, C. J. Senff, R. J. Alvarez II, R. M. Hardesty, B. J. Johnson, and S. J. Oltmans (2012), Stratospheric influence on surface ozone in the Los Angeles area during late spring and early summer of 2010, *J. Geophys. Res.*, *117*(D00V06), doi:10.1029/2011JD016766.

Lin, M., A. M. Fiore, O. R. Cooper, L. W. Horowitz, A. O. Langford, H. Levy II, B. J. Johnson, B. Naik, S. J. Oltmans, and C. J. Senff (2012a), Springtime high surface ozone events over the western United States: Quantifying the role of stratospheric intrusions, *J. Geophys. Res.*, *117*(D00V22), doi:10.1029/2012JD018151.

Lin, M., et al. (2012b), Transport of Asian ozone pollution into surface air over the western United States in spring, *J. Geophys. Res., 117*(D00V07), doi:10.1029/2011JD016961.

Neuman, J. A., et al. (2012), Observations of ozone transport from the free troposphere to the Los Angeles basin, *J. Geophys. Res.*, *117*(D00V09), doi:10.1029/2011JD016919.

Newell R.E., V. Thouret, J.Y.N. Cho, P. Stoller, A. Marenco and H.G. Smit (1999), Ubiquity of quasi-horizontal layers in the troposphere, *Nature, 398*, 316-319.

Ohara, T., H. Akimoto, J. Kurokawa, N. Horii, K. Yamaji, X. Yan and T. Hayasaka (2007), An Asian emission inventory of anthropogenic emission sources for the period 1980-2020. *Atmos. Chem. Phys., 7,* 4419-4444.

U.S. Environmental Protection Agency (U.S. EPA) (2007), Treatment of data influenced by exceptional events, *Fed. Regist., 72*(55), 13,560–13,581.

Synthesis of Results - Climate Processes/Transformation

Response to Question P

QUESTION P

What is the prevalence and spatial extent of the ozone weekend effect? What are the contributing factors?

BACKGROUND

The O_3 weekend effect is a phenomenon documented since the 1970s [*Cleveland et al.*, 1974; *Levitt and Chock*, 1976] in which ambient, daytime surface O_3 concentrations in some urban areas tend to be higher on weekends than on weekdays. An O_3 weekend effect in the SoCAB has been extensively studied, and decreased concentrations of NO_X emissions on weekends are considered to be the dominant cause of increased weekend O_3 concentrations [*Marr and Harley*, 2002a; b; *Yarwood et al.*, 2008]. A large decrease in on-road diesel-fueled vehicle activity on weekends accounts for the significant reductions in weekend NO_X (and BC) emissions. Reduced NO_X emissions on weekends can affect O_3 concentrations via two processes: 1) decreased O_3 loss by titration by freshly emitted NO and 2) increased O_3 production due to an increase in the ratio of VOCs to NO_X. The more recent studies [*Marr and Harley,* 2002a; b; *Yarwood et al.,* 2008] indicate that the second process, increased photochemical production of O_3, plays a significant role in increased weekend O_3 concentrations in and downwind of urban areas in California.

POLICY RELEVANCE
The changes in ambient ozone concentrations that are observed to occur in response to emission changes between weekdays and weekends can provide insights regarding the efficacy of NOx emission reduction policies. However, a comprehensive understanding of the day-of-week variations in ozone concentrations is necessary for this phenomenon to provide reliable guidance regarding long-term emission control strategies.

The O_3 weekend effect has been investigated using airborne and ground-based measurements from the CalNex field study conducted in May and June 2010. It must be noted that this is a statistically limited period with only a few weekends, which may have been on average warmer than the weekdays. Efforts have been made to compare the analysis of the CalNex data with analyses of more extensive data sets, such as the data from the South Coast Air Quality Management District monitoring network for the entire 2010 O_3 season and for other years.

FINDINGS

***Finding P1*: In the SoCAB, NO_X emissions are reduced by nearly half on weekends, while VOC emissions remain approximately constant. As a result, weekend hydroxyl radical concentrations are greater, giving 65%–75% faster photochemical processing. In addition, ozone production efficiency is 20%–50% higher. These effects yield 8-16 ppbv higher average midday ozone concentrations on weekends than on weekdays.**

Pollack et al. [2012] analyze the O_3 weekend effect by examining a wide variety of data sets collected in the SoCAB over many years. Consistent with previous work, they show that NO_X emissions are significantly reduced (by approximately half) on weekends (Figure P1) while no change could be discerned in CO, CO_2 and VOC emissions. Reduced diesel truck traffic on the weekends has been identified as the cause of the reduced NO_X emissions; *Pollack et al*. [2012] further support this identification by showing that black carbon emissions (primarily due to diesel-fueled vehicles) are also reduced by approximately half on weekends. These NO_X emission reductions lead to average increases of 48±8% and 43±22% in the weekend VOC/NO_X ratio as determined from the CalNex 2010 airborne and ground-based measurements, respectively.

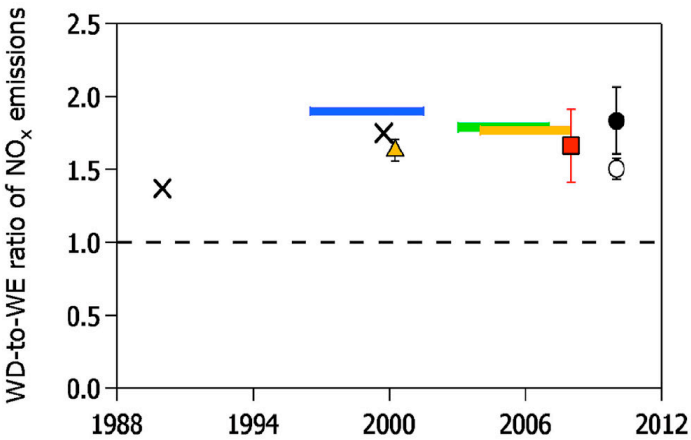

Figure P1. Weekday-to-weekend-day ratios of NO_X emissions derived for the LA basin from CalNex airborne (solid black circle) and ground-based (open circle) measurements, CARB flights of ARCTAS (red square), roadside/tunnel studies (crosses), ground-based network measurements (orange triangle), and satellite measurements from GOME (blue bar), SCIAMACHY (orange bar), and OMI (green bar). (Figure based on *Pollack et al*., 2012).

Reaction with NO_2 is the major sink for the hydroxyl radical (OH) in the Los Angeles atmosphere. Thus, one consequence of reduced NO_X emissions on weekends is an increased concentration of OH radicals. Since these radicals initiate the oxidation of VOCs, atmospheric photochemistry proceeds more rapidly on weekends. Figure P2 demonstrates this faster photochemistry by examining the relationships between VOCs and CO. The slope of the linear correlation of each VOC with respect to CO is defined as the enhancement ratio (ER) of the VOC to CO. CO is unreactive on the timescale of transport of pollutants out of the Los Angeles basin. In the absence of photochemical loss of the VOC, the ER is equal to the ratio of emissions of that VOC to CO. The same enhancement ratio is observed on weekdays and on weekends for VOCs that react only slowly (on a timescale of days), such as benzene in Figure P2a, while smaller enhancement ratios are observed on weekends for more reactive VOCs, such as toluene in Figure P2b. The decrease in ERs on weekends is due to faster removal of the reactive VOCs due to the higher OH concentrations. Figure P2c demonstrates that ERs are the same at night on weekends and on weekdays, showing that the emission ratios are the same throughout the week. However, the ERs are higher during weekday afternoons than on weekends by a factor that correlates with the reaction rate constant of the VOC with OH radicals. This behavior indicates that average daytime OH concentrations are larger on weekends by 65%–75% [*Warneke et al.*, 2013].

As a result of the lower NO_X emissions and the higher OH concentrations on weekends, NO_X is oxidized more rapidly and the O_3 formation efficiency per unit NO_X oxidized are both enhanced on weekends. Figure P3 shows the fraction of emitted NO_X that had not been oxidized to other NO_Y species at the time of measurement; this fraction is significantly smaller on weekends, demonstrating the faster weekend NO_X oxidation rate. Figure P4 shows the relationship between O_3 formed and NO_X oxidized in the airborne and ground-based measurements. Here O_X, which

equals $O_3 + NO_2$, rather than O_3 is plotted on the ordinate to avoid the influence of reaction of ambient O_3 with fresh emissions of NO. The slopes of these plots, which approximate the number of O_3 molecules formed per NO_X oxidized (i.e. the O_3 formation efficiency), are higher on weekends. These two effects are the fundamental cause of the higher O_3 concentrations on weekends [*Pollack et al.*, 2012].

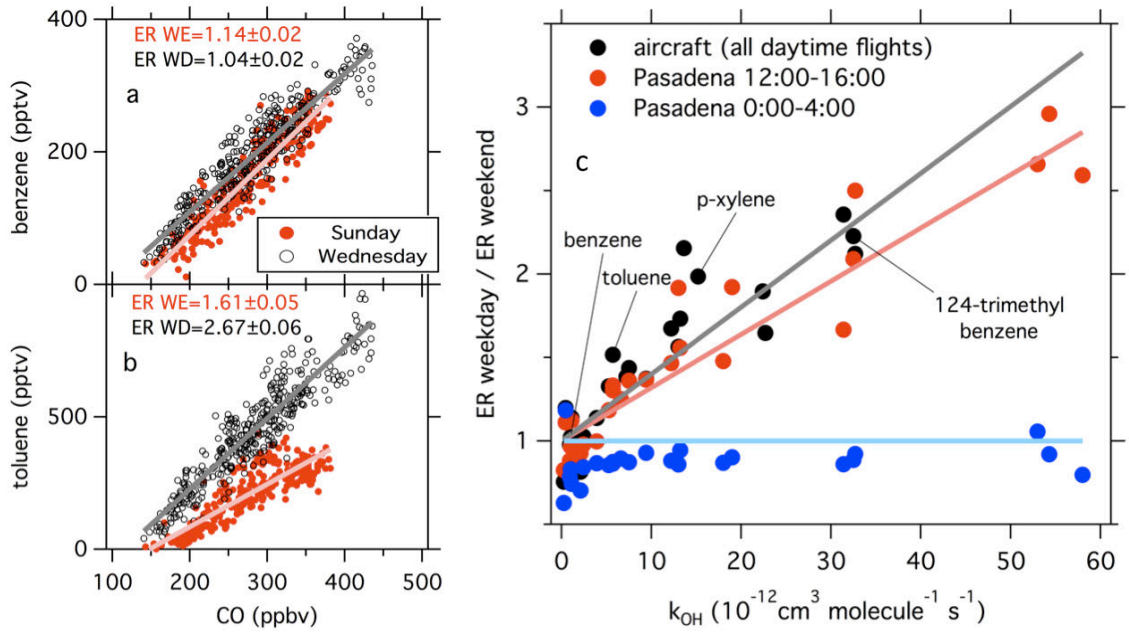

Figure P2. Correlation of **a)** benzene and **b)** toluene with CO measured during NOAA WP-3D flights on a weekday (black symbols) and a weekend day (red symbols). Linear least square fits are shown and the slopes with confidence limits are annotated. Each slope defines an enhancement ratio (ER) of the VOC with respect to CO. **c)** Ratio of weekday to weekend ERs measured on all daytime NOAA WP-3D flights (black symbols) and at the Pasadena ground site during the afternoon (red symbols) and during nighttime (blue symbols). The lines of the respective colors indicate linear least square fits forced to an intercept of unity. (Figure based on *Warneke et al.*, 2013).

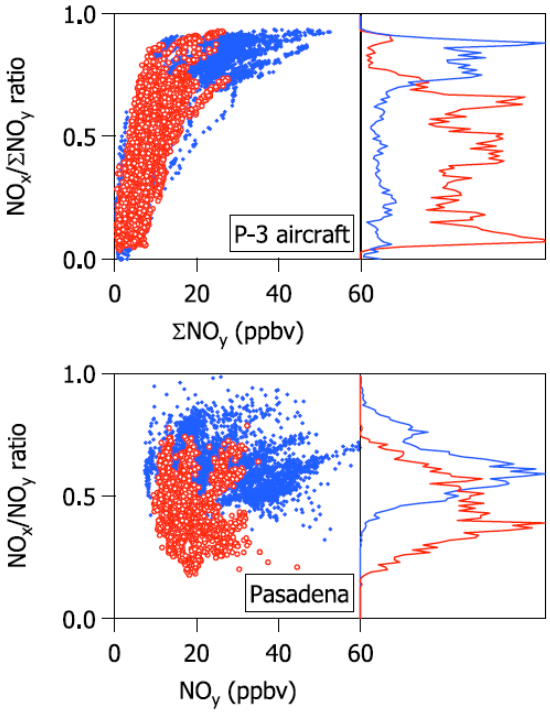

Figure P3. Plots of NO_X/NO_Y ratio versus NO_Y (left) and histogram (right) of the corresponding ratio on weekdays (blue) and weekends (red). Top plots are airborne observations over SoCAB, where ΣNO_Y represents NO_Y determined from the sum of all measured NO_Y species, and bottom plots are ground-based measurements from the CalNex Pasadena site, where NO_Y is a direct measurement. (Figure from *Pollack et al.*, 2012.)

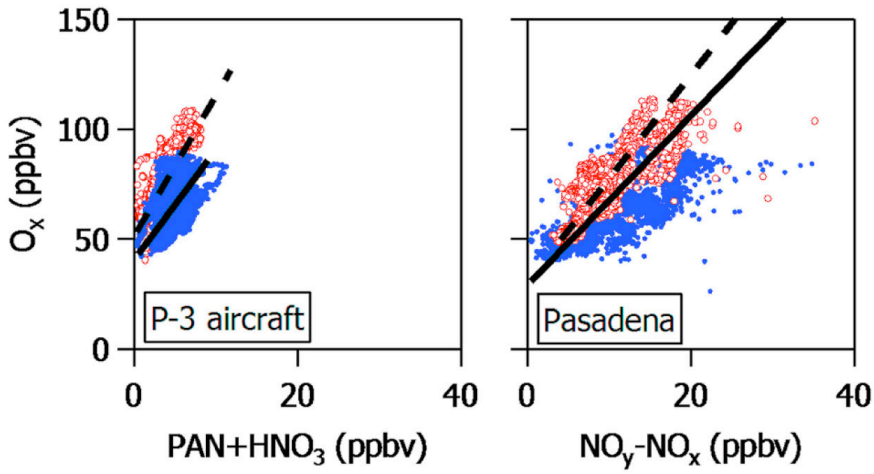

Figure P4. Plots of (left) airborne observations of O_X versus PAN+HNO_3 and (right) ground-based measurements of O_X versus NO_Y-NO_X on weekdays (blue dots, solid lines) and weekends (red circles, dashed lines). (Figure from *Pollack et al.,* 2012).

***Finding P2*: The weekend reduction of NO_X emissions, and the concomitant changes in the photochemical environment in the SoCAB, provides an opportunity to investigate certain aspects of urban photochemistry such as secondary aerosol formation.**

Bahreini et al. [2012] compare the formation of secondary organic aerosol in the SoCAB on weekdays with weekends. Even though diesel truck traffic is reduced by about a factor of two on weekends, SOA concentrations are about the same throughout the week in air masses with similar degrees of photochemical processing. This result indicates that the contribution to SOA formation from diesel emissions is zero within the uncertainties of their analysis. This work is discussed more fully in the Response to Question N.

***Finding P3*: Investigation of the history of the weekend O_3 effect in the San Joaquin Valley suggests that NO_X emissions reductions are now effective for reducing maximum O_3 concentrations in the southern and central SJV, or are poised to soon become so.**

Pusede and Cohen [2012] describe the effects of NO_X and organic reactivity reductions on the frequency of high O_3 days in the SJV. They use sixteen years of observations of O_3, NO_X, and temperature at sites upwind, within, and downwind of three cities located along the axis of the Valley to assess the probability of exceeding the California 8-h average O_3 standard of 70.4 ppb at each location. They show that reductions in organic reactivity have been very effective in the central and northern regions of the SJV but less so in the southern region, and present evidence for two distinct categories of organic reactivity sources: one source that has decreased and dominates at moderate temperatures, and a second source that dominates at high temperatures, particularly in the southern SJV, and has not changed over the last twelve years. They conclude that NO_X emissions reductions are already effective for reducing maximum O_3 concentrations, or are poised to become so, in the southern and central SJV. These are the regions of the SJV where O_3 violations are most frequent, and where conditions are transitioning to NO_X-limited chemistry on the days when air temperatures are hottest and high O_3 concentrations are most probable.

References

Bahreini, R., et al. (2012), Gasoline emissions dominate over diesel in formation of secondary organic aerosol mass, *Geophys. Res. Lett.*, *39*(L06805), doi:10.1029/2011GL050718.

Cleveland, W. S., et al. (1974), Sunday and workday variations in photochemical air-pollutants in New Jersey and New York, *Science, 186*(4168), 1037–1038, doi:10.1126/science.186.4168.1037.

Levitt, S. B., and D. P. Chock (1976), Weekday-weekend pollutant studies of Los Angeles Basin, *J. Air Pollut. Control Assoc., 26*(11), 1091–1092.

Marr, L. C., and R. A. Harley (2002a), Modeling the effect of weekday-weekend differences in motor vehicle emissions on photochemical air pollution in central California, *Environ. Sci. Technol., 36*(19), 4099–4106, doi:10.1021/es020629x.

Marr, L. C., and R. A. Harley (2002b), Spectral analysis of weekday-weekend differences in ambient ozone, nitrogen oxide, and non-methane hydrocarbon time series in California, *Atmos. Environ., 36*(14), 2327–2335, doi:10.1016/S1352-2310(02)00188-7.

Pollack, I. B., et al. (2012), Airborne and ground-based observations of a weekend effect in ozone, precursors, and oxidation products in the California South Coast Air Basin, *J. Geophys. Res.*, *117*(D00V05), doi:10.1029/2011JD016772.

Pusede, S. E. and R. C. Cohen (2012), On the observed response of ozone to NO_X and VOC reactivity reductions in San Joaquin Valley California 1995–present, *Atmos. Chem. Phys., 12*, 8323–8339.

Warneke, C., et al. (2013), Photochemical aging of volatile organic compounds in the Los Angeles basin: weekday - weekend effect*, J. Geophys. Res. Atmos., 118*, 5018–5028, doi:10.1002/jgrd.50423.

Yarwood, G., et al. (2008), Modeling weekday to weekend changes in emissions and ozone in the Los Angeles basin for 1997 and 2010, *Atmos. Environ., 42*(16), 3765–3779, doi:10.1016/j.atmosenv.2007.12.074.

Synthesis of Results - Climate Processes/Transformation

Response to Question Q

QUESTION Q

How do the different aerosol compositions in different areas influence radiative balances?

BACKGROUND

Aerosols affect climate through their direct and indirect interactions with radiation in the atmosphere. Aerosols can directly scatter and absorb short-wave (i.e., visible and near ultraviolet wavelengths) radiation and can emit long-wave (i.e., infrared) radiation. Aerosols can also affect cloud radiative properties by altering the cloud droplet number and size, and by changing cloud lifetime and extent. These properties in part determine the scattering and absorption of radiation by clouds.

It is recognized that these aerosol climate effects are likely large and represent primarily a net climate cooling, but that they are only poorly quantified [e.g., *IPCC*, 2007]. While it is important that earth-system models accurately simulate these effects, cloud-aerosol interactions are complex and nonlinear, leading to large uncertainties in estimates of indirect climate forcing. The CalNex field study included measurements of many aerosol properties, and these measurements have been analyzed from a variety of perspectives. The following material summarizes some of the results of these analyses.

POLICY RELEVANCE
Informed climate change mitigation policies must understand aerosol influences on climate, which arise primarily from aerosol effects on the radiative balance of the atmosphere. These effects are poorly understood and thus modeling results are uncertain. The CalNex measurements and analyses provide information to improve this understanding and provide benchmarks to which modeling results can be compared.

FINDINGS

***Finding Q1*: Climate models need more detailed treatment of direct radiative effects related to black carbon absorption enhancements and also of ammonium nitrate partitioning between aerosol and gas phases.**

Cappa et al. [2012; 2013] compared direct measurements of black carbon absorption enhancements from two different regions in California to show that the mixing state of aerosol BC enhances its ability to absorb solar radiation by relatively small factors of ~1.06 at 532 nm and ~1.13 at 405 nm. This analysis used the contrast between measurements made offshore from the R/V Atlantis during CalNex with those made in Sacramento, CA during the concurrent CARES project [*Zaveri et al.*, 2012], and concluded that climate models that use absorption enhancement dependence of up to a factor of two may produce significant overestimates of warming by BC under some conditions. The observed BC in these two data sets was dominated by diesel emissions [*Cappa et al.,* 2012]. *Adachi and* B*useck* [2013] examined the mixing of BC with other aerosol components by transmission electron microscope, and conclude that the

complex shapes of these mixed particles explains why light amplification by BC coatings are smaller than estimates from optical model calculations that assume simple spherical shapes. In contrast, a recent study [*Lack et al.,* 2012] measured the effect of coatings on absorption in biomass burning plumes and found that coatings of organic and inorganic material on BC enhanced absorption by up to a factor of 1.7 at 532 nm and up to a factor of three at 405 nm. The *Lack et al.* [2012] analysis also concluded that while absorption at 532 nm by particulate organic matter (POM) was very weak, significant variability of absorption at 404 nm was important in determining the overall mass absorption efficiency of POM at low wavelengths in the visible range. Taken together, the *Cappa et al.* [2012] and *Lack et al.* [2012] analyses suggest sufficiently large differences between the radiative effects of BC, and internal mixtures with BC, from anthropogenic and biomass sources to warrant their separate treatment in climate models.

LeBlanc et al. [2012] used spectral irradiance measurements taken on board the WP-3D aircraft when above and below an aerosol layer to estimate the aerosol direct radiative forcing. The observations were compared, using relative forcing efficiency, to direct radiative forcing from other field missions in different parts of the world. The CalNex relative forcing efficiency spectra agreed with earlier studies that found this parameter to be constrained at each wavelength within 20% per unit of aerosol optical thickness at 500 nm, and was found to be independent of aerosol type and location. The diurnally averaged below-layer forcing integrated over the wavelength range of 350-700 nm for CalNex was estimated to be 59±14 W/m^2 of cooling at the surface per unit optical depth.

Langridge et al. [2012] used WP-3D aircraft data to track the evolution of aerosol radiative properties during transport within and downwind of the Los Angeles basin. They documented that changes in aerosol hygroscopicity, secondary organic carbon content, and ammonium nitrate mass occurring during transport over the time scale of hours had significant effects on the aerosol extinction. In particular, they found that the semi-volatile partitioning of ammonium nitrate with gas phase ammonia and nitric acid was strongly affected by temperature and plume dilution, in accordance with thermodynamic models. They noted that the small spatial and temporal scales of variability of aerosol hygroscopicity require explicit, high-resolution treatment for accurate representation of aerosol direct radiative forcing in regional and large-scale climate models.

Zhang et al. [2011] analyzed water-soluble organic carbon (WSOC) aerosol data from the Pasadena ground site to show that nitroaromatics contribute significantly to the brown SOA in Los Angeles. They use aerosol radiocarbon (^{14}C) measurements to conclude that anthropogenic carbon dominated the aerosol budget in Los Angeles, in contrast to measurements in Atlanta, GA showing a minimal anthropogenic component to the water-soluble SOA.

***Finding Q2*: The hygroscopicity of particles in the Central Valley is consistent with the emerging global picture of a limited range of hygroscopicities, which may simplify the treatment of indirect aerosol effects in global climate models. However, considerable variability was found in aerosol hygroscopicity in the Los Angeles basin, which may complicate the treatment of this issue in regional climate models.**

Measurements of cloud condensation nuclei (CCN) concentrations throughout the boundary layer in the Los Angeles basin and Central Valley varied by two orders of magnitude (~10^2-10^4 cm^{-3} @ STP), and represented a substantial fraction of the total submicron particle concentration (~10^3-10^5 cm^{-3} @ STP). Organic species and fully-neutralized sulfate were found to constitute more than 75% of the particle mass in all regions, on average, with higher organic fractions

observed in the Central Valley than in the Los Angeles basin. Despite this variation, large changes in the regionally-averaged CCN-derived aerosol hygroscopicity were not observed, and most CCN were found to activate between 0.2-0.4% super saturation (κ ~ 0.1-0.4) [*Moore et al.*, 2012], where κ is the hygroscopicity parameter [*Petters and Kreidenweis*, 2007]. Hygroscopicities in this range reflect the dominance of inorganic and oxygenated organic species (particularly in the Central Valley) and are consistent with the emerging global picture of a continental aerosol hygroscopicity of κ ~ 0.3 [e.g., *Andreae and Rosenfeld*, 2008; *Pringle et al.*, 2010].

More significant compositional variation was observed within the Los Angeles basin than in the Central Valley, resulting in a more complex picture with regard to aerosol hygroscopicity. For example, *Langridge et al.* [2012] attributed measured changes in humidified aerosol optical extinction to gas-aerosol partitioning of organic and nitrate species as the urban LA plume moved inland into the warmer, eastern part of the basin. The gas-to-particle partitioning of SOA precursors and the evaporation of semi-volatile ammonium nitrate resulted in an overall decrease in hygroscopicity of the aging aerosol. This trend is consistent with *Hersey et al.* [2013], who also observed a decrease from west to east in the Los Angeles basin (from κ=0.4 to κ=0.2) in sub-saturated aerosol hygroscopicity for 150-250 nm aerosol measured aboard the CIRPAS Twin Otter. Meanwhile, concurrent CCN measurements aboard the CIRPAS Twin Otter showed the opposite trend, with supersaturated aerosol hygroscopicity increasing with plume photochemical age (κ=0.2 to κ=0.4) at 0.73% super saturation. This discrepancy likely reflects size-dependent changes in aerosol composition during plume aging – a conclusion that is supported by particle time-of-flight mass spectrometry compositional data [*Hersey et al.*, 2013]. This sort of size-dependent chemistry was also observed in measurements of a biomass-burning (BB) plume sampled by the CIRPAS Twin Otter in the Los Angeles basin, emphasizing the role of BB as a source of CCN even while being effectively non-hygroscopic at relative humidities less than 100%.

References

Adachi, K., and P. R. Buseck (2013), Changes of ns-soot mixing states and shapes in an urban area during CalNex, *J. Geophys. Res. Atmos., 118, 3723–3730, doi:10.1002/jgrd.50321*.

Andreae, M. O., and D. Rosenfeld (2008), Aerosol-cloud-precipitation interactions. Part 1. The nature and sources of cloud-active aerosols, *Earth Sci. Rev., 89*, 13–41, doi:10.1016/j.earscirev.2008.03.001.

Cappa, C. D., et al. (2012), Radiative absorption enhancements due to the mixing state of atmospheric black carbon, *Science*, *337*, 1078-1081, doi:10.1126/science.1223447.

Cappa, C. D.; et al. (2013), Response to Comment on 'Radiative absorption enhancements due to the mixing state of atmospheric black carbon', *Science*, *339*, 393-c, doi: 10.1126/science.1230260.

Hersey, S. P., et al. (2013), Composition and hygroscopicity of the Los Angeles Aerosol: CalNex, *J. Geophys. Res., 118, 3016–3036, doi:10.1002/jgrd.50307.*

IPCC, Intergovernmental Panel on Climate Change: Climate Change 2007: The Physical Science Basis. Contribution of Working Group I to the Fourth Assessment, Report of the Intergovernmental Panel on Climate Change [Solomon, S., D. Qin, M. Manning, Z. Chen, M. Marquis, K.B. Averyt, M. Tignor and H.L. Miller (eds.)]. Cambridge 1 University Press, Cambridge, United Kingdom and New York, NY, USA, 996 pp, 2007.

Lack, D. A., J. M. Langridge, R. Bahreini, C. D. Cappa, A. M. Middlebrook, and J. P. Schwarz (2012), Brown carbon and internal mixing in biomass burning particles, *Proceedings of the National Academy of Sciences*, *109*(37), 14802-14807, doi:10.1073/pnas.1206575109.

Langridge, J. M., et al. (2012), Evolution of aerosol properties impacting visibility and direct climate forcing in an ammonia-rich urban environment, *J. Geophys. Res., 117*(D00V11), doi:10.1029/2011JD017116.

LeBlanc, S. E., K. S. Schmidt, P. Pilewskie, J. Redemann, C. Hostetler, R. Ferrare, J. Hair, J. M. Langridge, and D. A. Lack (2012), Spectral aerosol direct radiative forcing from airborne radiative measurements during CalNex and ARCTAS, *J. Geophys. Res., 117*(D00V20), doi:10.1029/2012JD018106.

Moore, R. H., K. Cerully, R. Bahreini, C. A. Brock, A. M. Middlebrook, and A. Nenes (2012), Hygroscopicity and composition of California CCN during summer 2010, *J. Geophys. Res.*, *117*(D00V12), doi:10.1029/2011JD017352.

Petters, M. D., and S. M. Kreidenweis (2007), A single parameter representation of hygroscopic growth and cloud condensation nucleus activity, *Atmos. Chem. Phys., 7*, 1961-1971, doi:10.5194/acp-8-6273-2008.

Pringle, K. J., H. Tost, A. Pozzer, U. Pöschl, and J. Lelieveld (2010), Global distribution of the effective aerosol hygroscopicity parameter for CCN activation, *Atmos. Chem. Phys., 10*, 5241-5255, doi:10.5194/acp-10-5241-2010.

Zaveri, R. A., et al. (2012), Overview of the 2010 Carbonaceous Aerosols and Radiative Effects Study (CARES), *Atmos. Chem. Phys., 12*, 7647-7687, doi:10.5194/acp-12-7647-2012.

Zhang, X., Y.-H. Lin, J. D. Surratt, P. Zotter, A. S. H. Prévôt, and R. J. Weber (2011), Light-absorbing soluble organic aerosol in Los Angeles and Atlanta: A contrast in secondary organic aerosol, *Geophys. Res. Lett., 38*(L21810), doi:10.1029/2011GL049385.

Synthesis of Results - Atmospheric Transport

Response to Question R

QUESTION R

Is there evidence of pollutant transport between air basins or states?

POLICY RELEVANCE

Several regions within California have significant air quality challenges, and the emission sources throughout the State vary widely in magnitude and species emitted. Pollutants emitted in one region and transported to other regions may add significantly to the impact of the local emissions within the receptor regions. This transport may affect the effectiveness of air quality control measures taken within a particular receptor region.

BACKGROUND

California is a large state with several distinct regions, the more populated of which generally face air quality challenges. Air quality within some regions has been studied extensively (for example, the Los Angles Basin). However, less attention has been given to understanding the impacts of transport of air pollutants from one region to another. Previous studies showed that pollution produced in the Los Angeles area can be transported eastward to the deserts [see for example, *Langford et al.,* 2010; *Riley et al.,* 2008; *White and Macias,* 1990] and similarly, pollutants from the San Francisco Bay Area (SFBA) can affect the Central Valley and the foothills of the Sierra Nevada [see for example, *Bao et al.,* 2008; *Beaver and Palazoglu*, 2009; *Michelson and Bao*, 2008; *Riley et al.,* 2008]. Other possible interregional impacts are from Southern California and the San Francisco Bay Area to the coastal waters and from the Central Valley to the mountains, deserts, and Southern California. Transport between and within regions can take place in the free troposphere as well as in the boundary layer [*Neuman et al.,* 2012]. The CalNex field study included analysis of some of the transport patterns that were observed during that period; however, this period was limited and so these findings must be considered in context of previous work (some referenced above).

The focus of the response to this question is on transport between California's Air Basins and between Mexico and California across the southern border of California. The Response to Question T briefly discusses transport from California to other states.

FINDINGS

***Finding R1a*: San Francisco Bay Area anthropogenic emissions are transported efficiently to the Central Valley. Automotive CO emitted in the Bay Area is a significant fraction of total CO found in the San Joaquin Valley.**

***Finding R1b*: Agricultural emissions (as well as emissions from other sources) in the Central Valley can be transported aloft to the Southern California Bight.**

***Finding R1c*: Southern California emissions are typically transported to less-populated areas to the east.**

Angevine et al. [2013] apply the WRF/FLEXPART Lagrangian particle dispersion model to simulate the amounts of gaseous tracers that are transported within and among four regions: Southern California, the San Francisco Bay Area (SFBA), the Central Valley, and the rest of the State plus part of Nevada including the Las Vegas and Reno urban areas. They consider two completely inert tracers, whose emissions are set equal to those of carbon monoxide (CO) and ammonia (NH_3) to represent emissions from anthropogenic and agricultural sources, respectively. These species have quite different spatial emissions patterns throughout the State. The concentrations of the tracers from the simulations of the particle dispersion model are compared to airborne and ground-based measurements. The age of the tracers in each location is also presented. Vertical profiles and diurnal cycles are analyzed to help clarify important transport processes. The simulations cover the period of CalNex studies (May and June of 2010). So the analysis presented here applies only to the time period simulated (primarily early June). This period is expected to be representative of summer in general. The transport patterns could be quite different in other seasons of the year, particularly in winter.

The simulations of pollutant transport in May and June 2010 are illustrated in Figures R1 and R2. They conform to the basic picture developed over several decades of research (see references above). Southern California emissions are transported to the east and affect the desert areas. The SFBA emissions are an important source of pollutants in the San Joaquin Valley. Central Valley automobile emissions affect their local areas (e.g., Sacramento and Bakersfield) and the Sierra Nevada.

Angevine et al. [2013] also see some novel, or at least easily-visualized, results from the simulations. The Southern California Bight (i.e., the part of the Pacific Ocean bounded by the curved coastline of Southern California from Point Conception to San Diego including the Channel Islands) is filled with a mixture of aged CO tracer from Southern California and the SFBA, with the two sources dominating at different times of day and locations within the Bight. The SFBA emissions are transported through the San Jose area and into and beyond the valleys through the coastal mountains, where they join the offshore flow. The SFBA tracer is transported down the coast by the prevailing northwesterly winds, introduced into the western edge of the Bight, and then recirculated by the "Catalina" eddy. The Southern California tracer drifts out to Santa Monica Bay on the nocturnal land breeze and joins in the eddy circulation when present. Overall CO tracer mixing ratios are low. Air over the Bight is also affected by the Central Valley emissions represented by the NH_3 tracer (Figure R2).

In these simulations, there is no indication of transport from Southern California to the Central Valley. Emissions from the Central Valley do make their way to Southern California, as shown by the NH_3 tracer, but the contribution of automobile emissions from the Central Valley to southern California is negligible compared to the large emissions from automotive sources within southern California.

***Finding R2*: The primary direction of transport of Mexican emissions in the border area (as exemplified by daytime Tijuana emissions) was to the east or southeast. Under most conditions during May and June of 2010, the transport of emissions from the Mexican border regions into the San Diego area was not an important influence. However, nighttime Tijuana emissions, which were particularly rich in black carbon, were commonly transported into the US in a northeasterly direction.**

The Cal-Mex 2010 Field Study is a US-Mexico collaborative project to investigate cross-border transport of emissions in the California-Mexico border region, which took place from May 15 to June 30, 2010, and was loosely coordinated with CalNex. *Bei et al*. [2012] present an overview of the meteorological conditions and plume transport patterns during the study period based on the analysis of surface and vertical measurements (radiosonde, ceilometers and tethered balloon) conducted in Tijuana, Mexico and the modeling output using the WRF/FLEXPART model. Based on simulations with particles released in Tijuana in the morning, four representative plume transport patterns were identified. Most days during May and June were classified as plume-east and plume-southeast days, showing that the plumes in Tijuana were mostly carried to the southeast and east of Tijuana within the boundary layer during daytime, although some emissions may have trickled over the US-Mexico border near the eastern edge of California. This general transport pattern is consistent with the back trajectory simulations of *Takahama et al*. [2013], who found that under mean wind conditions, much of the oxygenated organic aerosol observed in Tijuana may have come from the Southern California Air Basin.

Shores et al. [2013] utilized forward trajectory analysis using meteorological fields generated by *Baker et al*. [2013] to model transport of black carborn (BC) emissions from Tijuana. Transport of these emissions, which occurred predominately at night, into the US was common, often entering in a northeastward direction east of San Diego-Tijuana and sometimes as far east as Imperial County at the eastern edge of California.

References

Angevine, W. M., et al. (2013), Pollutant transport among California regions, *J. Geophys. Res. Atmos., 118*, 6750–6763, doi:10.1002/jgrd.50490.

Baker, K. R., et al. (2013), Evaluation of surface and upper air fine scale WRF meteorological modeling of the May and June 2010 CalNex period in California, *Atmos. Environ., 80,* 299-309, doi: 10.1016/j.atmosenv.2013.08.006.

Bao, J. W., S. A. Michelson, P. O. G. Persson, I. V. Djalalova, and J. M. Wilczak (2008), Observed and WRF-simulated low-level winds in a high-ozone episode during the Central California Ozone Study, *J. Appl. Meteorol. Clim., 47*(9), 2372–2394.

Beaver, S., and A. Palazoglu (2009), Influence of synoptic and mesoscale meteorology on ozone pollution potential for San Joaquin Valley of California, *Atmos. Environ., 43*(10), 1779–1788.

Bei, N., et al. (2012), Meteorological overview and plume transport patterns during Cal-Mex 2010, *Atmos. Environ. 70,* 477–489, doi:10.1016/j.atmosenv.2012.01.065.

Langford, A. O., C. J. Senff, R. J. Alvarez II, R. M. Banta, and R. M. Hardesty (2010), Long-range transport of ozone from the Los Angeles Basin: A case study, *Geophys. Res. Lett., 37*, L06807, doi:10.1029/2010GL042507.

Michelson, S. A., and J.-W. Bao (2008), Sensitivity of low-level winds simulated by the WRF model in California's Central Valley to uncertainties in the large-scale forcing and soil initialization, *J. Appl. Meteorol. Clim., 47*, 3131–3149.

Neuman, J. A., et al. (2012), Observations of ozone transport from the free troposphere to the Los Angeles basin, *J. Geophys. Res., 117*, D00V09, doi:10.1029/2011JD016919.

Riley, W. J., D. Y. Hsueh, J. T. Randerson, M. L. Fischer, J. G. Hatch, D. E. Pataki, W. Wang, and M. L. Goulden (2008), Where do fossil fuel carbon dioxide emissions from California go? An analysis based on radiocarbon observations and an atmospheric transport model, *J. Geophys. Res., 113,* G04002, doi:10.1029/ 2007JG000625.

Shores, C.A., et al. (2013), Sources and transport of black carbon at the California-Mexico border, *Atmos. Environ., 70*, 490-499.

Takahama, S., et al. (2013), Submicron organic aerosol in Tijuana, Mexico, from local and Southern California sources during the CalMex campaign, *Atmos. Environ., 70*, 500–512.

White, W. H., and E. S. Macias (1990), Regional transport of the urban workweek: Methylchloroform cycles in the Nevada-Arizona desert, *Geophys. Res. Lett., 17*, 1081–1084, doi:10.1029/GL017i008p01081.

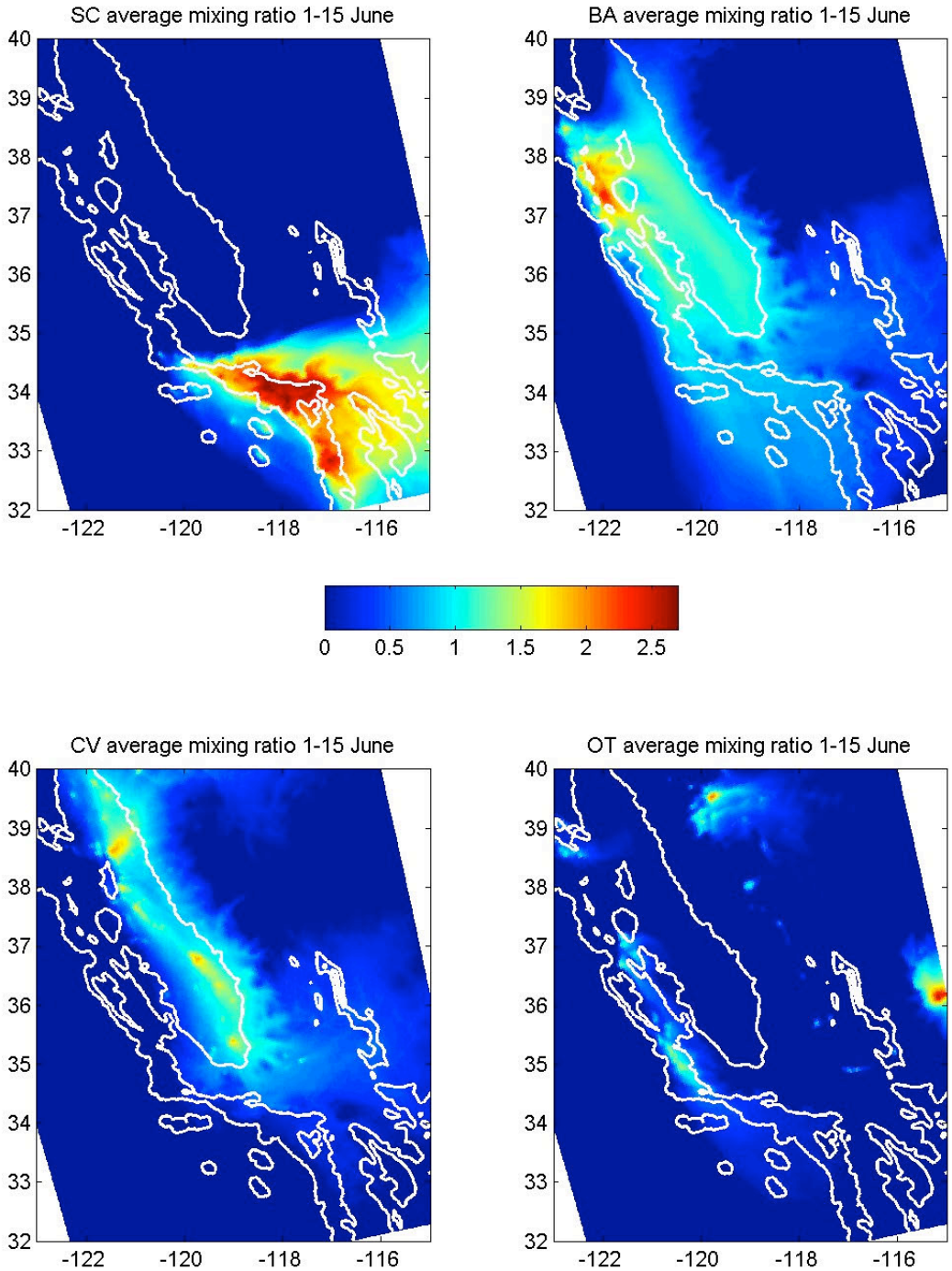

Figure R1: Average near-surface mixing ratios of each CO tracer (log10 (ppbv)) for all hours of 1-15 June, 2010. Log (base 10) scale is used to make small concentrations visible. The maps span from the Sacramento Valley in the northwest to the California-Mexico border in the southeast; the white lines show the 1 m and 500 m elevation contours. In the model calculation, a background CO concentration of 120 ppbv is assumed, but that background is not added in this figure. The tracers are identified according to their emission region: Southern California (SC), San Francisco Bay Area (BA), Central Valley (CV) and other regions (OT). [Figure from *Angevine et al.*, 2013].

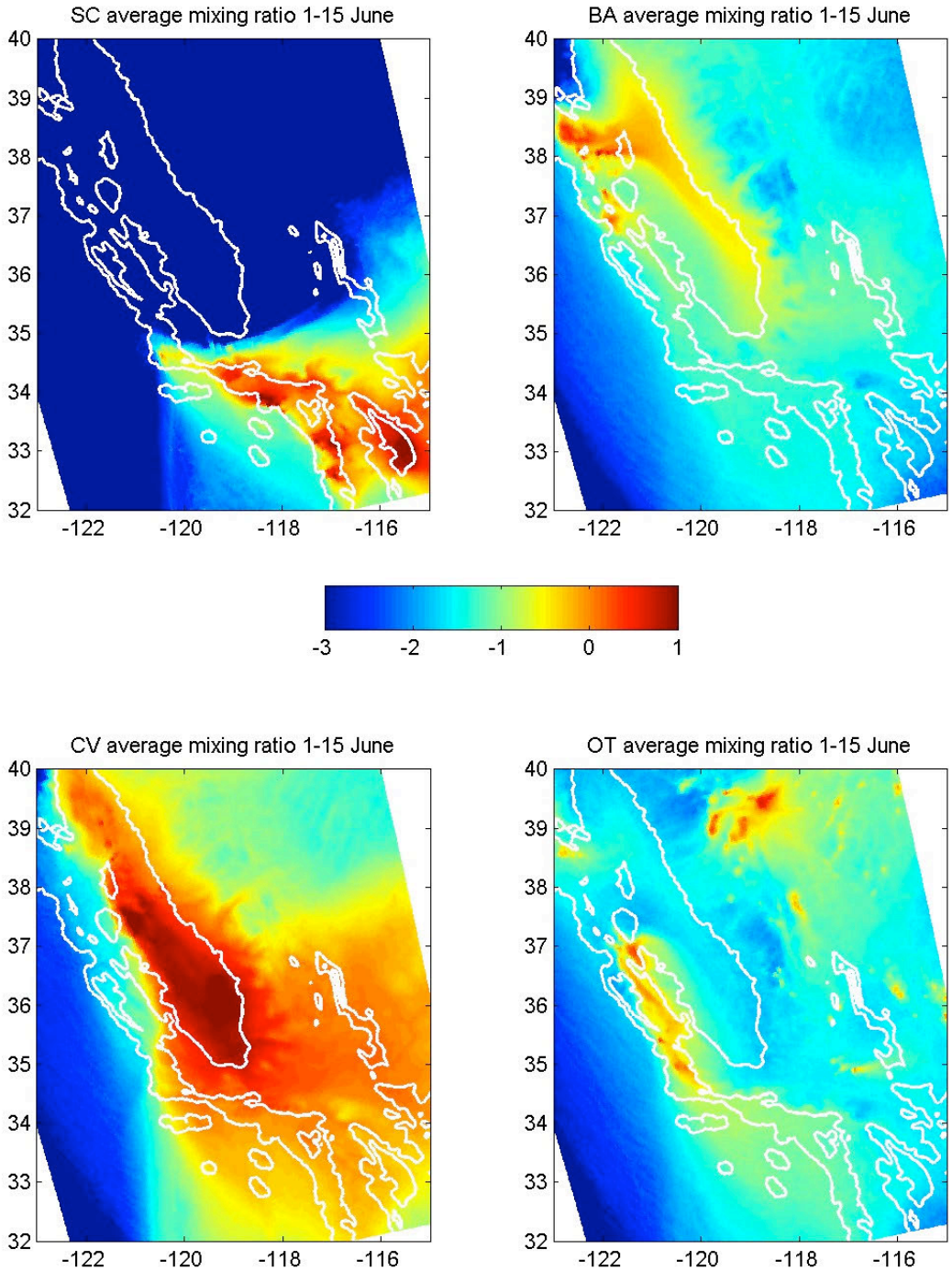

Figure R2: Average of near-surface mixing ratios (log 10 (ppbv)) of NH_3, used as a tracer of agricultural emissions from four source regions. All hours of 1-15 June 2010 are included. The log (base 10) scale is used to make small concentrations visible. The figure is in the same format as in Figure R1. [Adapted from *Angevine et al.*, 2013].

Synthesis of Results - Atmospheric Transport

Response to Question S

QUESTION S

Is there evidence of pollutant recirculation, particularly in the South Coast Air Basin (SoCAB)?

POLICY RELEVANCE

Air quality models are required to formulate and evaluate air pollution control strategies as well as to demonstrate attainment of air quality goals included in the State Implementation Plan (SIP). The ability of a model to reproduce situations where yesterday's pollution is recirculated within an air basin to contribute to today's concentration levels, as opposed to being dispersed by the prevailing winds between days, is a critical measure of model performance. Observational evidence of recirculation that can be compared to results from air quality models provides critical guidance in their development as regulatory tools.

BACKGROUND

California is a state with complex topographic features that interact with synoptic- and meso-scale meteorological patterns and can contribute to strong temperature gradients, both horizontal (e.g., between the ocean and land) and vertical (e.g., radiative, marine, subsidence inversions). These interactions and temperature gradients generate complex airflows that transport pollutants in complicated patterns - some of which can recirculate aged emissions back to their source area.

The response to this question discusses recirculation of pollutants within the SoCAB; related material is given in responses to other questions. Questions R and T discuss transport between air basins and transport of pollutants from upwind sources into California, respectively; both of these transport discussions have some relation to the transport mechanisms responsible for the recirculation of pollutants.

FINDINGS

***Finding S1*: Pollutants from the SoCAB can be recirculated within the Catalina Eddy in the boundary layer over the Southern California Bight. In the process, they can mix with pollutants from the San Francisco Bay Area, which can be transported down the coast. Although pollutant concentrations associated with San Francisco Bay Area emission sources that are offshore of southern California are generally small, they represent the bulk of the pollution in that area during the June 1-15 period of CalNex.**

Angevine et al. [2013] applied a Lagrangian particle dispersion model to determine the amounts of tracers that are transported within regions of the State, including southern California (see more complete description in Response to Question R). They selected carbon monoxide (CO) emissions from automobiles as a tracer to represent anthropogenic urban emissions and separately tracked the CO tracer emitted from four regions of the State: Southern California, San Francisco Bay Area, Central Valley and all other regions of the State. The simulations cover

May and June 2010, the CalNex field measurement period, and are likely only applicable to similar seasonal conditions. Tracer patterns in winter could be quite different.

The regional CO tracers (Figure S1) show the predominate sources of anthropogenic emissions in particular areas. The Southern California tracer is confined entirely to Southern California,

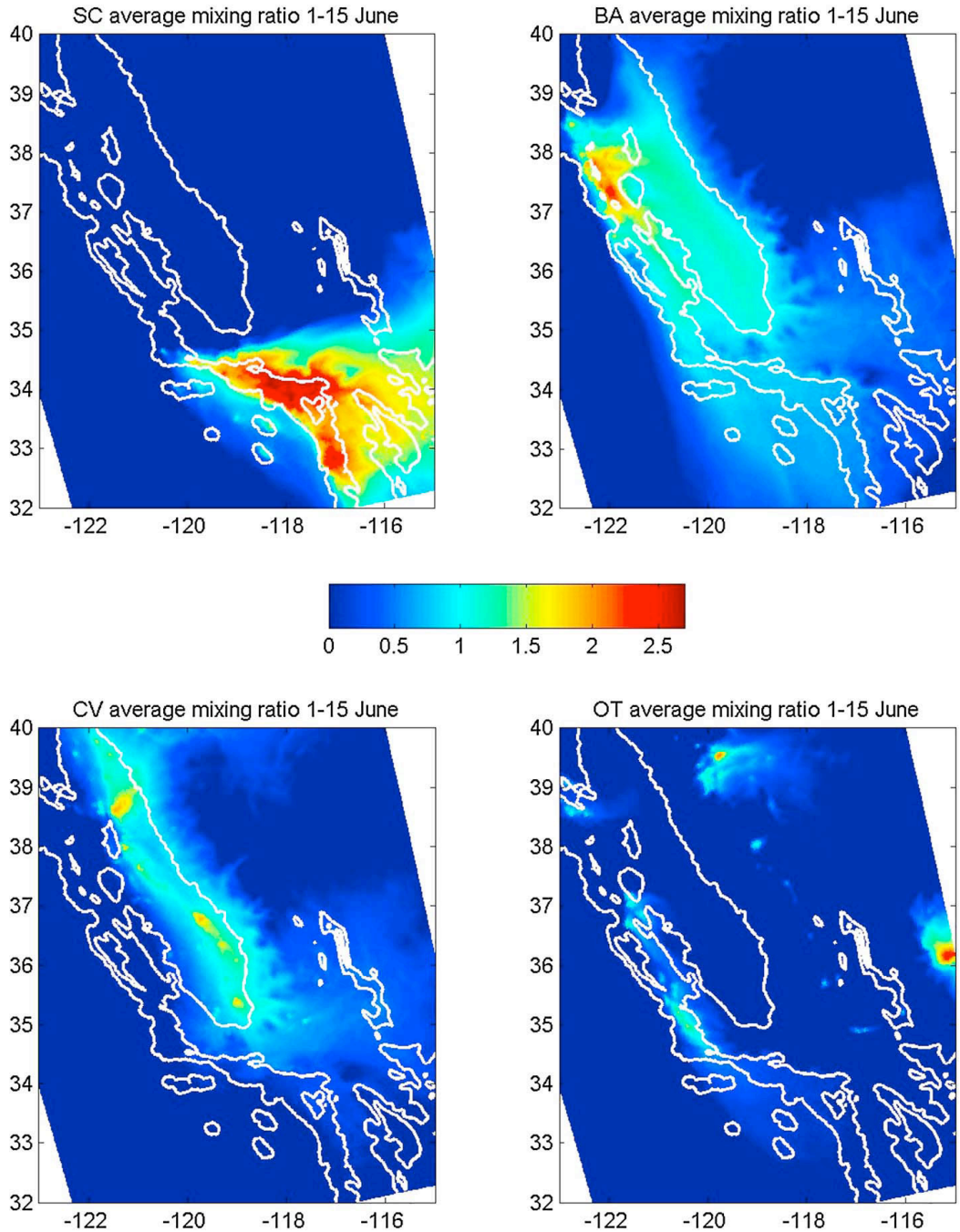

Figure S1: Near-surface mixing ratios of CO regional tracers for 1-15 June 2010. Each tracer is summed over all hours. The maps span from the Sacramento Valley in the northwest to the California-Mexico border in the southeast; the white lines show the 1 m and 500 m elevation contours. The tracers are identified according to their emission region: southern California (SC), San Francisco Bay Area (BA), Central Valley (CV) and other regions of the state (OT). [Figure from *Angevine et al.,* 2013].

with no detectable influence north of the mountains that mark the northern edge of the Los Angeles basin, except very small concentrations far to the east. Its influence is also present in the near-shore Southern California Bight. The most widely distributed tracer is from the San Francisco Bay Area (SFBA). It dominates over the Coastal Ranges south of the SFBA, as well as the western part of the Southern California Bight. It also dominates the San Joaquin Valley except for those areas with strong emissions of the CV tracer. *Angevine et al.,* [2013] show that the tracer is aged over the water in the Southern California Bight, with the oldest tracer material present near the coastline. *Angevine et al.* [2012] attribute this effect to the "Catalina" eddy , which circulates aged Southern California emissions (seen in their study as fresh tracer in Santa Monica Bay at 0400 LST) around and combines them with aged SFBA emissions brought down the coast. This air is returned ashore to the Los Angeles basin, but the concentrations are small as evidenced by the diminishing influence of the SFBA tracer inland from the coast. *Angevine et al.* [2013] caution that their findings are subject to errors in the meteorological model and in the emissions inventory.

***Finding S2*: The direction that emissions originating from Los Angeles exit from the basin varies with time of day. From late morning to early evening most emissions exit toward the east, while during the rest of the day significant emissions exit to the west and south in shallow layers over the ocean. Both the sea-land breeze circulation and the Catalina Eddy flow over the Southern California Bight bring emissions that had exited the LA basin to the west and south back into the source region. For NO_Y, total inflow from upwind sources and this return flux equals about 40% of that emitted within the basin when averaged over May of 2010.**

Analysis: S.A. McKeen, unpublished

An Eulerian, regional-scale air quality model, WRF/Chem [*Ahmadov et al*., 2012], has been applied to the May-July 2010 time period over the western U.S. (12 km x 12 km resolution), and over the southern two-thirds of California at 4 km x 4 km resolution in support of field measurement analysis and emission validation studies. *Angevine et al.* [2012] have shown that the WRF model adequately characterized meteorology in the Los Angeles region during the study period, thus allowing model results to be used for identifying transport and conversion pathways for several key gas-phase and aerosol-phase pollution constituents. Here, a 4-week period of emission fluxes (NO_Y is taken as the tracer) during May is used to demonstrate the mean diurnal pattern of in-flow and recirculation of O_3 precursors through an imaginary cylinder (Figure S2) placed over Los Angeles.

A 4-week average of NO_Y fluxes was derived from the 12 km x 12 km resolution model simulations described in *Brioude et al*. [2013]. This simulation included marine vessel emissions from within the Long Beach and Los Angeles harbors, but not over the ocean. Figure S2 shows the location of the cylindrical surface (36 km radius) through which the vertical and angular distribution of NO_Y flux was calculated. Figure S3 illustrates that flux for three specific hours of the day.

Figure S3a shows the transport before sunrise (5:00 am LDT). The land breeze carries NO_Y away from Los Angeles in a 200-meter layer heading west (over LAX) and a smaller flux into the area from the southeast (Anaheim direction). Downslope flow from the San Gabriel Mountains also brings a dilute NO_Y flux into the cylinder. At noon (7 hours later, Figure S3b), the sea breeze and mountain upslope flow have reversed the transport, with a return flux from the west over LAX and from over Long Beach. This oceanic inflow comes at a critical time for O_3

Figure S2. Base of imaginary cylinder (red circle) placed over Los Angeles for the purpose of calculating fluxes of pollutant emissions through the wall of the cylinder.

pollution over the LA basin, between sunrise and early afternoon when photolysis of NO_Y species can occur and contribute to O_3 formation. This onshore inflow is accompanied by large fluxes out of the basin both to the north over the San Gabriel Mountains and to the east-southeast through Covina and Anaheim. At 10:00 pm LDT, Figure S3c shows a southward NO_Y flux extending through a deep layer. Imbedded within this broad southerly outward flow is a sharp gradient in NO_Y flux with a low-level, 200-meter layer of inflow. At the surface, the strong southward outflow is just over and west of Long Beach, while just east of Long Beach, the inflow flux is strongly to the northwest along the southwestern flanks of the Santa Ana Mountains and Chino Hills. This inflow to the LA basin, attributable to the Catalina Eddy circulation, continues until sunrise (Figure S3a), combining the recirculated NO_Y with fresh Orange County emissions.

A vertically integrated (0-1.2km) budget analysis of emissions and outbound and inbound fluxes of NO_Y within the cylinder defined in Figure S2 concluded that inbound NO_Y fluxes are 40% of the NO_Y emitted within the cylinder, and a majority of this inbound flux is attributed to recirculated pollution.

References

Ahmadov, R., et al. (2012), A volatility basis set model for summertime secondary organic aerosols over the eastern United States in 2006, *J. Geophys. Res.*, 117, *D06301, doi:*10.1029/2011JD016831.

Angevine, W. M., L. Eddington, K. Durkee, C. Fairall, L. Bianco, and J. Brioude (2012), Meteorological model evaluation for CalNex 2010, *Monthly Weather Review*, doi:10.1175/MWR-D-12-00042.1

Angevine, W. M., et al. (2013), Pollutant transport among California regions, *J. Geophys. Res. Atmos., 118*, 6750–6763, doi:10.1002/jgrd.50490.

Brioude, J., et al. (2013), Top-down estimate of surface flux in the Los Angeles Basin using a mesoscale inverse modeling technique: Assessing anthropogenic emissions of CO, NO_x and CO_2 and their impacts, *Atmos. Chem. Phys.*, *13*, 3661–3677, doi:10.5194/acp-13-3661-2013.

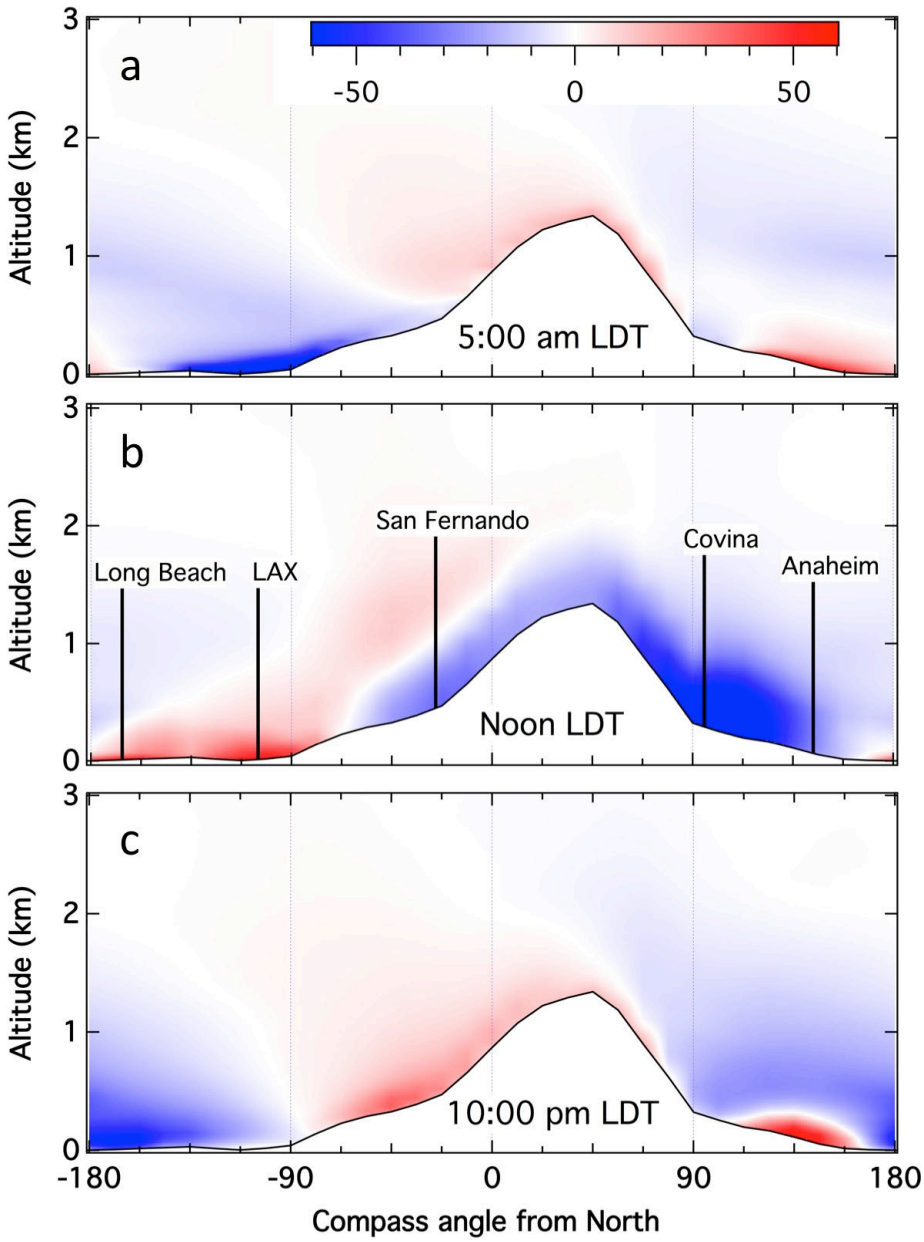

Figure S3. 28-day (4-31 May 2010) average NO_Y fluxes normal to the cylinder walls defined in Figure S2 at three hours during the day. Red (positive) signifies a flux into the cylinder, and blue signifies out of the cylinder. Fluxes are in units of mol/hr/Δangle/meter (vertical), where Δangle = 11.25°. The flux magnitude is indicated in the color bar in a). For orientation, the directions of 5 landmarks are indicated in b). In each panel, the black line with white below indicates the intersection of the cylinder wall with ground level.

Synthesis of Results - Atmospheric Transport
Response to Question T

QUESTION T

Is there evidence of long-range transport during CalNex? What were the relative contributions of the various sources outside the control of emissions within California (i.e., policy-relevant background ozone)?

BACKGROUND

The Response to Question D discusses "background" (better termed "baseline") concentrations observed during CalNex. Transport of these baseline concentrations into California provides the largest contributions to degraded air quality within the State that are outside the control of California. As discussed in that Response, important species are limited to O_3, PM, CO and peroxyacetyl nitrate (PAN). Transport of CO and PAN contribute O_3 precursors of importance in California, but the CalNex analyses thus far have not addressed these species beyond the discussion in the Response to Question D; their importance will not be discussed further here. PM is a pollutant whose long-range transport is primarily limited to extraordinary episodic events; causes of these events include large wildfires, extensive agricultural burning and dust storms. Each such event must be considered separately, and no such event was observed during CalNex. Hence, the response to this question is limited to the long-range transport of O_3. Within California's atmospheric boundary layer, local O_3 formation and destruction are rapid. These rapid processes combined with the strong non-linear dependence of O_3 formation on precursor concentrations make it difficult to accurately quantify the influence of long-range transport.

POLICY RELEVANCE
Transport of ozone into California from upwind regions is beyond the control of California policies. The fractional contribution from this transport to the state's ozone concentrations is growing as baseline ozone concentrations rise and local precursor emissions decrease. Particularly intense episodes of stratospheric O_3 may constitute “exceptional events” that can be excluded from regulatory consideration.

Quantification of source contributions to observed surface O_3 concentrations is a complicated bookkeeping issue that has significant subtleties. A useful concept is "policy-relevant background" or PRB O_3 concentration [*McDonald-Buller et al.*, 2011], which is defined as the concentrations that would exist in the United States in the absence of anthropogenic emissions in continental North America (i.e., the U.S., Canada, and Mexico). PRB O_3 is purely a model concept; it cannot be directly observed anywhere at anytime. Models are imperfect, but even if PRB O_3 could be accurately calculated, the difference between observed O_3 concentrations and the PRB O_3 cannot simply be attributed to anthropogenic O_3 formation, due to the non-linear character of tropospheric photochemistry. For example, local anthropogenic emissions of NO_X tend to increase the ambient concentrations of hydroxyl radicals, which leads to faster photochemical destruction of O_3, thereby reducing the PRB contribution. Higher PRB O_3 concentrations also increase radical concentrations, which leads to faster production of O_3 from anthropogenic precursors. The following discussion presents results of various analyses aimed to quantify the influence of long-range transport of O_3. No consistent bookkeeping system has been employed so subtleties remain in their interpretation. Since California is on the west coast

of North America and the prevailing winds are onshore, the focus of this work does not include transport from other regions of North America. These analyses focus on the 2010 late spring, early summer period of CalNex. This period is near the typical maximum season of long-range transport for both Asian pollution and stratospheric intrusions; 2010 was a particularly active year for transport of stratospheric air to the lower troposphere over California. Consequently, the results may be biased high to some extent.

Intense episodes of stratospheric O_3 transport are of particular policy relevance. The current guidelines from the U.S. Environmental Protection Agency (EPA) state that air quality monitoring data influenced by an extreme stratospheric O_3 intrusion may be excluded from regulatory determinations related to violations of the U.S. National Ambient Air Quality Standard (NAAQS) for ground-level O_3, since these naturally occurring "exceptional events" are not controllable by state agencies [*U.S. EPA*, 2007].

FINDINGS

***Finding T1*: Transport of baseline O_3 can enhance surface O_3 concentrations to such an extent that the margin for local and regional O_3 production before exceeding the NAAQS is greatly reduced or potentially eliminated, particularly if the NAAQS is revised downward to 60 ppbv.**

Langford et al. [2012] used principal component analysis and FLEXPART particle trajectory analysis to quantify the episodic contribution of transport of stratospheric O_3 to the surface of the greater Los Angeles area during the CalNex period (Figure T1). The May 29–30 episode (Figure T1; also illustrated in Figure O1) led to a peak 1-hour O_3 concentration of 88 ppbv at Joshua Tree National Park, and widespread entrainment of upper tropospheric air into the CBL increased local background O_3 concentrations over the entire greater Los Angeles area to ~55 ppbv. This background was 10–15 ppbv higher than the O_3 concentrations in marine air transported ashore from the Pacific Ocean. When combined with locally produced O_3, several exceedances of the current NAAQS occurred on the following day.

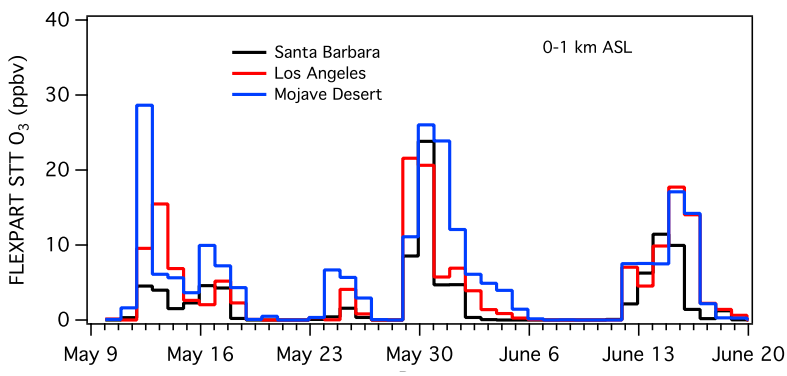

Figure T1. Time series of the contribution of stratospheric O_3 to surface concentrations at three sites in the greater Los Angeles area as calculated by the FLEXPART particle dispersion model. (Figure based on *Langford et al*, 2012).

Lin et al. [2012a,b] compare model results with surface measurements in order to quantify the impact of transported baseline O_3 on surface concentrations over the western U.S. They utilize a new global high-resolution chemistry-climate model (GFDL AM3) with full stratosphere-troposphere chemistry nudged to reanalysis winds, which is expected to give much more accurate results than earlier models. They find that AM3 successfully reproduces observed sharp ozone gradients above California, including the interleaving and mixing of Asian pollution and stratospheric air associated with complex interactions of mid-latitude cyclone air streams. Particular emphasis is placed on quantifying transport of stratospheric O_3 [*Lin et al.,* 2012a] and

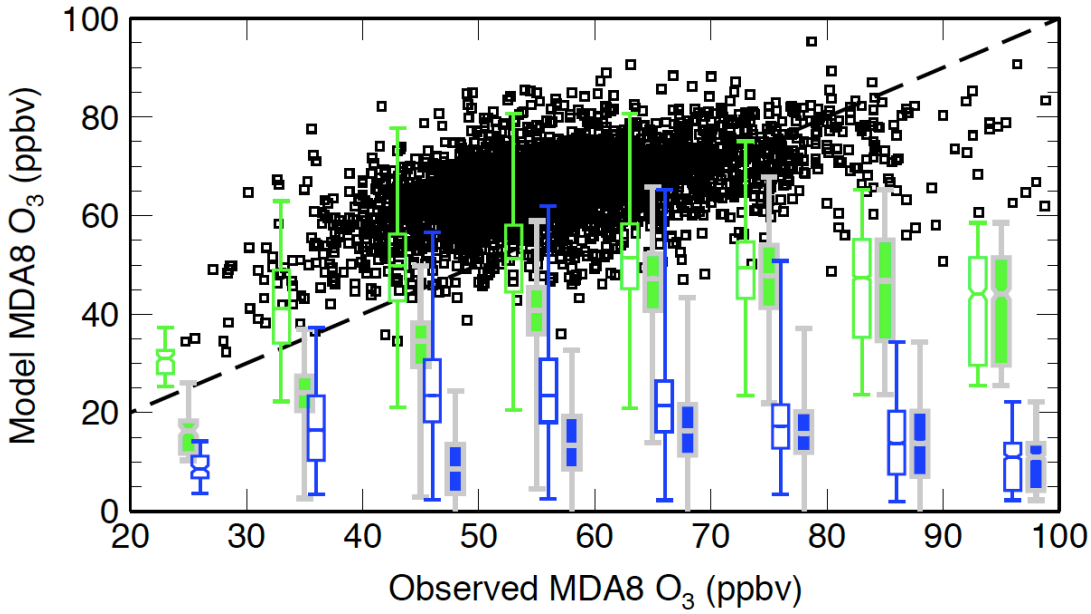

Figure T2. Model versus observed MDA8 surface O_3 for April–June 2010 at polluted sites in the densely populated regions of the Central Valley, Southern California, and Las Vegas, Nevada. The box-and-whisker plots (minimum, 25th, 50th, 75th percentiles, and maximum) concentrations give statistics of the PRB O_3 (green) and the stratospheric contribution (blue) for every 10-ppbv bin of observed O_3. Points greater than 80 ppbv are merged in the 70–80 ppbv range. The filled boxes are bias-corrected. The dashed line indicates the 1:1 relationship. (Figure based on *Lin et al,* 2012a).

Asian O_3 pollution [*Lin et al.,* 2012b] into California. Figure T2 shows results for the population centers of Southern California and Las Vegas from April to June 2010. In these areas transport of baseline O_3 to the surface can mix with high levels of locally produced O_3 pollution. The model calculates that stratospheric intrusions (solid blue symbols in Figure T2) can episodically increase surface maximum daily 8-hour average (MDA8) O_3 concentrations by 20 to 40 ppbv, including on days when observed O_3 concentrations exceed the NAAQS threshold. In these areas, PRB O_3 (solid green symbols in Figure T2) and its stratospheric component peak when observed O_3 is in the 60–80 ppbv range, and both tend to decline by 2–5 ppbv when observed O_3 increases to higher values. The PRB O_3 elevated by stratospheric intrusions reached maxima as high as 60–75 ppbv.

At high-elevation western U.S. sites, the model successfully reproduces the observed O_3 values in excess of 60 ppbv, and estimates a total PRB contribution of 83% and a North American anthropogenic contribution of 17%. The stratospheric contribution and Asian pollution account for 39% and 8% of the total, respectively. The 25th–75th percentile of the stratospheric contribution is 15–25 ppbv when observed MDA8 ozone is 60–70 ppbv, and increases to ~17–40 ppbv for the 70–85 ppbv range. These estimates are up to 2–3 times greater than previously reported. The dominant contribution from stratospheric O_3, and larger impacts with increasing O_3, indicates an important role for stratospheric intrusions in driving high concentration O_3 events at the surface during the springtime at high-elevation sites in the western U.S.

Figure T3 compares the stratospheric impacts on surface O_3 over the Mojave Desert as calculated by the AM3 [*Lin et al,* 2012a] and FLEXPART models [*Langford et al.,* 2012 and Figure T1]. The significantly larger impact from the AM3 calculation is more realistic, because it reflects the influence of the stratospheric impact on O_3 from all stratospheric intrusions in the northern

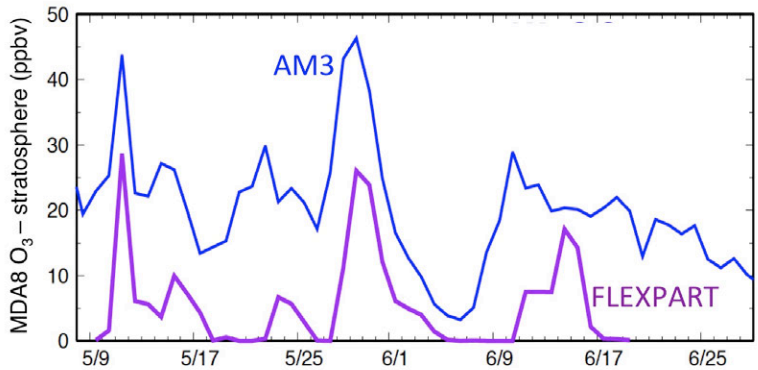

Figure T3. Time series of the contribution of stratospheric O_3 to MDA8 surface O_3 concentrations over the Mojave Desert calculated by the AM3 and FLEXPART models. (Figure based on *Lin et al,* 2012a).

hemisphere over the past months. In contrast, FLEXPART, as implemented for CalNex, directly treated transport of stratospheric O_3 from intrusions that occurred over only the North Pacific Ocean during the previous ten days. Hence, the O_3 contributions illustrated in Figure T1 represent lower limits for the total stratospheric impact.

***Finding T2*: Transport of baseline ozone accounts for a majority of surface ozone concentrations in California at urban as well as rural locations, both on average and during many exceedance events.**

To quantify ozone production within California, *Cooper et al.* [2011] compared inland ozone concentrations to baseline concentrations. Median values of lower tropospheric baseline O_3 are equal to more than 80% of the median O_3 measured within the daytime mixed layer above California's Central Valley. Similar comparisons across the polluted regions of southern California show that baseline O_3 is equal to 63–76% of the measured O_3 above Joshua Tree National Park and the LA basin.

The model calculations of *Lin et al.* [2012a,b] agree well with this observation-based estimate of *Cooper et al.* [2011]. Figure T2 shows that the median contribution of PRB O_3 (middle of solid green symbols) averages more than 50% of the observed MDA8 surface O_3 throughout the observed range, dropping to near 50% only at surface O_3 concentrations of 90 ppbv or greater. The observation-based analysis of *Parrish et al.* [2010] suggests that free tropospheric baseline O_3 transported to the surface of the northern Central Valley explains most of this region's O_3 variability, a conclusion generally consistent with the transport analysis presented by *Cooper et al.* [2011].

***Finding T3*: In addition to being a receptor of long-range pollutant transport, California is also a source of transport to downwind areas.**

Airborne lidar measurements of ozone above the Los Angeles Basin on 17 July 2009 during a "pre-CalNex" deployment of the NOAA Twin Otter aircraft show orographic lifting of ozone from the surface to the free troposphere by the San Gabriel Mountains. Mixing ratios in excess of 100 ppbv were measured ~4 km above mean sea level. These observations are in excellent agreement with published model studies, confirming that boundary layer venting by the so called "mountain chimney effect" is a potentially important pathway for removal of pollutants from the Los Angeles basin. The lofting of ozone and other pollutants into the free troposphere greatly increases the potential for long-range transport from the basin, and trajectory calculations suggest that some of this ozone was transported ~1000 km to eastern Utah and western Colorado [*Langford et al.,* 2010]. Model calculations [*Huang et al.,* 2013] show that contributions from southern California anthropogenic emissions to monthly mean MDA8 surface O_3 in the mountain states decrease with distance, ranging from <1 ppbv (in Wyoming) to 15 ppbv (in western

Arizona). These contributions show medium (>0.6) to strong (>0.8) positive correlations with the modeled surface MDA8 O_3. For the most strongly affected states of Arizona and New Mexico, these contributions have median values of ~3, ~2, ~5, and ~15 ppbv when the total surface MDA8 O_3 exceeds thresholds of 60, 65, 70, and 75 ppbv, respectively.

References

Cooper, O. R., et al. (2011), Measurement of western U.S. baseline ozone from the surface to the tropopause and assessment of downwind impact regions, *J. Geophys. Res., 116*, D00V03, doi:10.1029/2011JD016095.

Huang, M., K.W. Bowman, G. R. Carmichael, R. B. Pierce, H. M. Worden, M. Luo, O. R. Cooper, I. B. Pollack, T. B. Ryerson, and S. S. Brown (2013), Impact of Southern California anthropogenic emissions on ozone pollution in the mountain states: Model analysis and observational evidence from space, *J. Geophys. Res. Atmos., 118*, 12,784–12,803, doi:10.1002/2013JD020205.

Langford, A. O., C. J. Senff, R. J. I. Alvarez, R. M. Banta, and R. M. Hardesty (2010), Long-range transport of ozone from the Los Angeles Basin: a case study, *Geophys. Res. Lett.*, *37*(L06807), doi:10.1029/2010GL042507.

Langford, A. O., J. Brioude, O. R. Cooper, C. J. Senff, R. J. Alvarez II, R. M. Hardesty, B. J. Johnson, and S. J. Oltmans (2012), Stratospheric influence on surface ozone in the Los Angeles area during late spring and early summer of 2010, , *J. Geophys. Res., 117*(D00V06), doi:10.1029/2011JD016766.

Lin, M., A. M. Fiore, O. R. Cooper, L. W. Horowitz, A. O. Langford, H. Levy II, B. J. Johnson, B. Naik, S. J. Oltmans, and C. J. Senff (2012a), Springtime high surface ozone events over the western United States: Quantifying the role of stratospheric intrusions, *J. Geophys. Res.*, *117*(D00V22), doi:10.1029/2012JD018151.

Lin, M., et al. (2012b), Transport of Asian ozone pollution into surface air over the western United States in spring, *J. Geophys. Res.*, *117*(D00V07), doi:10.1029/2011JD016961.

McDonald-Buller, E.C., D.T. Allen, N. Brown, D.J. Jacob, D. Jaffe, C.E. Kolb, A.S. Lefohn, S. Oltmans, D.D. Parrish, G. Yarwood and L. Zhang (2011), Establishing Policy Relevant Background (PRB) Ozone Concentrations in the United States, *Environ. Sci. Technol., 45*(22), 9484-9497, doi:10.1021/es2022818.

Parrish, D. D., K. C. Aikin, S. J. Oltmans, B. J. Johnson, M. Ives, and C. Sweeny (2010), Impact of transported background ozone inflow on summertime air quality in a California ozone exceedance area, *Atmos. Chem. Phys., 10*, 10,093–10,109, doi:10.5194/acp-10-10093-2010.

U.S. EPA (2007), Treatment of data influenced by exceptional events, *Fed. Regist., 72*(55), 13,560–13,581.

Synthesis of Results - Modeling

Response to Question U

QUESTION U

How well did the meteorological and air quality forecast models perform during CalNex? What weaknesses need attention?

BACKGROUND

Angevine et al. [2012] provide meteorological fields for interpretation of chemical and aerosol measurements taken during the CalNex field campaign. The simulations have been used to support inverse modeling to improve estimates of emissions in the Los Angeles area and the Central Valley [*Brioude et al.,* 2013; *Kim et al.*, 2013], to understand transport and chemical evolution in the Los Angeles area and beyond [e.g., *Cooper et al.,* 2011; *Angevine et al.,* 2013] and to explore the characteristics and impact of marine stratocumulus clouds. For those purposes, *Angevine et al.* [2012] focus on boundary layer structure, clouds, and winds in the coastal zone of Southern California, the Los Angeles basin, and the San Joaquin Valley.

During the CalNex intensive period, results from seven real-time air quality forecast models were provided to NOAA/ESRL/CSD by four institutions: Environment Canada, NOAA/NCEP, NOAA/ESRL/GSD, and Baron Advanced Meteorological Services (BAMS). An additional real-time ensemble forecast based on four of the forecast models was also available to study participants. A graphical archive of the 24 and 48-hour forecasts from May 1 through July 18, 2010 is available at: http://www.esrl.noaa.gov/csd/groups/csd4/modeleval.

POLICY RELEVANCE

In air quality applications, meteorological fields from mesoscale models are used to drive Lagrangian or Eulerian transport and chemistry models. We need to understand the accuracy and uncertainty of the meteorological fields in order to know what confidence to place in the air quality modeling results. In a real sense, the transport and chemistry models are a synthesis of our understanding of the atmosphere, and provide our only means of evaluating emission control scenarios.

FINDINGS

***Finding U1*: Evaluation of different meteorological models against CalNex measurements shows that details of model configuration (physics, initialization, resolution) can impact performance for specific processes and regions. Particular attention needs to be paid to land surface and soil parameters and to clouds offshore. Significant but poorly characterized biases (for example, high wind speeds and weak land breeze) remain in the best available simulations.**

Angevine et al. [2012] evaluate the performance of mesoscale meteorological models for the coastal zone and Los Angeles area of Southern California, and for the San Joaquin Valley. Several configurations of the Weather Research and Forecasting Model (WRF) with differing

grid spacing, initialization, planetary boundary layer (PBL) physics, and land surface models are compared. One configuration of the Coupled Ocean–Atmosphere Mesoscale Prediction System (COAMPS) model is also included, providing results from an independent development and process flow. Specific phenomena of interest for air quality studies are examined. All model configurations are biased toward higher wind speeds than observed. The diurnal cycle of wind direction and speed (land–sea-breeze cycle) as modeled and observed by a wind profiler at Los Angeles International Airport is examined. Each of the models shows different biases in reproducing the cycle. Soundings from San Nicolas Island, a case study involving the Research Vessel (R/V) Atlantis and the NOAA P3 aircraft, and satellite images are used to evaluate simulation performance for cloudy boundary layers. In a case study, the boundary layer structure over the water is poorly simulated by all of the WRF configurations except one with the total energy–mass flux boundary layer scheme and ECMWF reanalysis. The original WRF configuration had a substantial bias toward low PBL heights in the San Joaquin Valley, which is improved in the final configuration. WRF runs with 12-km grids have larger errors in wind speed and direction than those present in the 4-km grid runs.

***Finding U2a*: Evaluation of several different real-time air quality forecasts against O_3 and PM2.5 observations show that none of the models perform statistically better than the persistence forecast (i.e., predicting that tomorrow's air quality will be exactly the same as today's air quality). All models show temporal correlations for maximum 8-hr O_3 that beat persistence, but model biases and poor spatial correlations limit overall forecast skill.**

***Finding U2b*: Incorporation of the RAQMS global forecast [*Pierce et al.*, 2003] to modify lateral boundary conditions improved temporal skill for O_3 forecasts but increased model bias.**

Analysis: S.A. McKeen, unpublished

The focus of this evaluation is a comparison of predicted maximum 8-hr average O_3, and 24-hr average PM2.5 with those observed. For example, Figure U1 shows AIRNow O_3 monitor locations, and compares observations with the NOAA/NCEP forecast (without incorporation of boundary conditions from the RAQMS global forecast) for the number of occurrences when maximum 8-hr average O_3 is greater than 75 ppbv. The forecast model tends to over-predict the number of occurrences throughout the sample area, except for the under-predictions east of the LA basin. Analysis attributes the overall O_3 over-prediction to NO_X emissions being too high, and the behavior east of the LA basin to titration effects from the resulting high NO_X in that region.

The performance of each of the seven forecast models was evaluated through several statistical comparisons of the model output with observations. For example, the overall r-correlation and median bias between the model predictions and the measurements are evaluation measures that cover both space and time. The benchmark selected for evaluating model performance is the same statistical comparison of the persistence forecast with observations, whereby tomorrow's forecast is simply taken to be today's observations. It is found that none of the models for forecasting O_3 can outperform persistence forecasting in terms of correlation, and that all but one model are biased high.

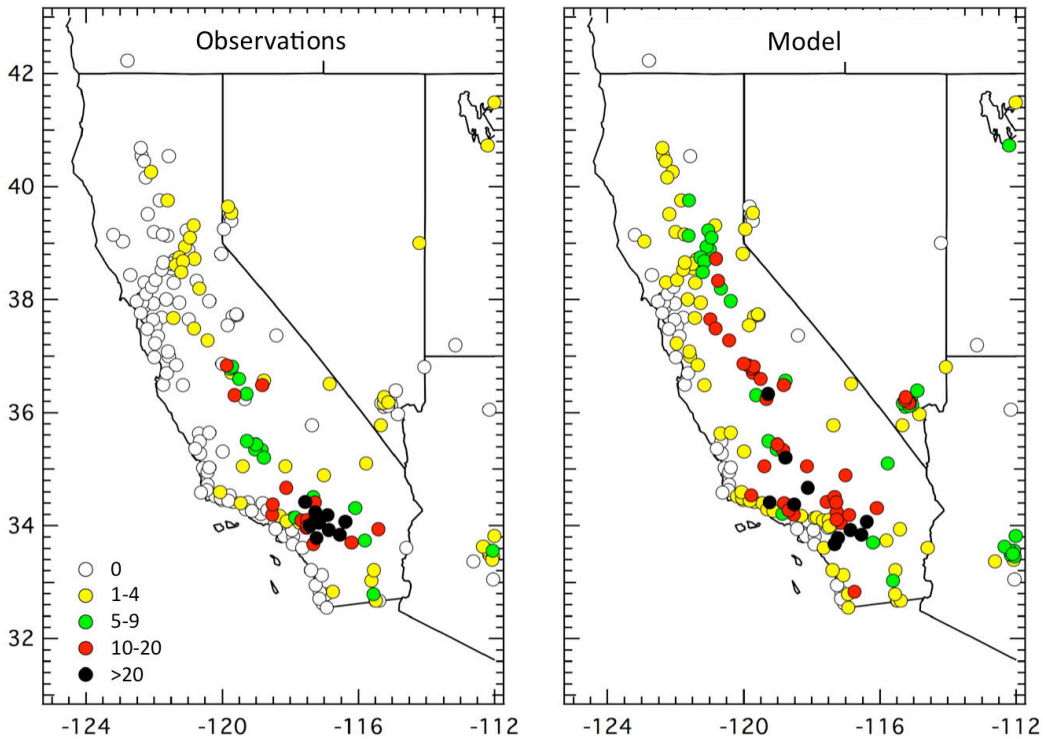

Figure U1. Number of days with maximum 8-hr average O_3 concentration ≥ 75 ppbv from 19 May to 15 July 2010. Observations are shown on the left and results from a model forecast are shown on the right.

All models do have more than 50% of their points with better temporal correlation than persistence. The inclusion of the RAQMS global forecast to provide lateral boundary conditions for the NCEP model significantly improves the O_3 r-correlation, but also significantly increases the positive bias of the model. The RAQMS forecast includes real-time assimilation of upper-tropospheric satellite O_3 data, which has the largest impact on high elevation stations and the eastern part of California.

For PM2.5, like O_3, none of the models can outperform the persistence forecast in terms of correlation or root mean square error. With a median observed average PM2.5 concentration of 10 $\mu g/m^3$, all but two models display low absolute bias. Unlike the O_3 forecasting, inclusion of the RAQMS global forecast for PM2.5 has a negative impact in terms of the correlation measures. Retrospective runs tested the impact of assimilating the global GOCART aerosol transport model into one of the WRF/Chem models; this approach improved forecast predictions over the base model, but r-correlation skill still remained less than that for the persistence forecast.

It should be noted that the use of persistence as a statistical reference puts the forecast models at a distinct disadvantage when applied to California in the summertime. Correlations of the persistence forecast are noticeably higher for California, when compared to the rest of the U.S. for the same time period, particularly for O_3 because of California's Mediterranean climate. Thus, individual model performance for California should not be extrapolated to other parts of the U.S. and Canada.

References

Angevine, W. M., L. Eddington, K. Durkee, C. Fairall, L. Bianco, and J. Brioude (2012), Meteorological model evaluation for CalNex 2010, *Monthly Weather Review*, doi:10.1175/MWR-D-12-00042.1.

Angevine, W. M., et al. (2013), Pollutant transport among California regions, *J. Geophys. Res. Atmos., 118*, 6750–6763, doi:10.1002/jgrd.50490.

Brioude, J., et al. (2013), Top-down estimate of surface flux in the Los Angeles Basin using a mesoscale inverse modeling technique: Assessing anthropogenic emissions of CO, NO_x and CO_2 and their impacts, *Atmos. Chem. Phys.*, *13*, 3661–3677, doi:10.5194/acp-13-3661-2013.

Cooper, O. R., et al. (2011), Measurement of western U.S. baseline ozone from the surface to the tropopause and assessment of downwind impact regions, *J. Geophys. Res.*, *116*(D00V03), doi:10.1029/2011JD016095.

Kim, S.W., et al. (2013), Evaluation of NO_X emission inventories in California using multi-satellite data sets, in-situ airborne measurements, and regional model simulations during CalNex 2010, *J. Geophys. Res.*, in preparation.

McKeen, S.A., G. Grell, S. Peckham, E.-Y. Hsie, W. Gong, S. Ménard, H. Landry, J. McQueen, Y. Tang, J. McHenry, D. Olerud, (2010-12-14), Evaluation of Real-time Air Quality Model Forecasts and Their Emissions During the CalNex-2010 Field Campaign. *American Geophysical Union, Fall Meeting*, San Francisco, CA, USA.

Pierce, R. B. et al. (2003), Regional Air Quality Modeling System (RAQMS) predictions of the tropospheric ozone budget over east Asia, *J. Geophys. Res.*, *108,* 8825, doi:10.1029/2002JD003176, D21.

Synthesis of Results - Climate and Air Quality Nexus

Response to Question V

QUESTION V

What pollution control efforts are likely to result in "win-win" or "win-lose" situations?

BACKGROUND

The California Research at the Nexus of Air Quality and Climate Change (CalNex) 2010 field project was undertaken to provide improved scientific knowledge for emissions control strategies to simultaneously address the two interrelated issues of air quality and climate change. Air quality and climate change issues are linked because in many cases, the agents of concern are the same and the sources of the agents are the same or intimately connected. Examples include tropospheric ozone, which is both an air pollutant and a greenhouse gas, and atmospheric particulate matter, which has effects on the radiative budget of the atmosphere as well as human and ecosystem health, visibility degradation, and acidic deposition. Efforts to address one of these issues can be beneficial to the other ("win-win" situations), but in some cases, policies addressing one issue without additional consideration can have unintended detrimental impacts on the other ("win-lose" situations). The goal of CalNex 2010 is to improve and advance the science needed to support continued and effective air quality and climate management policy for the State of California and the Nation as a whole.

POLICY RELEVANCE

Policies to address climate change and air quality degradation are more effective when both issues are considered together so that policies positively impact both issues ("win-win" situations) rather than improving one, but worsening the other ("win-lose" situations).

One clear example of a "win-win" control strategy is reduction in emissions of light-absorbing or black carbon (BC) aerosol. This material is emitted with widely varying emission factors from a variety of combustion processes, including heavy-duty diesel engines and biomass burning. It is a component of PM that is suspected to be particularly important in the negative health effects associated with aerosols [*Jansen et al.,* 2005], and thus constitutes an important air quality issue. It also acts as a warming agent in the atmosphere [*Bond et al.,* 2013] due to its light-absorbing properties, and thus constitutes an equally important climate change issue. Light absorbing aerosols like black carbon also generally act to reduce cloudiness [*Ackerman et al.*, 2000; *Koren et al.*, 2005], further warming the atmosphere. Thus, reducing BC emissions will create a "win-win" situation for both climate change and air quality in California.

It is also worth emphasizing here that any pollutant control effort that increases efficiency of energy use (e.g., increased fuel mileage of on-road vehicles, or increased use of mass transport to replace personal vehicle usage) is a "win-win" change for air quality and climate change. Less fuel burned implies both smaller air pollutant emissions and less CO_2 released to the atmosphere.

FINDINGS

The data set collected during the CalNex fieldwork provides a wide range of measurements that allow air quality and climate change policies to be developed with a full appreciation of the ways in which the policies will impact both issues. Until now, relatively few studies have considered both issues together. However, the following are two specific examples.

***Finding V1*: The approximately 75% reduction of burning crop residue from rice agriculture (a "win" for air quality) increased methane emissions (a "lose" for climate).**

Peischl et al. [2012] analyzed airborne measurements of methane (CH_4) and carbon dioxide (CO_2) taken over the rice growing region of California's Sacramento Valley in the late spring of 2010 and 2011. From these and ancillary measurements, they show that CH_4 mixing ratios were enhanced in the planetary boundary layer above the Sacramento Valley during the rice growing season than they were before it, which they attribute to emissions from rice paddies. They derive daytime emission fluxes of CH_4 between 0.6 and 2.0% of the CO_2 taken up by photosynthesis on a per carbon, or mole-to-mole, basis. They also use a mixing model to determine an average CH_4/CO_2 flux ratio of ~0.6% for one day early in the growing season of 2010. They conclude the CH_4/CO_2 flux ratio estimates from a single rice field in a previous study [*McMillan et al.,* 2007] are representative of rice fields in the Sacramento Valley. If generally true, the CARB greenhouse gas inventory emission rate [*Franco*, 2002, which is consistent with CARB's current on-line GHG inventory (http://www.arb.ca.gov/app/ghg/2000_2011/ghg_sector_data.php)] of 2.7 x 10^{10} g CH_4/yr is approximately three times lower than the range of probable CH_4 emissions (7.8–9.3 x 10^{10} g CH_4/yr) from rice cultivation derived in this study. They attribute this difference to decreased burning of the residual rice crop since 1991, which leads to an increase in CH_4 emissions from rice paddies in succeeding years, but which is not accounted for in the CARB inventory.

***Finding V2*: Marine vessel emissions changes due to fuel sulfur reductions and speed controls result in a net warming effect (a "lose" for climate), but have substantial positive impacts on local sulfur and primary PM emissions (a "win" for air quality).**

Lack et al. [2011] demonstrate the efficacy of California's shipping fuel quality regulation and vessel speed reduction (VSR) program in reducing emission factors and absolute emissions of SO_2, sulfate, and (somewhat unexpectedly) particulate organic matter (POM) and black carbon (BC). (See Response to Question E for more complete discussion.) The emission factors of N_{Tot} (total particle number) appear to increase due to the regulations, although these are small particles that will likely quickly condense or coagulate with existing particles. On an absolute scale (per kilometer of travel), mass reductions of SO_2, sulfate, and PM are in excess of 96%; BC and POM reductions are 75% and 88% respectively, and CO_2 reductions are 58%. The regulations significantly alter the direct climate cooling impacts of the emitted PM by reducing the sulfate that forms just after emission and through secondary formation from SO_2 oxidation. In areas where low sulfur fuel is used, significant reductions in the number of cloud condensation nuclei (CCN) as well as reductions in particle size will decrease the indirect cooling impacts associated with enhanced cloud formation, particularly in regions sensitive to inputs of CCN from shipping, such as at ~30° N. This reduced cooling is partially offset by a concurrent decrease in the climate warming impact of BC and CO_2 emissions. Their observations suggest that air quality benefits from the fuel quality regulation and the VSR program are likely to be substantial, although these air-quality benefits are likely to occur concurrently with a reduction in the anthropogenic cooling effect that results from shipping PM. If it is determined that air

pollution (i.e., human health and welfare) goals can be met through near-coast regulation, then the implementation of a more nuanced location-dependent global fuel quality regulation may be worthy of consideration.

References

Ackerman, A.S., O.B. Toon, D.E. Stevens, A.J. Heymsfield, V. Ramanathan, and E.J. Welton (2000), Reduction of tropical cloudiness by soot, *Science*, *288*, 1042-1047.

Bond, T. C., et al. (2013), Bounding the role of black carbon in the climate system: A scientific assessment, *J. Geophys. Res. Atmos., 118*, 5380–5552, doi: 10.1002/jgrd.50171.

Franco, G. (2002), Inventory of California greenhouse gas emissions and sinks: 1990–1999, Report 600–02–001F, Calif. Energy Comm., Sacramento.

Jansen, K. L., T. V. Larson, J. Q. Koenig, T. F. Mar, C. Fields, J. Stewart and M. Lippmann (2005), Associations between Health Effects and Particulate Matter and Black Carbon in Subjects with Respiratory Disease, *Environ. Health Perspect., 113*(12), 1741–1746, doi: 10.1289/ehp.8153.

Koren, I., Y.J. Kaufman, D. Rosenfeld, L.A. Remer, and Y. Rudich (2005), Aerosol invigoration and restructuring of Atlantic convective clouds, *Geophys. Res. Lett.*, *32*, L14828, doi:10.1029/2005GL023187.

Lack, D. A., et al. (2011), Impact of fuel quality regulation and speed reductions on shipping emissions: Implications for climate and air quality, *Environ. Sci. Technol.*, *45*, 9052-9060, doi:10.1021/es2013424.

McMillan, A. M. S., M. L. Goulden, and S. C. Tyler (2007), Stoichiometry of CH_4 and CO_2 flux in a California rice paddy, *J. Geophys. Res.*, *112*, G01008, doi:10.1029/2006JG000198.

Peischl, J., et al. (2012), Airborne observations of methane emissions from rice cultivation in the Sacramento Valley of California, *J. Geophys. Res.*, *117*(D00V25), doi:10.1029/2012JD017994.

Synthesis of Results - Climate and Air Quality Nexus

Response to Question W

QUESTION W

Could the same pollutant control efforts in different air basins (i.e., SJVAB and SoCAB) have different results with respect to changes in air quality and climate (i.e., move toward different nexus quadrants in the figure on the front page of this report)?

BACKGROUND

There are some circumstances where the same control efforts have markedly different effects on air quality. A well known example is the work of *Chameides et al.* [1988] who showed that control of anthropogenic VOC emissions is effective in reducing ambient O_3 concentrations in many urban areas, but much less effective in some urban areas (such as Atlanta, Georgia) that have large emissions of biogenic hydrocarbons. Such hydrocarbons are generally highly reactive and thus effective O_3 precursors. Consequently, their concentrations do not accumulate greatly in the ambient atmosphere despite their major role in photochemical O_3 production. In regions with large emissions of biogenic hydrocarbons, reduction of NO_X emissions may be a more effective control strategy than reduction of anthropogenic VOC emissions.

In California, the air basins with the most difficult air quality issues (i.e., SJVAB and SoCAB) are not thought to have large emissions of the biogenic hydrocarbons that are important in forested regions, although biogenic emissions in downslope flow from the Sierra Mountains contribute to nighttime formation of aerosols in the southern SJVAB [*Rollins et al.,* 2012]. In other air basins (e.g., the Mountain Counties), biogenic emissions may be important but such areas generally experience only modest ambient O_3 concentrations (due to limited NO_X emissions) unless O_3 is transported there from regions with large anthropogenic emissions. However, within either SJVAB or SoCAB, other unrecognized sources of reactive VOCs could possibly affect the efficacy of pollutant control efforts; such possible sources deserve investigation. The possible role of agricultural emissions in the SJVAB is a topic of increasing concern.

POLICY RELEVANCE

Many of California's air quality regulations, such as mobile source controls, are applicable throughout the entire State. However, other regulations address the individual needs of a specific region, as different air basins (e.g., SJVAB, and SoCAB) have important differences in the mix of air quality relevant emissions. It is important to understand this emission mix in developing appropriate control strategies

FINDINGS

***Finding W1*: The southern SJVAB has an unidentified, temperature-dependent VOC emission source that dominates O_3 production on the hottest days when the highest O_3 concentrations occur. As a consequence, NO_X emission controls are expected to be more effective for reducing maximum O_3 concentrations in the southern SJVAB than in the SoCAB.**

As more thoroughly discussed in the Response to Question J, *Pusede and Cohen* [2012] and *Pusede et al.* [2013] show that the NO_X versus VOC sensitivity of the O_3 photochemistry in the SJVAB changes markedly with ambient temperature, becoming much more NO_X sensitive on the hottest days, which are also the days that lead to most O_3 exceedances in this air basin. CalNex measurements from the Bakersfield site (Figure J2) have been analyzed to identify the cause of this change in photochemical regime as a particular VOC source that is rich in oxygenated VOCs. A similar analysis indicates that such a temperature dependent VOC source is not present in the SoCAB. As a consequence, NO_X emission controls are expected to be more effective in the SJVAB than in the SoCAB, and indeed may be required for further reduction of the highest O_3 levels in the southern SJVAB.

***Finding W2a*: In the SJVAB ammonia is in large excess compared to nitric acid; consequently NH_4NO_3 PM concentrations in the SJVAB will be more responsive to NO_X emissions reductions compared to ammonia emissions reductions.**

***Finding W2b*: In the SoCAB the response of NH_4NO_3 PM concentrations to emission reductions will depend upon meteorological conditions, other aerosol components, and the regional distribution of NH_3 and NO_X emissions.**

Ammonia (NH_3) is the dominant gas-phase base in the troposphere. Anthropogenic emissions of NO_x are oxidized in sunlight to form nitric acid (HNO_3), which can react in the atmosphere to form ammonium nitrate (NH_4NO_3) particulate matter (PM). In the SJVAB, two major NH_3 sources from agricultural activity, animal waste and crop fertilization, are particularly important. In general, in both the SoCAB and the SJVAB, agricultural activity (i.e., dairy farms and other livestock operations) and urban centers (i.e., Fresno, Los Angeles) are sources of ammonium nitrate gas-phase precursors. As more thoroughly discussed in the Response to Question I and J, *Nowak et al.* [2012a,b] utilize airborne measurements of NH_3, HNO_3, and particle composition made aboard the NOAA WP-3D aircraft to quantify NH_3 emissions from agricultural and vehicle sources, describe the vertical structure and transport of NH_3 from these sources, examine their impact on ammonium nitrate formation, and contrast the SoCAB and the SJVAB.

In the SJVAB during CalNex, ambient NH_3 concentrations were quite large, much larger on average than observed by the WP-3D aircraft in any other location; nevertheless NH_4NO_3 concentrations were relatively small. The amount of NH_4NO_3 that can be formed is limited by the amount of HNO_3 that can be formed from the relatively small NO_X emissions in the SJVAB. Consequently, ambient NH_4NO_3 concentrations will be much more responsive to NO_X emissions reductions compared to NH_3 emissions reductions.

The CalNex data were collected in late spring-early summer, but NH_4NO_3 concentrations are much larger in winter in the SJVAB. Since NO_X emissions are not expected to have a large seasonal variation, sensitivities to NO_X and NH_3 emissions reductions are expected to be similar throughout the year. Data collected during the Discover-AQ campaign in the Central Valley during January and February 2013 may provide a means to verify this expectation for winter.

The situation in the SoCAB is quite different. The relatively large NO_X emissions from the vehicle fleet and the relative small NH_3 emissions from dairies and vehicles cause the formation of ammonium nitrate aerosol to depend on many variables. Meteorological conditions (temperature, humidity and sunlight) will affect the thermodynamics and kinetics of NH_4NO_3 formation as well as the rate of conversion of NO_X to HNO_3. The regional distribution of NH_3 and NO_X emissions will determine which of the reactants is in excess at any particular location.

Additionally, the formation of NH_4NO_3 will also be affected by preexisting aerosol. Judging the most effective control strategy for NH_4NO_3 PM in the SoCAB must consider all of these variables.

***Finding W3a*: In both the SoCAB and the SJVAB, anthropogenic VOCs are believed to be the primary precursors of secondary organic aerosol; thus in both basins organic aerosol concentrations will be sensitive to VOC emissions control.**

***Finding W3b:* Biogenic VOCs oxidized in the presence of NO_X provides additional sources of secondary organic aerosol that are important for the SJVAB, but less so in the SoCAB. Thus, NO_X emissions reductions will be effective for controlling this source of organic aerosol in the SJVAB, but will have less impact in the SoCAB.**

As more thoroughly discussed in the Response to Questions L, anthropogenic VOCs are the primary precursors of secondary organic aerosol (SOA) in both the SoCAB and the SJVAB. Consequently, control of the emissions of these species is the obvious approach to reducing the SOA contribution to ambient PM concentrations in both air basins. Additionally, as discussed with regard to Finding L2, there are nighttime and daytime mechanisms involving NO_X that lead to additional SOA formation from the oxidation of biogenic VOCs. These mechanisms are more important in the SJVAB than the SoCAB. The nighttime mechanism directly involves NO_X, as the NO_3 radical is the biogenic VOC oxidant [Rollins et al., 2012]. NO_X is also believed to play a role in the daytime mechanism, where urban plumes are transported into the biogenic VOC rich environment of the Sierra foothills. Thus, this component of SOA formation from biogenic VOCs is expected to be sensitive to NOx emission controls.

References

Chameides, W.L., R.W. Lindsay, J. Richardson and C.S. Kiang (1988), The role of biogenic hydrocarbons in urban photochemical smog: Atlanta as a case study, *Science, 241*, 1473-1475.

Nowak, J. B., J. A. Neuman, R. Bahreini, A. M. Middlebrook, J. S. Holloway, S. A. McKeen, D. D. Parrish, T. B. Ryerson, and M. Trainer (2012a), Ammonia sources in the California South Coast Air Basin and their impact on ammonium nitrate formation, *Geophys. Res. Lett., 39*, L07804, doi:10.1029/2012GL051197.

Nowak, J. B. (2012b), Ammonia Emissions from Agricultural Sources and their Implications for Ammonium Nitrate Formation in California, presentation at ACS National Meeting, August 2012, Philadelphia, PA.

Pusede, S. E. and R. C. Cohen (2012), On the observed response of ozone to NOx and VOC reactivity reductions in San Joaquin Valley California 1995–present, *Atmos. Chem. Phys., 12*, 8323–8339.

Pusede, S. E., et al. (2013), On the temperature dependence of organic reactivity, ozone production, and the impact of emissions controls in San Joaquin Valley California, *Atmos. Chem. Phys. Disc*, *13*, 28511–28560, doi:10.5194/acpd-13-28511-2013.

Rollins, A. W., et al. (2012), Evidence for NO_X control over nighttime SOA formation, *Science*, *337*(6099), 1210-1212, doi:10.1126/science.1221520.

Recommendations for Further Analysis

As is expected in scientific research, progress in addressing a given set of questions raises new questions suggesting additional analysis. Specific examples of additional analysis suggested by the CalNex Findings are briefly discussed here.

1. Finding B1 notes recent, marked increases in the concentrations of ethanol in the SoCAB, but also continuing decreases in the concentrations of acetaldehyde (an air toxic), which is a secondary product of the atmospheric oxidation of ethanol. Research data sets indicate continuing acetaldehyde concentration decreases, but results from the Toxics Network shows slower acetaldehyde decreases, and increases in formaldehyde concentrations. It would be enlightening a) to resolve the inconsistencies between the research and Toxics Network results, and b) to follow the future evolution of acetaldehyde concentrations as most VOC concentrations continue to decrease, while the concentration of ethanol perhaps increases.
2. Finding C2 notes that the CalNex measurements cannot characterize the peak PM2.5 concentrations observed in the Central Valley in winter (January-February 2013). However, a systematic comparison of the PM characterization from CalNex with that from the DISCOVER-AQ study in winter should provide additional insights into PM formation in the Central Valley as well as in the SoCAB. Both the organic and NH_3NO_4 PM components could be investigated in this analysis.
3. Finding E2 notes that by some measures, O_3 concentrations have decreased more slowly in the SJV than in the SoCAB; however the cause and significance of this difference is ambiguous. Figure E2 presents a statistical investigation of the O_3 concentration trends in these two air basins. A systematic extension of this investigatory approach to many of California's air basins would provide insights into separately determining the roles played by transported baseline O_3 concentrations and the time scales of response to emission control policies in determining the temporal trends of ambient O_3 concentrations.
4. Finding F2a indicates that CH_4 emissions from the oil and gas sector in Los Angeles constitute the emissions missing from current inventories. However, it has not been determined if these emissions are due to leaks during the natural gas extraction and production activities within the SoCAB, or due to leaks from the domestic natural gas distribution system. Spatially-resolved measurements in Los Angeles, possibly including CH_4 stable isotope data, both in atmospheric samples and in direct samples of potential source emissions, are needed for more detailed identification and attribution of the excess CH_4 that appears to be a consistent feature of Los Angeles' atmosphere.
5. Finding F2b indicates that CH_4 emissions from dairies had large temporal variation during CalNex, possibly associated with manure management practices. Further investigation of this variability may provide guidance for reducing these CH_4 emissions.
6. Finding F3 suggests that improved quantification of agricultural N_2O sources in California may help the State reduce GHG emissions. More precise knowledge of the spatial distribution of sources, their magnitude, and their seasonality is necessary to critically evaluate State and National inventories and to assess the contribution of N_2O to the total GHG emissions of California.
7. Finding F6 indicates that top-down assessments of NO_X emissions are in general agreement with the CARB emission inventory. However, the CalNex analysis has not included a comparison between satellite column measurements of NO_2 with inventory NO_X emissions.

Combining the CalNex NOAA P-3 aircraft measurements with the satellite data and model calculations provides a powerful tool for assessing NO_2 emission inventories, e.g. *Kim et al*. [2011].

8. Finding G2 indicates that individual VOC to CO emission ratios observed in the SoCAB can disagree by a factor of four or more with the ratios derived from NEI 2005 and CARB 2008 emission inventories. The agreement is particularly poor for oxygenated VOCs. Although these disagreements did not have large implications for the accuracy of photochemical modeling of O_3 and PM formation, it would be useful to elucidate the cause of these discrepancies.
9. Finding J2 presents evidence for a temperature dependent, unidentified source of VOC emissions in the SJV, perhaps associated with agricultural activities or petroleum operations. This source plays an important role in O_3 exceedances in this air basin. Identification of this source would perhaps provide an attractive target for reducing SJV O_3 concentrations.
10. A major research focus of CalNex was the formation of secondary organic aerosol (SOA). There is general agreement that SOA constitutes the majority of the organic component of PM2.5, but no definitive picture has emerged regarding either the major precursors or the primary formation mechanisms. It is likely that the entire atmospheric chemistry research community will be occupied with fully developing this picture in years to come.
11. Finding M1 notes that nighttime chemical processes play multiple important air quality roles. Traditionally air quality models have primarily focused on daytime, photochemical reactions. It is important to ensure that the nighttime chemical processes are accurately included in the air quality modeling.
12. Finding N4 notes that there is disagreement regarding the relative importance of the gasoline versus diesel contributions to SOA formation. This disagreement should be resolved.
13. The Findings in Responses to Questions D, O and T have pointed to the growing importance of baseline O_3 transported into California. This importance is growing, because as local O_3 production decreases, transported O_3 constitutes an increasing fraction of ambient concentrations, a fraction that is not controllable by local efforts. An improved understanding of how this transport contributes to local O_3 concentrations is important - note relation to item 3) above.

References

Kim, S.-W., et al., (2011), Evaluations of NO_X and Highly Reactive VOC Emission Inventories in Texas and their Implications for Ozone Plume Simulations during the Texas Air Quality Study 2006, *Atmos. Chem. Phys.*, *11*,, 11361-11386, doi:10.5194/acp-11-11361-2011.

Contributors

The California Air Resources Board (CARB) and the National Oceanic and Atmospheric Administration (NOAA) gratefully acknowledge significant contributions to the success of the CalNex field research campaign by the many different organizations listed below. These contributions include significant financial and in-kind organizational support as well as the time and creative energy of individual scientists, engineers, post-doctoral fellows, and graduate students who joined in this collaborative enterprise.

These contributions include:

- Defining the objectives of CalNex,
- Instrumenting the various atmospheric measurement platforms and sites,
- Implementing and quality assuring the myriad field measurements during the course of the study,
- Completing the analysis, interpretation, and intercomparison of research results, and
- Publishing and reporting the research findings, so that they can be used for policy purposes by CARB and other stakeholders.

Cooperating State Government Organizations

California Air Resources Board
- Research Division, Atmospheric Processes Research Section
- Air Quality Planning and Science Division

California Energy Commission

Cooperating California Local Government Organizations

Sacramento Metropolitan Air Quality Management District
San Joaquin Valley Air Pollution Control District
San Luis Obispo County Air Pollution Control District
South Coast Air Quality Management District

Cooperating Federal Government Agencies

Centre National de la Recherche Scientifique (Toulouse, France), Laboratoire d'Aérologie
Department of Energy (DOE)
- Brookhaven National Laboratory (BNL)
- Pacific Northwest National Laboratory (PNNL)

Environment Canada (EC)
- Air Quality Research Division, Science and Technology Branch
- Meteorological Service of Canada

Lawrence Berkeley National Laboratory
- Chemical Sciences Division
- Environment and Energy Technologies Division

Meteorological Research Institute (Ibaraki, Japan)
National Aeronautics and Space Administration (NASA)
- Goddard Institute for Space Studies
- Headquarters Science Mission Directorate, Tropospheric Chemistry Program
- Langley Research Center (LRC)

National Oceanic and Atmospheric Administration (NOAA)
- Air Resources Laboratory (ARL)

- ESRL Chemical Sciences Division (CSD)
- ESRL Global Monitoring Division (GMD)
- ESRL Physical Sciences Division (PSD)
- Geophysical Fluid Dynamics Laboratory (GFDL)
- Health of the Atmosphere Program
- National Centers for Environmental Prediction (NCEP)
- Pacific Marine Environmental Laboratory (PMEL)
- National Weather Service (NWS)
- National Environmental Satellite Data and Information Service (NESDIS)
- Office of Marine and Aviation Operations (OMAO)

National Park Service, Air Resources Division
National Science Foundation (NSF)
- National Center for Atmospheric Research (NCAR)
  - Atmospheric Chemistry Division
  - Earth Observing Laboratory
  - Research Aviation Facility
- University Corporation of Atmospheric Research

Research Centre Jülich GmbH (Jülich, Germany), Institute for Chemistry of the Polluted Atmosphere
United States Environmental Protection Agency (USEPA), National Exposure Research Laboratory
United States Navy (USN), Point Mugu Naval Air Warfare Center

Cooperating Research Universities

Arizona State University
- Department of Chemistry and Biochemistry
- School of Earth and Space Exploration

Auburn University, School of Forestry and Wildlife Science
Baylor University, Department of Environmental Science
Boston College, Department of Chemistry
California Institute of Technology
- Division of Chemistry and Chemical Engineering
- Division of Engineering and Applied Science
- Division of Geological and Planetary Sciences
- Jet Propulsion Laboratory (JPL)
- Keck Institute for Space Studies

California State Polytechnic University, Pomona, Department of Mechanical Engineering
Colorado State University, Cooperative Institute for Research in Atmospheres (CIRA)
Columbia University
- Department of Earth and Environmental Sciences
- Lamont-Doherty Earth Observatory

Georgia Institute of Technology
- School of Earth and Atmospheric Sciences
- School of Chemical and Biomolecular Engineering

Harvard University
- Atmospheric and Environmental Chemistry
- School of Engineering and Applied Sciences
- Department of Earth and Planetary Sciences

Indiana University
- Center for Research in Environmental Science
- Department of Chemistry
- School of Public and Environmental Affairs

Massachusetts Institute of Technology
- Department of Civil and Environmental Engineering
- Department of Earth, Atmospheric and Planetary Sciences
- Molina Center for Energy and the Environment

Naval Postgraduate School, Center for Interdisciplinary Remotely-Piloted Aircraft Studies (CIRPAS)

North Carolina Agricultural and Technical State University, Interdisciplinary Scientific Environmental Technology Center (ISET)

Paul Scherrer Institut (Villigen, Switzerland), Laboratory of Atmospheric Chemistry

Peking University (Beijing, China)

Pennsylvania State University

Princeton University, Atmospheric and Oceanic Sciences

Scripps Institution of Oceanography

Seoul National University (Seoul, Republic of Korea), School of Earth and Environmental Sciences

Texas Tech University, Department of Chemistry & Biochemistry

Université Lille Nord de France (Lille, France)

Université Paris Est Créteil (Créteil, France), Laboratoire Interuniversitaire des Systèmes Atmosphériques

Université de Versailles Saint Quentin en Yvelines, (Gif-sur-Yvette, France), Laboratoire des Sciences du Climat et de l'Environnement

University of Alberta (Edmonton, Canada), Department of Mechanical Engineering

University of Arizona, Chemical and Environmental Engineering

University of Bern (Bern, Switzerland)
- Department of Chemistry and Biochemistry
- Oeschger Centre for Climate Change Research

University of Calgary (Calgary, Canada), Department of Chemistry

University of California, Berkeley
- Department of Chemistry
- Department of Civil and Environmental Engineering
- Department of Earth and Planetary Sciences
- Department of Environmental Science, Policy, and Management
- Transportation Sustainability Research Center

University of California, Davis
- Air Quality Research Center
- Department of Civil and Environmental Engineering

University of California, Irvine
- Department of Chemistry
- Department of Mechanical and Aerospace Engineering

University of California, Los Angeles, Department of Atmospheric and Oceanic Sciences

University of California, San Diego, Department Chemistry and Biochemistry

University of California, Santa Cruz, Department of Microbiology and Environmental Toxicology

University of Colorado

Cooperative Institute for Research in Environmental Science (CIRES)
Department of Atmospheric and Oceanic Sciences
Department of Chemistry and Biochemistry
Laboratory for Atmospheric and Space Physics
University of Colombia (Bogota, Colombia), Chemical Engineering and Environmental Studies
University of Delaware, Department of Chemistry and Biochemistry
University of Helsinki (Helsinki, Finland), Department of Physics
University of Houston, Department of Earth and Atmospheric Sciences
University of Iowa, Center for Global and Regional Environmental Research
University of Manchester (Manchester, UK)
National Centre for Atmospheric Science
School of Earth, Atmospheric and Environmental Sciences
University of Maryland, Joint Center for Earth Systems Technology
University of Miami, Rosenstiel School of Marine and Atmospheric Science
University of North Carolina at Chapel Hill, Department of Environmental Sciences and Engineering
University of Toronto (Toronto, Canada), Department of Chemistry
University of Virginia, Climate Change Research Center
University of Washington, Seattle
Department of Atmospheric Sciences
Department of Chemistry
University of Wisconsin, Madison
Department of Chemistry
Environmental Chemistry and Technology
Virginia Tech, Department of Civil and Environmental Engineering
Washington State University, Department of Civil and Environmental Engineering
York University (Toronto, Canada), Centre for Atmospheric Chemistry

Cooperating Private Sector Organizations

Aerodyne Research Inc.
Aerosol Dynamics Inc.
Alion Science and Technology
Atmospheric and Environmental Research, Inc.
Baron Advanced Meteorological Services
Bay Area Environmental Research Institute
Maersk Line
RTI International

Other Cooperating Organizations

Wisconsin State Laboratory of Hygiene, Environmental Health Division

Appendix A - Sites, Platforms and Instruments deployed during the CalNex 2010 Field Study

This Appendix provides a comprehensive summary of the platforms and sites deployed for the CalNex 2010 field study. It is reproduced directly from the CalNex 2010 Overview Paper [*Ryerson et al.,* 2013].

1. Longer-term sites: Existing networks of surface monitors

The State of California is divided into 15 air districts of somewhat distinctive geological, meteorological, and anthropogenic characteristics. CARB and local air quality districts operate monitoring networks to routinely measure the atmospheric parameters necessary to:

1) document air quality relative to ambient air quality standards (AAQS) that have been established to protect public health,
2) forecast daily atmospheric conditions so that efforts can be taken to protect personal health and reduce the emission of pollutants,
3) track progress towards attaining the federal and state AAQS and goals,
4) facilitate data analyses that improve understanding of pollutant emissions and atmospheric processes so that efforts to attain AAQS are effective, and
5) provide inputs for air quality and climate models that inform scientists and decision-makers about the likely impacts of potential actions within a complex system of interactions and feedbacks.

In general, these measurements are made with federal reference or equivalent methods (FRM/FEM) and are subjected to defined quality assurance and quality control programs (www.arb.ca.gov/aaqm/qa/qa.htm). The primary monitoring networks with relevance to CalNex are for criteria pollutants (pollutants for which ambient air quality standards have been established), climate change pollutants (pollutants that cause the atmosphere to warm or cool over the long term, *i.e.*, affect the radiative balance of the earth), and meteorological parameters (atmospheric conditions that can concentrate, disperse, transform, or remove pollutants).

a. Criteria pollutant network

The State and Local Air Monitoring Station (SLAMS) network for criteria pollutants in (or near) California during CalNex in 2010 was very similar to its current configuration (www.arb.ca.gov/adam/netrpt). The gaseous pollutant network monitored O_3 at 202 sites, carbon monoxide (CO) at 120 sites, nitrogen dioxide (NO_2) at 135 sites, and sulfur dioxide (SO_2) at 83 sites. The aerosol pollutant network measured PM <2.5 microns in diameter (PM2.5) at 88 sites and <10 microns in diameter (PM10) at 182 sites. Near-real-time and historical air quality data can be accessed via the CARB Air Quality and Meteorology Information System (AQMIS; www.arb.ca.gov/aqmis2/aqmis2.php). Historical air quality data and statistics can be accessed via the CARB Aerometric Data Acquisition and Management system (www.arb.ca.gov/adam).

b. Climate change network

Two sites of the nascent CARB GHG monitoring network were in operation during CalNex: Mt. Wilson in the San Gabriel Mountains and Arvin in the southern San Joaquin Valley. The continuous measurements at that time by CARB included CO_2 and CH_4 at both sites, and

ancillary measurements of CO at Arvin. Other sites with longer-term monitoring records are located on the Pacific coastline and include Scripps Pier in La Jolla (southern California) and Trinidad Head, a NASA Advanced Global Atmospheric Gases Experiment (AGAGE) site and a NOAA baseline observatory, near Arcata in northern California.

c. Meteorological network

The meteorological monitoring network acquires data from a variety of federal, state, regional, and local sources. During CalNex, the long-term meteorological monitoring network included wind speed and direction at 157 sites, air temperature at 139 sites, relative humidity at 62 sites, and solar radiation at 38 sites. Current and historical meteorological data can be accessed via the AQMIS site (www.arb.ca.gov/aqmis2/metselect.php).

2. CALGEM tall tower sites

Collaborative atmospheric measurements between the California Greenhouse Gas Emissions Measurement (CALGEM; calgem.lbl.gov) and the NOAA tall tower and cooperative flask sampling networks project were made from two towers, one located on Mount Sutro (STR; 37.7553 °N, 122.4517 °W, base at 262 m above sea level (ASL)), and one near Walnut Grove, California (WGC; 38.2650 °N, 121.4911 °W, base at 0 m ASL) (Fig. 1). Daily flask samples were collected from 91 and 485 m above ground level (AGL) at STR and WGC, respectively, at 1500 Pacific Standard Time for later analysis of the major greenhouse gases (e.g., CO_2, CH_4, N_2O, halocarbons) and a suite of other gases at the NOAA Earth Science Research Laboratory in Boulder, CO. Additionally, in-situ instruments at WGC measured CO_2, CH_4, and CO at 30, 91, and 483 m AGL on a 15-minute repeat cycle. Measurements from both flask and in-situ sampling are tied to WMO calibration scales, facilitating their use in studies of regional CH_4 and N_2O emissions from Central California [*Jeong et al.*, 2012a; *Jeong et al.*, 2012b].

3. Summer 2010 Intensive Measurements

a. Mobile platforms

i) NOAA WP-3D aircraft

The NOAA WP–3D aircraft was instrumented to measure a wide variety of trace gases, aerosol particle composition, microphysics, cloud nucleating and optical properties, hydrometeor concentration, size, and morphology, solar actinic fluxes, and solar irradiance (Tables 1b and 1c). In addition to instrumentation carried in prior field projects (e.g., [*C. A. Brock et al.*, 2011; *D. D. Parrish et al.*, 2009]) the CalNex P–3 payload included new measurements of methane (CH_4) [*Kort et al.*, 2011; *Peischl et al.*, 2012] nitrous oxide (N_2O) [*Kort et al.*, 2011], nitryl chloride ($ClNO_2$) [*Osthoff et al.*, 2008], and aerosol light absorption [*Lack et al.*, 2012]. Seventeen P–3 research flights during CalNex, totaling 127 flight hours and including five flights after dark, sampled the daytime and nighttime planetary boundary layer (PBL), marine surface layer (ML), and the overlying free troposphere (FT) throughout California and offshore (Table 1a, Fig. 2). These flights and the transit flights to and from the WP-3D base in Ontario, CA provide data on atmospheric emissions, chemistry, transport and mixing, and removal. The NOAA Air Quality and the NOAA Climate Change Programs supported these flights. The P–3 data from CalNex are publicly available at www.esrl.noaa.gov/csd/tropchem/2010calnex/P3/DataDownload.

ii) CIRPAS Twin Otter aircraft

The CIRPAS Twin Otter aircraft was instrumented to measure a wide variety of aerosol parameters including single-particle and bulk chemical composition, hygroscopicity, microphysics, cloud nucleating, and optical properties (Table 2b). Eighteen CIRPAS Twin Otter aircraft research flights during CalNex, totaling approximately 90 hours, were based in Ontario, California, and sampled the daytime PBL and overlying FT within the California South Coast Air Basin (SoCAB) containing the Los Angeles (LA) urban complex (Table 2a; Fig. 3). Three of the 18 flights were to the SJV. These flights were supported by the NOAA Climate Change Program. The CIRPAS Twin Otter deployment and flight plans were focused on providing data to better understand the origin, composition, hygroscopicity, and cloud nucleating behavior of aerosol particulate matter in LA, its outflow regions, and the SJV. The CIRPAS Twin Otter was also used to investigate the effect of photochemical aging on aerosol composition and oxidation state, and the radiative implications of the regional aerosol.

iii) NOAA Twin Otter aircraft

The NOAA Twin Otter aircraft was equipped with the TOPAZ differential absorption lidar (DIAL) to measure vertically–resolved O_3 and aerosol backscatter nadir profiles [*Alvarez II et al.*, 2011; *Langford et al.*, 2011], a scanning Doppler lidar to measure nadir wind fields [*Pearson et al.*, 2009], and an airborne multi-axis differential optical absorption spectrometer (AMAX–DOAS) to measure aerosol extinction and variety of trace gas column densities, among them nitrogen dioxide (NO_2), formaldehyde (HCHO), glyoxal (CHOCHO), and nitrous acid (HONO) [*Baidar et al.*, 2012; *Volkamer et al.*, 2009] (Table 3b). The NOAA Twin Otter also carried an *in situ* O_3 sensor, a radiometer to measure surface temperature, and upward and downward irradiance sensors to retrieve surface albedo at 360, 479, 630, and 868 nm. Fifty-one NOAA Twin Otter aircraft research flights during CalNex, totaling 207 hours, took place between May 19 and July 19, 2010. Of these, 33 flights were based in Ontario, California, and 15 were based in Sacramento, California in coordination with the DOE CARES program [*Zaveri et al.*, 2012] (Table 3a; Fig. 4), and three were transit flights to and from California. These flights were supported by CARB and the NOAA Air Quality Program. The NOAA Twin Otter deployment and flight plans were focused on providing data to better understand the emissions sources of NO_x to the atmosphere, the 3-dimensional distribution of O_3, NO_2, CHOCHO, and particulate matter in different regions of California, and the key transport processes affecting the spatial and temporal distributions of these pollutants. Preliminary DIAL O_3 data from the CalNex project are publicly available at http://www.esrl.noaa.gov/csd/lidar/calnex/data_archive.

Typically, the Twin Otter flew one of two generic flight plans during CalNex. Morning flights were dedicated to mapping horizontal distributions of trace gases and obtaining high-resolution vertical profiles of trace gases and the aerosol backscatter coefficient from the surface to 4 km ASL at selected locations in the LA basin, including a coastal site, over the high desert, and in the Central Valley. The morning observations were primarily aimed at constraining the boundary conditions of atmospheric models, characterizing pollutant concentrations aloft, and testing of satellite retrievals [*Oetjen et al.*, 2012]. During afternoon flights the plane stayed at one altitude, typically about 4 km ASL, to map out the ozone, wind and aerosol structure when photochemical production of ozone was high and to observe transport of O_3, NO_2, and aerosol into and out of the various air basins of Southern California.

iv) NASA B200 aircraft

The NASA B200 King Air aircraft provided an airborne remote–sensing capability and was equipped with a high–spectral–resolution lidar (HSRL) [*Hair et al.*, 2008; *Rogers et al.*, 2009] to provide calibrated measurements of vertically–resolved aerosol backscatter, extinction, and optical thickness (Table 4b). Mixed layer heights were also derived from the HSRL profiles of aerosol backscatter [*Fast et al.*, 2012; *Scarino et al.*, 2012]. The NASA B200 also carried the Research Scanning Polarimeter (RSP) to provide total and linearly polarized reflectance in nine spectral channels [*Knobelspiesse et al.*, 2011](Table 4b). Six NASA B200 aircraft research flights based in Ontario, CA and totaling 23 hours took place between May 11 and May 24, 2010 (Table 4a; Fig. 5). These flights were supported by the DOE Atmospheric Systems Research Program and the NASA Radiation Sciences and Tropospheric Chemistry Programs. The NASA B200 King Air deployment and flight plans were focused on providing data to better understand the vertical and horizontal distribution of aerosols and aerosol optical properties within and above the PBL, evaluation of CALIPSO satellite instrument retrieval algorithms, provide vertical context for *in situ* measurements on other CalNex aircraft, and use those *in situ* measurements to evaluate new combined (active + passive) aerosol retrieval algorithms. B200 flights during its deployment from Ontario were highly coordinated with the NOAA WP-3D to maximize the overlap between the in-situ and remotely sensed data provided by the two aircraft.

Following its deployment in collaboration with CalNex, the NASA B200 continued research flights in California from June 4 through June 28, 2010 in conjunction with the DOE CARES study based in Sacramento, CA [*Zaveri et al.*, 2012].

v) WHOI R/V *Atlantis*

The Woods Hole Oceanographic Institute (WHOI) R/V *Atlantis* provided both *in situ* and remote–sensing capabilities and was instrumented to measure a wide variety of trace gases, aerosol particle composition, microphysics, cloud nucleating, and optical properties, hydrometeor concentration, size, and morphology, solar actinic fluxes, solar irradiance, and meteorological and cloud parameters (Table 5b and c). The R/V *Atlantis* research cruise took place offshore California between May 14 and June 8, 2010 (Table 5a; Fig. 3). This cruise was supported by the NOAA Climate Change Program. The R/V *Atlantis* deployment and cruise tracks were focused on providing data to better understand atmospheric emissions from oceangoing shipping and port facilities, the chemistry of SOA formation in the clean and polluted marine boundary layer (MBL), nighttime halogen chemistry involving chloride–containing aerosols, the radiative and cloud microphysical effects of atmospheric aerosols, and the production and flux of sea spray particles to the atmosphere. The R/V *Atlantis* gas-phase data from the CalNex project are available at http://www.esrl.noaa.gov/csd/tropchem/2010calnex/Atlantis/DataDownload, and the aerosol data are available at http://saga.pmel.noaa.gov/data.

b. Surface sites

i) Pasadena

The CalNex Los Angeles (CalNex-LA) ground site was located on the campus of the California Institute of Technology (Caltech) in Pasadena, approximately 18 km northeast of downtown Los Angeles (34.1408 °N, 118.1223 °W, 230 m ASL)(Fig. 1). Measurements were made from 15 May through 16 June 2010. Close to 40 research groups participated at the field site, providing measurements of an extensive suite of atmospheric species (Tables 6a – 6c).

In-situ gas-phase measurements, including observations of radicals, reactive nitrogen compounds, volatile organic carbon compounds (VOCs), oxygenated VOCs, O_3, CO, CO_2, and solar actinic fluxes, were made from one of two 10 m high scaffolding towers located on an empty campus parking lot.

Remote sensing of O_3, NO_2, NO_3, HONO, HCHO and SO_2 was performed at five height intervals (covering 32–550 m AGL) by long-path differential optical absorption spectroscopy (DOAS) between the roof of the Caltech Millikan library and the mountains 5–7 km northeast of the library building. The library roof also housed in-situ NO_2 and CHOCHO measurements as well as a multi–axis DOAS system. Good agreement between in–situ and long–path observations of O_3, NO_2, and SO_2 showed that the ground site was generally representative for the larger area around Caltech, except for a few nights when near-surface air was isolated from air masses aloft. Only sporadically were very local emissions from vehicles close to the sampling site found to impact the measurements. The main ground site also hosted an aerosol backscatter ceilometer that provided a measurement of the local boundary layer height [*Haman et al.*, 2012].

A large number of aerosol instruments (Tables 6b and 6c) sampled from a second 10 m high scaffolding tower, or from the top of their respective laboratory trailers at the main ground site. The instruments included standard measurements of aerosol size distributions, aerosol mass spectrometers, aerosol extinction measurements, and more experimental instrumentation described elsewhere in this issue.

Fourteen aerosol samplers were also operated on the roof of a 3 story (12 m) building on the Caltech campus and were co-located with an extensive suite of meteorological measurements including turbulent momentum and heat fluxes (Table 6c).

ii) Bakersfield

The CalNex Bakersfield sampling site was located at the Kern Cooperative Extension compound in the southern part of the city (35.35 °N, 118.97 °W, 20 m ASL) (Fig. 1). Bakersfield is located in the southern portion of the SJV and is bordered on the west by the Coastal Range (~50 km), on the east by the Sierra Nevada Mountains (~25 km), and on the south by the Tehachapi Mountains (~25 km). Measurements were made from 19 May through 28 June 2010. More than 15 research groups participated at the field site, providing measurements of an extensive array of gas-phase and particle-phase species (Tables 7a and 7b).

Meteorological measurements included relative humidity, wind speed and direction, and photosynthetically active radiation. *In situ* gas-phase measurements, including measurements of radicals, ozone, reactive nitrogen species, VOCs, CO_2, N_2O, and CH_4 were made from various heights on the 20 m high scaffolding tower located at the sampling site. A large number of

aerosol instruments also sampled from the tower or from the tops of laboratory trailers that were located surrounding the tower. The instruments included an aerosol mass spectrometer, a Sunset Labs EC/OC instrument, and instruments to measure chemically speciated organics, organic nitrates, and water–soluble anions and cations. Multiple high–volume aerosol samplers were also operated at the base of the tower to provide filter samples for off-line analysis of organic compounds, organosulfates, and nitroxyorganosulfates.

iii) Mt. Wilson

Mt. Wilson is located in the San Gabriel Mountains 26 km northeast of downtown Los Angeles and immediately north of the LA basin (Fig. 1). The Mt. Wilson Observatory (34.22 °N, 118.06 °W, 1770 m ASL) provided a high–altitude site for both *in situ* and remote–sensing measurements. Samples at this site routinely show a strong diurnal trend in many trace gases [*Gorham et al.*, 2010]. Maxima in carbon monoxide (CO) and urban hydrocarbons are typically observed during the afternoon, when upslope flows transport boundary–layer air from the western LA basin to the site. Conversely, minima in these species are typically observed at this site after dark, when surface cooling inhibits upslope flow and the top of the boundary layer has subsided below the height of the Observatory. Downslope or synoptic flow then typically advects cleaner air to the site, resulting in different sampling footprints for daytime and nighttime samples. However, the variability within just daytime samples provides a measure of atmospheric emissions ratios of urban pollutants, integrated over the upwind western LA basin, for species that are conserved over the relevant atmospheric transport time scales [*Gorham et al.*, 2010; *Hsu et al.*, 2010].

Whole–air samples were taken at Mt. Wilson twice per day at approximately 0200 and 1400 Pacific standard time beginning on 30 April 30 2010 and continued beyond the conclusion of the CalNex field project. Samples were returned to the NOAA Global Monitoring Division laboratory in Boulder, CO and analyzed for a variety of halocarbon, hydrocarbon, greenhouse, and other gases (Table 8).

Spatial distributions of carbon dioxide (CO_2), CH_4, N_2O, CO, NO_2, HCHO and aerosol extinction in the Los Angeles basin were measured from the NASA-Jet Propulsion Laboratory (JPL) California Laboratory for Remote Sensing (CLARS) at Mt. Wilson by remote sensing Fourier–transform spectroscopy (FTS) in a joint project of the JPL and the University of California–Los Angeles (UCLA). This project was supported by NASA, NOAA, and CARB. Data were obtained on 31 non-cloudy days from 14 May through 20 June 2010, and continued beyond the conclusion of the CalNex field project.

iv) Radar wind profiler network

Twenty Doppler radar wind profilers (e.g., [*Carter et al.*, 1995]) from the Physical Sciences Division (PSD) at NOAA and from cooperative agencies in California were available for the CalNex study (Table 10, Fig. 1). These instruments provided hourly averaged wind profile measurements from ~120 m AGL up to ~4 km or higher, depending on atmospheric conditions. Radio acoustic sounding systems (RASS; [*May et al.*, 1990]) were operated in conjunction with nineteen of the wind profilers to measure temperature profiles up to ~1.5 km. The vertical resolutions of both the wind and temperature measurements were 60, 100, or 200 m depending

on instrument operating configurations. The wind profile observations were quality controlled after the data collection period using the continuity technique [*Weber et al.*, 1993] and by visual inspection (final wind profiler datasets are available at ftp://ftp1.esrl.noaa.gov/users/tcoleman/CalNex2010/). During CalNex, NOAA PSD provided an online tool (www.esrl.noaa.gov/psd/programs/2010/calnexqc/traj/; [*White et al.*, 2006]) that used real-time observations from the profiler network to calculate forward or backward trajectories. The trajectory tool was used during the study to assist with flight mission planning and, following the study and using the quality controlled wind profiles, to illustrate regional transport patterns and quantify pollution source apportionment.

c. IONS-2010 ozonesonde network

The Intercontinental Chemical Transport Experiment Ozonesonde Network Study (IONS)–2010 network [*Cooper et al.*, 2011] was implemented during CalNex to better define baseline O_3 from the surface to the tropopause along the US west coast. IONS–2010 was supported by the NOAA Health of the Atmosphere Program, the NASA Tropospheric Chemistry Program, the U. S. Navy, Environment Canada, and by the NOAA National Air Quality Forecast Capability. Ozonesondes were launched in the mid–afternoon Pacific time 6 days per week (Monday–Saturday) between May 10 and June 19, 2010 from the network of seven sites, one in southern British Columbia and six in California including Trinidad Head, where ozonesondes have been launched on a weekly basis since 1997 by NOAA GMD (Fig. 1). This network was implemented to provide data on pathways, abundance, and latitudinal variation of O_3 transported into the continental U.S., determine the influence of PBL processes on transport of FT O_3 to the surface [*Parrish et al.*, 2010], and provide an extensive data set for evaluation of O_3 simulations by chemical transport models and O_3 retrievals from satellites [*Cooper et al.*, 2011; *Lin et al.*, 2012a; *Lin et al.*, 2012b].

d. Satellite observations with relevance to CalNex

An integrated, multi-platform and multi-sensor approach that combined *in situ* and remotely sensed data from surface, aircraft, and satellite with numerical model simulations was essential to accomplish several of the stated science objectives of CalNex. This integrated approach was exemplified by cloud optical and microphysical measurements in persistent stratus cloud decks offshore that were performed in a highly coordinated fashion, using simultaneous measurements from in-situ and remote sensing instruments onboard the R/V *Atlantis*, the WP-3D aircraft, and NOAA and NASA satellites. A combination of *in situ* and remotely sensed measurements from the WP-3D and the *Atlantis* was used to validate stratus cloud drop effective radius retrievals from solar spectral flux radiometers (SSFRs) carried aboard both platforms. In turn, the SSFR retrievals were used to validate cloud optical thickness and effective radius retrievals from sensors aboard the NOAA Geostationary Operational Environmental Satellite (GOES) and the Moderate Resolution Imaging Spectroradiometer (MODIS) aboard the NASA Terra satellite [*McBride et al.*, 2012]. Further, GOES cloud fractions from Pathfinder Atmospheres Extended (PATMOS-x) retrievals [*Heidinger et al.*, 2012] were used to assess the fidelity of high-resolution Weather Research and Forecasting (WRF) and Naval Research Laboratory (NRL) Coupled Ocean/Atmosphere Mesoscale Prediction System (COAMPS) model coastal cloud forecasts [*Angevine et al.*, 2012]. These regional forecast models provided key

input information for deployment and optimal coordination of the research vessel and aircraft during CalNex.

Satellite data also contributed to CalNex planning activities through real-time assimilation of satellite O_3 and aerosol retrievals. O_3 profiles retrieved from microwave limb sounder (MLS) measurements [*Froidevaux et al.*, 2008; *Livesey et al.*, 2008] and aerosol optical depth (AOD) retrievals from MODIS measurements [*Chu et al.*, 2002; *Remer et al.*, 2005] were assimilated within the Real-time Air Quality Modeling System (RAQMS) [*Pierce et al.*, 2010; *Pierce et al.*, 2007] which provided daily chemical and aerosol forecasts at 2°×2° resolution of long-range transport for CalNex planning activities. Data denial experiments during CalNex demonstrated the positive impact of MLS O_3 profile and MODIS AOD assimilation on RAQMS forecasts.

Table 1a. NOAA WP–3D CalNex flights; dates are based on UTC takeoff times.

Flight Date in 2010	Description	Coordination & overflights
Fri. April 30	Transit from Denver to LA; San Juan, and Four Corners power plants; Phoenix urban plume	–
Tue. May 4	Emissions and chemistry in the LA Basin; export to desert	Pasadena
Fri. May 7	Southern San Joaquin Valley survey; Fresno and Bakersfield urban plumes; Harris Ranch plume; PBL heights over cultivated and fallow lands near Tulare Lake; transport layers; coastal upwelling in Morro Bay	Pasadena
Sat. May 8	Ships in the LA Bight; emissions and chemistry in the LA Basin; transport layers; export to desert	Pasadena
Tue. May 11	Emissions from Sacramento Valley rice fields prior to flooding and planting; stratospheric intrusion; urban emissions transported into Central Valley; coastal upwelling offshore Pt. Arena	WGC tower; Pasadena; Bakersfield
Wed. May 12	Oakland; Salinas, Silicon, and Northern San Joaquin Valleys; agriculture and dairy farm emissions; stratospheric intrusion; cloud study and coastal upwelling offshore Monterey	WGC tower; Pasadena; Bakersfield
Fri. May 14	Cloud study and coastal upwelling in LA Bight; emissions and chemistry in the LA Basin	Pasadena
Sun. May 16	Cloud study and coastal upwelling in LA Bight; emissions and chemistry in the LA Basin; export to desert	R/V *Atlantis*; MODIS; Pasadena; NASA B200
Wed. May 19	Emissions and chemistry in the LA Basin; aerosol direct radiative effects experiment; export to desert	CIRPAS Twin Otter; Pasadena; NASA B200
Fri. May 21	Maersk vessel fuel switch experiment (flight terminated early)	Pasadena; NASA B200
Mon. May 24	Day–into–night flight (4 PM–11 PM); southern San Joaquin Valley survey; transport layers; LA Basin survey	Pasadena; NASA B200
Sun. May 30	Day–into–night flight (7 PM–1:30 AM); outflow to LA Bight; LA Basin survey	NOAA Twin Otter
Mon. May 31	Night flight (10 PM–4 AM); outflow to LA Bight; LA Basin; export to desert and Salton Sea	–
Wed. June 2	Sunrise flight (1 AM–7 AM); outflow to LA Bight; LA Basin; export to desert and Salton Sea	–
Thu. June 3	Sunrise flight (1 AM–8 AM); outflow to LA Bight; LA Basin; export to desert and Salton Sea	–
	(June 7–11: Redeployed to Gulf of Mexico in support of the Deepwater Horizon oil spill response)	

Mon. June 14	Emissions from Sacramento Valley rice fields during growing season; PBL heights over different land use; Sacramento urban plume; cloud study and coastal upwelling offshore Pt. Arena	WGC tower; Bakersfield; Pasadena
Wed. June 16	Southern San Joaquin Valley survey; Fresno and Bakersfield urban plumes; Harris Ranch plume; PBL heights over cultivated and fallow lands near Tulare Lake	Bakersfield; Pasadena
Fri. June 18	Oakland; Salinas, Silicon, and Northern San Joaquin Valleys; agriculture and dairy farm emissions; offshore Monterey cloud study; coastal upwelling	WGC tower; DOE G1; NASA B200; NOAA Twin Otter; Bakersfield; Pasadena
Sun. June 20	Santa Barbara Channel; emissions and chemistry in the LA Basin; export to desert	Pasadena
Tue. June 22	Transit from LA to Denver; export to desert; Las Vegas urban plume; Moapa, San Juan, and Four Corners power plants; South Fork, NM and Flagstaff, AZ forest fires; Denver urban plume	BAO tower, Erie, CO

Table 1b. NOAA WP–3D Gas–Phase Measurements

Measurement	Reference	Technique	Sample interval	Accuracy at high S/N (±1–sigma)	Precision at low S/N (±1–sigma)
NO, NO_2, NO_y, and O_3	[*Pollack et al.*, 2010; *Ryerson et al.*, 1998; *Ryerson et al.*, 1999]	Gas–phase chemiluminescence	1 s	3, 4, 12, and 2%	10, 30, 40, and 15 pptv
NO_3, N_2O_5, NO, NO_2, and O_3	[*Wagner et al.*, 2011]	Cavity ring–down spectroscopy (CRDS)	1 s	20, 10, 5, 5, and 5%	2, 2, 70, 45, and 60 pptv
CO	[*Holloway et al.*, 2000]	Vacuum ultraviolet resonance fluorescence spectroscopy	1 s	5%	0.5 ppbv
CO_2, CH_4, CO, and N_2O	[*Kort et al.*, 2011]	Quantum cascade laser absorption spectroscopy (QCLS)	1 s	0.1 ppmv, 1, 3.5, and 0.2 ppbv	0.02 ppmv, 0.5, 0.15, and 0.1 ppbv
CO_2 and CH_4	[*Peischl et al.*, 2012]	Wavelength–scanned cavity ring–down spectroscopy (WS–CRDS)	1 s	0.1 ppmv and 1.2 ppbv	≤0.15 ppmv and ≤2 ppbv
HNO_3	[*Neuman et al.*, 2002]	SiF_5^- chemical ionization mass spectrometry (CIMS)	1 s	(15% + 40 pptv)	12 pptv
NH_3	[*Nowak et al.*, 2007]	protonated acetone dimer CIMS	1 s	(30% + 170 pptv)	80 pptv
SO_2	[*Ryerson et al.*, 1998]	Pulsed UV fluorescence	3 s	20%	250 pptv
C_2–C_{10} NMHCs	[*Colman et al.*, 2001]	GC–FID of whole air samples	3–8 s	5–10%	3 pptv
C_1–C_2 halocarbons	[*Schauffler et al.*, 2003]	GC–MS of whole air samples	3–8 s	<10%	<0.1 pptv
C_1–C_5 alkyl nitrates	[*Schauffler et al.*, 2003]	GC–MS of whole air samples	3–8 s	10–20%	0.2 pptv
CH_3CN, HCHO, isoprene, aromatics, and monoterpenes	[*de Gouw and Warneke*, 2006]	Proton–transfer–reaction mass spectrometry (PTRMS)	1s every 17 s	20%; (30–100% for HCHO)	
Peroxyacetyl nitrate (PAN) and $ClNO_2$	[*Osthoff et al.*, 2008; *W Zheng et al.*, 2011]	I^- CIMS	2 s	20%	5 and 50 pptv

280– 640 nm actinic flux; photolysis frequencies	[*Stark et al.*, 2007]	spectrally resolved radiometry	1 s	30% $jO(^1D)$ 15% jNO_2 9% jNO_3	$3 \times 10^{-7}\ s^{-1}$ $jO(^1D)$ $3 \times 10^{-7}\ s^{-1}$ jNO_2 $2 \times 10^{-5}\ s^{-1}$ jNO_3
300–1700 nm spectrally resolved irradiance; 4.5–40 μm broadband irradiance	[*Pilewskie et al.*, 2003]	VIS–NIR spectrometry; IR filter radiometry	1 s	5%	<0.05 $W/m^2/nm$
H_2O	–	chilled mirror hygrometry	1 s	1.0 °C	1.0 °C

Table 1c. NOAA WP–3D Aerosol Measurements

Measurement	Reference	Technique	Sample interval	Accuracy at high S/N (±1–sigma)	Precision at low S/N (±1–sigma)
Low turbulence inlet	[*Wilson et al.*, 2004]	Boundary layer suppression by suction	–	–	–
Size distributions 0.004–1.0 µm (fine), 1.0–8.3 µm (coarse)	[*Brock et al.*, 2008]	5 parallel CPCs, and white and laser light scattering	1 s	*(See note 1)*	*(See note 1)*
Single–particle refractory black carbon mass	[*Schwarz et al.*, 2008]	Single–particle soot photometry (SP2)	1 s	30%	greater of 12 ng/kg or 25%
Optical extinction (dry; 532 nm) and γ(RH)	[*Langridge et al.*, 2011]	Cavity ring–down spectroscopy	1 s, 10 s	<2%	4 Mm^{-1} at 10 Mm^{-1} ambient
Optical absorption (dry; 404, 532, 658 nm)	[*Lack et al.*, 2012]	Laser photoacoustic spectroscopy	1 s	10%	~1 Mm^{-1}
Optical absorption (467, 530, and 660 nm) on filter media	[*Bond et al.*, 2004]	Particle soot absorption photometry (PSAP)	1 s	<20%	~1 Mm^{-1}
Size–resolved non–refractory NH_4^+, NO_3^-, SO_4^{2-}, Cl^- and organic composition for PM_1	[*Bahreini et al.*, 2009]	Aerosol mass spectrometry (AMS)	10 s	17, 17, 18, 18, and 19%	0.06, 0.01, 0.01, 0.01, and 0.06 µg/m^3
Cloud condensation nuclei (CCN) concentration (cm^{-3} at STP) and supersaturation (%)	[*Moore and Nenes*, 2009; *Roberts and Nenes*, 2005]	Continuous–flow streamwise thermal–gradient CCN counter with scanning flow CCN analysis (SFCA)	1 s	10% relative in CCN cm^{-3}, 0.04% absolute in supersaturation	≤10 CCN cm^{-3}, 0.04% absolute in supersaturation
Cloud particle size distribution (0.6–50 µm)	[*Baumgardner et al.*, 2001]	Laser light forward and back scattering	1 s		
Cloud particle size distribution (3–50 µm)	[*Lance et al.*, 2010]	Laser light forward scattering	1 s		
Cloud particle size distribution (50–6000 µm), morphology	[*Lance et al.*, 2010]	Droplet imaging probe	1 s		

Cloud liquid water content	[*King et al.*, 1978]	Hot wire probe	1 s	10%	0.05 g/m^3

Note 1: Uncertainty of fine mode aerosol number is ±(9% + 14/cm^3), surface area is +(17% + 0.2 μm^2/cm^3), –(8% + 0.2 μm^2/cm^3), and volume is +(26% + 0.03 μm^3/cm^3), –(12% + 0.03 μm^3/cm^3). Uncertainty of coarse mode aerosol number is ±(20% + 0.02/cm^3), surface area is +(32% + 0.14 μm^2/cm^3), –(14% + 0.14 μm^2/cm^3), and volume is +(52% + 0.12 μm^3/cm^3), –(20% + 0.12 μm^3/cm^3).

Table 2a. CIRPAS Twin Otter CalNex Flights

Flight date in 2010	Description	Coordination & overflights
Tue. May 4	LA Basin with missed approaches at airports throughout the Basin	–
Wed. May 5	LA Basin with missed approaches at airports throughout the Basin	–
Thu. May 6	LA Basin after morning marine layer	–
Fri. May 7	LA Basin	–
Mon. May 10	LA Basin source characterization: focused on western side in clean, windy conditions	Pasadena
Wed. May 12	LA Basin with outflow to Salton Sea	Pasadena
Thu. May 13	LA Basin with outflow to Salton Sea	Pasadena
Fri. May 14	LA Basin	Pasadena
Sat. May 15	LA Basin, humid/hazy morning	Pasadena
Tue. May 18	San Joaquin Valley, day after passage of a front	Pasadena; Bakersfield
Wed. May 19	LA Basin	NOAA P–3; NASA B200
Thu. May 20	San Joaquin Valley, after cloudy morning in Bakersfield	Bakersfield; NASA B200
Fri. May 21	LA Basin with El Cajon and Banning Pass outflows	Pasadena; NASA B200
Sat. May 22	San Joaquin Valley, sampling north–south line between Bakersfield and Fresno	Bakersfield; NASA B200
Mon. May 24	LA Basin with El Cajon outflow to Apple Valley and Banning Pass outflow to Palm Springs; clear and cool, no marine layer but slight aerosol haze	Pasadena; NASA B200
Tue. May 25	LA Basin with El Cajon outflow to Apple Valley and Banning Pass outflow to Palm Springs	Pasadena; NASA B200
Thu. May 27	LA Basin after cloudy and cool morning	Pasadena
Fri. May 28	LA Basin with mostly clear morning	Pasadena

Table 2b. CIRPAS Twin Otter Aerosol Measurements

Measurement	Reference	Technique	Sample interval	Accuracy at high S/N (±1–sigma)	Precision at low S/N (±1–sigma)
Diffusion inlet	[*Hegg et al.*, 2005]	Two–stage diffuser	–	–	–
Dry particle size distributions: 0.005–0.2 µm and 0.015–1.0 µm	[*Russell et al.*, 1996; *Wang and Flagan*, 1990]	2 parallel differential mobility analyzers	1.5 min	~20%	~20%
Aerosol size distributions: 0.1–3 µm	–	Laser light forward scattering (PCASP)	1 s	~10%	~10%
Total particle number concentration	–	3 parallel CPCs	1 s	~5%	5 cm^{-3}
Size–resolved non–refractory NH_4^+, NO_3^-, SO_4^{2-}, Cl^- and organic composition for submicron particles	[*Bahreini et al.*, 2009]	Aerosol mass spectrometry (AMS)	1 min	17, 17, 18, 18, and 19%	0.06, 0.02, 0.01, 0.01, and 0.08 µg/m^3
Single particle composition and size	[*Pratt et al.*, 2009]	Aerosol time–of–flight mass spectrometer (ATOFMS)	1 min	–	–
Water–soluble organic carbon: D_p < 2.5 µm	[*Sullivan et al.*, 2006]	Particle–into–liquid sampler coupled to a total organic carbon analyzer (PILS–TOC)	4 min	10%	0.1 µg/m^3
Cloud condensation nuclei concentration (STP cm^{-3}) and supersaturation (%)	[*R H Moore and Nenes*, 2009], [*Roberts and Nenes*, 2005]	Continuous–flow streamwise thermal–gradient CCN counter employing scanning flow CCN analysis (SFCA)	1 s	10% relative in CCN cm^{-3}, 0.04% absolute in supersaturation	≤10 CCN cm^{-3}, 0.04% absolute in supersaturation
Aerosol hygroscopicity (growth factors) for 150, 175, 200, and 225 nm dry particles at 74 and 92% relative humidity	[*Sorooshian et al.*, 2008]	Differential aerosol sizing and hygroscopicity spectrometer probe (DASH–SP)	17–45 s	4.3%	Growth Factor of 0.04–0.13
Single–particle refractory black carbon mass and coating state	[*Schwarz et al.*, 2008]	Single–particle soot photometry (SP2)	1 s	30%	30%
Optical absorption and scattering (405, 532, and 781 nm)	[*Arnott et al.*, 1999]	Photoacoustic Soot Spectrometer (PASS3)	2 s	~30%	~30%

Optical absorption (467, 530, and 660 nm) on filter media	[*Bond et al.*, 2004]	Particle soot absorption photometry (PSAP)	1 s	20%	~1 Mm^{-1}

Table 3a. NOAA Twin Otter CalNex Flights

Flight date in 2010	Description	Coordination & overflights
Wed. May 19	2nd leg of the transit flight from Colorado to California; pollution survey over LA Basin	Pasadena
Sun. May 23	O_3 distribution over Southern California associated with a stratospheric intrusion	
Tue. May 25 A	Pollution survey over LA Basin	Pasadena
Tue. May 25 B	Pollution survey over LA Basin	Pasadena
Sat. May 29	O_3 distribution over LA Basin and Mojave Desert associated with a stratospheric intrusion	Pasadena
Sun. May 30	Day–into–night flight (6 PM–9:30 PM); pollutant distribution over LA Basin and LA Bight	NOAA P-3; Pasadena
Mon. May 31 A	Pollution survey over LA Basin	Pasadena
Mon. May 31 B	Pollution survey over eastern LA Basin; Doppler lidar test	
Tue. June 1	Outflow of pollution from LA Basin to Mojave Desert; NO_2 comparison with OMI satellite	Pasadena
Thu. June 3 A	Dawn flight: Pollution survey over LA Basin	Fontana-Arrow
Thu. June 3 B	Pollution survey over LA Basin	Pasadena
Fri. June 4	Pollution survey over LA Basin; transport to Mojave Desert and Imperial Valley	Pasadena
Sat. June 5 A	Pollution survey over LA Basin	Pasadena
Sat. June 5 B	Pollution survey over LA Basin; transport to Mojave Desert and Imperial Valley	
Mon. June 7 A	Pollution survey over LA Basin	Pasadena
Mon. June 7 B	Pollution survey over LA Basin; transport to Mojave Desert and Imperial Valley	Pasadena
Tue. June 15 A	1st leg of transit flight from Ontario to Sacramento; pollution survey over Bakersfield area; NO_2 comparison with OMI satellite	Bakersfield
Tue. June 15 B	2nd leg of transit flight from Ontario to Sacramento; pollution survey over San Joaquin Valley	
Fri. June 18 A	Pollution survey over Sacramento area and northern San Joaquin Valley	WGC tower
Fri. June 18 B	Pollution survey over San Joaquin Valley	NOAA P-3; DOE G1; NASA B200; Bakersfield
Mon. June 21 A	Pollution survey over Sacramento and east of Bay Area	

Mon. June 21 B	Pollution survey over Sacramento, southern Bay Area, and northern San Joaquin Valley	
Tue. June 22 A	Pollution survey over Sacramento and east of Bay Area	WGC tower
Tue. June 22 B	Inflow of Asian pollution over Northern Coast and Sacramento Valley; OMI	
Wed. June 23	Pollution survey over Sacramento, east of Bay Area, and over Sierra Nevada Foothills	
Thu. June 24 A	Pollution survey over Sacramento and east of Bay Area	
Thu. June 24 B	Pollution survey over Sacramento, east of Bay Area, and over Sierra Nevada Foothills	
Sat. June 26	Pollution survey over Sacramento and east/south of Bay Area; transport to San Joaquin Valley, inflow of Asian pollution	WGC tower
Sun. June 27 A	Pollution survey over Sacramento and east of Bay Area	
Sun. June 27 B	Pollution survey over Sacramento, east of Bay Area, and over Sierra Nevada Foothills	WGC tower
Mon. June 28	Pollution survey over Sacramento and east of Bay Area	WGC tower
Tue. June 29 A	1st leg of transit flight from Sacramento to Ontario; pollution survey near Point Reyes, north and east of Bay Area	WGC tower
Tue. June 29 B	2nd leg of transit flight from Sacramento to Ontario; pollution survey near over San Joaquin Valley and Mojave Desert; transport of pollutants between air basins	
Wed. June 30 A	Pollution survey over Salton Sea, along Mexican border, and over portion of northern Mexico; cross-border pollution transport	
Wed. June 30 B	Pollution survey over San Diego, near Mexican border, and between San Diego and LA; cross-border pollution transport	
Fri. July 2	Pollution survey over LA Basin; transport to Mojave Desert and Imperial Valley	Pasadena
Sun. July 4	Pollution survey over LA Basin; transport to Mojave Desert and Imperial Valley	Pasadena
Mon. July 5 A	Pollution survey over LA Basin and transport to Mojave Desert; OMI	Pasadena
Mon. July 5 B	Pollution survey over LA Basin; transport to Mojave Desert and Imperial Valley	Pasadena
Tue. July 6	Pollution survey over LA Basin; transport to Mojave Desert and Imperial Valley	Pasadena
Mon. July 12	Pollution survey over LA Basin and transport to Mojave Desert; OMI	Pasadena
Wed. July 14	Ontario to Monterey; pollution survey over San Joaquin Valley and Sierra Nevada; transport by mountain slope flows	Bakersfield

Thu. July 15 A	Day–into–night flight (7 PM–11 PM); Monterey to Ontario: pollution survey over San Joaquin Valley and Sierra Nevada; transport by mountain slope flows and low level jet	Bakersfield
Thu. July 15 B	Pollution survey over LA Basin and transport to Mojave Desert	Pasadena
Fri. July 16 A	Pollution survey over LA Basin; transport to Mojave Desert and Imperial Valley	Pasadena
Fri. July 16 B	Pollution survey over LA Basin; transport to Mojave Desert and Imperial Valley	Pasadena
Sat. July 17	Pollution survey over LA Basin; transport to Mojave Desert and Imperial Valley	Pasadena
Sun. July 18 A	Dawn flight: Pollution survey over LA Basin	Fontana-Arrow
Sun. July 18 B	Pollution survey over San Diego, near Mexican border, and between San Diego and LA; cross-border pollution transport	
Mon. July 19 A	1st leg of the transit flight from California to Colorado; pollution transport from LA Basin to Mojave Desert and southern Nevada	
Mon. July 19 B	2nd leg of the transit flight from California to Colorado; Four Corners and San Juan Power plants	

Table 3b. NOAA Twin Otter Measurements

Measurement	Reference	Technique	Sample interval	Accuracy at high S/N (±1–sigma)	Precision at low S/N (±1–sigma)
O_3 profiles	[*Alvarez II et al.*, 2011]; [*Langford et al.*, 2011]	Differential absorption lidar	10 s	5 – 10 % (up to 30% for low SNR)	< 5% (up to 15% for low SNR)
Aerosol backscatter profiles (300 nm)	[*White et al.,* 1999; *Davis et al.,* 1999]	Differential absorption lidar	10 s	~ 10 %	< 30 %
BL height	[*Pearson et al.,* 2009]	Differential absorption lidar	10 s	~ 50 m	~ 50 m
Line-of-sight wind speed profiles (@ 4 azimuth angles)	[*Pearson et al.,* 2009]	Doppler lidar	2 - 6 s	0.1 m/s	up to 0.1 m/s
Relative aerosol backscatter profiles (1.6 µm)		Doppler lidar	1 s	uncalibrated	uncalibrated
O_3	*www.twobtech.com/model_202.htm*	UV light absorption	10 s	1 ppbv / 2%	1 ppbv / 2%
Temperature	*www.ti.com/lit/ds/symlink/lm35.pdf*	Thermistor	1 s	< 0.2 K	0.2 K
Surface temperature	*www.heitronics.com/fileadmin/content/ Prospekte/KT15IIP_e_V510.pdf*	IR pyrometer	1 s	0.06 K	0.5 K
NO_2 vertical column density (VCD)		AMAX-DOAS	2s	~7%	1.5 x10^{15} molec cm^{-2}
NO_2, HCHO, CHOCHO vertical profiles		AMAX-DOAS	Ascent/ descent	~10%	depends on gas & averaging time
Aerosol extinction profiles (360, 477, 630 nm)		AMAX-DOAS	Ascent/ descent	~5%	~ 0.01− 0.03 km^{-1}
Surface albedo		4-channel UV and vis irradiance	30s		~5%

Table 4a. NASA B200 CalNex Flights

Flight date in 2010	Description	Coordination & overflights
Wed. May 12	Transit from Tucson AZ	-
Thu. May 13	Salton Sea and LA basin	-
Sun. May 16	LA Basin. San Gabriel and San Bernardino Mtns.	Pasadena; NOAA P–3
Wed. May 19	LA Basin, export to desert. Catalina Is. low level cloud study	Pasadena; NOAA P–3, CIRPAS Twin Otter
Thu. May 20	LA Basin. Southern San Joaquin Valley	Pasadena; CIRPAS Twin Otter
Fri. May 21	LA Basin, export to desert	Pasadena; CIRPAS Twin Otter
Sat. May 22	San Joaquin Valley, Salton Sea, Over water near Catalina Is., LA Basin	Pasadena; CIRPAS Twin Otter
Mon. May 24	LA Basin. Salton Sea. Catalina Is.	Pasadena; CIRPAS Twin Otter
Tue. May 25	LA Basin. Salton Sea, Southern San Joaquin Valley, Transit to Sacramento	Pasadena; CIRPAS Twin Otter
(June 3-28)	*(Redeployed to Sacramento for DOE CARES Mission, see Zaveri et al. 2012)*	
Mon. June 14	Sacramento urban plume, SF Bay area inflow	NOAA P–3; DOE T0, T1 sites
(Flight 2 on this day)		
Fri. June 18	Sacramento, Northern San Joaquin Valley, Intercomparison	NOAA P–3; DOE G1; DOE T0 T1 sites

Table 4b. NASA B200 Measurements

Measurement	Reference	Technique	Sample interval	Measurement Precision	Bias/Systematic Uncertainty
Backscatter Ratio (532 nm)	[*Hair et al.*, 2008]	High Spectral Resolution Lidar	10 s	5%	0.01
Backscatter coefficient (532 and 1064 nm)	[*Hair et al.*, 2008]	High Spectral Resolution Lidar	10 s	5%	0.16 $(\text{Mm-sr})^{-1}$ (532 nm)
Extinction coefficient (532 nm)	[*Hair et al.*, 2008]	High Spectral Resolution Lidar	1 min	10%	10 Mm^{-1}
Depolarization Ratio (532 and 1064 nm)	[*Hair et al.*, 2008]	High Spectral Resolution Lidar	10 s	3%	0.004
Aerosol Optical Thickness (532 nm)	[*Hair et al.*, 2008]	Research Scanning Polarimeter	1 min	10%	0.02

Table 5a. WHOI R/V Atlantis sampling locations

Category	Start time, UTC	End time, UTC	Details
Offshore/background (clean marine) air	14 May/1800	15 May/1130	Transit San Diego to Santa Monica Bay
	16 May/1800	16 May/2300	Coordinated cloud study with WP-3D aircraft
	23 May/0000	23 May/0800	Catalina Island
	23 May/1530	23 May/2000	Catalina Island
	25 May/1730	26 May/0130	Shipping lanes off Santa Monica Bay
	27 May/1930	28 May/0130	Sea lanes south of Pt. Fermin
	30 May/0600	30 May/0730	Catalina Island; WP-3D flyover at 0710
	30 May/2300	31 May/0530	West of Santa Barbara
	01 Jun/0200	02 Jun/0000	Transit Santa Barbara to Monterey Bay
	02 Jun/0000	02 Jun/1700	Monterey Bay
	02 Jun/1700	02 Jun/2330	Transit Monterey Bay to Golden Gate
	06 Jun/1900	07 Jun/1900	Farallon Islands; whales
Santa Monica Bay; LAX approaches	15 May/1130	16 May/1500	Santa Monica Bay 1-5 nm offshore
	17 May/0130	17 May/0730	Santa Monica Bay 1-5 nm offshore
	21 May/1000	21 May/2000	Santa Monica Bay 1-5 nm offshore
	24 May/0600	24 May/2130	Santa Monica Bay 1-5 nm offshore
	25 May/0530	25 May/1700	Santa Monica Bay 1-5 nm offshore
	29 May/0500	29 May/1600	On station west of Palos Verdes Pt.
	29 May/1600	30 May/0400	Transit Santa Monica Bay coastline
	30 May/0800	30 May/1300	Santa Monica Bay near Palos Verdes
	30 May/1830	30 May/2130	Transit Santa Monica Bay coastline

Santa Barbara Channel area	18 May/0930	18 May/2200	Off Port Hueneme
	31 May/0800	31 May/1500	Off Ventura
	31 May/1900	01 May/0200	Off Santa Barbara; methane seeps
Los Angeles/Long Beach harbors	20 May/1600	20 May/2000	Transit LA harbor to Long Beach harbor and return
	22 May/0200	22 May/2200	LA harbor; cruise ship terminal
	26 May/1630	27 May/1600	LA harbor; west basin
	27 May/1600	27 May/1730	Transit through Long Beach harbor to San Pedro Bay
	28 May/1300	28 May/2030	San Pedro Bay; LA harbor; media event at dock
San Pablo Bay; San Francisco/Oakland harbors	03 Jun/0000	03 Jun/0300	Golden Gate to Martinez/San Pablo Bay
	06 Jun/0100	06 Jun/1530	East of Martinez at Anchorage 26
	06 Jun/1530	06 Jun/1900	Transit Anchorage 26 to Golden Gate
	06 Jun/1900	07 Jun/2330	Oakland harbor
	07 Jun/2330	08 Jun/1400	Anchored east of San Francisco
Sacramento River transits; Sacramento harbor	03 Jun/1530	03 Jun/2200	Transit Martinez to W. Sacramento/DOE G-1 at 2005
	03 Jun/2200	04 Jun/2230	West Sacramento turning basin
	04 Jun/2230	05 Jun/0400	Transit south and back to West Sacramento
	05 Jun/1930	06 Jun/0100	Transit from West Sacramento to Anchorage 26
Marine vessel emission studies	17 May/1300	18 May/0000	Santa Barbara/Port Hueneme ships and oil platforms
	18 May/0000	18 May/0400	NOAA R/V *Miller Freeman*

	19 May/0530	20 May/1600	San Pedro Bay anchorage
	23 May/1000	23 May/1500	San Pedro Bay shipping lanes
	23 May/2200	24 May/0330	San Pedro Bay shipping lanes
	24 May/2230	25 May/0230	San Pedro Bay shipping lanes
	25 May/0300	25 May/0345	Offshore; *Margrethe Maersk* experiment
	26 May/0800	26 May/1500	East of San Pedro Bay shipping lanes
	28 May/0330	28 May/1300	San Pedro Bay; Huntington Beach
	29 May/0200	29 May/0300	San Pedro Bay shipping lanes; cruise ship
	30 May/1300	30 May/1400	Offshore; *Mathilde Maersk* experiment
Ocean-derived aerosol studies	14 May/2150	15 May/0110	Off La Jolla
	15 May/2230	16 May/0155	Santa Monica Bay
	18 May/1600	18 May/2200	South of sea lanes off Port Hueneme
	23 May/0120	23 May/0550	South of Catalina Island
	23 May/1510	23 May/1930	South of Catalina Island
	24 May/1800	24 May/2100	Santa Monica Bay
	25 May/1900	26 May/0110	Sea lanes south of Pt. Dume
	27 May/1930	28 May/0115	Sea lanes south of Pt. Fermin
	30 May/2330	31 May/0510	South of sea lanes off Port Hueneme
	31 May/2325	01 June/0155	Off Santa Barbara
	06 June/2030	07 June/0200	Southeast of Farallon Islands

Table 5b. WHOI R/V Atlantis gas-phase measurements

Measurement	Reference	Technique	Sample interval	Accuracy at high S/N (±1–sigma)	Precision at low S/N (±1–sigma)
NO, NO_2	[*Lerner et al.*, 2009]	Gas–phase chemiluminescence; LED photolysis	1 min	4%, 11%	0.020 ppbv, 0.030 ppbv
NO, NO_2	[*Fuchs et al.*, 2009]	Cavity ring–down spectroscopy (CRDS)	1 min	3%, 3%	0.10, 0.10 ppbv
N_2O_5	[*Wagner et al.*, 2011]	Cavity ring–down spectroscopy (CRDS)	1 min	10%	2 pptv
NO_y	[*Williams et al.*, 2009]	Gas–phase chemiluminescence; heated Au tube	1 min	25%	0.050 ppbv
O_3	[*E J Williams et al.*, 2006]	UV absorption; gas–phase chemiluminescence	1 min, 1 min	2%, 2%	1 ppbv, 0.1 ppbv
O_3	[*Bates et al.*, 2008]	UV absorption	1 min	2%	1 ppbv
$ClNO_2$ and Cl_2	[*Kercher et al.*, 2009]	Chemical Ionization Mass Spectrometry (I^-)	5 min	30%	2 and 11 pptv
HCOOH and HCl	[*Bertram et al.*, 2011]	Chemical Ionization Mass Spectrometry (ToF-CIMS)	1 s	<30% and <50%	15 pptv
H_2O_2	[*Lee et al.*, 1995]	Aqueous collection, HPLC separation, fluorescence detection	30 s every 150 s	(5% + 10 pptv)	10 pptv
CH_3OOH	[*Lee et al.*, 1995]	Aqueous collection, HPLC separation, fluorescence detection	30 s every 2.5 m	(10% + 20 pptv)	20 pptv
CH_2O	[*Heikes*, 1992]	Aqueous collection, fluorescence detection	1 min	(10% + 25 pptv)	25 pptv
CO	[*Lerner et al.*, 2009]	Vacuum ultraviolet resonance fluorescence spectroscopy	1 min	3%	1 ppbv
CO_2	[*Lerner et al.*, 2009]	Non-dispersive infrared absorption spectroscopy	1 min	0.08 ppmv	0.07 ppmv
SO_2	[*Williams et al.*, 2009]	Pulsed UV fluorescence	1 min	10%	0.13 ppbv
SO_2	[*Bates et al.*, 2008]	Pulsed UV fluorescence	1 min	5%	0.10 ppbv

C_2–C_7 NMHCs	[*Bon et al.*, 2011]	In-situ GC–FID	30 min	=~10%	~2 pptv
$(CH_3)_2S$, CH_3CN, isoprene, methanol, acetone, acetaldehyde, aromatics, and monoterpenes	[*de Gouw and Warneke*, 2006]	Proton-transfer-reaction mass spectrometry (PTRMS)	1 min	20%	(18,23,33,267,37,99, 14,31 pptv)
HCHO, OCS	[*Herndon et al.*, 2007]	Quantum cascade laser absorption spectroscopy (QCLS)	1 min, 1 min	7%, 15%	75 pptv, 10 pptv
Gaseous elemental mercury (GEM)	[*Landis et al.*, 2002]	Cold vapor atomic fluorescence spectroscopy (CVAFS)	5 min	5%	25 pg Hg m^{-3}
H_2O	–	chilled mirror hygrometry	1 s	1.0 °C	1.0 °C
Radon	[*Whittlestone and Zahorowski*, 1998]	Radon gas decay	13 min		
280–640 nm actinic flux; photolysis frequencies	[*Stark et al.*, 2007]	3-wavelength filter radiometry	1 min	30% $jO(^1D)$ 15% jNO_2 9% jNO_3	3×10^{-7} s^{-1} $jO(^1D)$ 3×10^{-7} s^{-1} jNO_2 2×10^{-5} s^{-1} jNO_3
300–1700 nm spectrally resolved irradiance; 4.5–40 μm broadband irradiance	[*Pilewskie et al.*, 2003]	VIS–NIR spectrometry; IR filter radiometry	1 s	5%	<0.05 $W/m^2/nm$

Table 5c. WHOI R/V Atlantis aerosol, cloud, meteorological, and seawater measurements

Measurement	Reference	Technique	Sample interval	Accuracy at high S/N (±1–sigma)	Precision at low S/N (±1–sigma)
Aerosol number concentration	[*Bates et al.*, 2001]	CNC (TSI 3010, 3025)	1 s	10%	
Aerosol size distributions 0.02 -10 µm	[*Bates et al.*, 2005]	Parallel Aitken DMPS, accumulation mode DMPS, and an Aerodynamic Particle Sizer	5 min	10%	
Aerosol thermal volatility 0.02 – 0.5 µm at 230°C	[*Bates et al.*, 2012; *Russell et al.*, 2009]	Parallel (heated and unheated) SMPSs	5 min	10%	
Sub-1 and sub-10 µm scattering and backscattering (450, 550, 700 nm) and γ(RH)	[*Quinn and Bates*, 2005]	Parallel TSI 3563 Nephelometers	1 min	14%	0.13 Mm^{-1}
Sub-1 and sub-10 µm optical extinction (405, 532, 662 nm) and γ(RH)	[*Baynard et al.*, 2007; *Langridge et al.*, 2011]	Cavity ring-down spectroscopy	2-5 s	<2%	0.5 Mm^{-1} at 532 nm (varies with l)
Sub-1 and sub-10 µm optical absorption (dry: 406, 532 nm; thermodenuded: 406, 532 nm)	[*Lack et al.*, 2012]	Laser photoacoustic spectroscopy	2 s	10%	~1 Mm^{-1}
Sub-1 and sub-10 µm optical absorption (467, 530, and 660 nm) on filter media	[*Bond et al.*, 1999]	Particle soot absorption photometry (PSAP)	1 s	>20%	~1 Mm^{-1}
Aerosol Optical Depth	[*Quinn and Bates*, 2005]	Microtops sun photometer	Inter-mittent	20%	0.015 at 500 nm
Single-particle refractory black carbon mass and coating state	[*Schwarz et al.*, 2008]	Single-particle soot photometry (SP2)	1 s	40%	greater of 12 ng/kg or 25%
Concentration of BC non-refractory coating material	[*Cappa et al.*, 2012]	Soot Particle Aerosol Mass Spectrometer (SP-AMS)	1 min		0.03 $\mu g/m^3$
Volatility and hygroscopicity of aerosol particles (50, 100, and	[*Villani et al.*, 2008]	Volatility-hygroscopicity tandem differential mobility analyzer	20 min	0.05 units in growth	

145 nm)				factor	
Air ion size distribution (0.8 – 0.42 nm)	[*Mirme et al.*, 2007]	Air ion spectrometer	1.5 min	10^1 #/cm^{-3}	
Cloud condensation nuclei concentration for sub-1 µm aerosol at 5 supersaturations	[*Quinn et al.,* 2008]	Continuous-flow thermal-gradient CCN counter	5 min	10%	5 cm^{-3}
Cloud condensation nuclei concentration for 60 nm aerosol at 5 supersaturations	[*Quinn et al.*, 2008]	Continuous-flow thermal-gradient CCN counter coupled with an SMPS	5 min	10%	5 cm^{-3}
Sub-1 and sub-10 µm composition of inorganic ions, trace elements, OC, EC and total aerosol mass	[*Bates et al.*, 2008]	Impactors with IC, XRF, thermal-optical, and gravimetric analysis	3 to 16 hrs	6 – 31%	
Sub-1 µm alkane, hydroxyl, amine, and carboxylic acid functional groups and total submicron mass	[*Russell et al.*, 2009]	Fourier transform infrared (FTIR) spectroscopy	3 to 16 hrs	20%	0.09, 0.02, 0.01, and 0.008 µmol bond
Size-resolved chemistry of single particles	[*Gard et al.*, 1997]	Aerosol time-of-flight Mass Spectrometry (ATOFMS)	300 s	15-20%	N/A
Cloud liquid water path	[*Turner et al.*, 2007]	Microwave radiometer	15 s	N/A	N/A
Cloud–base height	[*Fairall et al.*, 1997]	Ceilometer	15 s		30 m
Cloud structure and precip	[*Lhermitte*, 1987]	W band cloud radar	1 hr		
Temperature/RH profiles	[*Wolfe et al.*, 2007]	Radiosondes	5 s		0.3C and 4%
Wind profiles	[*Law et al.*, 2002]	915-MHz wind profiler	5 min		1.4 m s^{-1}
Wind profiles/microscale turbulence	[*Frisch et al.*, 1989]	C band radar	5 min		1.0 m s^{-1}
High resolution boundary layer turbulence structure		Doppler mini-Sodar			
Turbulent fluxes	[*Bradley and Fairall*,	Bow-mounted eddy covariance	20 s,		25% at 1 hr

	2006]		10 min, 1 hr		
Seawater DMS	[*Bates et al.*, 2000]	sulfur chemiluminescence	15 min	8%	0.2 nM

Table 6a. Pasadena ground site gas–phase measurements

Measurement	Reference	Technique	Sample interval	Accuracy at high S/N (±1–sigma)	Precision at low S/N (±1–sigma)
O_3, NO_2, SO_2, NO_3, HONO, HCHO profiles	[*Wang et al.*, 2006]	Long–path differential optical absorption spectrometry (DOAS)	30 min	3, 4, 3, 10, 5, and 5%	0.8 ppbv and 60, 25, 1.2, 23, and 170 pptv
C_2–C_{10} NMHCs	[*Kuster et al.*, 2004]	GC–MS			
C_1–C_2 halocarbons	[*Kuster et al.*, 2004]	GC–MS			
O_3		UV absorption			
NO, NO_2, and NO_y	[*Drummond et al.*, 1985; *Pollack et al.*, 2010; *Williams et al.*, 1988]	Gas–phase chemiluminescence	10 sec		
SO_2		Pulsed UV fluorescence			
CO	[*Gerbig et al.*, 1999]	Vacuum ultraviolet resonance fluorescence spectroscopy		4%	0.2 ppbv
CO_2	[*Peischl et al.*, 2010]	NDIR absorption	1 min	0.14 ppmv	0.02 ppmv
CO_2 and $^{13}CO_2$		WS–CRDS		0.10 ppmv and 0.35 ‰	
NO_2	[*Fuchs et al.*, 2009]	CRDS	1 min	3%	4 pptv
HONO and CHOCHO	[*Washenfelder et al.*, 2008]	Incoherent broadband cavity–enhanced absorption spectrometry	10 min	15 and 30%	13 and 52 pptv
HNO_3, HONO, HNCO, and organic acids	[*Veres et al.*, 2008]	Negative–ion proton–transfer chemical ionization mass spectrometry	1 min	30%	40 pptv
PAN and $ClNO_2$	[*Mielke et al.*, 2011]	I^- CIMS			
PAN	[*Flocke et al.*, 2005]	GC-electron capture detection (ECD)			
HCHO		Liquid–phase fluorescence using the Hantzsch			

		reaction			
HO, HO_2, and HO reactivity	[*Dusanter et al.*, 2009]	Laser–induced fluorescence			
280– 420 nm actinic flux; photolysis frequencies	[*Shetter and Müller*, 1999]	spectrally resolved radiometry			
Volatile and semivolatile organic compounds	[*Holzinger et al.*, 2010]	High resolution proton transfer reaction time–of–flight mass spectrometry			
Water–soluble gas–phase organic carbon	[*Hennigan et al.*, 2008]	Mist chamber and online TOC measurement			
Total gas–phase volatile and semivolatile organic carbon		High–resolution electron impact time–of–flight mass spectrometry			
Gas–phase semivolatile organic carbon	[*Bouvier-Brown et al.*, 2013]	Sorbent tubes and offline solvent extraction with GC–MS	3 hr	22%	10 – 80 pptv
Meteorology and eddy covariance					
NO_2, HCHO, HONO, CHOCHO	[*Coburn et al.*, 2011]	Multi–axis DOAS	5 min	5, 10, 10, and 10%	(2.5, 10, 3, and 1.5) × 10^{14} molec/cm^2 vertical column density
CH_3CN, isoprene, aromatics, and monoterpenes	[*Warneke et al.*, 2005]	Proton–transfer ion trap mass spectrometry	5 min	15 – 25%	15 – 120 pptv
NH_3	[*Ellis et al.*, 2010]	Quantum cascade tunable infrared laser differential absorption spectrometry			
NO_2 and CHOCHO	[*Thalman and Volkamer*, 2010]	Light–emitting–diode cavity–enhanced DOAS	1 min	5%	11 and 7 pptv
HONO		Wet chemical derivitization/HPLC	10 min	6%	10 pptv

Table 6b. Pasadena ground site continuous and semi–continuous aerosol measurements

Measurement	Reference	Technique	Sample interval	Accuracy at high S/N (±1–sigma)	Precision at low S/N (±1–sigma)
Size–resolved non–refractory NH_4^+, NO_3^-, SO_4^{2-}, Cl^- and organic composition for PM_1	[*DeCarlo et al.*, 2006]	high–resolution time–of–flight aerosol mass spectrometry (HR–ToF–AMS)	5 min	30%	10-100 ng/m^3
Potential aerosol mass	[*Kang et al.*, 2007]	AMS and SMPS following exposure of ambient air to OH			
Submicron number distribution		Scanning mobility particle sizing	5 min	5% for size; 15% for concentratio n	
Submicron number distribution		UHSAS	1 min		
Total particle number		Condensation particle counter	1 min		
Number distribution (300 nm – 10 µm)		Optical particle counter	1 min		
Submicron aerosol volatility	[*Huffman et al.*, 2008]	Thermal denuder with AMS and SMPS	2 hr		
Organic and elemental carbon		Thermal–optical analysis	1 hr		
Water–soluble organic carbon	[*Weber et al.*, 2001]	Particle–into–liquid sampling and TOC measurement (PiLS–TOC)	10 min		
Carboxylic acids for aerodynamic diameter < 2.5 µm		PiLS–ion chromatography			
Speciated organic composition	[*Canagaratna et al.*, 2007; *B J Williams et al.*, 2006]	Combined thermal desorption aerosol GC–MS (TAG) and HR-ToF-AMS: TAG-AMS	1 hr		
Speciated organic composition	[*Worton et al.*, 2012]	Two–dimensional TAG	2 hrs		
Speciated organic composition	[*Holzinger et al.*, 2010]	High–resolution PTR–TOF–MS			

Water–soluble organic– and nitrogen–containing compounds	[*Bateman et al.*, 2010]	PiLS followed by high–resolution electrospray ionization mass spectrometry	30 min		
Single–particle refractory black carbon mass and coating state	[*Schwarz et al.*, 2008]	Single–particle soot photometry (SP2)	5 min	2.5%	10%
Single–particle refractory black carbon mass and coating composition	[*Onasch et al.*, 2012]	SP–AMS	5 min		
Black carbon mass	[*Arnott et al.*, 2005]	Aethalometry	5 min	45%	50%
Optical absorption	[*Arnott et al.*, 2006]	Photoacoustic soot spectrometer	5 min	0.7 Mm^{-1} at 532 nm	5% at 532 nm
Optical extinction (523 and 630 nm)	[*Massoli et al.*, 2010]	Cavity–attenuated phase shift spectroscopy	1 sec	0.8 Mm–1	5%
Aerosol extinction, scattering, and albedo	[*Dial et al.*, 2010; *Thompson et al.*, 2012]	CRDS/integrating sphere nephelometry	1 min	1-2 Mm^{-1}	
Single–particle optical size and single–scattering albedo at 672 nm	[*Sanford et al.*, 2008]	Laser scattering and extinction in a high–Q cavity			
Single–particle composition and number fractions for particle classes	[*Froyd et al.*, 2009; *Murphy et al.*, 2006]	Particle analysis by laser mass spectrometry (PALMS)	15% for particle classifi ciation number fraction		
Single–nanoparticle composition	[*Zordan et al.*, 2008]	Nano-aerosol mass spectrometer			
Size–resolved cloud condensation nuclei	[*Roberts and Nenes*, 2005]	Continuous–flow streamwise cloud condensation nuclei (CCN) spectrometry			
Vertically–resolved backscatter (355, 532, and 1064 nm)	[*Kovalev et al.*, 2009]	Scanning LIDAR			

Column aerosol optical depth	[*Holben et al.*, 2001]	AERONET sun photometry			
Boundary layer backscatter and mixing height	[*Haman et al.*, 2012]	Aerosol backscatter gradient ceilometer	5 min	20 m (stable conditions) to 100 m (unstable conditions)	2 m (stable conditions) to 20 m (unstable conditions)
Size-resolved particle number concentrations for 0.5<D<5 µm	[*Hayes et al.*, 2012]	White-light optical particle counter	10 sec		

Table 6c. Pasadena ground site aerosol sampler measurements

Measurement	Reference	Technique	Sample interval	Accuracy at high S/N (±1–sigma)	Precision at low S/N (±1–sigma)
Organosulfates and Nitrated Organosulfates	[*Surratt et al.*, 2008; *Zhang et al.*, 2011]	Filter collection with subsequent UPLC/DAD/ESI-HR-Q-TOFMS analyses	Every 3–6 hrs and 23 hrs	10-30%	1%
Nitro-Aromatics	[*Surratt et al.*, 2008; *Zhang et al.*, 2011]	Filter collection with subsequent UPLC/DAD/ESI-HR-Q-TOFMS analyses	Every 3–6 hrs and 23 hrs	10-30%	1%
WSOCs		Filter collection with subsequent H-NMR analyses	Every 3–6 hrs and 23 hrs		
Organic Acids	[*Kristensen and Glasius*, 2011]	Filter collection with subsequent HPLC/ESI-HR-Q-TOFMS analyses	Every 3–6 hrs and 23 hrs	25%	0.5-1.5 ng LOD
^{14}C of OC and TC	[*Szidat et al.*, 2006]	Filter collection with subsequent off-line accelerator mass spectrometry	Every 3–4 hrs	1-5%	5-15%
OC/EC	[*Schauer et al.*, 2003]	Filter collection with subsequent thermal-optical measurements	Every 3–4 hrs	OC 5-15% and EC 25%	OC LOD 0.3µgC/cm^2
Organics		Filter collection with subsequent solvent extraction, with and without prior derivatization, for GC/MS analyses	Every 3–6 hrs and 23 hrs		
Oxidized Organics		Filter collection with subsequent 2D-GC/ToFMS	Every 3–6 hrs and 23 hrs	10-30%	5%
Organics	[*Goldstein et al.*, 2008]	Filter collection with subsequent TAG-2D-GC/MS analyses with prior derivatization	Every 3–6 hrs and 23 hrs		
Submicron alkane, organic hydroxyl, amine, carboxylic acid, and non-acid carbonyl functional groups and total submicron organic	[*Gilardoni et al.*, 2007; *Russell et al.*, 2009]	Filter collection with subsequent Fourier transform infrared (FTIR) spectroscopy analyses	Every 3–6 hrs and 23 hrs	21% (Total organic mass)	0.09, 0.02, 0.01. 0.008, and 0.005 µmol of bond

mass					
Precursor-specific SOA tracers		Filter collection with subsequent GC/MS analyses with prior derivatization	Daily (23 hrs)	21% for total organic mass	0.09, 0.02, 0.01, 0.008, and 0.005 µmol of bond
Primary organic tracers and compound-specific stable isotope analysis	[*Sheesley et al.*, 2004]	Filter collection with subsequent GC/MS and GC-IRMS analysis	Every 3–6 hrs and 9–13 hrs	20%	5%
^{14}C and OC/EC	[*Schauer et al.*, 2003]	Filter collection with subsequent offline accelerator mass spectrometric analyses for ^{14}C and thermal-optical measurement for OC/EC	Daily (23 hrs)	1% for ^{14}C and 20% for OC/EC	1% for ^{14}C and 5% for OC/EC
Elements and Metals	[*Bukowiecki et al.*, 2009]	Rotating drum impactor (RDI) and subsequent synchrotron radiation-induced XRF analysis	2 hrs	30-40%	5%
Molecular characterization of organics in bulk samples; Microscopy and microanalysis of individual particles	[*Laskin et al.*, 2006; *Moffett et al.*, 2010a; *Moffett et al.*, 2010b; *Nizkorodov et al.*, 2011; *Roach et al.*, 2010]	MOUDI impactor with different substrates for subsequent analysis by Nano-DESI-HR-Orbitrap MS[†]; Computer Controlled SEM/EDX[‡]; Scanning Transmission X-ray Microscopy[#]	6 hrs	N/A	N/A
Microanalysis	[*Adachi and Buseck*, 2008]	Microanalysis particle samplers with subsequent transmission electron microscopy (TEM) analyses	4.8 min	N/A	N/A
VOCs		Tenax tubes with subsequent thermal desorption-GC/MS analyses	3 hrs	10%	25%

Table 7a. Bakersfield ground site gas–phase measurements

Measurement	Reference	Technique	Sample interval	Accuracy at high S/N (±1–sigma)	Precision at low S/N (±1–sigma)
HO, HO_2, OH loss rate, naphthalene, and potential aerosol mass					
NO_2, $\sum RO_2NO_2$, $\sum RONO_2$, HNO_3					
NO					
O_3	[*Gearn*, 1961]	UV absorption	1 min	±0.5%	±1 ppbv
CO, N_2O, CH_4, CO_2, H_2O, and stable isotopes of CO_2					
VOCs		GC–MS and GC–FID	15 min	±5–20%	
HCHO		Laser–induced fluorescence	30 s	±30%	±70 pptv
Glyoxal and α–dicarbonyls		Laser–induced phosphorescence	30 s	±20%	5 pptv
NH3, HNO3, HCl, HONO, SO2					
HONO	[*Ren et al.*, 2010]	CRDS	1 min	±15%	1 ppbv
HNO3, organic acids, peroxides, and oxygenates		CF_3O^- CIMS	16 s	±25%	25 pptv
PAN, PPN, MPAN, and other acyl peroxynitrates		I^- TD–CIMS	1 min	±(3 pptv + 21%) ±(3 pptv + 21%) MPAN	± 3 pptv

Table 7b. Bakersfield ground site aerosol measurements

Measurement	Reference	Technique	Sample interval	Accuracy at high S/N (±1–sigma)	Precision at low S/N (±1–sigma)
Size–resolved non–refractory NH_4^+, NO_3^-, SO_4^{2-}, Cl^- and organic composition for PM_1		Aerosol mass spectrometry (AMS)	5 min	30%	0.03 µg/m^3
IR-active functional groups	[*Russell*, 2003; *Russell et al.*, 2009]	Fourier transform infrared spectroscopy on filter sample extracts	2–4 hrs	21% for total organic mass	0.001–0.09 µmol of analyte
Trace elements in fine aerosol	[*Liu et al.*, 2009]	X-ray fluorescence on filter samples	2–4 hrs	6–40%	0.001–0.16 µg
Water-soluble anions and cations					
Speciated organics		Thermal desorption aerosol GC–MS (TAG)			
Organic nitrates in the gas/particle phase					
Organic and elemental carbon					
MOUDI impactor		Nano–DESI with high–resolution MS			
Speciated organics	[*Williams et al.*, 2006; *Kreisberg et al.*, 2009]		30 or 90 mins	15% for non-carboxylic acid compounds	
Organosulfates and α–dicarbonyls					
Nitrooxy– and organosulfates		UPLC/ESI-HR-Q-TOFMS	23 hrs	1–30%	1%
Nitrooxy– and organosulfates					

Table 8. Species measured in whole–air samples by NOAA GMD at Mt. Wilson, CA during CalNex.

Halocarbons	Hydrocarbons	Others
$CHBr_3$	C_6H_6	CO
CCl_4	C_2H_2	CO_2
CH_3I	C_3H_8	$^{14}CO_2$
$CHCl_3$	n–C_4H_{10}	CH_4
CH_2Br_2	n–C_5H_{12}	N_2O
CH_2Cl_2	i–C_5H_{12}	SF_6
CH_3Br		CS_2
CH_3Cl		OCS
C_2Cl_4		
CCl_3F (CFC–11)		
CCl_2F_2 (CFC–12)		
$CClF_3$ (CFC–13)		
$C_2Cl_3F_3$ (CFC–113)		
C_2ClF_5 (CFC–115)		
CHF_3 (HFC–23)		
C_2HF_5 (HFC–125)		
CH_2FCF_3 (HFC–134a)		
$C_2H_3F_3$ (HFC–143a)		
$C_2H_4F_2$ (HFC–152a)		

CF_2ClBr (Halon 1211)
$CBrF_3$ (Halon 1301)
$C_2Br_2F_4$ (Halon 2402)
$CHClF_2$ (HCFC–22)
$C_2H_3ClF_2$ (HCFC–142b)

Table 9. Species measured by remote sensing techniques at Mt. Wilson, CA during CalNex.

Measurement	Reference	Technique	Sample interval
NO_2, HCHO, glyoxal, aerosol extinction (O_4)	[*Pikelnaya et al.*, 2007]	Multi-axis DOAS	1 min
CO_2, CH_4, N_2O, CO, O_2		Near-IR Fourier Transfer Spectroscopy	1 min

Table 10a. CalMex ground sites gas–phase measurements

Measurement	Reference	Technique	Sample interval, s	Accuracy at high S/N (±1–sigma)	Precision at low S/N (±1–sigma)
H_2SO_4	[*J Zheng et al.*, 2011; *Zheng et al.*, 2010]	Atmospheric pressure NO_3^- chemical ionization mass spectrometry (API-CIMS)	30	36%	0.004 pptv
Methanol, acetonitrile, formaldehyde, isoprene, acetaldehyde, acetone, methyl ethyl ketone, and aromatics	[*Fortner et al.*, 2009]	Proton-transfer-reaction mass spectrometry (PTR-MS)	300	25%; (40-80% for formaldehyde due to RH change)	< 400 pptv (3.0 ppbv for methanol and 1.2 ppbv for formaldehyde)
CO_2, CO, NO_x	[*T O Moore et al.*, 2009]	Infrared absorption (CO_2 and CO) and chemiluminescence (NO_x)	60[(a)]	2%, 5%, 5%	0.5 ppmv, 0.04 ppmv, 0.05 ppbv
column NO_2	[*Johansson et al.*, 2008]	Differential Optical Absorption Spectroscopy	300		2.67E15 molecules/cm^2 [(b)]
O_3	[*Dunlea et al.*, 2006; *McAdam et al.*, 2011]	UV absorption	60		0.6 ppb[(c)]
NO/NOx	[*Dunlea et al.*, 2007; *McAdam et al.*, 2011]	Chemiluminescence (non-specific for NO_2)	60		0.4 ppb[(c)]
CO	[*McAdam et al.*, 2011]	Infrared gas filter correlation	60		0.04 ppm[(d)]
SO_2	[*McAdam et al.*, 2011]	Pulsed UV fluorescence	60		1 ppb[(e)]
NOy-HNO_3	[*Fitz et al.*, 2003]	Chemiluminescence with dual external converters and nylon filter	60		0.5 ppb[(c)]
NO_2 and peroxyacetyl nitrate (PAN)		Luminol chemiluminescence	One instantaneous sample		1 ppb[(f)]

			every 5 minutes	
CH_4 and NMHC	[*Zhou et al.*, 2007]	GC-FID	One sample every 70 s	20 ppb CH4 150 ppb NMHC [(g)]
Benzene, toluene, ethylbenzene, o-xylene, m-xylene	[*Król et al.*, 2010]	Gas-chromatography Retention TENAX	15 minutes	0.004[(h)]
Hg	[*Obrist et al.*, 2008]	Atomic Fluorescence	60[i]	0.2 ng/m^3[(i)]

[(a)]Faster (0.1-1 s) data available upon request.

[(b)]Detection limit at 2sigma.

[(c)]Low detection limit with range of 500 ppb and ±10% expected precision.

[(d)]Low detection limit with range of 50 ppm and ±0.1 ppm expected precision.

[(e)]Low detection limit with range of 500 ppb and 1% reading expected precision.

[(f)]Low detection limit with range of 500 ppb and 20% expected precision.

[(g)]Low detection limit with range of 20 ppb and 2% of measured value expected precision.

[(h)]Low detection limit with range of 300 ppb and 10% of measured value expected precision.

[(i)]Low detection limit with range of 1000 ppm and 10% of measured value expected precision.

Table 10b. CalMex ground sites aerosol measurements

Measurement	Reference	Technique	Sample interval	Accuracy at high S/N (±1–sigma)	Precision at low S/N (±1–sigma)
Submicron organic functional groups and total organic mass	[*Russell*, 2003; *Russell et al.*, 2009]	Fourier Transform Infrared Spectroscopy (FTIR)	2.2 to 4.3 hrs	21% (Total organic mass)	10-130 ng/m^3
Elemental composition	[*Hyslop and White*, 2008]	X-ray fluorescence (XRF)	2.2 to 4.3 hrs	8-41%, 68% (Cl)	0.3-75 ng/m^3
Submicron non-refractory NH_4^+, NO_3^-, SO_4^{2-}, Cl^- and organic composition	[*Ng et al.*, 2011]	Aerosol Chemical Speciation Monitor (ACSM)	15 to 30 min	20-25%	13-200 ng/m^3
Single-particle refractory black carbon mass and coating state	[*Schwarz et al.*, 2008; *Subramanian et al.*, 2010]	Single-particle soot photometry (SP2)	5 min	20% for time-averaged mass conc.	<100% detection efficiency for particles <0.7 fg
Single-particle morphology and composition	[*Stöhr*, 1992]	X-ray spectromicroscopy (STXM-NEXAFS)	Single-particle	[*Takahama et al.*, 2010]	
$PM_{2.5}$ trace elements composition	[*Querol et al.*, 2008]	Acid digestion followed by ICP-MS analysis	24 hours	< 20%	depends on the element
$PM_{2.5}$ EC/OC content	[*Zielinski et al.*, 1997]	CM5014 analyzer (UIC, Joliet, IL)	12 hours	10%	3 ng/m^3
Size distributions 0.03–0.4 µm (RH<10%)	[*Khalizov et al.*, 2009b; *Wu et al.*, 2007]	DMA-CPC (TSI 3081 and 3760A)	2 min	10%	1 cm^{-3}
Aerosol density (RH<10%: 46, 81, 151, and 240 nm)	[*Tajima et al.*, 2011]	Aerosol particle mass analyzer (APM)	10 min	5%	0.05 g cm^{-3}
Optical extinction	[*Khalizov et al.*, 2009a; *Pettersson et*	Cavity ring-down spectroscopy	90 s	1%	0.5 Mm^{-1}

(RH<10%: 532 nm)	*al.*, 2004]				
Optical Scattering (RH<10%: 450, 550, and 700 nm)	[*Anderson and Ogren*, 1998; *Khalizov et al.*, 2009a]	TSI 3563 nephelometer	90 s	1%	0.5 Mm^{-1}
$PM_{2.5}$, particle number (3-1000 nm), active surface area, total polycyclic aromatic hydrocarbons, black carbon	[*Marr et al.*, 2006]	Light scattering, diffusion charging, aerosol photoemission, light absorption	60 s[(a)]	50%, 10%, 20%, 20%, 10%	1 µg m^{-3}, 1 cm^{-3}, 10 mm^2 m^{-3}, 10 ng m^{-3}, 0.1 µg m^{-3}
Black carbon particle mass	[*Allen et al.*, 1999]	Light absorption by suspended aerosol particles at two wavelengths: 880 nm (black carbon) and 370 nm (UV-PM)	5 min	5.2%[(b)] r^2 =0.92 against EC Quartz filter	5.2%[(b)]
PM2.5, particle mass	www.thermo.com	TEI personal DataRAM nephelometer	60 s	±5% of reading [(c)]	±0.2% of reading [(d)]or ±0.0005 mg/m^3
PM1, particle mass	[*Green et al.*, 2009]	Tapered element oscillating microbalance	10 min	0.1[(e)]$\mu g/m^3$	
PM0.1, particle count	[*Hagler et al.*, 2009]	Condensation particle counter	60 s	*5%*	±3–12%

[(a)]Faster (1 s) data available upon request.

[(b)]Personal communication Tony Hansen, Magee Scientific, Oakland, CA.

[(c)]Accuracy referred to gravimetric calibration with SAE Fine (ISO Fine) test dust (mmd = 2 to 3 µm, óg = 2.5, as aerosolized).

[(d)]Precision/repeatability (2-sigma) at constant temperature and full battery voltage.

[(e)]Low detection limit with range of 0 to 1,000,000 $\mu g/m^3$ and expected precision of 2.0 $\mu g/m^3$ (1-hour), 1.0 $\mu g/m^3$ (24-hour)

Table 11. Radar wind profiler and radio acoustic sounding system network operational during CalNex.

Location	Designation	Latitude, degrees	Longitude, degrees	Elevation, m	Sponsor
Bakersfield	BKF	35.35	-118.98	120	NOAA/PSD[1]
Bodega Bay	BBY	38.32	-123.07	12	NOAA/PSD
Chico	CCO	39.69	-121.91	41	NOAA/PSD
Chowchilla	CCL	37.11	-120.24	76	NOAA/PSD
Gorman	GMN	34.72	-118.80	912	NOAA/PSD
Irvine	IRV	33.69	-117.73	122	SCAQMD[2]
Livermore	LVR	37.70	-121.90	109	BAAQMD[3]
Los Angeles	USC	34.02	-118.28	67	SCAQMD
Lost Hills	LHS	35.62	-119.69	80	NOAA/PSD
Miramar	MRM	32.90	-117.10	126	SDAPCD[4]
Moreno Valley	MRV	33.87	-117.22	452	SCAQMD
Oakhurst	OHT	37.38	-119.63	955	NOAA/PSD
Ontario	ONT	34.06	-117.58	280	SCAQMD
Pacoima	WAP	34.26	-118.41	300	SCAQMD
Sacramento	SAC	38.30	-121.42	6	SMAQMD[5]
San Nicolas Island	SNS	33.28	-119.52	15	NOAA/PSD
Simi Valley	SIM	34.30	-118.80	283	VCAPCD[6]
Tracy	TCY	37.70	-121.40	60	SJVAPCD[7]
Truckee	TRK	39.32	-120.14	1796	NOAA/PSD
Visalia	VIS	36.31	-119.39	81	SJVAPCD[7]

All locations except Truckee were equipped with a radio-acoustic sounding system (RASS). [1]NOAA Physical Sciences Division; [2]South Coast Air Quality Management District (AQMD); [3]Bay Area AQMD; [4]San Diego Air Pollution Control District (APCD); [5]Sacramento Metropolitan AQMD; [6]Ventura County APCD; [7]San Joaquin Valley APCD.

References

Adachi, K., and P. R. Buseck (2008), Internally mixed soot, sulfates, and organic matter in aerosol particles from Mexico City, *Atmospheric Chemistry and Physics*, *8*, 6469–6481, doi:10.5194/acp-8-6469-2008.

Allen, G. A., J. Lawrence, and P. Koutrakis (1999), Field validation of a semi-continuous method for aerosol black carbon (aethalometer) and temporal patterns in summertime hourly black carbon measurements in southwestern PA, *Atmospheric Environment*, *33*, 817-823.

Alvarez II, R. J., et al. (2011), Development and application of a compact tunable solid–state airborne ozone lidar system for boundary layer profiling, *Journal of Atmospheric and Oceanic Technology*, *28*, 1258-1272, doi:10.1175/JTECH-D-10-05044.1.

Anderson, T. L., and J. A. Ogren (1998), Determining aerosol radiative properties using the TSI 3563 integrating nephelometer, *Aerosol Science and Technology*, *29*(1), 57-69.

Angevine, W. M., L. Eddington, K. Durkee, C. Fairall, L. Bianco, and J. Brioude (2012), Meteorological model evaluation for CalNex 2010, *Monthly Weather Review*, doi:10.1175/MWR-D-12-00042.1

Arnott, W. P., H. Moosmüller, C. F. Rogers, T. Jin, and R. Bruch (1999), Photoacoustic spectrometer for measuring light absorption by aerosol: instrument description, *Atmospheric Environment*, *33*, 2845–2852.

Arnott, W. P., K. Hamasha, H. Moosmüller, P. J. Sheridan, and J. A. Ogren (2005), Towards aerosol light-absorption measurements with a 7-wavelength aethalometer: evaluation with a photoacoustic instrument and 3-wavelength nephelometer, *Aerosol Science and Technology*, *39*(1), 17–29, doi:10.1080/027868290901972.

Arnott, W. P., J. W. Walker, H. Moosmüller, R. A. Elleman, H. H. Jonsson, G. Buzorius, W. C. Conant, R. C. Flagan, and J. H. Seinfeld (2006), Photoacoustic insight for aerosol light absorption aloft from meteorological aircraft and comparison with particle soot absorption photometer measurements: DOE Southern Great Plains climate research facility and the coastal stratocumulus imposed perturbation experiments, *Journal of Geophysical Research*, *111*(D05S02), doi:10.1029/2005JD005964.

Bahreini, R., et al. (2009), Organic aerosol formation in urban and industrial plumes near Houston and Dallas, Texas, *Journal of Geophysical Research*, *114*(D00F16), doi:10.1029/2008JD011493.

Baidar, S., H. Oetjen, S. Coburn, B. Dix, I. Ortega, R. Sinreich, and R. Volkamer (2012), The CU Airborne MAX-DOAS instrument: ground based validation, and vertical profiling of aerosol extinction and trace gases, *Atmospheric Measurement Techniques Discussions*, *5*, 7243-7292, doi:10.5194/amtd-5-7243-2012.

Bateman, A. P., S. A. Nizkorodov, J. Laskin, and A. Laskin (2010), High-resolution electrospray ionization mass spectrometry analysis of water-soluble organic aerosols collectred with a particle into liquid sampler, *Analytical Chemistry*, *82*, 8010-8016, doi:10.1021/ac1014386.

Bates, T. S., P. K. Quinn, D. S. Covert, D. J. Coffman, J. E. Johnson, and A. Wiedensohler (2000), Aerosol physical properties and processes in the lower marine boundary layer: a comparison of shipboard sub-micron data from ACE–1 and ACE–2, *Tellus*, *52B*(2), 258–272.

Bates, T. S., P. K. Quinn, D. Coffman, J. E. Johnson, T. L. Miller, D. S. Covert, A. Wiedensohler, S. Leinert, A. Nowak, and C. Neusüss (2001), Regional physical and chemical properties of the marine boundary layer aerosol across the Atlantic during Aerosols99: An overview, *Journal of Geophysical Research*, *106*(D18), 20,767–720,782.

Bates, T. S., P. K. Quinn, D. Coffman, J. E. Johnson, and A. M. Middlebrook (2005), Dominance of organic aerosols in the marine boundary layer over the Gulf of Maine during NEAQS 2002 and their role in aerosol light scattering, *Journal of Geophysical Research*, *110*(D18202), doi:10.1029/2005JD005797.

Bates, T. S., et al. (2008), Boundary layer aerosol chemistry during TexAQS/GoMACCS 2006: Insights into aerosol sources and transformation processes, *Journal of Geophysical Research*, *113*(D00F01), doi:10.1029/2008JD010023.

Bates, T. S., et al. (2012), Measurements of ocean derived aerosol off the coast of California, *Journal of Geophysical Research*, *117*(D00V15), doi:10.1029/2012JD017588.

Baumgardner, D., H. Jonsson, W. Dawson, D. O'Connor, and R. Newton (2001), The cloud, aerosol, and precipitation spectrometer: a new instrument for cloud investigations, *Atmospheric Research*, *59–60*, 251-264.

Baynard, T., E. R. Lovejoy, A. Pettersson, S. S. Brown, D. Lack, H. Osthoff, P. Massoli, S. Ciciora, W. P. Dubé , and A. R. Ravishankara (2007), Design and application of a pulsed cavity ring- down aerosol extinction spectrometer for field measurements, *Aerosol Science and Technology*, *41*(4), 447–462, doi:10.1080/02786820701222801.

Bertram, T. H., J. R. Kimmel, T. A. Crisp, O. S. Ryder, R. L. N. Yatavelli, J. A. Thornton, M. J. Cubison, M. Gonin, and D. R. Worsnop (2011), A field-deployable, chemical ionization time-of-flight mass spectrometer, *Atmos. Meas. Tech.*, *4*, 1471–1479, doi:10.5194/amt-4-1471-2011.

Bon, D. M., et al. (2011), Measurements of volatile organic compounds at a suburban ground site (T1) in Mexico City during the MILAGRO 2006 campaign: measurement comparison, emission ratios, and source attribution, *Atmospheric Chemistry and Physics*, *11*, 2399–2421, doi:10.5194/acp-11-2399-2011.

Bond, T. C., T. L. Anderson, and D. Campbell (1999), Calibration and intercomparison of filter-based measurements of visible light absorption by aerosols, *Aerosol Science and Technology*, *30*(6), 582–600, doi:10.1080/027868299304435.

Bond, T. C., D. G. Streets, K. F. Yarber, S. M. Nelson, J.-H. Woo, and Z. Klimont (2004), A technology–based global inventory of black and organic carbon emissions from combustion, *Journal of Geophysical Research*, *109 (D14203)*, doi:10.1029/2003JD003697.

Bouvier-Brown, N. C., K. Chang, T. Nguyen, E. Carrasco, D. Ruiz, J. Karz, J. Gilman, W. Kuster, and J. de Gouw (2013), Portable and inexpensive quantification of VOCs: a method using a solid adsorbent, solvent extraction, and quantification by GC-MS, *Journal of Geophysical Research (in preparation)*.

Bradley, F., and C. Fairall (2006), A Guide to Making Climate Quality Meteorological and Flux Measurements at Sea, *Technical Memorandum Rep.*, 108 pp. pp, NOAA.

Brock, C. A., et al. (2008), Sources of particulate matter in the northeastern United States in summer: 2. Evolution of chemical and microphysical properties, *Journal of Geophysical Research*, *113*(D8), doi: 10.1029/2007JD009241.

Brock, C. A., et al. (2011), Characteristics, sources, and transport of aerosols measured in spring 2008 during the aerosol, radiation, and cloud processes affecting Arctic Climate (ARCPAC) Project, *Atmospheric Chemistry and Physics*, *11*, 2423–2453, doi:10.5194/acp-11-2423-2011.

Bukowiecki, N., A. Richard, M. Furger, E. Weingartner, M. Aguirre, T. Huthwelker, P. Leinemann, R. Gherig, and U. Baltensperger (2009), Deposition uniformity and particle size distribution of ambient aerosol collected with a rotating drum impactor, *Aerosol Science and Technology*, *43*(9), 891-901, doi:10.1080/02786820903002431.

Canagaratna, M. R., et al. (2007), Chemical and microphysical characterization of ambient aerosols with the Aerodyne aerosol mass spectrometer, *Mass Spectrometry Reviews*, *26*, 185-222, doi:10.1002/mas.20115.

Cappa, C. D., et al. (2012), Radiative absorption enhancements due to the mixing state of atmospheric black carbon, *Science*, *337*, 1078-1081, doi:10.1126/science.1223447.

Carter, D. A., K. S. Gage, W. L. Ecklund, W. M. Angevine, P. E. Johnston, A. C. Riddle, J. Wilson, and C. R. Williams (1995), Developments in UHF lower tropospheric wind profiling at NOAA's Aeronomy Laboratory, *Radio Science*, *30*, 977-1001.

Chu, D. A., Y. J. Kaufman, C. Ichoku, L. A. Remer, D. Tanre, and B. N. Holben (2002), Validation of MODIS aerosol optical depth retrieval over land, *Geophysical Research Letters*, *29*(12), 1617.

Coburn, S., B. Dix, R. Sinreich, and R. Volkamer (2011), The CU ground MAX-DOAS instrument: characterization of RMS noise limitations and first measurements near Pensacola, FL of BrO, IO, and CHOCHO, *Atmos. Meas. Tech.*, *4*, 2421-2439.

Colman, J. J., A. L. Swanson, S. Meinardi, B. Sive, D. R. Blake, and F. S. Rowland (2001), Description of the analysis of a wide range of volatile organic compounds in whole air samples collected during PEM-Tropics A and B, *Analytical Chemistry*, *73*, 3723-3731, doi:10.1021/ac010027g.

Cooper, O. R., et al. (2011), Measurement of western U.S. baseline ozone from the surface to the tropopause and assessment of downwind impact regions, *Journal of Geophysical Research*, *116*(D00V03), doi:10.1029/2011JD016095.

Davis, K. J., N. Gamage, C. R. Hagelberg, C. Kiemle, D. H. Lenschow, and P. P. Sullican (1999), An objective method for deriving atmospheric structure from airborne lidar observations, *Journal of Atmospheric and Oceanic Technology*, 17, 1455-1468.

de Gouw, J., and C. Warneke (2006), Measurements of volatile organic compounds in the Earth's atmosphere using proton-transfer-reaction mass spectrometry, *Mass Spectrometry Reviews*, *26*, 223-257, doi:10.1002/mas.20119.

DeCarlo, P. F., et al. (2006), Field–deployable, high–resolution, time–of–flight aerosol mass spectrometer, *Analytical Chemistry*, *78*(24), 8281–8289, doi:10.1021/ac061249n.

Dial, K. D., S. Hiemstra, and J. E. Thompson (2010), Simultaneous measurement of optical scattering and extinction on dispersed aerosol samples, *Analytical Chemistry*, *82*, 7885-7896, doi:10.1021/ac100617j.

Drummond, J. W., A. Volz, and D. H. Ehhalt (1985), An optimized chemi-luminescence detector for tropospheric NO measurements, *Journal of Atmospheric Chemistry*, *2*(3), 287-306.

Dunlea, E. J., et al. (2006), Technical Note: Evaluation of standard ultraviolet absorption ozone monitors in a polluted urban environment, *Atmospheric Chemistry and Physics*, *6*, 3163-3180.

Dunlea, E. J., et al. (2007), Evaluation of nitrogen dioxide chemiluminescence monitors in a polluted urban environment, *Atmospheric Chemistry and Physics*, *7*, 2691-2704.

Dusanter, S., D. Vimal, P. S. Stevens, R. Volkamer, and L. T. Molina (2009), Measurements of OH and HO2 concentrations during the MCMA-2006 field campaign – Part 1: Deployment of the Indiana University laser-induced fluorescence instrument, *Atmospheric Chemistry and Physics*, *9*, 1665-1685.

Ellis, R. A., J. G. Murphy, E. Pattey, R. van Haarlem, J. M. O'Brien, and S. C. Herndon (2010), Characterizing a quantum cascade tunable infrared laser differential absorption spectrometer (QC-TILDAS) for measurements of atmospheric ammonia, *Atmos. Meas. Tech.*, *3*, 397-406.

Fairall, C. W., A. B. White, J. B. Edson, and J. E. Hare (1997), Integrated Shipboard Measurements of the Marine Boundary Layer, *Journal of Atmospheric and Oceanic Technology*, *14*, 338–359.

Fast, J. D., et al. (2012), Transport and mixing patterns over Central California during the carbonaceous aerosol and radiative effects study (CARES), *Atmospheric Chemistry and Physics*, *12*, 1759-1783, doi:10.5194/acp-12-1759-2012.

Fitz, D. R., K. Bumiller, and A. Lashgari (2003), Measurement of NOy during the SCOS97-NARSTO, *Atmospheric Environment*, *37 Supplement No. 2*, S119-S134, doi:10.1016/S1352-2310(03)00385-6.

Flocke, F. M., A. J. Weinheimer, A. L. Swanson, J. M. Roberts, R. Schmitt, and S. Shertz (2005), On the measurement of PANs by gas chromatography and electron capture detection, *Journal of Atmospheric Chemistry*, *52*, 19-43, doi:10.1007/s10874-005-6772-0.

Fortner, E. C., J. Zheng, R. Zhang, W. Berk Knighton, R. M. Volkamer, P. Sheehy, L. Molina, and M. André (2009), Measurements of volatile organic compounds using proton transfer reaction - mass spectrometry during the MILAGRO 2006 campaign, *Atmospheric Chemistry and Physics*, *9*, 467-481.

Frisch, A. S., B. E. Martner, and J. S. Gibson (1989), Measurement of the vertical flux of turbulent kinetic energy with a single Doppler radar, *Boundary Layer Meteorology*, *49*, 331–337, doi:10.1007/BF00123648.

Froidevaux, L., et al. (2008), Validation of Aura Microwave Limb Sounder stratospheric ozone measurements, *Journal of Geophysical Research*, *113*(D15S20), doi:10.1029/2007JD008771.

Froyd, K. D., D. M. Murphy, T. J. Sanford, D. S. Thomson, J. C. Wilson, L. Pfister, and L. Lait (2009), Aerosol composition of the tropical upper troposphere, *Atmospheric Chemistry and Physics*, *9*, 4363–4385.

Fuchs, H., W. P. Dubé, B. M. Lerner, N. L. Wagner, E. J. Williams, and S. S. Brown (2009), A sensitive and versatile detector for atmospheric NO_2 and NO_x based on blue diode laser cavity ring-down spectroscopy, *Environmental Science & Technology*, *43*(20), 7831–7836, doi:10.1021/es902067h.

Gard, E., J. E. Mayer, B. D. Morrical, T. Dienes, D. P. Fergenson, and K. A. Prather (1997), Real-Time Analysis of Individual Atmospheric Aerosol Particles: Design and Performance of a Portable ATOFMS, *Analytical Chemistry*, *69*(20), 4083–4091, doi:10.1021/ac970540n.

Gearn, A. G. (1961), Absorption of ozone in the ultra–violet and visible regions of the spectrum, *Proceedings of the Physical Society*, *78*, 932.

Gerbig, C., S. Schmitgen, D. Kley, A. Volz-Thomas, K. Dewey, and D. Haaks (1999), An improved fast-response vacuum-UV resonance fluorescence CO instrument, *Journal of Geophysical Research*, *104*(D1), 1699-1704.

Gilardoni, S., et al. (2007), Regional variation of organic functional groups in aerosol particles on four U.S. east coast platforms during the International Consortium for Atmospheric Research on Transport and Transformation 2004 campaign, *Journal of Geophysical Research*, *112*(D10S27), doi:10.1029/2006JD007737.

Goldstein, A. H., D. R. Worton, B. J. Williams, S. V. Hering, N. M. Kreisberg, O. Panić, and T. Górecki (2008), Thermal desorption comprehensive two-dimensional gas chromatography for in-situ measurements of organic aerosols, *Journal of Chromatography A*, *1186*, 340-347, doi:10.1016/j.chroma.2007.09.094.

Gorham, K. A., N. J. Blake, R. A. VanCuren, H. E. Fuelberg, S. Meinardi, and D. R. Blake (2010), Seasonal and diurnal measurements of carbon monoxide and nonmethane hydrocarbons at Mt. Wilson, California: Indirect evidence of atomic Cl in the Los Angeles basin, *Atmospheric Environment*, *44*, 2271–2279.

Green, D. C., G. W. Fuller, and T. Baker (2009), Development and validation of the volatile correction model for PM_{10} - an empirical method for adjusting TEOM measurements for their loss of volatile particulate matter, *Atmospheric Environment*, *43*, 2132-2141, doi:10.1016/j.atmosenv.2009.01.024.

Hagler, G. S. W., R. W. Baldauf, E. D. Thoma, T. R. Long, R. F. Snow, J. S. Kinsey, L. Oudejans, and B. K. Gullett (2009), Ultrafine particles near a major roadway in Raleigh, North Carolina: downwind attenuation and correlation with traffic-related pollutants, *Atmospheric Environment*, *43*, 1229-1234, doi:10.1016/j.atmosenv.2008.11.024.

Hair, J. W., C. A. Hostetler, A. L. Cook, D. B. Harper, R. A. Ferrare, T. L. Mack, W. Welch, L. R. Izquierdo, and F. E. Hovis (2008), Airborne High Spectral Resolution Lidar for profiling aerosol optical properties, *Applied Optics*, *47*(36), 6734–6753.

Haman, C. L., B. Lefer, and G. A. Morris (2012), Seasonal variability in the diurnal evolution of the boundary layer in a near-coastal urban environment, *Journal of Atmospheric and Oceanic Technology*, *29*, 697-710, doi:10.1175/JTECH-D-11-00114.1.

Hayes, P. L., et al. (2012), Aerosol composition and sources in Los Angeles during the 2010 CalNex campaign, *Journal of Geophysical Research (in review)*.

Hegg, D. A., D. S. Covert, H. Jonsson, and P. A. Covert (2005), Determination of the transmission efficiency of an aircraft aerosol inlet, *Aerosol Science and Technology*, *39*(10), 966-971, doi:10.1080/02786820500377814.

Heidinger, A., A. Evan, M. Foster, and A. Walther (2012), A naive Bayesian cloud detection scheme derived from CALIPSO and applied within PATMOS-x, *Journal of Applied Meteorology and Climatology*, doi:10.1175/JAMC-D-11-02.1.

Heikes, B. G. (1992), Formaldehyde and Hydroperoxides at Mauna Loa Observatory, *Journal of Geophysical Research*, *97*(D16), 18,001–018,013.

Hennigan, C. J., M. H. Bergin, J. E. Dibb, and R. J. Weber (2008), Enhanced secondary organic aerosol formation due to water uptake by fine particles, *Geophysical Research Letters*, *35*(L18801), doi:10.1029/2008GL035046.

Herndon, S. C., M. S. Zahniser, D. D. J. Nelson, J. Shorter, J. B. McManus, R. Jiménez, C. Warneke, and J. A. de Gouw (2007), Airborne measurements of HCHO and HCOOH during the New England Air Quality Study 2004 using a pulsed quantum cascade laser spectrometer, *Journal of Geophysical Research*, *112*(D10S03), doi:10.1029/2006JD007600.

Holben, B. N., et al. (2001), An emerging ground–based aerosol climatology: aerosol optical depth from AERONET, *Journal of Geophysical Research*, *106*, 12,067–012,097.

Holloway, J. S., R. O. Jakoubek, D. D. Parrish, C. Gerbig, A. Volz-Thomas, S. Schmitgen, A. Fried, B. Wert, B. Henry, and J. R. Drummond (2000), Airborne intercomparison of vacuum ultraviolet fluorescence and tunable diode laser absorption measurements of tropospheric carbon monoxide, *Journal of Geophysical Research*, *105*, 24,251-224,261.

Holzinger, R., J. Williams, F. Herrmann, J. Lelieveld, N. M. Donahue, and T. Röckmann (2010), Aerosol analysis using a Thermal-Desorption Proton-Transfer-Reaction Mass Spectrometer (TD-PTR-MS): a new approach to study processing of organic aerosols, *Atmospheric Chemistry and Physics*, *10*, 2257–2267.

Hsu, Y. K., T. VanCuren, S. Park, C. Jakober, J. Herner, M. FitzGibbon, D. R. Blake, and D. D. Parrish (2010), Methane emissions inventory verification in southern California, *Atmospheric Environment*, *44*, 1-7, doi:10.1016/j.atmosenv.2009.10.002.

Huffman, J. A., P. J. Ziemann, J. T. Jayne, D. R. Worsnop, and J. L. Jimenez (2008), Development and characterization of a fast-stepping/scanning thermodenuder for chemically-resolved aerosol volatility measurements, *Aerosol Science and Technology*, *42*, 395-407.

Hyslop, N. P., and W. H. White (2008), An evaluation of interagency monitoring of protected visual environments (IMPROVE) collocated precision and uncertainty estimates, *Atmospheric Environment*, *42*, 2691-2705.

Jeong, S., C. Zhao, A. E. Andrews, L. Bianco, J. M. Wilczak, and M. L. Fischer (2012a), Seasonal variation of CH_4 emissions from central California, *Journal of Geophysical Research*, *117*(D11306), doi:10.1029/2011JD016896.

Jeong, S., C. Zhao, A. E. Andrews, E. J. Dlugokencky, C. Sweeney, L. Bianco, J. M. Wilczak, and M. L. Fischer (2012b), Seasonal variations in N_2O emissions from central California, *Geophysical Research Letters*, *39*(L16805), doi:10.1029/2012GL052307.

Johansson, M., B. Galle, T. Yu, L. Tang, D. Chen, H. Li, J. X. Li, and Y. Zhang (2008), Quantification of total emission of air pollutants from Beijing using mobile mini-DOAS, *Atmospheric Environment*, *42*, 6296-6933, doi:10.1016/j.atmosenv.2008.05.025.

Kang, E., M. J. Root, D. W. Toohey, and W. H. Brune (2007), Introducing the concept of potential aerosol mass (PAM), *Atmospheric Chemistry and Physics*, *7*, 5727–5744.

Kercher, J. P., T. P. Riedel, and J. A. Thornton (2009), Chlorine activation by N_2O_5: simultaneous, in situ detection of $ClNO_2$ and N_2O_5 by chemical ionization mass spectrometry, *Atmos. Meas. Tech.*, *2*, 193-204.

Khalizov, A. F., H. Xue, L. Wang, J. Zheng, and R. Zhang (2009a), Enhanced light absorption and scattering by carbon soot aerosol internally mixed with sulfuric acid, *Journal of Physical Chemistry A*, *113*, 1066-1074.

Khalizov, A. F., R. Zhang, D. Zhang, H. Xue, J. Pagels, and P. H. McMurry (2009b), Formation of highly hygroscopic soot aerosols upon internal mixing with sulfuric acid vapor, *Journal of Geophysical Research*, *114*(D05208), doi:10.1029/2008JD010595.

King, W. D., D. A. Parkin, and R. J. Handsworth (1978), A hot-wire liquid water device having fully calculable response characteristics, *Journal of Applied Meteorology*, *17*, 1809-1813.

Knobelspiesse, K., et al. (2011), Combined retrievals of boreal forest fire aerosol properties with a polarimeter and lidar, *Atmospheric Chemistry and Physics*, *11*, 7045-7067, doi:10.5194/acp-11-7045-2011.

Kort, E. A., P. K. Patra, K. Ishijima, B. C. Daube, R. Jiménez, J. Elkins, D. Hurst, F. L. Moore, C. Sweeney, and S. C. Wofsy (2011), Tropospheric distribution and variability of N_2O: evidence for strong tropical emissions, *Geophysical Research Letters*, *38*(L15806), doi:doi:10.1029/2011GL047612.

Kovalev, V. A., A. Petkov, C. Wold, S. Urbanski, and W. M. Hao (2009), Determination of smoke plume and layer heights using scanning lidar data, *Applied Optics*, *48*(28), 5287–5294.

Kreisberg, N. M., S. V. Hering, B. J. Williams, D. R. Worton, and A. H. Goldstein (2009), Quantification of Hourly Speciated Organic Compounds in Atmospheric Aerosols, Measured by an In-Situ Thermal Desorption Aerosol Gas Chromatograph (TAG), *Aerosol Sci. Tech.*, *43*(1), 38-52.

Kristensen, K., and M. Glasius (2011), Organosulfates and oxidation products from biogenic hydrocarbons in fine aerosols from a forest in North West Europe during spring, *Atmospheric Environment*, *45*(27), 4546-4556, doi:doi:10.1016/j.atmosenv.2011.05.063

Król, S., B. Zabiegała, and J. Namieśnik (2010), Monitoring VOCs in atmospheric air I. On-line gas analyzers, *Trends in Analytical Chemistry*, *29*(9), 1092-1100, doi:10.1016/j.trac.2010.05.007.

Kuster, W. C., B. T. Jobson, T. Karl, D. Riemer, E. Apel, P. D. Goldan, and F. C. Fehsenfeld (2004), Intercomparison of volatile organic carbon measurement techniques and data at La Porte during the TexAQS2000 air quality study, *Environmental Science and Technology*, *38*(1), 221-228, doi:10.1021/es034710r.

Lack, D. A., M. S. Richardson, D. Law, J. M. Langridge, C. D. Cappa, R. J. McLaughlin, and D. M. Murphy (2012), Aircraft instrument for comprehensive characterization of aerosol optical

properties, part 2: black and brown carbon absorption enhancement measured with photo acoustic spectroscopy, *Aerosol Science and Technology*, *46*(5), 555-568, doi:doi:10.1080/02786826.2011.645955.

Lance, S., C. A. Brock, D. Rogers, and J. A. Gordon (2010), Water droplet calibration of the Cloud Droplet Probe (CDP) and in–flight performance in liquid, ice, and mixed–phase clouds during ARCPAC, *Atmos. Meas. Tech.*, *3*, 1683-1706, doi:10.5194/amt-3-1683-2010.

Landis, M. S., R. K. Stevens, F. Schaedlich, and E. M. Prestbo (2002), Development and characterization of an annular denuder methodology for the measurement of divalent inorganic reactive gaseous mercury in ambient air, *Environmental Sciene & Technology*, *36*(13), 3000–3009, doi:10.1021/es015887t.

Langford, A. O., C. J. Senff, R. J. I. Alvarez, R. M. Banta, R. M. Hardesty, D. D. Parrish, and T. B. Ryerson (2011), Comparison between the TOPAZ airborne ozone lidar and in situ measurements during TexAQS 2006, *Journal of Oceanic and Atmospheric Technology*, *28*, 1243-1257, doi:10.1175/JTECH-D-10-05043.1.

Langridge, J. M., M. S. Richardson, D. Lack, D. Law, and D. M. Murphy (2011), Aircraft instrument for comprehensive characterization of aerosol optical properties, part I: wavelength-dependent optical extinction and its relative humidity dependence measured using cavity ringdown spectroscopy, *Aerosol Science and Technology*, *45*(11), 1305-1318, doi:10.1080/02786826.2011.592745.

Laskin, A., J. P. Cowin, and M. J. Iedema (2006), Analysis of individual environmental particles using modern methods of electron microscopy and X-ray microanalysis,, *Journal of Electron Spectroscopy and Related Phenomena*, *150*, 260–274, doi:10.1016/j.elspec.2005.06.008.

Law, D. C., S. A. McLaughlin, M. J. Post, B. L. Weber, D. C. Welsh, D. E. Wolfe, and D. A. Merritt (2002), An electronically stabilized phased array system for shipborne atmospheric wind profiling, *Journal of Atmospheric and Oceanic Technology*, *19*(6), 924–933, doi:10.1175/1520 - 0426.

Lee, M., B. C. Noone, D. O'Sullivan, and B. G. Heikes (1995), Method for the collection and HPLC analysis of hydrogen peroxide and C_1 and C_2 hydroperoxides in the atmosphere, *Journal of Atmospheric and Oceanic Technology*, *12*, 1060–1070.

Lerner, B. M., P. C. Murphy, and E. J. Williams (2009), Field measurements of small marine craft gaseous emission factors during NEAQS 2004 and TexAQS 2006, *Environmental Science & Technology*, *43*(21), 8213–8219, doi:doi:10.1021/es901191p.

Lhermitte, R. (1987), A 94-GHz Doppler radar for cloud observations, *Journal of Atmospheric and Oceanic Technology*, *4*, 36-48.

Lin, M., A. M. Fiore, O. R. Cooper, L. W. Horowitz, A. O. Langford, H. Levy II, B. J. Johnson, B. Naik, S. J. Oltmans, and C. J. Senff (2012a), Springtime high surface ozone events over the western United States: Quantifying the role of stratospheric intrusions, *Journal of Geophysical Research*, *117*(D00V22), doi:10.1029/2012JD018151.

Lin, M., et al. (2012b), Transport of Asian ozone pollution into surface air over the western United States in spring, *Journal of Geophysical Research*, *117*(D00V07), doi:10.1029/2011JD016961.

Liu, S., S. Takahama, L. M. Russell, S. Gilardoni, and D. Baumgardner (2009), Oxygenated organic functional groups and their sources in single and submicron organic particles in MILAGRO 2006 campaign, *Atmospheric Chemistry and Physics*, *9*, 6849–6863.

Livesey, N. J., et al. (2008), Validation of Aura Microwave Limb Sounder O_3 and CO observations in the upper troposphere and lower stratosphere, *Journal of Geophysical Research*, *113*(D15S02), doi:10.1029/2007JD008805.

Marr, L. C., K. Dzepina, J. L. Jimenez, F. Reisen, H. L. Bethel, J. Arey, J. S. Gaffney, N. A. Marley, L. T. Molina, and M. J. Molina (2006), Sources and transformations of particle-bound polycyclic aromatic hydrocarbons in Mexico City, *Atmospheric Chemistry and Physics*, *6*, 1733-1745.

Massoli, P., P. L. Kebabian, T. B. Onasch, F. B. Hills, and A. Freedman (2010), Aerosol light extinction measurements by cavity attenuated phase shift (CAPS) spectroscopy: laboratory validation and field deployment of a compact aerosol particle extinction monitor, *Aerosol Science and Technology*, *44*(6), 428–435, doi:10.1080/02786821003716599.

May, P. T., R. G. Strauch, K. P. Moran, and W. L. Ecklund (1990), Temperature sounding by RASS with wind profiler radars: a preliminary study, *IEEE Transactions Geosciences and Remote Sensing*, *28*, 19-28.

McAdam, K., P. Steer, and K. Perrotta (2011), Using continuous sampling to examine the distribution of traffic related air pollution in proximity to a major road, *Atmospheric Environment*, *45*, 2080-2086, doi:10.1016/j.atmosenv.2011.01.050.

McBride, P. J., K. S. Schmidt, P. Pilewskie, A. Walther, A. K. Heidinger, D. E. Wolfe, C. W. Fairall, and S. Lance (2012), CalNex cloud properties retrieved from a ship-based spectrometer and comparisons with satellite and aircraft retrieved cloud properties, *Journal of Geophysical Research*, *117*(D00V23), doi:10.1029/2012JD017624.

Mielke, L. H., A. Furgeson, and H. D. Osthoff (2011), Observation of ClNO2 in a mid-continental urban environment, *Environmental Science & Technology*, *45*, 8889-8896, doi:10.1021/es210955u.

Mirme, A., E. Tamm, G. Mordas, M. Vana, J. Uin, S. Mirme, T. Bernotas, L. Laakso, A. Hirsikko, and M. Kulmala (2007), A wide-range multi-channel air ion spectrometer, *Boreal Environment Research*, *12*(3), 247–264.

Moffett, R. C., T. Henn, A. Laskin, and M. K. Gilles (2010a), Automated chemical analysis of internally mixed aerosol particles using X-ray spectromicroscopy at the carbon K-edge, *Analytical Chemistry*, *82*, 7906–7914, doi:10.1021/ac1012909.

Moffett, R. C., A. Tivanski, and M. K. Gilles (2010b), Scanning transmission X-ray microscopy: applications in atmospheric aerosol research, in *Fundamentals and Applications in Aerosol Spectroscopy*, edited by R. Signorelli and J. Reid, pp. 420–462, CRC Press.

Moore, R. H., and A. Nenes (2009), Scanning flow CCN analysis – a method for fast measurements of CCN spectra, *Aerosol Science and Technology*, *43*(12), 1192-1207, doi:10.1080/02786820903289780.

Moore, T. O., D. C. Doughty, and L. C. Marr (2009), Demonstration of a mobile flux laboratory for the atmospheric measurement of emissions (FLAME) to assess emissions inventories, *Journal of Environmental Monitoring*, *11*(2), 259-268, doi:10.1039/b810798j.

Murphy, D. M., D. J. Cziczo, K. D. Froyd, P. K. Hudson, B. M. Matthew, A. M. Middlebrook, T. E. Peltier, A. SUllivan, D. S. Thomson, and R. J. Weber (2006), Single-particle mass spectrometry of tropospheric aerosol particles, *Journal of Geophysical Research*, *111*(D23S32), doi:10.1029/2006JD007340.

Neuman, J. A., et al. (2002), Fast-response airborne in situ measurements of HNO_3 during the Texas 2000 Air Quality Study, *Journal of Geophysical Research*, *107*(4436), doi:10.1029/2001JD001437.

Ng, N. L., et al. (2011), An aerosol chemical speciation monitor (ACSM) for routine monitoring of the composition and mass concentrations of ambient aerosol, *Aerosol Science and Technology*, *45*(7), 780-794, doi:10.1080/02786826.2011.560211.

Nizkorodov, S. A., J. A. Laskin, and A. Laskin (2011), Molecular chemistry of organic aerosols through the application of high resolution mass spectrometry, *Physical Chemistry Chemical Physics*, *13*, 3612–3629, doi:10.1039/c0cp02032j.

Nowak, J. B., J. A. Neuman, K. Kozai, L. G. Huey, D. J. Tanner, J. S. Holloway, T. B. Ryerson, G. J. Frost, S. A. McKeen, and F. C. Fehsenfeld (2007), A chemical ionization mass spectrometry technique for airborne measurements of ammonia, *Journal of Geophysical Research*, *112*, doi:10.1029/2006JD007589.

Obrist, D., A. G. Hallar, I. McCubbin, B. B. Stephens, and T. Rahn (2008), Atmospheric mercury concentrations at Storm Peak Laboratory in the Rocky Mountains: evidence for long-range transport from Asia, boundary layer contributions, and plant mercury uptake, *Atmospheric Environment*, *42*, 7579-7589, doi:10.1016/j.atmosenv.2008.06.051.

Oetjen, J., S. Baidar, N. A. Krotkov, L. N. Lamsal, M. Lechner, and R. Volkamer (2013), Airborne MAX-DOAS measurements over California: testing the NASA OMI tropospheric NO_2 product, *Journal of Geophysical Research (in review)*.

Onasch, T. B., A. Trimborn, E. C. Fortner, J. T. Jayne, G. L. Kok, L. R. Williams, P. Davidovits, and D. R. Worsnop (2012), Soot particle aerosol mass spectrometer: development, validation, and initial application, *Aerosol Science and Technology*, *46*(7), 804-817, doi:10.1080/02786826.2012.663948.

Osthoff, H. D., et al. (2008), High levels of nitryl chloride in the polluted subtropical marine boundary layer, *Nature Geoscience*, *1*, 324–328, doi:10.1038/ngeo177.

Parrish, D. D., et al. (2009), Overview of the Second Texas Air Quality Study (TexAQS II) and the Gulf of Mexico Atmospheric Composition and Climate Study (GoMACCS), *Journal of Geophysical Research*, *114*(D00F13), doi:doi:10.1029/2009JD011842.

Parrish, D. D., K. C. Aikin, S. J. Oltmans, B. J. Johnson, M. Ives, and C. Sweeney (2010), Impact of transported background ozone inflow on summertime air quality in a California ozone exceedance area, *Atmospheric Chemistry and Physics*, *10*, 10093–10109, doi:doi:10.5194/acp-10-10093-2010.

Pearson, G., F. Davies, and C. Collier (2009), An analysis of the performance of the UFAM pulsed doppler lidar for observing the boundary layer, *Journal of Atmospheric and Oceanic Technology*, *26*, 240-250.

Peischl, J., et al. (2010), A top-down analysis of emissions from selected Texas power plants during TexAQS 2000 and 2006, *Journal of Geophysical Research*, *115*(D16303), doi:10.1029/2009JD013527.

Peischl, J., et al. (2012), Airborne observations of methane emissions from rice cultivation in the Sacramento Valley of California, *Journal of Geophysical Research*, *117*(D00V25), doi:10.1029/2012JD017994.

Pettersson, A., E. R. Lovejoy, C. A. Brock, S. S. Brown, and A. R. Ravishankara (2004), Measurement of aerosol optical extinction at 532 nm with pulsed cavity ring down spectroscopy, *Journal of Aerosol Science*, *35*, 995-1011, doi:10.1016/j.jaerosci.2004.02.008.

Pierce, R. B., et al. (2007), Chemical data assimilation estimates of continental U.S. ozone and nitrogen budgets during the Intercontinental Chemical Transport Experiment–North America, *Journal of Geophysical Research*, *112*(D12S21), doi:10.1029/2006JD007722.

Pierce, R. B., et al. (2010), Impacts of background ozone production on Houston and Dallas, Texas, air quality during the Second Texas Air Quality Study field mission, *Journal of Geophysical Research*, *114*(D00F09), doi:10.1029/2008JD011337.

Pikelnaya, O., S. C. Hurlock, S. Trick, and J. Stutz (2007), Intercomparison of multiaxis and long-path differential optical absorption spectroscopy measurements in the marine boundary layer, *Journal of Geophysical Research*, *112*(D10S01), doi:10.1029/2006JD007727,.

Pilewskie, P., J. Pommier, R. Bergstrom, W. Gore, S. Howard, M. Rabbette, B. Schmid, P. V. Hobbs, and S. C. Tsay (2003), Solar spectral radiative forcing during the Southern African Regional Science Initiative, *Journal of Geophysical Research*, *108*(D13), doi:10.1029/2002JD002411.

Pollack, I. B., B. M. Lerner, and T. B. Ryerson (2010), Evaluation of ultraviolet light-emitting diodes for detection of atmospheric NO_2 by photolysis - chemiluminescence, *Journal of Atmospheric Chemistry*, *65*(2-3), 111-125, doi:10.1007/s10874-011-9184-3.

Pratt, K. A., et al. (2009), Development and characterization of an aircraft aerosol time-of-flight mass spectrometer, *Analytical Chemistry*, *81*, 1792–1800, doi:10.1021/ac801942r.

Querol, X., et al. (2008), PM speciation and sources in Mexico during the MILAGRO-2006 campaign, *Atmospheric Chemistry and Physics*, *8*, 111-128.

Quinn, P. K., and T. S. Bates (2005), Regional aerosol properties: Comparisons of boundary layer measurements from ACE 1, ACE 2, Aerosols99, INDOEX, ACE Asia, TARFOX, and NEAQS, *Journal of Geophysical Research*, *110*(D14202), doi:10.1029/2004JD004755.

Quinn, P. K., T. S. Bates, D. Coffman, and D. S. Covert (2008), Influence of particle size and chemistry on the cloud nucleating properties of aerosols, *Atmospheric Chemistry and Physics*, *8*, 1029–1042.

Remer, L. A., et al. (2005), The MODIS aerosol algorithm, products, and validation, *Journal of the Atmospheric Sciences*, *62*(4), 947-973.

Ren, X., et al. (2010), Measurement of atmospheric nitrous acid at Blodgett Forest during BEARPEX2007, *Atmospheric Chemistry and Physics*, *10*, 6283–6294, doi:10.5194/acp-10-6283-2010.

Roach, P. J., J. Laskin, and A. Laskin (2010), Molecular characterization of organic aerosols using nanospray desorption electrospray ionization mass spectrometry,, *Analytical Chemistry*, *82*, 7979–7986, doi:10.1021/ac101449p.

Roberts, G. C., and A. Nenes (2005), A continuous–flow streamwise thermal–gradient CCN chamber for atmospheric measurements, *Aerosol Science and Technology*, *39*(3), 206–221, doi:10.1080/027868290913988.

Rogers, R. R., et al. (2009), NASA LaRC airborne high spectral resolution lidar aerosol measurements during MILAGRO: observations and validation, *Atmospheric Chemistry and Physics*, *9*, 4811-4826, doi:10.5194/acp-9-4811-2009.

Russell, L. M., S. H. Zhang, R. C. Flagan, J. H. Seinfeld, M. R. Stoltzenburg, and R. Caldow (1996), Radially classified aerosol detector for aircraft-based submicron aerosol measurements, *Journal of Atmospheric and Oceanic Technology*, *13*(3), 598–609.

Russell, L. M. (2003), Aerosol organic–mass–to–organic–carbon ratio measurements, *Environmental Science & Technology*, *37*(13), 2982–2987, doi:10.1021/es026123w.

Russell, L. M., S. Takahama, S. Liu, L. N. Hawkins, D. S. Covert, P. K. Quinn, and T. S. Bates (2009), Oxygenated fraction and mass of organic aerosol from direct emission and atmospheric processing measured on the R/V *Ronald Brown* during TEXAQS/GoMACCS 2006, *Journal of Geophysical Research*, *114*(D00F05), doi:10.1029/2008JD011275.

Ryerson, T. B., et al. (1998), Emissions lifetimes and ozone formation in power plant plumes, *Journal of Geophysical Research*, *103*(D17), 22,569-522,583.

Ryerson, T. B., L. G. Huey, K. Knapp, J. A. Neuman, D. D. Parrish, D. T. Sueper, and F. C. Fehsenfeld (1999), Design and initial characterization of an inlet for gas-phase NOy measurements from aircraft, *Journal of Geophysical Research*, *104*, 5483-5492.

Ryerson, T.B., et al. (2013), The 2010 California Research at the Nexus of Air Quality and Climate Change (CalNex) field study. *J. Geophys. Res.-Atmos.,*in review.

Sanford, T. J., D. M. Murphy, D. S. Thomson, and R. W. Fox (2008), Albedo measurements and optical sizing of single aerosol particles, *Aerosol Science and Technology*, *42*(11), 958–969, doi:10.1080/02786820802363827.

Scarino, A. J., et al. (2012), Comparison of mixed layer heights from airborne high spectral resolution lidar, ground-based measurements, and the WRF-Chem model during CalNex and CARES, *Journal of Geophysical Research (in preparation)*.

Schauer, J. J., et al. (2003), ACE-Asia intercomparison of a thermal–optical method for the determination of particle-phase organic and elemental carbon, *Environmental Science & Technology*, *37*(5), 993–1001, doi:10.1021/es020622f.

Schauffler, S., E. L. Atlas, S. G. Donnelly, A. Andrews, S. A. Montzka, J. W. Elkins, D. F. Hurst, P. A. Romashkin, G. S. Dutton, and V. Stroud (2003), Chlorine budget and partitioning during the Stratospheric Aerosol and Gas Experiment (SAGE) III Ozone Loss and Validation

Experiment (SOLVE), *Journal of Geophysical Research*, *108*(D5), 4173, doi:10.1029/2001JD002040.

Schwarz, J. P., et al. (2008), Measurement of the mixing state, mass, and optical size of individual black carbon particles in urban and biomass burning emissions, *Geophysical Research Letters*, *35*(13), doi: 10.1029/2008GL033968.

Sheesley, R. J., J. J. Schauer, E. Bean, and D. Kenski (2004), Trends in Secondary Organic Aerosol at a Remote Site in Michigan's Upper Peninsula, *Environmental Science & Technology*, *38*(24), 6491–6500, doi:10.1021/es049104q.

Shetter, R. E., and M. Müller (1999), Photolysis frequency measurements using actinic flux spectroradiometry during the PEM–Tropics mission: Instrumentation description and some results, *Journal of Geophysical Research*, *104*(D5), 5647–5661.

Sorooshian, A., S. Hersey, F. J. Brechtel, A. Corless, R. C. Flagan, and J. H. Seinfeld (2008), Rapid, size-resolved aerosol hygroscopic growth measurements: Differential aerosol sizing and hygroscopicity spectrometer probe (DASH-SP), *Aerosol Science and Technology*, *42*(6), 445–464, doi:10.1080/02786820802178506.

Stark, H., B. M. Lerner, R. Schmitt, R. Jakoubek, E. J. Williams, T. B. Ryerson, D. D. Parrish, and F. C. Fehsenfeld (2007), Atmospheric in situ measurement of nitrate radical (NO_3) and other photolysis rates using spectroradiometry and filter radiometry, *Journal of Geophysical Research*, *112*(D10), doi:10.1029/2006JD007578.

Stöhr, J. (1992), *NEXAFS Spectroscopy*, 407 pp., Springer Verlag, Berlin.

Subramanian, R., et al. (2010), Black carbon over Mexico: the effect of atmospheric transport on mixing state, mass absorption cross-section, and BC/CO ratios, *Atmospheric Chemistry and Physics*, *10*, 219-237, doi:10.5194/acp-10-219-2010.

Sullivan, A. P., R. E. Peltier, C. A. Brock, J. A. de Gouw, J. S. Holloway, C. Warneke, A. G. Wollny, and R. J. Weber (2006), Airborne measurements of carbonaceous aerosol soluble in water over northeastern United States: Method development and an investigation into water-soluble organic carbon sources, *Journal of Geophysical Research*, *111*(D23S46), doi:10.1029/2006JD007072.

Surratt, J. D., et al. (2008), Organosulfate formation in biogenic secondary organic aerosol, *Journal of Physical Chemistry A*, *112*, 8345–8378, doi:10.1021/jp802310p.

Szidat, S., T. M. Jenk, H. A. Synal, M. Kalberer, L. Wacker, I. Hajdas, A. Kasper-Giebl, and U. Baltensperger (2006), Contributions of fossil fuel, biomass-burning, and biogenic emissions to carbonaceous aerosols in Zurich as traced by ^{14}C, *Journal of Geophysical Research*, *111*(D07206), doi:10.1029/2005JD006590.

Tajima, N., N. Fukushima, K. Ehara, and H. Sakurai (2011), Mass range and optimized operation of the aerosol particle mass analyzer, *Aerosol Science and Technology*, *45*(2), 196-214, doi:10.1080/02786826.2010.530625.

Takahama, S., S. Liu, and L. M. Russell (2010), Coatings and clusters of carboxylic acids in carbon-containing atmospheric particles from spectromicroscopy and their implications for cloud-nucleating and optical properties, *Journal of Geophysical Research*, *115*(D01202), doi:10.1029/2009JD012622.

Thalman, R., and R. Volkamer (2010), Inherent calibration of a blue LED-CE-DOAS instrument to measure iodine oxide, glyoxal, methyl glyoxal, nitrogen dioxide, water vapour and aerosol extinction in open cavity mode, *Atmos. Meas. Tech.*, *3*, 1797–1814, doi:10.5194/amt-3-1797-2010.

Thompson, J. E., P. L. Hayes, J. L. Jimenez, K. Adachi, X. Zhang, J. Liu, R. J. Weber, and P. R. Buseck (2012), Aerosol optical properties at Pasadena, CA during CalNex 2010, *Atmospheric Environment*, *55*, 190-200, doi:10.1016/j.atmosenv.2012.03.011.

Turner, D., S. Clough, J. Liljegren, E. Clothiaux, K. Cady-Periera, and K. Gaustad (2007), Retrieving Liquid Water Path and Precipitable Water Vapor From the Atmospheric Radiation Measurement (ARM) Microwave Radiometers, *Transactions on Geoscience and Remote Sensing*, *45*(11), 3680-3690.

Veres, P., J. M. Roberts, C. Warneke, D. Welsh-Bon, M. Zahniser, S. Herndon, R. Fall, and J. de Gouw (2008), Development of negative-ion proton-transfer chemical-ionization mass spectrometry (NI-PT-CIMS) for the measurement of gas-phase organic acids in the atmosphere, *International Journal of Mass Spectrometry*, *274*, 48-55, doi:10.1016/j.ijms.2008.04.032.

Villani, P., D. Picard, V. Michaud, P. Laj, and A. Wiedensohler (2008), Design and validation of a volatility hygroscopic tandem differential mobility analyzer (VH-TDMA) to characterize the relationships between the thermal and hygroscopic properties of atmospheric aerosol particles, *Aerosol Science and Technology*, *42*(9), 729–741, doi:10.1080/02786820802255668.

Volkamer, R., S. Coburn, B. Dix, and R. Sinreich (2009), MAX-DOAS observations from ground, ship, and research aircraft: maximizing signal-to-noise to measure "weak" absorbers, *Proceedings of the SPIE*, *7462*, 746203-746209, doi:10.1117/12.826792.

Wagner, N. L., W. P. Dubé, R. A. Washenfelder, C. J. Young, I. B. Pollack, T. B. Ryerson, and S. S. Brown (2011), Diode laser-based cavity ring-down instrument for NO_3, N_2O_5, NO, NO_2, and O_3 from aircraft, *Atmos. Meas. Tech.*, *4*, 1227-1240, doi:10.5194/amt-4-1227-2011.

Wang, S., R. Ackermann, and J. Stutz (2006), Vertical profiles of O3 and NOx chemistry in the polluted nocturnal boundary layer in Phoenix, AZ: I. Field observations by long-path DOAS, *Atmospheric Chemistry and Physics*, *6*, 2671–2693.

Wang, S. C., and R. C. Flagan (1990), Scanning electrical mobility spectrometer, *Aerosol Science and Technology*, *13*(2), 230-240, doi:10.1080/02786829008959441.

Warneke, C., J. A. de Gouw, E. R. Lovejoy, P. C. Murphy, W. C. Kuster, and R. Fall (2005), Development of proton–transfer ion trap–mass spectrometry: on-line detection and identification of volatile organic compounds in air, *Journal of the American Society for Mass Spectrometry*, *16*, 1316–1324.

Washenfelder, R. A., A. O. Langford, H. Fuchs, and S. S. Brown (2008), Measurement of glyoxal using an incoherent broadband cavity enhanced absorption spectrometer, *Atmospheric Chemistry and Physics*, *8*, 7779-7793.

Weber, B. L., D. B. Wuertz, D. C. Welsh, and R. McPeek (1993), Quality controls for profiler measurements of winds and RASS temperatures, *Journal of Atmospheric and Oceanic Technology*, *10*(452-464).

Weber, R. J., D. Orsini, Y. Daun, Y.-N. Lee, P. J. Klotz, and F. Brechtel (2001), A particle-into-liquid collector for rapid measurements of aerosol bulk chemical composition, *Aerosol Science and Technology*, *35*(3), 718-727, doi:10.1080/02786820152546761.

White, A. B., C. J. Senff, and R. M. Banta (1999), A comparison of mixing depths observed by ground-based wind profilers and an airborne lidar, Journal of Atmospheric and Oceanic Technology, 16, 584-590.

White, A. B., C. J. Senff, A. N. Keane, L. S. Darby, I. V. Djalalova, D. C. Ruffieux, D. E. White, B. J. Williams, and A. H. Goldstein (2006), A wind profiler trajectory tool for air quality transport applications, *Journal of Geophysical Research*, *111*(D23S23), doi:10.1029/2006JD007475.

Whittlestone, S., and W. Zahorowski (1998), Baseline radon detectors for shipboard use: Development and deployment in the First Aerosol Characterization Experiment (ACE 1), *Journal of Geophysical Research*, *103*(D13), 16,743–716,751.

Williams, B. J., A. H. Goldstein, N. M. Kreisberg, and S. V. Hering (2006), An in-situ instrument for speciated organic composition of atmospheric aerosols: thermal desorption aerosol GC/MS–FID (TAG), *Aerosol Science and Technology*, *40*(8), 627–638, doi:10.1080/02786820600754631.

Williams, E. J., F. C. Fehsenfeld, B. T. Jobson, W. C. Kuster, P. D. Goldan, J. Stutz, and W. A. McClenny (2006), Comparison of ultraviolet absorbance, chemiluminescence, and DOAS instruments for ambient ozone monitoring, *Environmental Science & Technology*, *40*(18), 5755–5762, doi:10.1021/es0523542.

Williams, E. J., B. M. Lerner, P. C. Murphy, S. C. Herndon, and M. S. Zahniser (2009), Emissions of NO_x, SO_2, CO, and HCHO from commercial marine shipping during Texas Air Quality Study (TexAQS) 2006, *Journal of Geophysical Research*, *114*(D21306), doi:10.1029/2009JD012094.

Williams, E. J., D. D. Parrish, M. P. Buhr, F. C. Fehsenfeld, and R. Fall (1988), Measurement of soil NO_x emissions in Central Pennsylvania, *Journal of Geophysical Research*, *93*(D8), 9539-9546.

Wilson, J. C., B. G. LaFleur, H. Hilbert, W. R. Seebaugh, J. Fox, D. W. Gesler, C. A. Brock, B. J. Huebert, and J. Mullen (2004), Function and performance of a low turbulence inlet for sampling supermicron particles from aircraft platforms, *Aerosol Science and Technology*, *38*(8), 790-802, doi:10.1080/027868290500841.

Wolfe, D. E., et al. (2007), Shipboard multisensor merged wind profiles from the New England Air Quality Study 2004, *Journal of Geophysical Research*, *112*(D10S15), doi:10.1029/2006JD007344.

Worton, D. R., N. M. Kreisberg, G. Isaacman, A. P. Teng, C. McNeish, T. Gorecki, S. V. Hering, and A. H. Goldstein (2012), Thermal desorption comprehensive two-dimensional gas chromatography: an improved instrument for in-situ speciated measurements of organic aerosols, *Aerosol Science and Technology*, *46*(4), 380-393, doi:10.1080/02786826.2011.634452

Wu, Z., M. Hu, S. Liu, B. Wehner, S. Bauer, A. Maßling, A. Wiedensohler, T. Petäjä, M. Dal Maso, and M. Kulmala (2007), New particle formation in Beijing, China: Statistical analysis

of a 1-year data set, *Journal of Geophysical Research*, *112*(D09209), doi:10.1029/2006JD007406.

Zaveri, R. A., et al. (2012), Overview of the 2010 Carbonaceous Aerosols and Radiative Effects Study (CARES), *Atmospheric Chemistry and Physics Discussions*, *12*, 7647-7687, doi:10.5194/acp-12-7647-2012.

Zhang, H., J. D. Surratt, Y. H. Lin, J. Bapat, and R. M. Kamens (2011), Effect of relative humidity on SOA formation from isoprene/NO photooxidation: enhancement of 2-methylglyceric acid and its corresponding oligoesters under dry conditions, *Atmospheric Chemistry and Physics*, *11*, 6411–6424, doi:10.5194/acp-11-6411-2011.

Zheng, J., A. Khalizov, L. Wang, and R. Zhang (2010), Atmospheric pressure-ion drift chemical ionization mass spectrometry for detection of trace gas species, *Analytical Chemistry*, *82*(17), 7302-7308, doi:10.1021/ac101253n.

Zheng, J., et al. (2011), Measurements of gaseous H_2SO_4 by AP-ID-CIMS during CAREBeijing 2008 Campaign, *Atmospheric Chemistry and Physics*, *11*, 7755-7765, doi:10.5194/acp-11-7755-2011.

Zheng, W., F. M. Flocke, G. S. Tyndall, A. Swanson, J. J. Orlando, J. M. Roberts, L. G. Huey, and D. J. Tanner (2011), Characterization of a thermal decomposition chemical ionization mass spectrometer for the measurement of peroxy acyl nitrates (PANs) in the atmosphere, *Atmospheric Chemistry and Physics*, *11*, 6529–6547, doi:10.5194/acp-11-6529-2011.

Zhou, L., Y. Zeng, P. D. Hazlett, and V. Matherne (2007), Ambient air monitoring with auto-gas chromatography running in trigger mode, *Analytica Chimica Acta*, *596*(1), 156-163.

Zielinski, M., H. Riimmelt, and G. Fruhmann (1997), Ambient air soot concentrations in Munich public transportation systems, *Science of the Total Environment*, *196*, 107-110.

Zordan, C. A., S. Wang, and M. V. Johnston (2008), Time–resolved chemical composition of individual nanoparticles in urban air, *Environmental Science and Technology*, *42*(17), 6631–6636, doi:10.1021/es800880z.

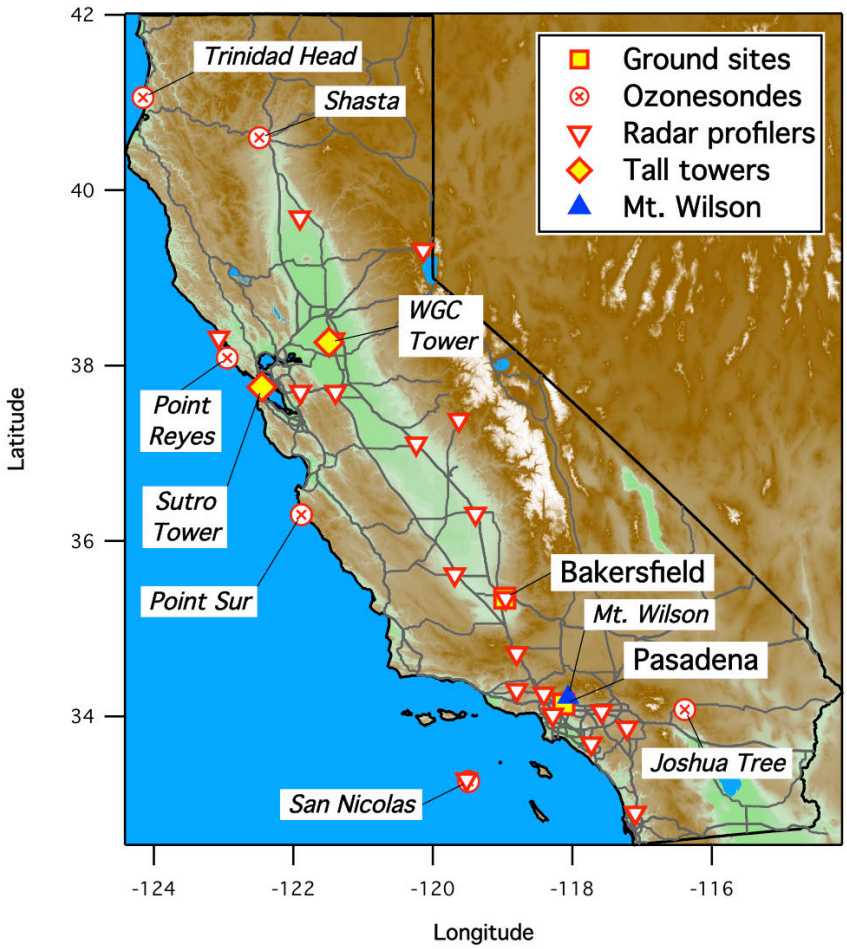

Figure 1. Map of selected ground sites relevant to the CalNex project in 2010.

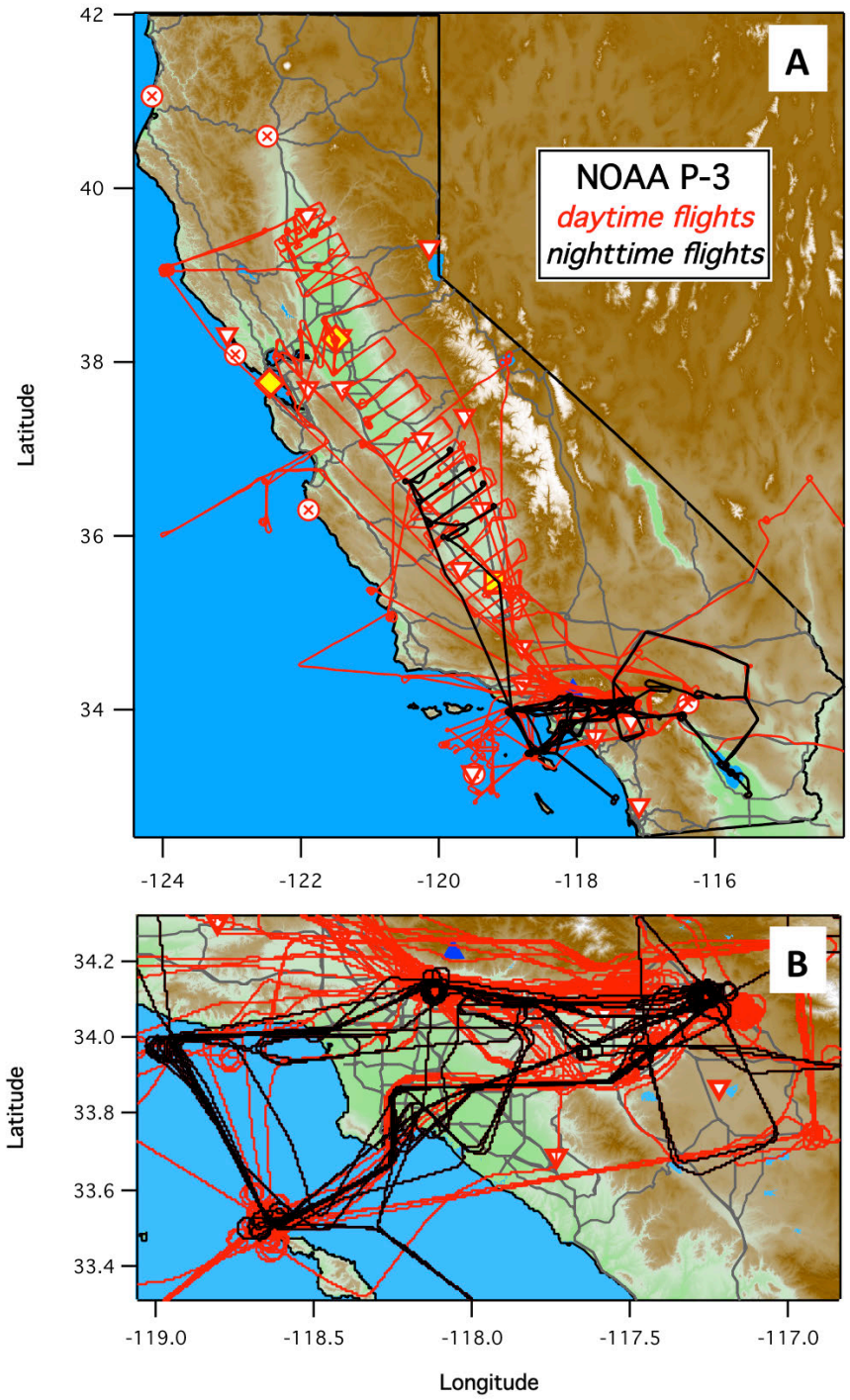

Figure 2. A). Daytime (red lines) and nighttime (black lines) NOAA P–3 research aircraft flight tracks in California between 30 April and 22 June 2010. B). As in A, showing details of P–3 flight segments within the South Coast Air Basin.

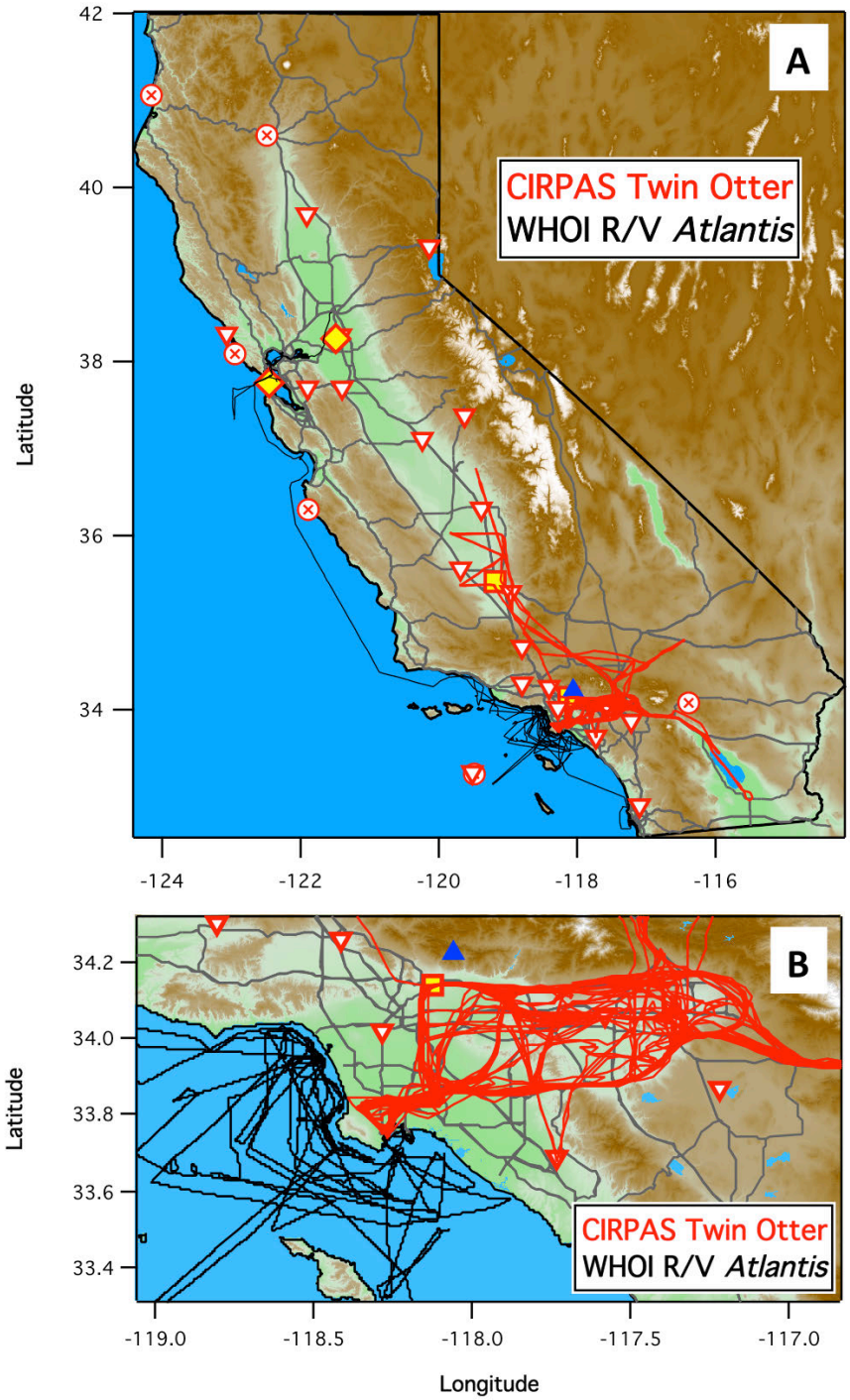

Figure 3. As in Fig. 2, for the CIRPAS Twin Otter flight tracks between 4 May and 28 May 2010 (red lines) and the R/V *Atlantis* cruise track between 14 May and 8 June 2010 (black lines).

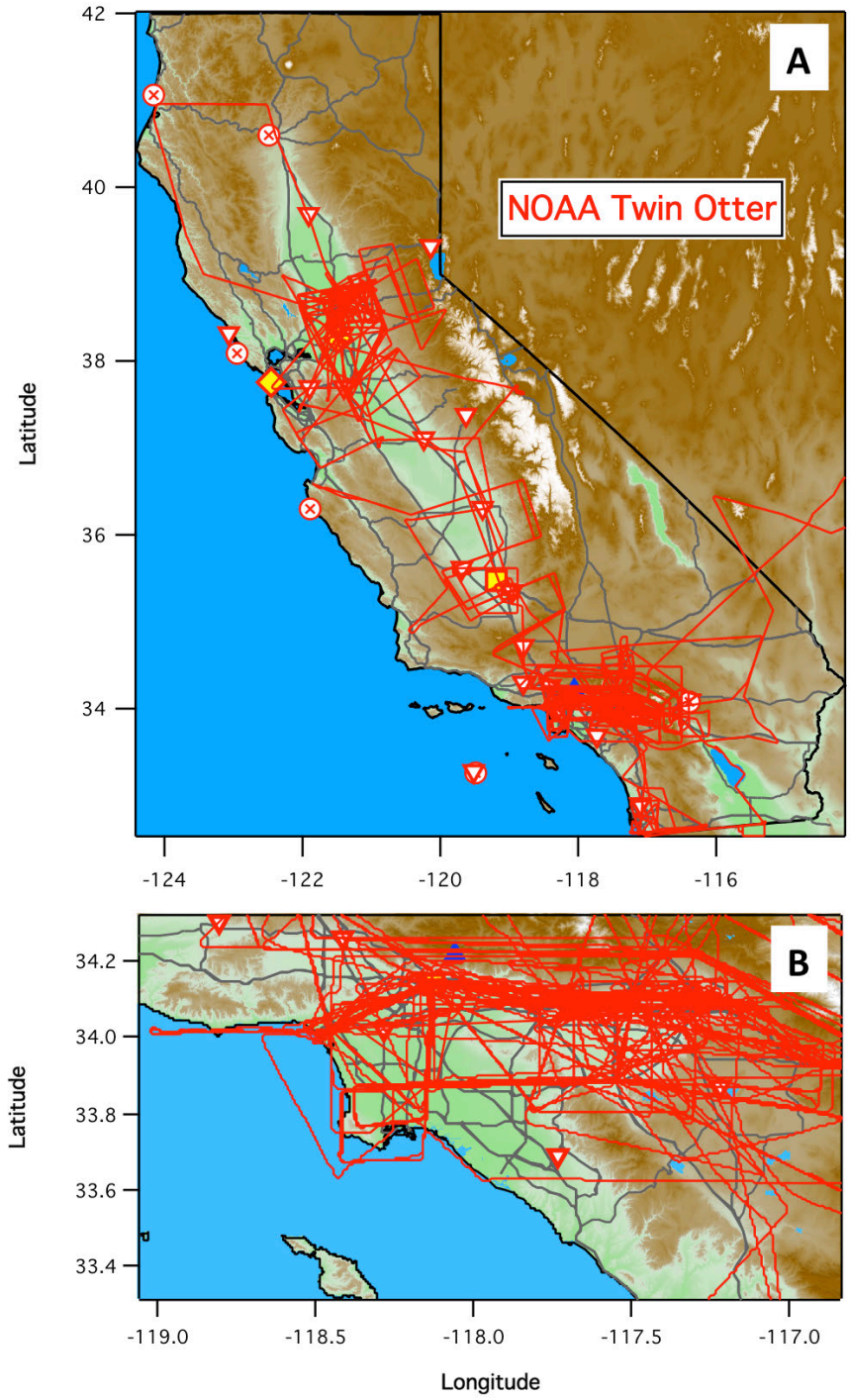

Figure 4. As in Fig. 2, for the NOAA Twin Otter flight tracks between 19 May and 19 July 2010 (red lines).

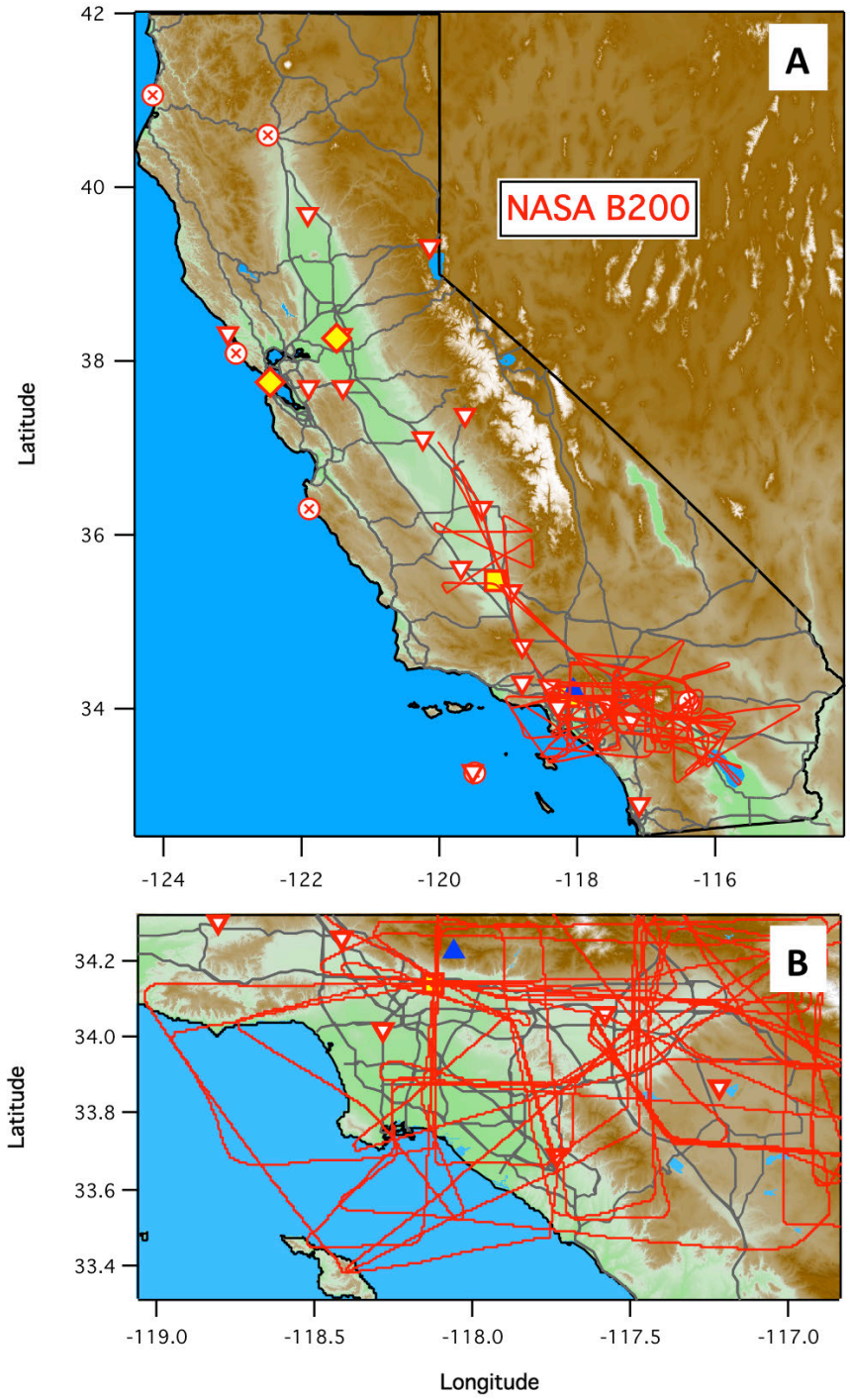

Figure 5. As in Fig. 2, for the NASA B200 flight tracks between 12 May and 25 May 2010 (red lines).